

Development of an automated trace analyser and a novel passive sampling device for the monitoring of ammonia in marine environments



Lenka O'Connor Šraj

ORCID: 0000-0002-2353-1037

Doctor of Philosophy (Chemistry)

School of Chemistry, The University of Melbourne

ABSTRACT

Ammonia is commonly used as an indicator of water quality, to assess the impacts of anthropogenic activity on ecosystem function and health. Water quality assessment often relies on the use of expensive equipment requiring a high degree of operator skill, or periodic, discrete, manual sampling and laboratory-based analysis, which is laborious, costly and without the guarantee that episodic pollution events will be detected. Low-cost, portable and/or field-deployable analytical tools are required to overcome this challenge. Hence, research conducted in the context of this thesis involves the development of novel analytical tools for the monitoring of ammonia in marine waters, covering both active and passive sampling.

A flow-based analytical method was designed and developed for the determination of total ammonia over a wide concentration range in marine waters using the gas-diffusion spectrophotometric method. Limits of detection similar to that of highly sensitive fluorometric methods was achieved. A novel flow approach was adopted whereby a continuous stream of sample was merged with the sodium hydroxide reagent stream and delivered to a gas-diffusion ammonia separation unit, allowing large sample volumes to be used, rather than being limited by the use of discrete samples. The working range and sensitivity of the method could be tailored by simple modification of the sample volumes used, and by minor adjustments to the program used to control the instrument, without the need to make changes to the manifold. Three working ranges were obtained, and the analytical figures of merit are described. This project was an enabling step in the development of an ammonia gas-diffusion passive sampling device, as it allowed the measurement of low concentrations often found in field samples, as well as high concentrations accumulated in the passive sampler's receiving solution, using the same instrumentation and reagents.

A passive sampling device based on gas-diffusion across a hydrophobic membrane was developed and successfully applied for the determination of the time-weighted average concentration (C_{TWA}) of ammonia in marine waters for a period of 3 to 7 days. Molecular ammonia (NH_3) present in the sampled source solution (SS) diffuses through a hydrophobic membrane into an acidic receiving solution where it is ionised and accumulated as NH_4^+ which

is directly proportional to the NH_3 concentration in the SS. Biofouling limited the application of the first gas-diffusion-based passive sampler (GD-PS) prototype to 3 days, and a number of antifouling strategies were therefore assessed, with a copper mesh enabling the sampling period to be extended to 7 days. The effects of environmental variables (temperature, pH and salinity) on NH_3 accumulation were also investigated, and the Group Method of Data Handling (GMDH) Algorithm was used to develop a single calibration model for a range of environmental conditions (10 to 30 °C, pH 7.8 to 8.2, salinity 20 to 35). PSDs were deployed at four estuarine and marine sites in *Nerm* (Port Phillip Bay), south eastern Australia, achieving good agreement between passive and automated discrete sampling methods (maximum relative error between -12 % to -19 %). The GD-PS covers the revised water quality trigger value ($160 \mu\text{g L}^{-1} \text{NH}_3\text{-N}$) and allows for episodic pollution events to be successfully detected, highlighting this as an exciting new tool for water quality assessment.

DECLARATION

I, Lenka O'Connor Šraj, declare that:

1. This thesis comprises only my original work, except where indicated, and with appropriate acknowledgement provided
2. Due acknowledgment has been made in the text to all other material used, particularly with respect to third-party copyright material
3. Permissions were obtained in all cases to use third-party copyright material in the open access version of this thesis
4. The thesis is less than the maximum word limit in length



PREFACE AND ACKNOWLEDGEMENT

I would like to acknowledge the Boon Wurrung, Wurundjeri and Wathaurong Sovereign Clans of the Kulin Nation as the Traditional Custodians of the waterways and lands upon which research for my doctoral studies was undertaken. I currently live on Wurundjeri Country and I would like to pay my respects to all First Nations elders, past, present and emerging. Furthermore, I recognise the significant contributions made by our First Nations custodians in terms of Indigenous knowledge and understandings of sustainability and caring for Country, including for our precious waterways and coastal areas. Throughout this work, the original First Nations place names have been used, italicised, together with the colonial place names in brackets.

All research work and thesis preparation were carried out under the supervision of Professor Spas D. Kolev with guidance, advice, support and editorial assistance provided by Professor Stephen Swearer (co-supervisor), Dr Ian D. McKelvie, Dr Richard Morrison, and Dr Maria Inês G. S. Almeida.

I would like to thank Ms Chelsea Bassett for assistance with preliminary passive sampling experiments, and the Environment Protection Authority Victoria for the loan of field equipment and assistance from staff, including Chris Garland, Adele McKenzie and Mick Ernest, and also Professor Vincent Pettigrove (RMIT University, former CEO of the Centre for Aquatic Pollution Identification and Management) for the loan of field equipment and assistance in setting up field experiments. I would also like to thank Mr Simon Sharp and Mr Andrew Longmore who provided extensive assistance in setting up field experiments and sampling guidance, Mr. Roger Eastham and the Royal Yacht Club of Victoria for allowing field work in their marina, Parks Victoria for permitting field work in the coastal waters of *Nerm* (Port Phillip Bay) and the Werribee River estuary, and Melbourne Ports for allowing field work to be undertaken in the *Birrarung* (Yarra River) estuary.

Mr Marcus Hammarstedt and Mr Benham Rasooli assisted with digitising graphics for publication, and I am grateful to the University of Melbourne for the award of a postgraduate scholarship.

Firstly, I would like to thank my wonderful family for their support and encouragement over the years, particularly my mother and father who worked tirelessly to provide me with an incredible education. I dedicate this thesis to you both, as you were instrumental in getting me to a point where I could take on this project. To my brothers and my partner, you are the most amazing people, and I am so lucky to have your continued and ongoing friendship and your help and assistance along this journey. On many occasions you helped me with my field work, with editorial and design assistance, you have looked after me when I have been busy trying to get my work done, and so thank you. I am so grateful to you all for being there for me, supporting me in this endeavour and for helping me along the way.

I would like to thank my encouraging and incredibly supportive supervisors Professor Spas D. Kolev and Professor Stephen Swearer firstly for taking me on as a PhD student, and for providing me with inspiration and assistance over the course of my graduate studies. It has been an honour to work with Professor Kolev. You taught me to be an inquisitive and independent researcher and you have often challenged me to think more broadly about my work. I am so grateful to have been given the opportunity to work with such an amazing scientist, and to be a member of the Kolev research group. I would like to thank Professor Kolev for being a most wonderful supervisor and mentor over the years. Professor Stephen Swearer you were always there when I needed assistance and always offered a fresh and invaluable perspective to the challenges I faced during the course of my research. I have thoroughly enjoyed our discussions over the years and look forward to continuing these into the future.

I would like to thank Dr Ian McKelvie and Dr Richard Morrison for all their assistance, guidance, mentorship and life-changing advice over the years. I feel so lucky to have been able to collaborate with you both on a multitude of projects, and I look forward to our continued work with the Kolev research group. You have given me so much inspiration, support and friendship over the years and I am forever grateful.

Finally, I would like to thank Dr Maria Inês G. S. Almeida for your supervision, guidance, mentorship, and friendship over the years. You were there for me every single day and I am so thankful for the many hours you have spent teaching me new techniques, working through problems with me, helping me with both lab and field work and supporting and encouraging me when experiments didn't go to plan. I feel so privileged to have been able to work with you and you have been an inspiration to me. I look forward to many years of friendship to come.

TABLE OF CONTENTS

CHAPTER 1:

General introduction	1
1.1 Aquatic ammonia pollution	3
1.2 Challenges for the analytical chemist	5
1.3 Flow-based methodologies	8
1.4 Passive sampling	28
1.5 General comments and research objectives	60

CHAPTER 2:

Determination of trace levels of ammonia in marine waters using a simple environmentally-friendly ammonia (SEA) analyser	84
2.1 Introduction	88
2.2 Materials and methods	91
2.3 Results and discussion	99
2.4 SEA analyser system performance	105
2.5 Validation of the SEA analyser	107
2.6 Conclusions	109
2.7 Appendix	111

CHAPTER 3:

Gas-diffusion-based passive sampler for ammonia monitoring in marine waters	116
3.1 Introduction	120
3.2 Materials and methods	121
3.3 Results and discussion	124
3.4 Conclusions	130

CHAPTER 4:

Monitoring of ammonia in marine waters using a passive sampler with biofouling resistance and neural network-based calibration	133
4.1 Introduction	137
4.2 Materials and methods	139
4.3 Results and discussion	144
4.4 Conclusions	157
4.5 Appendix	158

CHAPTER 5:

Conclusions and future work	177
-----------------------------	-----

LIST OF FIGURES

CHAPTER 1

Figure 1-1.	Biogeochemical cycling of aquatic nitrogen and transformations in the water column.	4
Figure 1-2.	Average concentration of the major ions in seawater accounting for the overall total salinity of 34.5.	6
Figure 1-3.	Schematic diagrams of commonly used flow systems.	8
Figure 1-4.	Distribution graph of flow-based methodologies developed for the determination of total ammonia in estuarine and marine waters.	9
Figure 1-5.	Results obtained by different sampling methods commonly used in environmental monitoring.	29
Figure 1-6.	Schematic diagrams and typical deployment configuration of a SPMD filled with triolein receiving phase.	35
Figure 1-7.	Single-phase polymer-based PSDs.	41
Figure 1-8.	Schematic diagrams and typical deployment configuration of the POCIS for the passive sampling of hydrophilic organic compounds.	44
Figure 1-9.	Schematic diagram and typical deployment configuration of the Chemcatcher®.	46
Figure 1-10.	Summary of the log K_{ow} ranges successfully tested for various Chemcatcher® receiving phase and membrane combinations.	48
Figure 1-11.	Schematic diagram and typical deployment configuration of the diffusive gradient in thin-films passive sampling device.	54

CHAPTER 2

Figure 2-1.	Schematic diagram of the fully automatic SEA analyser using a FiaLab 3500 flow system and Cetac autosampler.	94
Figure 2-2.	Different GDU configurations tested in order to select the configuration that achieved the highest sensitivity.	97
Figure 2-3.	(a) Effect of the donor stream flow rate on the analytical signal for three different ammonium standards; (b) effect of the sample and reagent volume on the maximum absorbance for three different ammonium standards.	100
Figure 2-4.	(a) Performance of different GDU configurations; (b) Performance of different porous hydrophobic membranes was examined using the sandwich type GDU.	103
Figure 2-5.	(a) Blank corrected absorbance response for for 1.4 μM (o) and 2.8 μM (\diamond) ammonium standards as a function of baseline absorbance; (b) absorbance response for different colour indicator dye solutions, as single dyes or as mixtures; (c) the working range of the method can be extended when mixed indicator solutions are used.	105

Figure 2-6.	Three typical concentration working ranges based on sample volume	106
Figure 2-7.	Sampling sites around the Port Phillip Bay Study Area with the average range of concentrations of ammonia nitrogen measured with the SEA analyser	108
Figure 2-8.	Spiked recoveries of seawater samples of varying salinity from around Port Phillip Bay (PPB), and Bancoora Surf Beach.	109
 CHAPTER 3		
Figure 3-1.	(a) Gas-diffusion-based PS assembly; (b) cross section of the gas-diffusion-based PS (membrane thickness not drawn to scale), and schematic illustration of the diffusion process of dissolved ammonia ($\text{NH}_{3(\text{aq})}$) from the source solution through the pores of the hydrophobic GDM	124
Figure 3-2.	(a) Transient concentration of ammonium in the receiving solution versus sampling time; (b) laboratory-based calibration of the gas-diffusion PS	129
 CHAPTER 4		
Figure 4-1.	A) GD-PS assemblage with antifouling mesh. B) Cross-section of the GD-PS showing the process of selective accumulation of dissolved $\text{NH}_{3(\text{aq})}$ from the source solution.	143
Figure 4-2.	Membrane antifouling strategies under laboratory conditions. A) Effect of the different antifouling strategies on the ammonium concentration accumulated in the receiving solution after 7 or 8 days of sampling in the laboratory; B) effect of the different antifouling strategies on the extent of biofilm formation on the surface of the GDMs	146
Figure 4-3.	Effect of salinity (A), pH (B) and temperature (C) on the GD-PS accumulation	150
Figure 4-4.	Field validation of the GD-PS with copper mesh (Cu-100) using the GMDH calibration model, A) <i>Birrarung</i> (Yarra River) estuary (Site 1) and B) Werribee River estuary mouth (Site 3)	154
Figure S4-1.	Port Phillip Bay field study sites and water collection point (datum: GDA94).	159
Figure S4-2.	Receiving solution composition and membrane optimisation	160
Figure S4-3.	GD-PS accumulation over 7 days using Cu-100 (◆), Cu-200 (○) and AgNP (◇) antifouling mesh and no treatment (●).	160
Figure S4-4.	Multivariate study of temperature, salinity and pH parameters	161
Figure S4-5.	GMDH model for GD-PS between pH 7.8 to 8.2 and temperature 10 to 30 °C.	164
Figure S4-6.	GMDH model figures of merit.	164

Figure S4-7.	Field validation of the GD-PS with copper mesh (Cu-100) using the GMDH calibration model, A) Hobsons Bay (Site 2) and B) Werribee River estuary 5 km upstream from river mouth (Site 4).	166
Figure S4-8.	Linear calibration of GD-PS with studentised residuals.	168
Figure S4-9.	Werribee river estuary mouth (Site 3) dissolved oxygen and tidal data. A) Tide and salinity data; B) pH and dissolved oxygen data; C) calculated source solution molecular ammonia and measured total ammonia data.	169
Figure S4-10.	Satellite images showing proximity of stockpiled agricultural chemicals to Werribee River estuary (Sites 3 and 4).	170

LIST OF TABLES

CHAPTER 1

Table 1-1.	Analytical features of flow-based methodologies using the indophenol blue reaction.	11
Table 1-2.	Analytical features of flow-based methodologies using analyte separation and/or preconcentration.	16
Table 1-3.	Analytical features of flow-based methodologies using fluorometric detection.	20
Table 1-4.	Stability and storage of reagents involved in the determination of ammonium.	27

CHAPTER 2

Table 2-1.	Gas-diffusion configurations comparing various aspect ratios (exposed membrane area to channel volume ratio).	97
Table 2-2.	Hydrophobic membranes tested.	98
Table 2-3.	Analytical figures of merit of the SEA analyser for three typical working ranges.	107
Table 2-4.	Method validation using a diluted CRM in 0.6 M NaCl, for the calibration range 0.28 – 13.9 μM NH_4^+ .	107
Table A2-1.	Programmable flow procedure for the determination of ammonia nitrogen in seawater.	111

CHAPTER 3

Table 3-1.	Membrane characteristics.	122
Table 3-2.	Study of the gas-diffusion membranes and the receiving solution composition.	126

CHAPTER 4

Table 4-1.	Comparison between discrete grab sampling and GD-based passive sampling (time-weighted average ammonia concentration ($[\text{NH}_3]_{\text{TWA}}$)) using the GMDH model.	154
Table S4-1.	Field site codes, location and GPS coordinates (datum: GDA94)	159
Table S4-2.	Experimental conditions for the multivariate study.	161
Table S4-3.	Experimental conditions for the univariate study.	162
Table S4-4.	Effect of the flow pattern on the error obtained when comparing discrete grab sampling (SS) and GD-based passive sampling ($[\text{NH}_3]_{\text{TWA}}$ determined using the GMDH model).	168

ABBREVIATIONS

ABA, Autonomous batch analysis	HAB, Harmful algal bloom
AgNP, Silver nanoparticle	HLB, Hydrophilic-Lipophilic Balance
ANAMOX, Anaerobic ammonium oxidation	HOC, Hydrophobic organic compound
ANZG, Australian and New Zealand Guidelines	HF, Hollow fibre
AOA, Ammonia oxidizing archaea	HPLC, High-performance liquid chromatography
AQUA-GAPS, Aquatic global passive sampling program	H-SDME: Headspace single-drop microextraction
BTB, Bromothymol blue	IC, Ion chromatography
CA, Cellulose acetate	IDA, Iminodiacetate groups
CRM, Certified reference material	IL, Ionic liquid
C_{TWA} , Time-weighted average concentration	IPB, Indophenol blue
CyDTA, 1,2 Cyclohexane diamine tetraacetic acid	iSEA, Integrated syringe-pump-based environmental-water analyser
DGT, Diffusive gradients in thin films	LDPE, Low-density polyethylene
DIC, Dichloroisocyanurate	LED, Light emitting diode
DRP, Dissolved reactive phosphorous	LFA, Loop flow analysis
EDTA, Ethylenediaminetetraacetic acid	LOD, Limit of detection
EU-WFD, European Union Water Framework Directive	LOQ, Limit of quantification
EVA, Ethylvinyl acetate	LWCC, Liquid waveguide capillary cell
FIA, Flow injection analysis	MCFIA, Multicommutated FIA
FL, Fluorescence	MOPA, 4-methoxyphthalaldehyde
GBR, Great Barrier Reef	M ₂ OPA, 4,5-dimethoxyphthalaldehyde
GC-MS, Gas chromatograph mass spectrometry	MPFS, Multipumping flow systems
GD, Gas-diffusion	MPV, Multiposition valve
GDM, Gas-diffusion membrane	MSA, Methane sulphonic acid
GDU, Gas-diffusion unit	MSFIA, Multi-syringe FIA
μ GDU, Micro gas-diffusion unit	N ₂ , Nitrogen
GMDH, Group Method Data Handling	NH ₃ , Molecular ammonia
	NH ₄ ⁺ , Ammonium
	NH ₃ /NH ₄ ⁺ , Total ammonia
	NPOE, Nitrophenyl octyl ether

OPA, Orthophthaldialdehyde
OPP, *o*-phenylphenol
PAH, Polyaromatic hydrocarbon
PBDE, Polybrominated diphenyl ethers
PCB, Polychlorinated biphenyl
PDMS, Polydimethylsiloxane
PES, Polyethersulfone
PFAS, Perfluoroalkyl substances
PFC, Perfluorinated chemicals
PIM, Polymer inclusion membrane
PIMS, Passive integrative mercury sampler
PMT, Photomultiplier tube
POCIS, Polar organic chemical integrative sampler
POM, Polyoxymethylene
PP, Polypropylene
PPB, *Nerm* (Port Phillip Bay)
PS, Passive sampler
PSD, Passive sampling device
PRC, Performance reference compound
PTFE, Polytetrafluoroethylene
P&T, Purge-and-trap
PVDF, polyvinylidene difluoride
rFIA, Reversed FIA
RTD, resistance temperature detector
 R_s , Sampling rate
SBSE, Solventless stir bar sorptive extraction
SD, Steam distillation
SFA, Segmented flow analysis
SIA, Sequential injection analysis
SLM, Supported liquid membranes
SPATT, Solid-phase adsorption toxin tracking
SP, Syringe pump
SPE, Solid-phase extraction
SPMD, Semipermeable membrane device
SR, Silicone rubber
TOMAS, Trioctylmethylammonium salicylate
TOMATS, Trioctylmethylammonium thiosalicylate
UV, Ultraviolet
WTP, Western Treatment Plan

CHAPTER 1: General introduction

Foreword

This thesis has been written in the format of a '*Thesis by Publication*'. The chapters of this work comprise a series of peer-reviewed papers which have been published in high-impact factor journals. These chapters are bookended by a substantial *General introduction* chapter and a *Conclusions and future work* chapter. Where a chapter (or section of a chapter) of this thesis has been published, it will be highlighted in the *Foreword* section at the beginning of each chapter, with information on the journal article appearing as a citation for the readers easy reference.

The following section encompasses a literature review looking at flow-based methodologies developed to monitor ammonia in marine waters, in addition to a description of passive sampling technologies that have been developed for monitoring environmental pollutants in natural waters, with a particular emphasis on those applied to estuarine, coastal and marine environments. The advantages and challenges of flow methods and passive sampling techniques is evaluated.

The content of the sections describing flow techniques for ammonia determination in estuarine and marine waters was published in 2014 in the journal *Trends in Analytical Chemistry*, and it has been further updated to cover the period 2014-2020. The section describing passive sampling techniques applied to high salinity matrices is currently in the process of being prepared for submission to a journal and is thus written in the style of a review paper.

O'Connor Šraj, L., Almeida, M. I. G. S., Swearer, S. E., Kolev, S. D., McKelvie, I. D. *Analytical challenges and advantages of using flow-based methodologies for ammonia determination in estuarine and marine waters*, TrAC Trends Analytical Chemistry, 59 (2014) 83-92, doi.org/10.1016/j.trac.2014.03.012

Contents

1.1	Aquatic ammonia pollution	3
1.2	Challenges for the analytical chemist	5
1.3	Flow-based methodologies	8
1.3.1	Indophenol blue method	10
1.3.2	Gas-diffusion method	16
1.3.3	Fluorometric method	20
1.3.4	Field applications	24
1.4	Passive Sampling	28
1.4.1	Semipermeable membrane devices (SPMDs)	34
1.4.1.1	Single-phase passive samplers	38
1.4.1.1.1	Low-density polyethylene (LDPE)	39
1.4.1.1.2	Silicone Rubber (SR)	40
1.4.1.1.3	Polyoxymethylene (POM) & ethylene-vinyl acetate (EVA)	42
1.4.2	Polar organic chemical integrative sampler (POCIS)	42
1.4.3	Chemcatcher®	46
1.4.3.1	Chemcatcher® for non-polar compounds	48
1.4.3.2	Chemcatcher® for polar compounds	49
1.4.3.3	Chemcatcher® for metals and organometallics	50
1.4.4	Solid-phase adsorption toxin tracking (SPATT)	52
1.4.5	Diffusive gradients in thin-films (DGT)	53
1.4.6	GELLYFISH for metals	56
1.4.7	Liquid membrane-based passive samplers	57
1.4.8	Ammonium PSDs applied to freshwaters	59
1.5	General comments and research objectives	60
	References	63

1.1 Aquatic ammonia pollution

Ammonia is an ecologically important nutrient in the nitrogen cycle of coastal and oceanic waters (Figure 1-1). It is naturally found at low concentrations in the environment as a by-product of protein metabolism and the decomposition of organic matter. However, it is increasingly entering the environment as a result of urban, industrial and agricultural processes, predominantly as a result of large-scale diffuse run-off from agricultural land [1]. Hence, the creation of guidelines for ammonia in estuarine and marine water systems is critical in order to achieve a sustainable use of water resources, and for the protection of aquatic life from acute and chronic effects of ammonia. Although this issue remains a challenge [2], some countries have established guideline values for ammonia in marine or salt waters [3-6].

The toxicity of ammonium/ammonia is dependent on pH. Below pH 8.75, ammonium (NH_4^+) is the predominant relatively non-toxic form, and above pH 9.75, ammonia (NH_3), the toxic form, is dominant [7]. Therefore, in most aquatic environments, ammonium is the major form and ammonia is present to a much lesser extent. Despite the lower toxicity of ammonium, it should be considered important because of its much greater concentrations than un-ionised ammonia [8].

There are several consequences of excessive ammonia/ammonium concentrations in the aquatic environment. In the presence of nitrifying bacteria, ammonium and ammonia can be converted to nitrate [1], both of which are utilised by phytoplankton, macrophytes and cyanobacteria. At elevated concentrations, ammonia/ammonium can stimulate primary production in planktonic communities causing rapid algal growth and eutrophication, contributing to widespread and even irreversible changes to a whole range of coastal and marine ecosystems [1, 9]. Microbial respiration fuelled by an increase in dissolved organic matter from algal senescence causes dissolved oxygen depletion, resulting in hypoxia in the water column [10]. The sensitivity of marine fish and invertebrates to ammonia toxicity is amplified in hypoxic waters, with both stressors exhibiting a synergistic effect [1]. Most marine fish and invertebrates excrete ammonia and ammonium directly, as the major metabolic waste products, to the surrounding water [11]. Although the precise mechanisms of excretion in fish are still the subject of research, it is believed that this process occurs via passive diffusion, from blood plasma to the water surrounding the gills [11]. The high ionic permeability of the gills of

marine fish allows for ammonia to enter as either the un-ionised or ionised forms, which may make them more prone to ammonia and ammonium toxicity than their fresh water counterparts [11]. Ammonia exposure is particularly detrimental to the growth and development of larval and juvenile life stages of fish and invertebrates. In mature fish, exposure to ammonia is known to cause pathohistological damage to the gills, kidneys and blood, neurotoxicity, hyperventilation, and convulsions. Over sustained periods of time, build-up of the toxin in the blood can result in the extinction of entire populations, thus threatening many globally important ecosystems and fisheries [12].

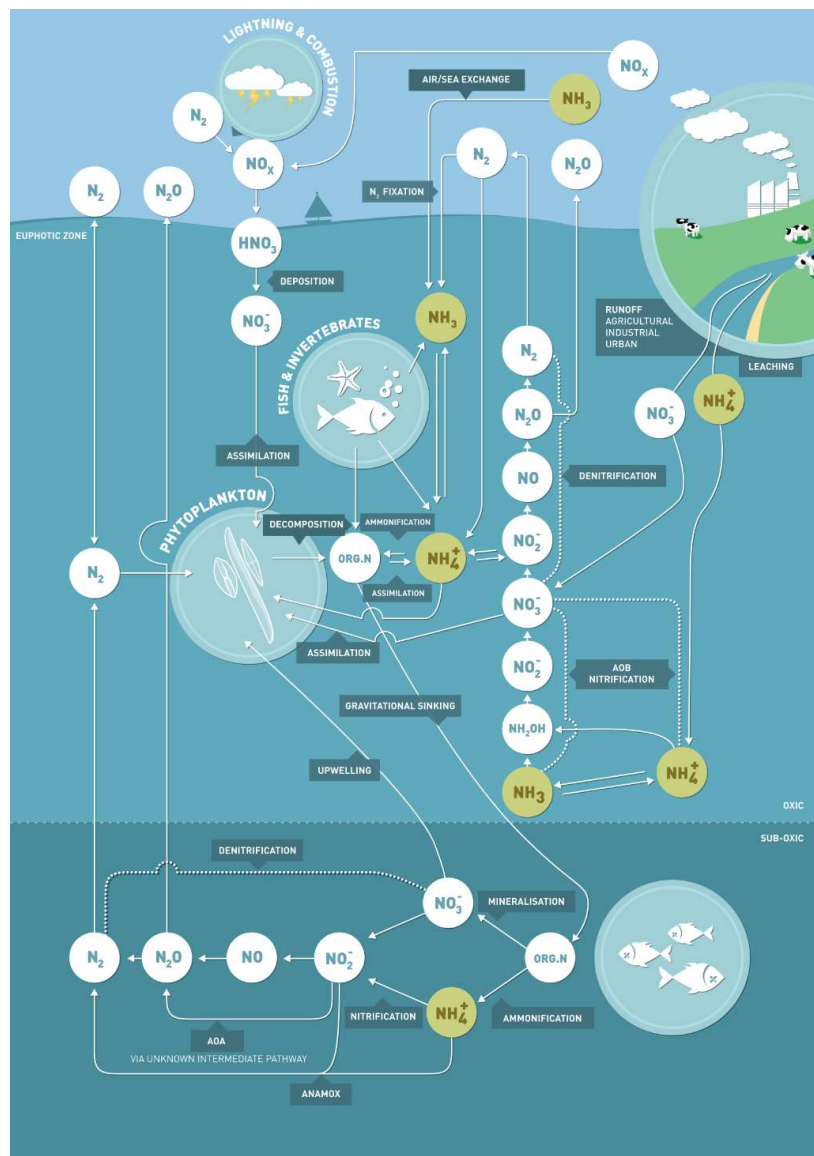


Figure 1-1. Biogeochemical cycling of aquatic nitrogen and transformations in the water column.

The global nitrogen cycle is complex and dynamic, and many aspects are still not fully understood. For example, it is only recently that ammonia oxidizing archaea (AOA) have been discovered in the oceans. These may be the key organism responsible for production of the potent greenhouse gas nitrous oxide (N_2O) [13], which has been described as having a global warming potential 310 times greater than CO_2 [14]. The rate of N_2O produced by AOA from ammonia is high under hypoxic conditions. The occurrence of hypoxic waters is predicted to increase exponentially with continual anthropogenic nutrient loading of coastal waters and global climatic changes, and this in turn may lead to increased production of N_2O in the oceans, and higher concentrations of N_2O in the atmosphere [13].

The total ammonia concentration (i.e. the sum of both ammonia and ammonium) is thus an indicator of water quality as well as an ecological stressor [7]. The measurement of total ammonia concentrations and fluxes, coupled with an understanding of the complex biogeochemical processes, is imperative for sustainable management and conservation of important marine ecosystems and their catchments [15]. Analytical methods that are fast, sensitive, reliable and preferably portable or capable of *in situ* analysis, are therefore essential tools in achieving such goals. The following section will thus review the challenges facing the analytical chemist as well as the flow-based and *in situ* methodologies developed for the determination of ammonia in marine, coastal and estuarine waters. Furthermore, an overview of the passive sampling techniques described in the literature will be provided, specifically when applied to high salinity matrices. Passive sampling has become a popular technique for *in situ* monitoring of environmental pollutants in aquatic environments, however passive sampling techniques specifically for ammonia monitoring in marine waters have not previously been described prior to the gas-diffusion-based passive samplers developed as part of the research reported in this thesis (see Chapters 3 and 4).

1.2 Challenges for the analytical chemist

Marine environments, including estuarine, coastal and open ocean waters are increasingly the focus of research with respect to the detection of anthropogenic pollutants [16]. However, the low analyte concentrations, variable salinity and matrix complexity of these waters (e.g. the potential interferences from cations such as Mg^{2+} and Ca^{2+}) make that task difficult [17]. To

illustrate the complexity of the seawater matrix, Figure 1-2 summarizes the average concentrations of the major ions in seawater, accounting for the overall total salinity of 34.5 [18]. Additionally, estuarine, coastal and oceanic waters represent different ecological systems which have substantially different chemical environments (as described below), and it is often difficult to find analytical methods that can be applied universally to all three types of matrix.

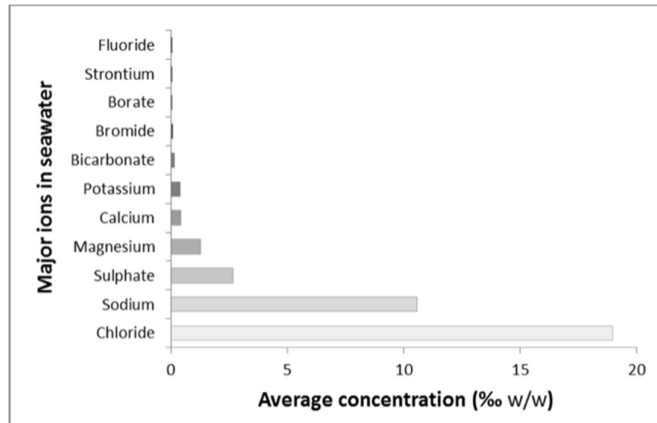


Figure 1-2. Average concentration of the major ions in seawater accounting for the overall total salinity of 34.5 [18].

Estuarine environments are where fresh water from rivers mix with saline water from the ocean and are characterised by salinities ranging from 0.5 to 35 [19]. They are dynamic, transient and exhibit a unique and complex biogeochemistry, with a wide range of chemical compositions (they often exhibit salinity stratification) that change with the tides, season, weather, biota, surrounding landscape and anthropogenic inputs of dissolved organic and inorganic materials [19]. Estuaries are some of the most biologically diverse and productive ecosystems, providing habitat for a variety of unique plants and animals (i.e. marine fish and invertebrates) [20].

In the oceans, salinity, temperature and nutrient-concentration profiles are typically vertically stratified [21]. The euphotic zone at the surface exhibits relatively uniform physicochemical properties due to winds, shallow currents and small-scale eddies that facilitate mixing [21]. However, due to mainly thermohaline stratification, the upper ocean surface is generally characterised by warm, highly saline, nutrient deficient waters, whereas the deeper water masses tend to be cooler, denser and containing higher concentrations of re-mineralised

inorganic nutrients, which have been accumulated by the gravitational sinking of decomposing phytoplankton and dissolved organic matter from the euphotic zone [21]. Essential nutrients are redistributed in the water column as a result of mesoscale ocean currents and circulation patterns, resulting in diapycnal three-dimensional mixing, coastal upwelling of cold, nutrient rich waters along western coastlines in the Pacific, Indian and Atlantic oceans, and to a lesser extent, contributions from diazotrophic nitrogen fixation, atmospheric deposition and inputs from river run-offs into estuaries and coastal waters [22].

Another challenge often encountered by the analytical chemist is the collection, storage and preservation of estuarine or marine water samples. Samples collected manually should be stored in glass or polyethylene bottles (0.5 – 1 L capacity) and analysed immediately. If that is not logistically feasible, they should be at least refrigerated or preferably deep-frozen [23]. Changes in analyte concentration may however be significant after more than a few days storage [24]. Acid preservation (i.e. conversion of all ammonia to ammonium) is used to extend the period between sample collection and analysis, however prior to analysis, samples must be neutralised [25].

Additionally, the exposure of reagents and standards to ambient air can potentially lead to contamination; this can be minimised by using a nitrogen glove box to keep and process all solutions [26], or by using acidic treatment [27].

The chemical variability of estuarine and marine systems significantly affects the selection and performance of the analytical method used for ammonia analysis. Most of the analytical methods available for ammonia determine not only ammonia but the combination of both molecular ammonia and ammonium (i.e. total ammonia). However, for consistency, the term ‘ammonium’ is used throughout this chapter to express the total ammonia.

The indophenol blue (IPB) method based on the Berthelot reaction is most commonly used as the reference method for the determination of ammonium in aqueous samples [28-30]. Other analytical methods have been proposed in the past 30 years including the fluorometric method, and methods involving analyte separation and preconcentration techniques, such as the gas-diffusion (GD) method. These analytical methods and their various automated versions have been applied in estuarine and marine waters for the determination of ammonium and are described in detail in the following sections. Automatic methodologies of analysis are flow-

based and have been developed with the aim of meeting the challenges mentioned above, thus providing fast, sensitive, accurate and even portable analytical tools. A brief and general description regarding flow-based methodologies (viz. principle, advantages, and disadvantages) is given in the following section. However, the focus will be on the analytical strategies used, rather than on a comparison between the various methods.

1.3 Flow-based methodologies

The flow analysis concept emerged during the 1950's, with the advent of segmented flow analysis, where the aim was to perform chemical analysis in an automatic fashion. Since then the concept has evolved and several flow-based methodologies have been developed [31].

Figure 1-3 shows schematic diagrams of basic and commonly used flow systems.

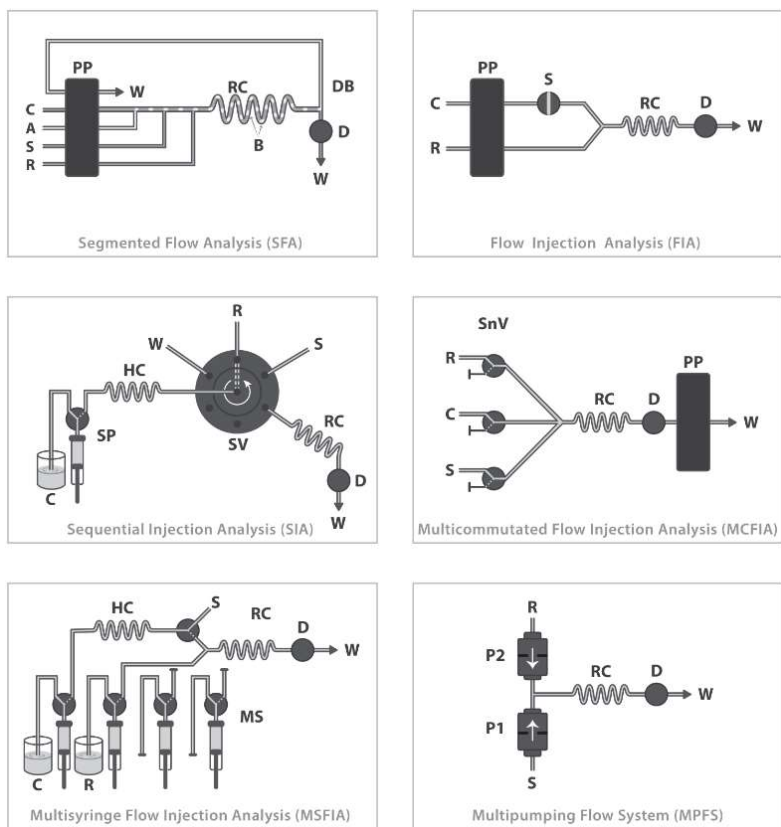


Figure 1-3. Schematic diagrams of commonly used flow systems: Carrier (C); Reagent (R); Air (A); Sample (S); Air bubble (B); Detector (D); Waste (W); Reaction coil (RC); Peristaltic pump (PP); Debubbler (DB); Syringe pump (SP); Holding coil (HC); Selection valve (SV); Solenoid valve (SnV); Multisyringe pump (MS); Solenoid micro-pumps (P1, P2).

The distribution of flow-based techniques that have been applied to the determination of ammonium in estuarine and marine waters is illustrated in Figure 1-4.

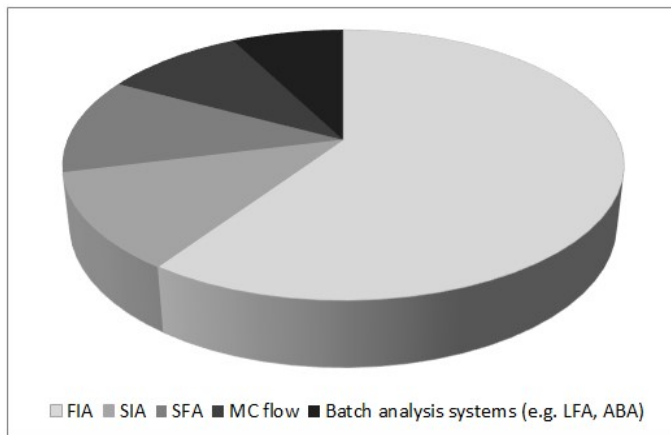


Figure 1-4. Distribution graph of flow-based methodologies developed for the determination of total ammonia in estuarine and marine waters (according to ISI Web of Knowledge, February 2020).

Segmented flow analysis (SFA), was designed to perform measurements similarly to discrete analysis, and consists of a continuous flowing stream segmented by air bubbles (Figure 1-3). Despite the disadvantages of air bubble segmentation (e.g. slow start-up times, higher reagent use and waste production), this technique has been widely adopted to automate oceanographic analytical methods including those for ammonium determination [32]. Unlike SFA, flow injection analysis (FIA) is characterized by a non-segmented flow stream where the sample is inserted in a carrier/reagent stream through an injection valve, in a reproducible fashion and with controlled dispersion (Figure 1-3). Consequently, enhanced sample throughput, simplicity of operation, low cost and greater potential for portability are some of the advantages of this technique, features that are particularly useful in oceanographic studies. Accordingly, more than half of the papers regarding the determination of ammonium in estuarine and marine waters apply FIA as the flow technique (Figure 1-4).

Apart from FIA, there are more recent flow techniques such as sequential injection analysis (SIA) and multicommutated flow techniques (e.g. multicommutated FIA (MCFIA), multi-syringe FIA (MSFIA), multipumping flow systems (MPFS)) that offer additional advantages and also with their own limitations (Figure 1-3). SIA was conceived to sequentially aspirate sample and

reagent plugs through a selection valve toward a holding coil, which are directed to the detector by flow reversal. Versatility, reagent saving, computer control and robustness are the main advantages of this technique.

Multicommutated flow techniques, highlighted by Cerdà and Pons [33], are based on a flow network comprising individual solenoid devices (valves in MCFIA/MSFIA and pumps in MPFS) controlled by computer software. These techniques have similar features as SIA, with the added potential of miniaturization and portability. A few studies have shown the potential of these techniques to assist in the challenge of ammonium monitoring in estuarine and seawater samples (Figure 1-4). Some batch-analysis systems have also been proposed in the context of this application (e.g. loop flow analysis (LFA), autonomous batch analysis (ABA)).

Flow-based methodologies have the advantage of not only performing automated analysis, but also of improving sensitivity, with the possibility of miniaturization and/or portability (e.g. shipboard measurements). Such features are ideal for the nanomolar level ammonium concentrations and analysis can even be performed on-line or immediately after sample collection, thus avoiding sample storage issues (e.g. loss of analyte).

With an emphasis on the strategies adopted to face the challenges described above, the following sections describe the flow techniques that have been developed for the determination of ammonium in estuarine and marine waters (including other saline samples) according to the analytical method applied, namely the IPB method, the GD method (this may need to be updated) and the fluorometric method (the analytical features of each method are described in Tables 1-1 to 1-3 below).

1.3.1 Indophenol blue method

Molecular absorption spectrophotometry is one of the most widely used analytical detection techniques, as it is accessible, versatile, accurate and generally inexpensive. Most colorimetric methods published for ammonia determination in estuarine and marine waters use some variation of the IPB chemistry, based on the reaction between ammonia and hypochlorite to form monochloroamine that then reacts with a phenolic compound to produce the coloured indophenol blue complex, which is measured spectrophotometrically [24]. To increase the reaction kinetics, a catalyst (e.g. nitroprusside) and reaction temperatures of the order of 60

°C are usually applied [24, 34]. Additionally, the reaction occurs at high pH which makes the method prone to interference from the precipitation of Mg²⁺ and Ca²⁺ hydroxides [35, 36]. This, together with the lack of sensitivity, comprises the main drawbacks of this method. Nevertheless, these issues can be overcome by using chelating agents and an absorption cell with a longer optical path, respectively [24, 37]. The analytical features and performance of methods using indophenol blue chemistry are listed in Table 1-1.

Table 1-1. Analytical features of flow-based methodologies using the indophenol blue reaction.

Analytical method	Reagent	Flow method	Optical path length (cm)	LOD (µM)	Concentration range (µM)	Sampling rate (h ⁻¹)	Type of sample	Ref.
Indophenol blue (Spectrophotometry)	Phenol	SFA	3	0.12	Up to 40	90	Seawater	[38]
		FIA	1	< 278	278 - 4444	40	Aquaculture	[39]
		FIA	1	1.4	Up to 107	-	Aquaculture	[40]
		SIA-SPE	3	0.0035	Up to 0.428	3	Seawater	[41]
		LFA	5	0.36	Up to 1.07	24	Spiked seawater	[36]
	SFA	200	0.005	Up to 1	30	Seawater	[42]	
		FIA	250	0.0036	0.02 to 0.5	22	Surface seawater	[43]
	SFA-GD	100	5.5 13	Up to 0.2 Up to 10	10	Oligotrophic seawaters, excretion planktonic copepods	[44]	
	Salicylate	FIA	Not quoted	< 35.7	35.7 - 214	36	Fish farming, seawater	[45]
	1-Naphthol	FIA	1	0.72	Up to 222	26	River, lake and seawater	[46]
		OPP	rFIA	3	0.08	Up to 35	30	Estuarine and coastal
	SIA (iSEA)	3	0.15	Up to 200	12	Underway coastal	[48]	
		SFA	100/200	6/4	Up to 200	< 4	Oligotrophic seawaters	[49]

Tartrate, citrate or ethylene diamine tetraacetic acid (EDTA) are typically used as chelating agents. As an alternative, Jodo et al. [38] proposed the use of 1,2-cyclohexane diamine tetraacetic acid (CyDTA) to mask the interference from magnesium in an SFA method to determine ammonium, nitrite, nitrate and phosphate in seawater. CyDTA proved to be more effective than citrate/tartrate for masking magnesium interference, although no information is given regarding other interferents. A mixture of both citrate and EDTA has also been used

for the same purpose [36, 42], and Li et al. [42] developed a SFA system using a mixture of citrate (54 mM) and EDTA (5.4 mM) which was shown to be enough to prevent the precipitation of divalent metal ions in seawater in a pH range between 11 and 12. Additionally, matching the salinity of the wash solution with that of the sample was required in order to avoid pronounced refractive index differences, which are problematic when analysing samples with different salinities.

FIA systems have been developed using indophenol blue chemistry for the simultaneous monitoring of ammonium and nitrite [39] and phosphate [40] in aquaculture. In the FIA system described by Ariza et al. [39], no complexing agent was used and a tolerance ratio between foreign ion (e.g. Na^+ , K^+ , Hg^{2+} , NO_3^- , CN^- , SCN^-) and ammonium of 100:1 was achieved. No mention was given to the formation of precipitate, which would be expected since the phenol solution was adjusted to pH 12. The FIA system proposed by Tovar et al. [40] used citrate as complexing agent.

Chen et al. [41] used solid-phase extraction (SPE) coupled to a SIA system as a strategy to enhance the sensitivity of the IPB method. Phenol, sodium dichloroisocyanurate (DIC) mixed with citrate, and nitroprusside were sequentially added into a vessel containing exactly 200 mL of sample where the indophenol blue compound was formed. After 10 min this solution was pumped through a commercial Oasis® Hydrophilic-Lipophilic Balance (HLB) cartridge where the indophenol blue compound was extracted, followed by elution with a mixture of ethanol and NaOH and spectrophotometric monitoring. No salt effect was observed, (i.e. no difference was observed between the reference signal in freshwater (low ionic strength) and seawater). Thus, a calibration curve prepared in deionized water could be used to analyse samples with different salinities. An LOD of 3.5 nM was achieved, although the sample throughput was compromised (i.e. 3 samples per hour).

As an alternative to the toxic phenol reagent, salicylate [45], 1-naphthol [46] and *o*-phenylphenol (OPP) [49], 4-methoxyphthalaldehyde (MOPA) [50], and 4,5-dimethoxyphthalaldehyde (M₂OPA) [51], have been used to form an IPB azo dye derivative for the spectrophotometric determination of ammonium. Muraki et al. [45] employed the sodium salicylate-hypochlorite reaction in a simple flow system for application in seawater from fish farms. The authors used potassium sodium tartrate to mask the interference from

Ca^{2+} and Mg^{2+} , however, precipitates were formed at pH 10-11 and consequently the pH of the samples had to be adjusted to 6-7 prior to injection.

A FIA system based on a modified Berthelot reaction was proposed by Shoji and Nakamura [46]. 1-Naphthol was used as an alternative to phenol and DIC instead of sodium hypochlorite. Citrate was used as a complexing reagent and no interference of foreign ions was observed. Good recoveries were obtained for the analysis of ammonium in river, lake and seawater samples.

Ma et al. [52], Lin et al. [47], and Li et al. [48], all reported the development of methods using the OPP-phenate chemistry with DIC in the presence of sodium nitroprusside (sodium nitroferricyanide) catalyst. Trisodium citrate was employed as the complexing agent to prevent precipitation of divalent alkaline metals (Ca^{2+} and Mg^{2+}) at high pH, and each method used a 3-cm optical pathlength detection cell. Ma et al. [52] described the use of a manually operated colorimetric method where the authors undertook a comprehensive study of the reaction kinetics of the OPP-IPB chemistry under different reagent concentrations and temperature conditions, and the potential salinity interference effects were also investigated. Under optimised reaction conditions a limit of detection (LOD) of 200 nM was achieved with a linear calibration range up to 100 μM and no salinity effect observed. Reagents were shown to be stable for a period of up to 10 days and heating was shown to increase the rate of colour development which in turn improved the sample throughput. However, temperature conditions chosen (room temperature 20 – 30 °C) to minimise hydrolysis of organic nitrogen compounds resulted in a low sample throughput of 3 h^{-1} . Reverse FIA (rFIA) involves the injection of reagents into a carrier stream of sample, allowing for reagent consumption to be minimised when sample volumes are not restricted [53], and Lin et al. [47] developed an automated method based on this approach with a sample throughput of approximately 30 h^{-1} , an LOD of 80 nM and a linear range of up to 35 μM in seawater. The salinity effect was investigated, and correction equations were necessary when the method was applied to estuarine and coastal water samples. An integrated syringe-pump-based (*i*SEA) system was developed by Li et al. [48] in the same research laboratory as the previous two studies, utilising an on-line filtration system for underway analysis of coastal environments over the course of 7 cruises and 716 analyses. Sample throughput of 12 h^{-1} , LOD of 150 nM and a linear range of up to 200 μM were described. Ma et al. [52] and Lin et al. [47] validated their methods against

two reference methods including the IPB-method described by the U.S. Environment Protection Authority [29], and the commonly used fluorescence method using OPA and sulphite. Li et al. [48] only used the batch method described by Ma et al. [52] for validation purposes. All comparisons showed good agreement, and a recovery study with spiked samples was performed to show method reliability.

However, spectrophotometric methods may be insufficiently sensitive, particularly when applied to oligotrophic waters containing trace levels of total ammonia. Several techniques are commonly applied to overcome this limitation, including chemical derivatisation to a species with a higher molar absorptivity [54, 55], analyte separation and preconcentration (see 1.3.2 Analyte separation and preconcentration methods), and increasing the optical pathlength of the detection flow cell [56]. According to the Beer-Lambert law, increasing the optical pathlength will result in an increase in the sensitivity of the colorimetric method, and several flow-based analytical methods have capitalised on the incorporation of a long path liquid waveguide capillary cell (LWCC) to enhance sensitivity and decrease LODs [42-44, 49]. LWCCs are typically low volume (125 to 1250 μL) and long optical pathlength (50 to 500 cm) detection cells which are connected to a light source and spectrophotometer via fiber optic cables [56]. Light is confined to the 'liquid' core of the LWCC by total internal reflection at the interface of the low refractive index core/wall, passing through the sample at specific angles. An in-depth review of recent analytical applications and performance of LWCCs is provided by Pascoa et al. [56].

In the SFA system described by Li et al. [42] the incorporation of a LWCC allowed the optical path length to be increased significantly (i.e., to 2 m) and consequently an LOD in the nanomolar range was achieved (i.e., 5 nM). Zhu et al. [43] likewise developed an automated, on-line colorimetric method for trace ammonium analysis in seawater using an FIA system coupled with a 2.5-meter LWCC. Phenol and DIC were used as colorimetric reagents with sodium nitroprusside as catalyst. Citrate or EDTA were used as chelating agents and the method was optimised to obtain high signal to noise ratio and sensitivity by decreasing reagent injection volumes, allowing for an LOD of 3.6 nM to be achieved. The authors report linearity from 20 to 500 nM, with the possibility of achieving a wider linear range (at the expense of sensitivity) by adjusting the detection wavelength and reaction temperature. An overall sample throughput of 22 h^{-1} was achieved, and the method was applied for 24-h on-line monitoring of

ammonium in the surface seawater of Wuyuan Bay and South China Sea. The method was compared to its batch-analysis counterpart (using IPB-chemistry) and a good agreement was shown between both methods.

Kodama et al. [44] employed two strategies to increase method sensitivity, namely GD-based analyte separation and preconcentration coupled with a 1.0-meter LWCC in a gas-segmented flow analysis colorimeter using IPB chemistry and sodium hypochlorite in place of DIC. The minimum LOD reported was 5.5 ± 1.8 nM at a wavelength of 630 nm, with linearity up to 0.2 μ M. Similarly to what was reported by Zhu et al. [43], Kodama et al. [44] were also able to extend the working range by measuring the absorbance at a lower wavelength (530 nm) allowing for concentrations up to 10 μ M to be determined. The LOD at 530 nm was 13 ± 5.3 nM and a sample throughput of 10 h⁻¹ was reported. The method was used to determine the vertical distribution of ammonium concentrations in the vicinity of the Kuroshio current oligotrophic waters off the coast of Japan, in addition to estimating the ammonium excretion rates from planktonic copepods.

Hashihama et al. [49] used OPP as an alternative to phenol for the determination of nanomolar concentrations of ammonium in seawater with a long pathlength LWCC (100 cm and 200 cm) and an UltraPath (200 cm), with internal diameters of 0.55 mm and 2 mm, respectively. The larger internal core of the UltraPath minimised baseline drift due to cell clogging, and the LODs determined for the 100 cm and 200 cm LWCCs, and the 200 cm UltraPath were 6, 4, and 4 nM, respectively, with a linear range up to 200 nM and an approximate sampling rate of ≤ 4 h⁻¹. The system was applied to underway surface monitoring and vertical profiling was undertaken in the South Pacific oligotrophic waters.

While the incorporation of LWCCs has the clear advantage of increasing method sensitivity and LODs, they present challenges to their successful use, specifically the necessity to perform some type of sample filtration to remove suspended particulates, complications associated with the formation and expulsion of bubbles which are more likely to form in longer pathlength optical cells, longer sample residence time in the cell which will invariably affect the rate of analysis, and difficulties associated with removal and cleaning of solid particulates from the internal cell, and biofilm formation during extended periods of use [56].

1.3.2 Analyte separation and preconcentration methods

The introduction of a gas-diffusion (GD) unit to the flow system offers another means for improving selectivity by separating the analyte from interferences and thus minimizing matrix effects. The sample is merged with sodium hydroxide in the donor channel of the GD device, thus converting ammonium ions into ammonia. Ammonia thus produced diffuses through the gas-permeable membrane (e.g. PTFE plumbing tape, Durapore® hydrophobic membrane [57]) present in the GD device into the acceptor channel which contains an acceptor solution. The diffused ammonia in the acceptor stream is detected using either the indophenol blue reaction, a pH sensitive indicator in the acceptor stream, or by measurement of the resultant pH or ionic strength change of the acceptor solution [57]. This can be achieved using spectrophotometric detection if the acceptor stream contains an acid-base indicator [35, 58-60], potentiometric pH [61] or conductimetric [62-64] measurements. This approach has allowed the determination of ammonium in samples with wide ranging salinities (Table 1-2).

Table 1-2. Analytical features of flow-based methodologies using analyte separation and/or preconcentration.

Analytical method	Acceptor stream	Flow method	LOD (μM)	Concentration range (μM)	Sampling rate (h^{-1})	Type of sample	Ref.
Analyte separation and preconcentration	BTB	GD-FIA	1	Up to 100	100	Canal water	[58]
		GD-FIA	0.2	1 - 50	30	Seawater	[61]
		GD-rFIA	0.21 ^a /0.64	Up to 11.4 ^a /214	60 ^a /135	Estuarine water	[59]
	Phenol red	GD-SIA	1.5 ^b /3	Up to 55.6 ^b /222	20 ^b /28	Estuarine, coastal and well water	[60]
		GD-MCFIA	1	2.8 – 55.6	20	Estuarine and seawater	[35]
		H-SDME	1.8	Up to 25	17	Seawater	[65]
	HCl	GD-FIA	0.05	Up to 10	60	Ammonia excretion, ocean mapping	[66]
		GD-MPFS	< 0.2	Up to 252	< 9	Estuarine, coastal and shelf water*	[62]
		GD-MSFIA	2.5	4.2 – 20,000	32	Coastal water	[63]
		GD-MPFS	0.27	0.5 - 25	17	Coastal seawater	[64]
	MSA	GD-FIA-IC	0.02-0.04	Up to 2	Very low	Estuarine, sea, aquaria and pore waters	[67]
		GD-FIA-IC	0.03	Up to 1	Very low	Seawater	[68]
	OPA-Sulphite	P&T-FIA	0.0074	0.01 – 0.2	< 4	Seawater	[69]

* Field application

A further advantage of this approach is that it obviates any Schlieren effects (i.e. the refractive index effect that is observed in conventional flow analysis systems when samples of different concentrations or salinities are injected into a carrier with a different refractive index) because the process of analyte detection occurs after ammonia diffusion into the acceptor stream has occurred. Moreover, different parameters can be optimized in order to enhance sensitivity, namely the GD configuration and surface area [70] as well as the flow pattern [71]. Fluorometric detection after GD separation has also been used (see Section 3.3 Fluorometric method).

Even though the gas-permeable membrane used in GD-based flow methods separates the donor stream from the acceptor stream, the formation of insoluble Mg^{2+} and Ca^{2+} hydroxides as a consequence of the addition of base to the seawater sample can block the membrane pores and the system manifold, thus compromising precision, sensitivity and sample throughput [61]. The formation of hydroxide precipitates, however, can be reduced by adding a chelating agent such as citrate or EDTA to the sodium hydroxide stream. Even using this strategy, Willason and Johnson [66] noticed gradual clogging of the membrane over time. Flushing the FIA system with 1% HCl every 5 h was shown to remedy this problem allowing the membrane to last for at least 24 h of continuous sampling. Good sensitivity was achieved due to the large diffusion area attained with an “S” shaped GD unit with a swept length of at least 240 mm.

Aiming to reduce the reagent consumption and waste generation, Gray et al. [59] proposed a reversed FIA (rFIA) system where the reagent (sodium hydroxide) was injected into a sample stream instead of injecting sample into a reagent stream. A multiple injection sequence of NaOH/sample/NaOH produced good sensitivity. To minimize interference from dissolved carbon dioxide, the sample stream was buffered at pH 8.4. Under these conditions, ammonium could be detected even in the presence of a wide range of alkalinity (29-131 $mg\ CaCO_3\ L^{-1}$) and salinity (0.02-36). This approach also avoided the addition of complexing agents because the amount of $Ca(OH)_2$ or $Mg(OH)_2$ precipitate formed was small and was flushed out of the system by the continuously flowing stream of sample.

Segundo et al. [60] developed an SIA system where two dynamic ranges could be obtained according to the number of sample plugs aspirated. Thus, a concentration range between 5.56 and 55.6 μM was attained with the sequence NaOH/sample/NaOH, and the range 55.6-222

μM was achieved with the sequence NaOH/sample/NaOH/sample/NaOH. The system was successfully applied to samples with a wide range of salinities (i.e. estuarine, well and coastal water samples). Moreover, they used a reagent recirculation approach in order to minimize reagent consumption. The buffer capacity of the indicator was restored daily to keep sensitivity constant. This approach was proposed and used by Oliveira et al. [35] who developed a MCFIA with in-line prevention of metal hydroxide precipitation. EDTA, tartrate and EDTA in combination with boric acid successfully prevented the precipitation of metal hydroxides in saline waters, although tartrate was chosen because it was considered more environmentally friendly. Accurate results were obtained in a wide range of salinities (9.6-34.8). An *in situ* analyser for monitoring of ammonium in estuarine and coastal shelf waters based on an MPFS was designed by Plant et al. [62] and is described in Section 4 (field applications).

FIA-GD systems using ion chromatography (IC) post gas-diffusion for separation for the determination of ammonium and methylamines have also been proposed [67, 68]. The sample was pumped and mixed with a solution containing NaOH and EDTA in the donor channel to raise the pH above 12 with no precipitation of metal oxides, followed by diffusion of all the volatile gaseous forms (e.g. ammonia, amines) into an acidic acceptor stream, such as HCl [67] or methane sulphonic acid (MSA) [68], and then a subsample was injected into the IC. The ability to chromatographically resolve both ammonium and methylamines is an advantage, but because of the chromatographic separation step, the sample throughput is very low and the system is much more complex in comparison with other flow methods. Moreover, a declining response ratio was noticed with increasing salinity [67].

In 2013 Henríquez et al. [63] reported a multi-syringe FIA system applying GD as the separation technique with conductometric detection. The method had a sample throughput of 32 h^{-1} , and a wide working range $4.2 \mu\text{M} - 20 \text{ mM}$ with an LOD of $2.5 \mu\text{M}$. Another flow-based method was proposed in 2014 by the same authors [64] this time using a multi-pumping flow system with a series of solenoid micropumps for propulsion. This method offered a greater precision than the previous method ($< 1\%$) with an order of magnitude lower LOD of $0.27 \mu\text{M}$, largely due to the use of a sample volume 3.3 times higher. The linear range was $0.5 - 25 \mu\text{M}$ and a sample throughput of 17 h^{-1} was achieved.

Several methods have recently been reported involving the use of a variety of matrix separation and preconcentration techniques: steam distillation, purge-and-trap (P&T), and headspace single-drop microextraction (H-SDME). These techniques are used as sample pre-treatment steps and are described below. While the LODs reported are mostly higher when compared to the earlier GD-based separation methods, their advantage is that they don't suffer from membrane longevity issues or blocking by the precipitation of divalent cations present in the sample, and therefore the use of complexing agents is not necessary.

P&T has commonly been applied as a separation technique for volatile organic compounds in wastewater and other complex matrices. It has been successfully applied to ammonia separation and preconcentration in seawater, and the process involves bubbling an inert gas through a sample of seawater that has been made basic by the addition of sodium hydroxide to convert total ammonia to molecular ammonia. Dissolved ammonia then moves from the aqueous to the vapour phase and is collected by a trap [72]. Compared to the GD separation method, P&T can process very large sample volumes increasing the enrichment factor and in turn facilitating improved method sensitivity. Ferreira et al. [73] developed a steam distillation separation technique coupled with an IC detection method which was capable of resolving monomethyl- and monoethylamine from total ammonia without interference from sodium and potassium ions. The LOD for this method was 1.7 μM with a linear range of 13.9 – 55.6 μM , a sample throughput of less than 4 h^{-1} , and the method was successfully applied to high salinity samples from the Brazilian oil industry with spiked recoveries in the order of 90 – 105%. Ferreira et al. [74] further described a P&T extraction system using ultrasonication to accelerate the extraction process, again using IC as the detection method. The sample throughput described by Ferreira et al. was, however, very low (i.e., < 2 h^{-1}). The LOD was 1.1 μM with a linear range of 13.9 – 111.1 μM and an optimum extraction time of 30 minutes per sample was chosen. Zhu et al. [69] proposed a more sensitive method by coupling a home-made P&T system with fluorescence spectrometry using the OPA-sulphite chemistry which is described in Section 1.3.3 Fluorometric method.

Šrámková et al. [65] developed a novel system for the separation and preconcentration of ammonia using in-syringe analysis and H-SDME with colorimetric detection. Drop formation was accurately controlled by a syringe pump. The drop reagent was pumped through a channel drilled into the syringe piston, and the drop was formed at the end that channel. The syringe

barrel was filled with the sample, which was made basic while stirring a magnetic stirring bar, allowing for total ammonia to be converted to molecular ammonia. Ammonia then evaporated into the syringe headspace reacting with the droplet containing an acid-base indicator, and on-drop spectrophotometric analysis was performed. An LOD of 1.8 μM was reported with method linearity of up to 25 μM . Washing the syringe between each sample took a considerable amount of time and a sample throughput of 17 h^{-1} was reported.

1.3.3 Fluorometric method

The fluorometric method involves the reaction of ammonium with orthophthaldialdehyde (OPA) in alkaline medium and in the presence of a strong reducing agent (e.g. 2-mercaptoethanol or sodium sulphite) [55]. An intensely fluorescent product is formed which allows the fluorometric assay to reach the nanomolar range [26]. However, the method can be used to measure either ammonium or amino acids [75]. Therefore, if ammonium determination is the main goal, some strategies must be adopted to avoid the interference by primary amines thus improving the selectivity of the method (described further in this section). Table 1-3 summarizes the analytical features of flow-based methods using the fluorometric method.

Table 1-3. Analytical features of flow-based methodologies using fluorometric detection.

Analytical method	Reagents	Flow method	LOD (nM)	Concentration range (μM)	Sampling rate (h^{-1})	Type of sample	Ref.
Fluorimetry	OPA-2-Mercaptoethanol	FIA-GD	~ 1	> 2	30	Fresh and seawater	[55]
	OPA-sulphite	FIA-GD	~ 1	Not quoted	18	Seawater*	[76]
		SFA	1.5/7 ^a	Up to 0.16/12 ^a	20/40	Estuarine and seawaters	[54]
		FIA-GD	7	Up to 4	30	Seawater*	[26]
		FIA	30	Up to 50	9 ^b /40	Coastal, estuarine and fresh waters	[77]
		FIA	1.1	Up to 0.6	8/3600 ^c	Seawater*	[27]
		FIA	< 5	Up to 25	12	Seawater*	[78]
		SIA	1000	Up to 20	120	River and marine waters*	[79]
		SIA	60	Up to 20	> 100	River and marine waters*	[80]
		MPFS	13/210	Up to 1/16	32	Surface seawater	[81]
		ABA	1/4.6/58	Up to 1/4/25	8	Coastal seawater*	[82]
		ABA	10	0.05 – 10	4	Marine waters*	[83]
		Flow-batch	< 1.2	Up to 0.3	5	Open ocean water*	[84]
	FIA	2.1	Up to 0.3	36	Estuarine and seawater*	[85]	

^a On-line dilution; ^b Stop-flow mode; ^c rFIA mode. * Field application

Jones [55] developed an FIA-GD system using fluorescence detection with OPA with 2-mercaptoethanol as the reducing agent. The GD step reduced interferences from primary amines and dissolved amino acids, but nevertheless was subject to likely interference from volatile amines. A similar version of a fluorescent-based FIA-GD system was used by Masserini and Fanning [76] in a sensor package for the simultaneous determination of nitrite, nitrate and ammonium in seawater.

Use of sodium sulphite as the reductant instead of 2-mercaptoethanol, reduces the sensitivity to amino acids, thus making the method more specific to ammonium [86]. Watson et al. [26] developed an FIA-GD system for seagoing applications that aimed to combine the advantages of Jones's GD method [55] with the OPA-sulphite approach. A GD cell, placed between the NaOH reservoir and the peristaltic pump, was used to remove ammonia contamination from the NaOH reagent (using 10% H₂SO₄ as a trap). Consequently, lower blank concentrations were obtained, thus improving the LOD. A comparison between 35 g L⁻¹ NaCl standards and standards made in seawater showed similar results in the absence of chelating agents. Since the reaction of ammonium with OPA and sulphite is more selective to ammonium than to primary amines, the GD unit becomes unnecessary, as shown by K  rouel and Aminot [54]. They developed an SFA system for the direct analysis of ammonium in estuarine and seawaters, which was not only free from primary amine interferences (including volatile amines) but also from a salt effect (less than 3.1% deviation in the salinity range of 0.2 to 35). Three ammonium concentration ranges were attained: nanomolar range (up to 100 nM), micromolar range (up to 12 µM) and submillimolar range (up to 250 µM), the last one was attained by adding on-line dilution to the SFA system. This method was adapted to FIA by Aminot et al. [77], for a potential *in situ* application. No salt effect was noticed in the salinity range of 5-35. No other interferences were observed, except for sulfide (deviation of -9% at 100 µM S²⁻). Using the same chemistry, Horstkotte et al. [81] designed a portable multipumping flow analyser system for possible shipboard monitoring. The method sensitivity was adjustable by the gain of the photomultiplier tube, thus allowing for applications across a wide range of concentrations (up to 16 µM). A detection cell was specially made and combined with a commercial photomultiplier tube, a long-pass optical filter and a UV-LED as the excitation light source.

When using the fluorometric method for the determination of ammonium in aquatic matrices, background fluorescence is frequently reported. This fluorescence results from substances in

the sample that autofluoresce, thus this effect can be corrected by measuring the sample fluorescence in the absence of OPA. A GD unit could also be used to avoid this issue, nevertheless a salt effect might be noticeable due to change in the ammonia solubility [55].

The fluorometric method involving the reaction of ammonium with OPA in the presence of sulphite reducing agent is attractive largely due to its high sensitivity and selectivity, allowing for nanomolar concentrations of ammonia nitrogen to be determined in complex high-salinity matrices. While the stability of reagent solutions has been identified as a disadvantage of the method, the addition of stabilising reagents such as formaldehyde to prevent oxidation of sulphite have shown promise in extending the lifetime of reagents and applicability to *in situ* shipboard analysis.

Hu et al. [75] developed a manual operation method using OPA, sulphite and formaldehyde reagents with EDTA-NaOH used to make the sample medium alkaline. EDTA was used to prevent precipitation of divalent alkaline earth metals from solution at high pH, which could interfere and depress the fluorescence signal. At high pH the amount of reaction product was increased thus enhancing the method sensitivity to nanomolar levels without enrichment. The working range of the method could be tailored to the desired range by changing the excitation/emission slit used, and an LOD of 9.9 nM was reported and linearity in the range of 32 – 500 nM was achieved when using an excitation/emission slit of 3 nm/5 nm, respectively. While the sampling rate reported was low (1.2 h^{-1}), the authors stated that it was possible to perform up to 10 samples simultaneously. Nevertheless, given many automated techniques using fluorescence have been described in the literature, manual methods seem only to provide interesting insights to reaction kinetics of novel reagent and chemical combinations.

Zhu et al. [85] used the same chemistry as described by Hu et al. [75] with the only difference being the choice of chelating agent (sodium tetraborate buffer instead of EDTA). Zhu et al. described the development of a portable home-made fluorescence detector comprising a UV-LED, two band pass filters, a photomultiplier tube (PMT), a modified flow-cell to reduce the interference of air bubbles in the fluorescence signal, and an electronic circuit with a constant voltage and current supply. The detector described was smaller than its commercially available PMT-FL counterpart with an increase in sensitivity greater than 11%. The detector was incorporated into an FIA system using OPA, sulphite and formaldehyde as reagents and the system was used for underway sampling in the Jiulongjiang estuary.

While the OPA-sulphite reaction is the most widely reported fluorescence method for ammonium determination in natural waters, functionalisation of OPA with the electron-donating methoxy groups to form 4-methoxyphthalaldehyde (MOPA) and 4,5-dimethoxyphthalaldehyde (M₂OPA) has been recently described showing promise to increase method sensitivity as the reaction products exhibit higher fluorescence intensity when compared to the ammonium-OPA product [50, 51]. MOPA was successfully synthesised by Liang et al. [50] and used in a manual batch method using sulphite, formaldehyde and sodium tetraborate buffer. The MOPA rapidly reacted with ammonium at room temperature and a 15-minute reaction time was selected as a compromise between sample throughput and sensitivity. An LOD of 5.8 nM was reported for the linear calibration range of 25 – 300 nM. The synthesis and use of M₂OPA in a custom-made hand-held portable fluorometer with a laser diode as the light source was reported by Zhang et al. [51] allowing for *in situ* analysis. M₂OPA was reported to have a rapid reaction time and enhanced fluorescence intensity when compared to the OPA and MOPA reaction products, and the hand-held portable laser diode fluorometer was reportedly used in single- or dual-laser beam modes, allowing for different working ranges to be achieved (0 – 5 µM and 0 – 2 µM, respectively) with different LODs (6.5 nM and 3.5 nM, respectively). While the newly developed device was suitable for field use, it was nevertheless still used in 'batch mode' where a sampling rate of 1 h⁻¹ was described.

The major limitation of the fluorescence methods described above, is the slow reaction kinetics, which can be improved by increasing reaction temperature. However, the need for an energy intensive heating device incorporated into the manifold, limits the use and application of fluorescence methods in long-term monitoring and field based applications. Nevertheless, a few shipboard FIA [26, 27, 76, 78], SIA [79, 80] and autonomous batch analysers (ABA) [82, 83] systems have been described for field applications using the fluorometric reaction NH₄⁺-OPA with sulphite reduction, and these are described in the following section.

1.3.4 Field applications

In situ monitoring has the potential to reduce or even avoid all the problems commonly encountered during manual collection, storage and preservation of samples of estuarine or marine waters. In the last decade there has been substantial progress in the development of

portable and miniaturised flow analysis devices which has allowed for shipboard laboratories to conduct real-time monitoring and mapping of nutrient distributions [27, 76, 79].

The fluorometric method with the OPA-sulphite reaction has been employed as the preferred method for *in situ* field analysis of ammonium, with one exception where the GD method with conductimetric detection was used [62]. This particular *in situ* flow analyser (called NH₄⁺-Digiscan) used micro-solenoid pumps to promote the flow. For *in situ* application all the electronic components were placed in housings and reagents in bags. The system was shown to be suitable for fixed location monitoring of ammonium in estuarine and coastal shelf environments at depths of up to 3 m. It was capable of performing *in situ* auto-calibration and exhibited stability when deployed for 30 days, without the loss of drift or analytical signal. An adequate LOD was achieved (Table 1-2), although the rate of analysis was relatively low (< 9 h⁻¹) when compared with other flow systems.

Several FIA systems have been developed and used in shipboard laboratories [26, 27, 76, 78]. Masserini and Fanning [76] developed a sensor package capable of simultaneous fluorometric detection of nitrite, nitrate and ammonium in oligotrophic seawater. Jones's technique [55] was used to determine ammonium, although slightly modified in order to adapt it to the nutrient sensor package. Discrete sections of tubing were carried through a heat exchanger as opposed to heating the entire manifold, and a larger flow-cell was used in the fluorescence detector (i.e. 40 µL instead of 12 µL) allowing for an LOD of approximately 1 nM to be achieved with a throughput of 18 samples per hour. Watson et al. [26] combined the OPA-sulphite chemistry with GD for the determination of ammonium. Samples were collected manually and immediately analysed or stored frozen. To avoid atmospheric contamination, a 150 L glove box flushed with N₂ was used for storing reagents and handling samples. Removal of ammonia contamination from reagents required the use of an in-line diffusion cell placed between the reagent reservoir and the peristaltic pump, using H₂SO₄ to remove the ammonia from the reagent stream.

Amornthammarong et al. [27] proposed an FIA analyser for the measurement of wastewater discharges into Florida coastal waters, incorporating a modified OPA-sulphite reaction, in which sodium sulphite was dissolved in 5 mM formaldehyde solution. They suggested that the precipitates did not form at high pH due to the high concentration of sulphite, dilution of seawater by reagents, and kinetic hindrance. A sample throughput of 8 h⁻¹ was achieved when

manual injection was performed, but for high-resolution analysis, rFIA was used, which increased the sample throughput to an incredible 1 s^{-1} (i.e. 3600 h^{-1}). Such high frequency measurements allowed for the modelling of an ammonium outfall plume and its dispersion by ocean currents. Rapid changes in ammonium concentrations were detected in only 2 h, clearly demonstrating the importance of high-frequency analysis.

The ammonium flow analyser described by Abi Kaed Bey et al. [78] was designed to determine ammonium in oligotrophic seawater. The instrument was designed “in-house” and allowed for the automated switching between reagent, sample and standard streams, which were sequentially pumped into the analyser mixing chamber. The mixed solution was then pumped to the heater and the detection unit, which included the following: a quartz flow-cell; a low-power UV-LED excitation source; a photon multiplier tube as the emission detector; and, two optical filters. The system described suffered from up to 85% reductions in signal at low concentration (5 nM) due to salinity variations, and the potential fluorescence interference from phytoplankton was found to be up to 12% by artificial simulation of a bloom. Interference from commonly encountered amines and amino acids at low concentrations were negligible, however at high concentrations the signal was depressed. The analyser was used for field analysis in the North Atlantic Ocean, and seawater was pumped from 5 m below to the bow of the ship towards the analyser.

Frank et al. [79, 80] developed an SIA system for the determination of both phosphate and ammonium as part of a “ferrybox” system that operated autonomously and continuously at sea in commercial ferry vessels. The “ferrybox” consisted of an automated sampling system. Samples were thus collected automatically and on-line, through a system comprising a centrifugal pump constantly directing sample from the hull of the ship to the “ferrybox”, which is connected with the SIA instrument. The flow rate of the sample was maintained high enough to ensure sample freshness, with the excess sample being diverted to waste. The sample stream was pumped via a peristaltic pump to the SIA system, where further samples were drawn from the continuously supplied filtrate stream. Off-line samples were simultaneously taken and analysed by an SFA system in order to validate the on-line system. However, the correlation between the ammonium results of the two methods was described as only “acceptable” [79]. This was due to the on-line results being contaminated by the destruction of plankton cells in the secondary centrifugal pump of the “ferrybox”, resulting in the release

of cell contents into the on-line sample stream. The off-line results were also affected by contamination, inappropriate sample storage and detector noise. Additional data analysis was outlined in a further paper, in order to verify the performance of the system [80].

More recently, Amornthammarong et al. proposed the design and use of a portable ABA for the determination of trace amounts of ammonium in coastal seawater [82, 83]. The ABA described utilizes a carefully designed mixing chamber, comprising one syringe pump (where the syringe acts as the primary mixing chamber), an eight-way distribution valve and a 5 mL pipette tip (which acts as the secondary mixing chamber). The standards and sample were mixed with the reagent in the syringe chamber, and the mixture was then pumped into the top of the pipette and drawn back into the syringe chamber from the pipette tip. Complete mixing occurred after 5 mixing cycles and the solution was then injected to the fluorescence detector. The syringe chamber, pipette tip and detector were flushed with deionized water three times prior to every subsequent measurement, which resulted in a sample frequency of approximately 8 h^{-1} .

In an improved version of the ABA, the commercial fluorescence detector [82] was replaced by an LED photodiode-based fluorescence detector, which was more sensitive and allowed for the assembly of a smaller apparatus [83]. This ABA system was also equipped with a filtering system allowing for measurements to be conducted in turbid waters. It was deployed at two field sites for measurement of ammonium concentrations in the intracoastal waterways of Florida, and diurnal ammonium concentration cycles were recorded. The advantages of such batch analysers include their low reagent consumption and ability to construct a calibration curve by auto-dilution from a single standard solution. However, one of the major drawbacks of batch analysers is their lower sampling frequency, due to the need for thorough washing of the mixing chamber to prevent sample cross contamination.

For the determination of ultra-trace ($< 1 \text{ nM}$) ammonium in seawater, Zhu et al. [84] used a flow-batch system accommodating a HLB cartridge to perform SPE. The OPA method as described by Amornthammarong et al. [83] was used, and the fluorescence reaction product was extracted onto the SPE cartridge, separating the analyte complex from the seawater matrix. The fluorescent products were eluted with ethanol and delivered to the fluorescence detector, and each cartridge could be used for over 50 seawater sample analyses. The benefits of employing SPE with the fluorescence method as described include improved sensitivity,

reduced reagent consumption and negligible salinity and matrix effects. This method was applied in the field in the South China Sea during a cruise in August 2012, and vertical ammonium profiles were determined as well as the distribution of ammonium in surface seawater.

The stability of reagents might not be an issue when working under laboratory conditions, however for analysis in the field, (e.g. in shipboard laboratories), it should be taken into consideration as it could be a limitation. Table 1-4 presents the stability of the main reagents involved in each of the methods described.

Table 1-4. Stability and storage of reagents involved in the determination of ammonium.

Method	Reagents	Stability and storage	Ref.
Indophenol blue Spectrophotometry	Phenol	Prepared fresh daily	[29]
	Salicylate	Prepared fresh daily	[45]
	1-Naphthol	Not listed	[46]
	Sodium nitroprusside 0.5%	Store in an amber bottle for up to 1 month	[87]
Gas-diffusion	Sodium hypochlorite	Unstable, prolonged storage should be avoided	[87]
	Bromothymol Blue*	Stored in gas-tight containers with CO ₂ traps	[35]
	Phenol red*	Stored in a bottle with an Ascarite guard to avoid CO ₂ uptake	[60]
	Methane sulfonic acid 40 mM†	Prepared routinely via a stock solution	[77]
Fluorimetry	2-Mercaptoethanol	Stable for at least 72 h	[78]
	Sodium sulphite 8 g L ⁻¹	Stable for at least 2 months at room temp. in a glass bottle	[81]
	Sulphite in phosphate buffer	Prepared daily	[80]
	OPA 10 mM (no buffer)	Stored refrigerated for 1 week	[80]
	OPA 40 g L ⁻¹ (no buffer)	Stored refrigerated in a glass bottle for at least 2 months	[81]
	OPA 0.37 M + sulphite (buffered)	Stored for several weeks in the dark at room temp.	[26]
	Mixed Reagent (OPA, sulphite, buffer, wetting agent)	Stored in the dark at room temp. for at least 2 months	[81]
	MOPA 7.8 g L ⁻¹ in MeOH and water + sulphite + formaldehyde	Prepared fresh daily	[50]
	M ₂ OPA 1.8 g L ⁻¹ in MeOH and water + sulphite + formaldehyde	Prepared fresh daily	[51]

* Spectrophotometric detection, † Ion chromatography

Flow-methodologies have the capability to provide high frequency data and pollutant concentration profiles, which is important when monitoring ammonium concentrations in highly variable estuarine and marine environments, with the added benefit of sample collection and pre-treatment steps being automated. However, many flow methods require the use of specialised and sometimes expensive or custom-made equipment and are often not

commercially available off-the-shelf instruments. Therefore, deploying flow systems over large spatiotemporal scales relevant for extensive water quality monitoring may be prohibitively laborious and expensive, especially as most equipment requires an energy source to control mechanical parts. Passive sampling could be used as an alternative *in situ* monitoring strategy, as it provides the average concentration of the target chemical species for the period that the sampler was deployed without the need for power, moving parts or complicated electronics. In comparison with flow-based methodologies, passive sampling is a cheaper and simpler water quality monitoring technique, which can be advantageous in allowing for sampling programs to be developed over large spatial and temporal scales. An overview of the passive sampling techniques reported in the literature for the monitoring of aquatic environments with high or variable salinity is provided in the following section.

1.4 Passive sampling

Most water quality monitoring programs involve the collection of periodic discrete grab or spot samples. Spot samples should be collected in a way that ensures they are representative of the medium being sampled, and when undertaking trace analysis, it may be necessary for very large volumes of sample to be collected [88, 89]. After collection, spot samples are transported to a laboratory for analysis, during which time they often need to be preserved [24]. The analytical procedure may involve some type of sample pre-treatment, including sample filtration, analyte preconcentration and separation from the matrix and/or derivatisation prior to analysis [24]. These sample handling steps are commonly laborious and expensive. Moreover, it is possible that during sample collection, transport or during any manual handling, contamination may occur leading to inaccurate results [24]. Additionally, periodic spot sampling only provides a snapshot of the levels of pollutants in the sampled medium at the time of collection, and episodic pollution events may be missed leading to an under representation of pollution concentrations in the environment (Figure 1-5) [89, 90]. Even though flow-based methodologies can be used to automate the overall analytical process, such systems are rarely used in commercial laboratories or in routine field monitoring applications, largely owing to the significant upfront costs of purchasing a system, the complexity and high degree of operator skill required for successful operation and maintenance, and high energy

consumption which may prohibit long-term deployment of the equipment in the field. Automatic water sampling units (autosamplers) are commonly used in routine water quality monitoring programs and can be programmed to collect composite or discrete samples over time, which can then be analysed in a laboratory [91]. While an autosampler allows for high-frequency spot sampling which increases the likelihood of pollution event detection, autosamplers have the disadvantage of being expensive, having significant energy requirements for long-term deployment, still suffer from the need for significant sample handling and manipulation, and can be difficult to deploy in coastal settings where sampling often requires the use of a boat (Figure 1-5).

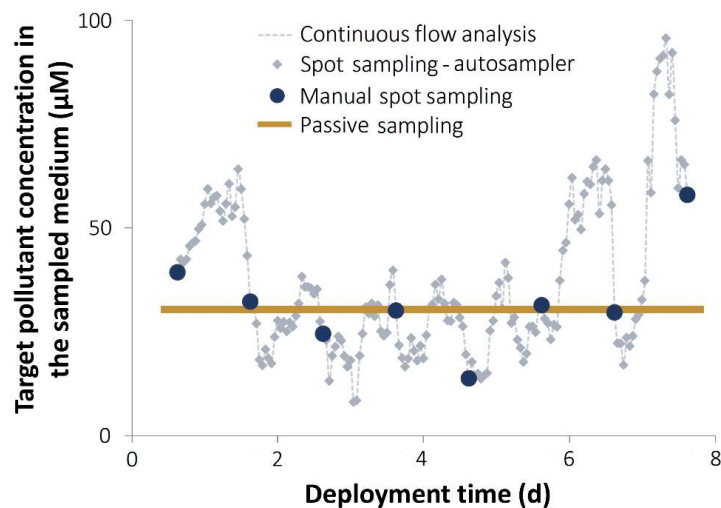


Figure 1-5. Results obtained by different sampling methods commonly used in environmental monitoring (data discussed in detail in Section 4.3.2 of Chapter 4).

Significant progress has been made over the past few decades in the field of aquatic passive sampling techniques, which essentially overcomes several challenges of spot sampling-based monitoring programs and the difficulties associated with the deployment of flow-based systems for *in situ* analysis, especially with respect to associated costs, both in terms of energy requirements and labour [91].

Passive sampling techniques have gained popularity over the last three decades and considerable work has been undertaken to improve and standardise passive sampling

methodologies in order to enable their incorporation into regulatory water quality monitoring programs globally [92-97].

The ideal passive sampling device (PSD) should be inexpensive, commercially available, and simple to assemble, prepare, deploy, retrieve and analyse, while being precise, accurate, sensitive and selective towards the analyte(s) of interest [88, 92]. Aquatic passive sampling has been defined as any sampling technique involving the free flow and accumulation of analyte molecules from the sampled medium (sampling source solution) to the PSDs collecting medium (receiving phase), with mass transfer driven by a difference in the chemical potential of the analyte molecules between the sample and collecting mediums [98].

A PSD generally consists of a receiving phase which is separated from the external environment being sampled by a semi-permeable membrane and/or a diffusion-limiting barrier. The uptake and accumulation of the target analyte(s) from the bulk matrix being sampled into the receiving phase occurs via processes of diffusion, permeation or chemically facilitated transport of the analyte through the membrane/barrier to the receiving phase, although in some applications (e.g., single-phase passive samplers) the membrane itself can act as the primary accumulation site for the analyte [99].

The process of passive sampling usually involves deployment of a PSD into the aquatic environment being monitored and subsequent collection of the sampler after a given period of time, after which the receiving phase can either be directly analysed or the analyte can be chemically stripped and processed.

PSDs are commonly categorised by their sampling regime with two types of samplers described in the literature, including the equilibrium-based and the integrative or kinetic passive samplers. Equilibrium passive sampling involves exposing the PSD to the aquatic environment to be sampled for a sufficient amount of time to reach a thermodynamic equilibrium, allowing for a stable concentration of analyte(s) between the sampled medium and the PSDs receiving phase to be achieved [89, 100, 101]. Mayer et al. provided an in-depth review of the principles and operation of equilibrium-based PSDs, highlighting three basic requirements for their successful operation, including ensuring that the capacity of the sampler is not overcome, avoiding saturation during analyte uptake, and making sure that the device response time is shorter than any fluctuations in analyte concentrations experienced in the environment being

sampled [100]. When using equilibrium-based PSDs the concentration of analyte(s) measured in the receiving phase will be similar to that measured using spot sampling, however there are advantages to using this sampling approach over conventional sampling methods, especially when measuring the partitioning and fugacity of analyte(s) in multicompartiment systems such as sediments, pore waters and/or their overlying waters [100].

While some PSDs can be used in both equilibrium and integrative accumulation regimes (depending on the analyte class and sampler type), many of the samplers discussed below are used exclusively in the integrative (linear) uptake mode. Integrative or kinetic passive samplers work on the assumption that the rate of mass transfer of analyte from the bulk sample to the receiving phase is linearly proportional to the difference between the activity of the analyte in the water and receiving phase [89]. An integrative PSD should exhibit 'zero sink' behaviour, where analyte species are effectively accumulated, and trapped species are retained even if their concentration around the sampler decreases to zero [98]. However, whilst some PSDs exhibit this behaviour, it is not always the case, and modelling approaches and corrections have been developed to describe mass accumulation in the PSD and to offset deviations from ideal behaviour [101].

During deployment, the analyte(s) of interest are passively accumulated from the aquatic environment to the receiving phase where they can be selectively pre-concentrated, allowing for the time-weighted average concentration (C_{TWA}) to be determined for the duration of deployment (Figure 1-5). The C_{TWA} is representative of the concentration of analyte(s) in the sampled medium for the duration of deployment, thus allowing for transient pollution events to be captured where they could be missed with infrequent spot sampling programs. The integrative uptake phase can be described by Equation (1-1) below [89]:

$$C_{TWA} = M_s/R_s(t) \quad (1-1)$$

where the term M_s refers to the mass of analyte accumulated in the receiving phase of the PSD after a given exposure time (t), R_s is the sampling rate, and C_{TWA} is the time-weighted average concentration of analyte in the sampled medium over the period of PSD deployment [89]. The R_s is dependent on the first-order rate constant for the accumulation of the analyte from the sampled medium to the receiving phase [89], and is commonly measured in laboratory-based calibration experiments for each analyte of interest [102]. The R_s can be affected by water

temperature, hydrodynamic conditions around the sampler, degree of biofouling and on the diffusional surface area of the PSD [102]. The C_{TWA} can be determined for the duration of the PSD exposure (t), when a) the R_s is known, and b) by quantifying the amount of analyte accumulated in the receiving phase post deployment (M_s) [89].

Environmental conditions have been reported to affect the diffusion of analytes across the semi-permeable barrier, thus affecting accumulation in the PSD receiving phase. For example, the effect of temperature on passive sampling results has been studied and shown to affect the sampling rate and the sampler-water partition coefficient [88, 103-105]. Water flow velocity and turbulence has also been shown to affect the mass transfer of analyte when uptake is controlled by diffusion through the water boundary layer [88]. In addition to temperature and turbulence or flow pattern of water around the device, there are several other environmental factors that can affect the performance of a PSD, namely salinity, pH, dissolved organic matter (DOM) and biofouling of the device. [89, 96, 106-109].

Biofouling is known to limit the deployment lifetime of scientific instruments especially when immersed in nutrient rich and productive aquatic environments [110, 111]. Biofouling occurs when exposed surfaces are colonised by periphytic microorganisms forming a biofilm, allowing further attachment of macroorganisms such as macrofauna [112]. The presence of a biofilm on the surface of passive sampling membranes and/or exposed receiving phases will increase the tortuous pathway of the diffusing analyte(s) from the bulk sample phase to the receiving phase, reducing the overall accumulation efficiency of the PSD [99].

The effect of biofouling on the performance of various passive sampling tools is well documented in the literature [89, 113-116]. Richardson et al. [117] found that the uptake of a range of organic contaminants was reduced in a semi-permeable membrane device (SPMD) by up to 50% under fouling conditions, and Huckins et al. [118] similarly observed that in severe cases the uptake of polyaromatic hydrocarbons (PAHs) was reduced by 20 – 70%.

Strategies to reduce microalgal colonisation of the SPMD, including mounting the device in between copper mesh screens [119], and the addition of the antifouling agents Irgarol and capsaicin to the receiving phase, were shown to be largely ineffective in mitigating the effects of biofilm formation on the surface of the SPMD studied [116]. Performance reference compounds having similar chemical properties to the analyte(s) under investigation, were used

to correct the sampling rate, by dissipating at a similar rate to the assimilation of analyte(s) into the passive sampler [106, 116]. The effects of biofouling, temperature and water turbulence could be corrected for using the PRCs, however, this approach is limited to isotropic exchange in hydrophobic passive sampling, and it is not suitable for sorption-based PSDs [107].

Whilst many researchers have documented the effects of biofouling on the performance of PSDs, different approaches to reducing or quantifying the effects have been shown to be effective, with no universally applicable strategy. Schäfer et al. observed that fouling did not occur in their 1-day pulse contamination experiments using a Chemcatcher® when a polyethersulfone diffusion-limiting membrane was used compared the configuration without the membrane which exhibited fouling and a four-fold reduction in analyte uptake [120]. Harman et al. observed that fouling between both SPMD and POCIS samplers varied when immersed in the same media, with markedly different effects in performance, where a SPMD exhibited a reduction in analyte uptake due to fouling, whereas a POCIS saw a significant increase in the uptake of alkylated phenols [121]. When sampling for metals [122, 123] and orthophosphate [124], the performance of a diffusive gradients in thin films (DGT) passive sampler was also reportedly impacted by the presence of biofilm, which blocked the pores of the device and changed the way analyte molecules were able to move through the diffusive gel layer. Uher et al. [125] found that the addition of a polycarbonate protective membrane minimised the effect of biofouling on some target metals, but adversely affected others. DGTs treated with silver nanoparticles were shown to inhibit the growth of biofilms without affecting the performance of a device for mercury determination [123], and antifouling efficacy of the antibiotic chloramphenicol and two metal iodides (copper and silver) was tested for a DGT technique for monitoring reactive phosphorus [126]. The silver iodide provided the longest protection (21 days), followed by the copper iodide (14 days), however, the antibiotic chloramphenicol did not appear to be effective in preventing the colonisation of microorganisms on the device for any of the deployment times tested.

Over the last two decades, several reviews have described and assessed a variety of passive sampling techniques applied to water quality monitoring in aquatic environments for a range of chemical species including organics, inorganics and heavy metals [89, 98, 127-132], with a particular emphasis on the monitoring of polar [104, 109, 133-135], and non-polar pollutants of concern [88, 96, 136]. While many reviews have focussed on the development and

application of passive sampling techniques for low salinity freshwater matrices, Mills et al. [137] and Schintu et al. [102] provide comprehensive book chapters evaluating passive sampling technologies commonly applied for water quality monitoring specifically in coastal and marine environments.

Two passive sampling devices have been developed and applied for the monitoring of ammonium in freshwaters including DGTs comprising a protective filter membrane, a diffusive gel layer and various sorbent receiving phases [138-142], and the polymer inclusion membrane based passive sampler using a membrane bound ionic liquid to facilitate transport and accumulation across the membrane using ion exchange processes [143]. However, both methods suffer from interference from competing alkali (Na^+ and K^+) and alkaline earth (Ca^{2+} , Mg^{2+} and Sr^{2+}) metal cations in solution, which in estuarine and seawaters are several orders of magnitude higher in concentration, leaving these PSDs ineffective for use in saline matrices.

A summary of the PSDs developed and applied for water quality monitoring in marine environments will be outlined in the following section, highlighting their construction, operation, application to water quality monitoring and their respective advantages and limitations. Moreover, an outline of the steps that were taken to study or mitigate the effect of the environmental variables above mentioned, in addition to a description of the calibration procedures applied to ensure appropriate quality control, will also be provided.

1.4.1 Semipermeable membrane devices (SPMDs)

SPMDs were first reported in 1990 by Huckins et al. [144], and are one of the most widely studied passive samplers, commonly used to monitor the concentration, occurrence, transport, fate and bioavailability of semi-volatile, non-polar, persistent organic pollutants in aquatic environments and air [88, 145-147]. The hydrophilicity/hydrophobicity of nonionic compounds can be described by the octanol-water partition coefficient ($\log K_{ow}$) which is a measure of a compound's partition between the lipophilic octanol and the hydrophilic water phase [148]. The more positive the value of $\log K_{ow}$, the more hydrophobic the compound, whereas hydrophilic compounds tend to exhibit low or even negative $\log K_{ow}$ values. SPMDs are suitable for hydrophobic compounds with $\log K_{ow}$ values ≥ 3 [147].

The most widely used SPMD comprises a 91.4 cm long by 2.5 cm wide sealed, transparent low-density polyethylene (LDPE) tube, commonly filled with 1 mL of a high purity, high molecular weight lipid such as triolein as the receiving phase (Figure 1-6A) [144]. The LDPE is an amorphous non-porous plastic, containing transient cavities up to 10 Å in size [89, 145, 146], allowing for small hydrophobic molecules to be absorbed by the polymer and excluding larger molecules or those adsorbed to suspended colloids, particulates or humic acids [89]. Triolein is the most common receiving phase used in SPMDs, primarily due to similarities between the octanol-water and triolein-water partition coefficients for a number of important hydrophobic organic compounds (HOCs) [89, 146], its low permeability in LDPE membranes [147], and as it is a major storage lipid found in a wide range of aquatic organisms thus allowing for PSDs to mimic uptake rates in the fatty tissue of marine invertebrates [145, 147, 149].

To ensure consistent surface area exposure during deployment, the layflat tubes of the SPMD are threaded between several spindles in a 'spider carrier' to prevent the tubes from self-adhering, and to minimise contact between the SPMD and the deployment canister walls (Figure 1-6B) [150]. The 'spider carrier' is mounted into a marine-grade stainless steel mesh deployment canister (Figure 1-6B) designed to protect the SPMD from mechanical damage during deployment, periods of which can range from one week to several months [151], or even over a year in deep-ocean environments [152].

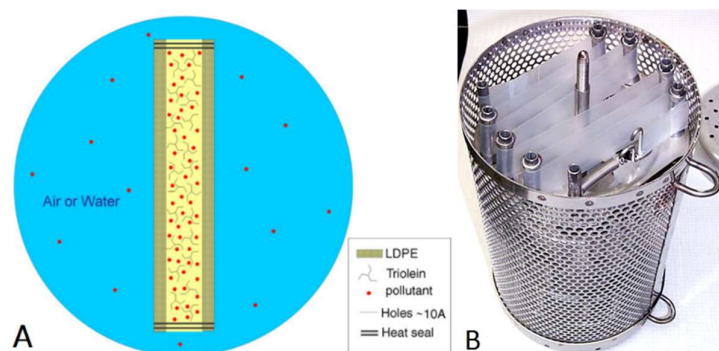


Figure 1-6. Schematic diagrams and typical deployment configuration of a SPMD filled with triolein receiving phase. (A) highlights the mechanism of analyte accumulation, and (B) showing the SPMD threaded onto the spindles of a 'spider carrier' and fitted into a commercially available cannister. Figure 1-6A is reproduced from ref. [146] with permission from Elsevier, and 1-6B is from ref. [151] with permission from the Office of Ocean Exploration and Research, National Oceanic and Atmospheric Administration.

A significant advancement in the development and application of SPMDs has been the use of performance reference compounds (PRCs), which are spiked into the lipid receiving phase prior to membrane enclosure, allowing for site-specific sampling rates to be determined and *in situ* calibration to be performed [99, 106, 153, 154]. If isotropic exchange kinetics apply to the uptake of analyte(s) and dissipation of PRCs then the respective uptake and dissipation rates can be correlated [106, 153, 154]. PRCs should be analytically non-interfering compounds such as isotopically labelled analogues of the analyte(s) under investigation (e.g., deuterium and/or ^{13}C and ^{14}C labelled), exhibit similar physicochemical properties to the analyte(s), and in the case of surrogate compounds should not be present in the environment in quantities above the limit of detection of the analytical method [99, 155]. Using PRCs, allows for exposure-specific effects (flow/turbulence, biofouling and temperature) and compound-specific effects (diffusion coefficients and sampler-water partition coefficients) to be compensated for during deployment, thus allowing for in-field calibration to be performed [96, 106]. The use of PRCs is commonplace with SPMDs having also been applied successfully to a small number of other aquatic PSDs for measuring HOCs.

SPMDs have been widely adopted for monitoring HOCs in the aquatic environment, and are well described in the literature with extensive studies outlining sampler performance and application in the field, including for use in complex matrices such as estuarine [156, 157], deep-ocean [152], tropical [158, 159], and cold polar environments [160, 161]. Concurrent monitoring of atmospheric concentrations allows for mass-transfer of HOCs at the air-water interface to be determined [162], and similarly the monitoring of pore waters and sediments has allowed for quantification of sediment-water mass transfer to be studied [163-165]. The SPMD with triolein lipid receiving phase was intended to be biomimetic, essentially acting as an effective surrogate for HOC accumulation in animal tissue. However, studies where SPMDs were deployed alongside trophically diverse biota have shown that substantial differences in HOC accumulation ratios can occur [149, 166, 167], largely due to environmental factors affecting the study organisms such as temperature, salinity, dissolved oxygen concentrations, or due to physiological parameters such as foraging behaviours, reproductive status, exposure to environmental stressors, metabolic activity and excretion of harmful substances [168]. Nevertheless, SPMDs provide a good tool for understanding the concentration of dissolved

HOCs (i.e., not bound to particulates or organic acids) in the aquatic environment, including in marine waters.

In marine environments SPMDs have been used to assess environmental concentrations of non-polar organochlorine pesticides [152, 167, 169-171], polyaromatic hydrocarbons (PAHs) [166, 170, 172-174], dioxins and furans [175-177], polychlorinated biphenyls (PCBs) [170, 174], polybrominated diphenyl ethers (PBDEs) [178], organotin [179, 180], and halogenated natural products produced by algae, sponges and other marine organisms [158].

As many HOCs are commonly found in air, precautions must be taken to minimise vapour phase contamination during deployment and transport, and strategies to minimise exposure to UV radiation should be used to minimise the possibility of photodegradation of PRCs and/or sequestered analytes which would lead to an underrepresentation in C_{TWA} estimates [150, 181].

Besides the relatively high cost of triolein-based SPMDs compared to other commercially available PSDs, one of the main limitations of this technique includes time-consuming and labour-intensive sample handling steps required for the recovery of analytes from the triolein receiving phase prior to analysis. These steps usually involve dialysis (requiring large amounts of organic solvents), pre-concentration, solvent exchange, and complicated extract clean-up prior to chromatographic separation [88, 146, 182]. In order to simplify the method, Leonard et al. [183] replaced the triolein receiving phase with isooctane, and Zhao et al. [184] with the ionic liquid (IL) 1-butyl-3-methylimidazolium hexafluorophosphate. The use of isooctane inhibited periphytic growth and biofouling of the PSD and analysis of the receiving phase did not require clean-up or back-extraction procedures. However, one of the main disadvantages of the isooctane-based SPMD is the leaching of the solvent receiving phase to the surrounding environment during deployment [183]. The benefit to using the IL as receiving phase was that it was retained by the semipermeable LDPE membrane, and it has been described as an environmentally friendly alternative to conventional organic solvents, able to be directly analysed by high performance liquid chromatography (HPLC) without the need for dialysis or clean-up procedures as required by the triolein-filled SPMD. However the IL-based SPMD exhibited reduced sensitivity when compared to its triolein-SPMD counterpart [184].

Similar in principle to the triolein filled SPMD, Brumbaugh et al. [185] described the development of a passive integrative mercury sampler for monitoring neutral Hg^0 species in air, synthetic fresh and seawater, comprising a lay-flat LDPE tube and a receiving phase of nitric acid and gold chloride. This sampler was able to extract dissolved gaseous mercury species, and Hg^0 uptake rates were shown to be linear for a period of two weeks, with the sampling in freshwater being more efficient than in seawater, likely due to a large fraction of aqueous mercury present as the charged chloro-anion complex preventing it from permeating through the transient cavities of the LDPE membrane [185]. This sampler was described as useful for screening applications in environmental waters primarily due to its 'proof of concept' stage of development, requiring further work to evaluate the usefulness of the sampler in water, in particular its ability to differentiate between dissolved gaseous and other neutral Hg^0 species.

Research was undertaken by Booij et al. to examine the uptake kinetics of the SPMD compared to triolein-free SPMD to determine the effect of triolein on HOC partition, with results highlighting that the LDPE membrane alone was only slightly less efficient at accumulating HOCs than the triolein-filled SPMD [154]. This encouraged further research into the suitability of membrane-water partitioning as a passive sampling method [186-188], giving rise to the development of several monophasic polymer based PSDs, several of which are described in the following section below (1.4.1.1 Single-phase passive samplers).

1.4.1.1 Single-phase passive samplers

Single-phase PSDs generally comprise a non-polar polymer membrane which acts as the receiving phase allowing for absorption of the analyte(s) directly into the elastomer. The polymer membrane of such samplers usually has a pre-determined thickness and surface area to volume ratio, which can be tailored to the analytes(s) of interest, and can determine the sampling regime of the PSD (equilibrium or kinetic) [189]. A wide variety of configurations have been described in the literature, including strips or sheets [176, 190, 191], as well as thin-film coatings on glass substrates such as capillaries [192], fibres [193] and beads [194].

Adams et al. [195] reported the first comprehensive study into the application of single-phase polyethylene membranes as PSDs in 2007, and in the same year Rusina et al. [196] published their investigating into the critical properties of 13 different single-phase polymer membranes

and their suitability for use as aquatic PSDs. In the last decade, single-phase PSDs have increased in popularity for monitoring HOCs, largely due to the simplicity of their preparation, ease of analyte stripping for analysis, and economical cost. However inconsistencies in polymer formulation between different manufacturers and suppliers and a lack of commercial availability of some single-phase PSDs may limit their widespread use and adoption as water quality monitoring tools [88].

The majority of studies reported in the literature describing the use of single-phase polymers as PSDs in marine environments have focussed on LDPE, silicone rubber also known as polydimethylsiloxane (PDMS), polyoxymethylene (POM) and ethylene-vinyl acetate (EVA) [88]. A summary of each of these PSDs is provided in the following sections.

1.4.1.1.1 Low-density polyethylene (LDPE)

The first study investigating the potential use of low density polyethylene (LDPE) sheets as an alternative to triolein-filled SPMDs was undertaken by Müller et al. in 2001 [186]. LDPE polymer consists of repeating ethylene units $[-CH_2-CH_2-]_n$ and its structure comprises highly branched chains, yielding a low-density amorphous polymer. Comparatively, high density polyethylene exhibits minimal branching, is semi-crystalline and has very different physicochemical characteristics, making it unsuitable for use in passive sampling.

Single-phase PSDs are becoming popular, as strips of polymer are simply cut up and deployed (Figure 1-7C), and analyte absorption processes into the polymer matrix are considered more straightforward compared to the SPMD-based PSDs, and difficult analyte stripping and purification procedures are avoided [88, 186]. It was not until 2007, that Adams et al. [195] undertook a comprehensive study into the use of polyethylene devices as PSDs for HOCs in aquatic matrices, investigating the effects of temperature, salinity and exposure time on the polyethylene-water partition coefficients and uptake of a number of PAHs, PCBs and one dioxin. Diffusion coefficients for a number of HOCs with wide ranging hydrophobicities were determined for LDPE in addition to two types of commercially available silicone rubber [197]. A review regarding LDPEs partition and diffusion coefficients for trace organic contaminants including an assessment of the implications of its use as a PSD was published in 2011 by Lohmann [198]. Similarly to triolein-based SPMDs, *in situ* exchange kinetics can be established

with the use of PRCs, which are equilibrated with the LDPE [198]. LDPE-PSDs have been found to have a high reproducibility compared to other commonly used single-phase PSDs [199]. The benefits of using single-phase LDPE-PSDs for environmental analysis is the facile preparation and straightforward stripping of analytes for analysis, the low cost of the material [92], and the fact that mechanical damage will not affect the performance of the PSD, as there is no risk of the receiving phase leaking due to its absence [195]. LDPE-PSDs have been selected alongside silicone rubber (SR) as the PSD of choice for the aquatic global passive sampling program (AQUA-GAPS) (Figure 1-7D) [92, 95], and have been successfully deployed to provide a) high resolution vertical distributions of organic contaminants in surface and sub-surface waters [200], b) to monitor the mass flux of HOCs between coastal waters and the overlying atmosphere [191, 201], and c) to monitor HOC concentrations between marine sediments and overlying waters [202, 203].

1.4.1.1.2 Silicone Rubber (SR)

Similar to LDPE, polydimethylsiloxane (PDMS) or more commonly known as SR has become a popular and well characterised single-phase polymeric PSD used to measure lipophilic organic compounds in aquatic environments [88, 197, 204, 205]. SR is a simple organosilicon polymer made up of repeating $[-\text{SiO}(\text{CH}_3)_2-]_n$ units. It has been extensively used for a range of analytical applications [206], including as a stationary phase in gas chromatographic separation columns [207], as a sorbent in solventless stir bar sorptive extraction (SBSE) [208, 209] and in solid-phase microextraction (SPME) techniques (Figure 1-7A and 1-7B) [192, 210-212], and as personal passive samplers in the form of wristbands [213-216]. A significant advantage of using SBSE and SPME is the ability for the PSDs to be directly analysed using on-line thermal desorption gas chromatography mass spectrometry (GC-MS), thereby greatly simplifying the overall analytical procedure [192, 206]. However, SPME and SBSE techniques are limited by the dimensions of the glass capillary and stir bar, respectively, which may reduce the sensitivity of the PSD, and limit their use for trace analysis [217].

Sampling cages have been designed to accommodate 30 (LDPE/SR or other polymer) strips (Figure 1-7D), and each strip can be placed in a Soxhlet extraction tube allowing for sequential solvent extraction and concentration of the analytes into a refluxing solvent [218]. The simple construction, facile stripping of analyte(s) and high partition coefficients and low transport

resistance make SR an attractive polymer for aquatic passive sampling [88, 197]. However, one of the main drawbacks is the necessity to remove trace oligomers from the polymer prior to deployment which may otherwise interfere with the quantification of the target analytes thus affecting the analysis accuracy [219]. SR passive samplers have been applied to a wide variety of marine waters globally, including but not limited to: a four year monitoring study undertaken at three Belgian coastal harbours to assess the freely dissolved concentrations of PAHs and PCBs [218]; at strategically important locations within the AQUA-GAPS water quality monitoring program [95]; alongside clams and mussels in a mangrove ecosystem to determine partitioning and bioaccumulation of legacy and emerging HOCs [190]; in a study linking passive sampling in the field to passive dosing in laboratory ecotoxicity testing [220]; and more recently the SR passive sampler was used to detect the presence of organotin compounds in tropical coastal waters in the Zanzibar archipelago [221].

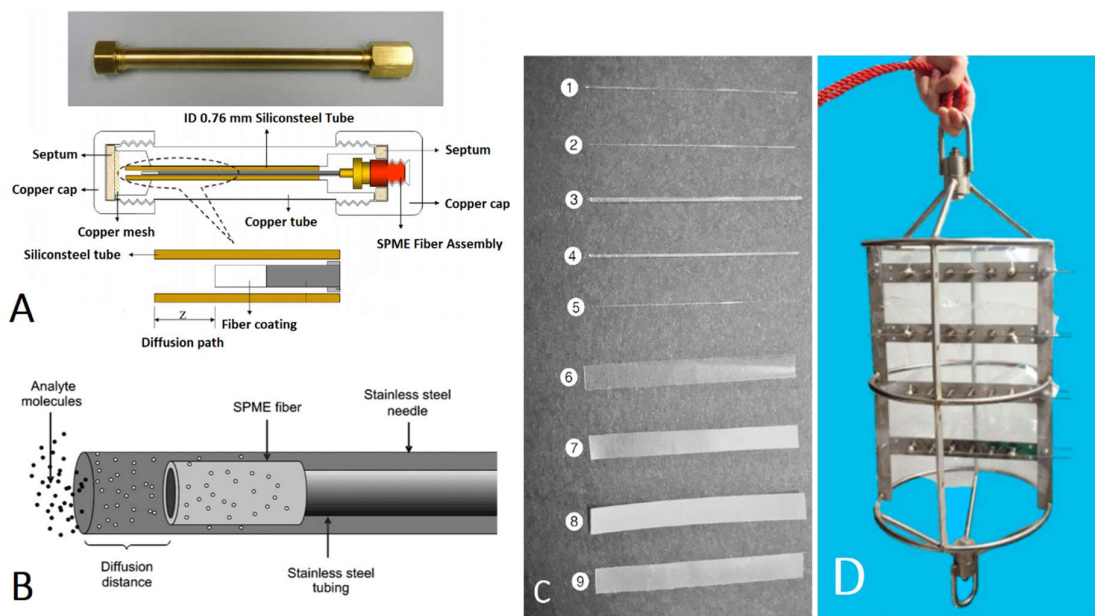


Figure 1-7. Single-phase polymer-based PSDs. A) Schematic representation of a SPME passive sampler with protective copper casing and mesh. B) Mechanism of analyte absorption into the polymer of the SPME fibre. C) Different polymer fibres and sheets including SR (1 – 4, 9), polyacrylate (5), polyethylene (6), and POM (8). D) Passive sampler holder deployed in coastal water during AQUA-GAPS using both LDPE and SR strips. Figures 1-7A and 1-7B are reproduced from ref. [222] and [223], respectively, both with permission from Elsevier; 1-7C is reproduced from ref. [224] with permission from Springer Nature, and 1-7D is reproduced from ref. [95] with permission from the American Chemical Society.

1.4.1.1.3 Polyoxymethylene (POM) & ethylene-vinyl acetate (EVA)

The polymer polyoxymethylene (POM) contains a repeating polar (H-bond accepting) group $[-CH_2-O-]_n$ in its molecular structure making it suitable as a PSD for a diverse range of polar and non-polar compounds including hormones, pharmaceuticals and biocides [225]. It exhibits a higher resistance to analyte mass transfer for a range of HOCs compared to the very lipophilic LDPE and SR membranes, and uptake and selectivity is defined as being polymer controlled rather than water boundary layer controlled [196]. This characteristic allows for typically long exposure/deployment times to be applied without reaching partitioning equilibrium [189], and for sampling work to be undertaken in highly contaminated environments where LDPE and SR samplers would become rapidly oversaturated. POM samplers (used as strips) (Figure 1-7C, number 8) have been deployed alongside passive air samplers in the overlying atmosphere to monitor the aerosol-water distribution of dioxins and PCBs and in marine waters in the Baltic Sea [226], and at surface and seafloor depths to investigate the flux of HOCs from the sediment pore water to the overlying waters [176].

Like POM, ethylene-vinyl acetate (EVA) is a hydrophilic polymer due to its polar acetate group $[-CH_2-CH_2-]_n[CH_2-CH(OCOCH_3)-]_m$, and it is, therefore, expected that its hydrophilic properties will allow for its use over an expanded range of target analytes that are currently not accommodated for in other more lipophilic passive sampling polymers (LDPE/SR) [194]. EVA has been used for passive sampling of cypermerthrin in the salmon farm industry [193], and more recently for soluble munitions compounds in marine and freshwater environments, where the polymer composition could be tailored to the analyte of interest [227].

1.4.2 Polar organic chemical integrative sampler (POCIS)

The polar organic chemical integrative sampler (POCIS) has been developed to accumulate a broad spectrum of hydrophilic organic compounds, which characteristically have one or more polar functional groups or a significant dipole moment, such as polar pesticides, pharmaceuticals, illicit drugs, antibiotics, hormones, personal care products, phosphate based flame retardants, surfactants, and their metabolites and degradation products [102]. Over 300 chemicals have been reported in the literature as having been detected and quantified by POCIS in both the laboratory setting and *in situ* in environmental waters [113]. The POCIS is

commonly deployed in conjunction with SPMDs to enable monitoring of a diverse range of persistent organic pollutants and emerging contaminants in environmental waters, including 75% of the priority substances listed under the European Union's Water Framework Directive (EU-WFD) [102].

POCIS samplers are most commonly applied to monitoring hydrophilic organic compounds with $\log K_{ow}$ values ≤ 3 , however Alvarez et al. (2007) illustrated the performance of both POCISs and SPMDs as a function of $\log K_{ow}$ values, highlighting the overlap in their suitability for detection and accumulation of organics in the range of $\log K_{ow}$ 3 to 4 [228]. Furthermore, POCISs have been successfully applied to monitoring a range of priority pollutants ($\log K_{ow} > 4$) identified in the EU-WFD [229], with some compounds exhibiting both polar and non-polar physicochemical characteristics (e.g., octylphenol and nonylphenol with $\log K_{ow}$ values from 4.1 to 4.5, respectively [230]), and other compounds being ionisable (e.g., pentachlorophenol $\log K_{ow}$ 5.1 [231]) and existing as both deprotonated or neutral species based on matrix pH [232-234].

The POCIS comprises a solid receiving phase (sorbent), sandwiched in between two identical microporous diffusion-limiting membranes (usually polyethersulphone (PES) with a pore size of 0.1 μm) compressed together by two stainless steel washers that hold the sampler together [232]. The 'membrane-sorbent-membrane' sandwich configuration maximises the surface area (commonly 45.8 cm^2) of the PSD as both sides of the sampler are exposed to the sampled medium and are able to accumulate analyte from the solution (Figure 1-8) [235]. Unlike the polyethylene membrane in the SPMD which is transparent, the PES membrane in POCIS is opaque, and therefore photodegradation is less likely to affect the performance of the device [233]. Arrays of POCIS are commonly deployed at each sampling location by mounting several samplers on a support rod with the advantage of combining the sorbents from multiple samplers to increase the sensitivity of measurements (Figure 1-8) [223].

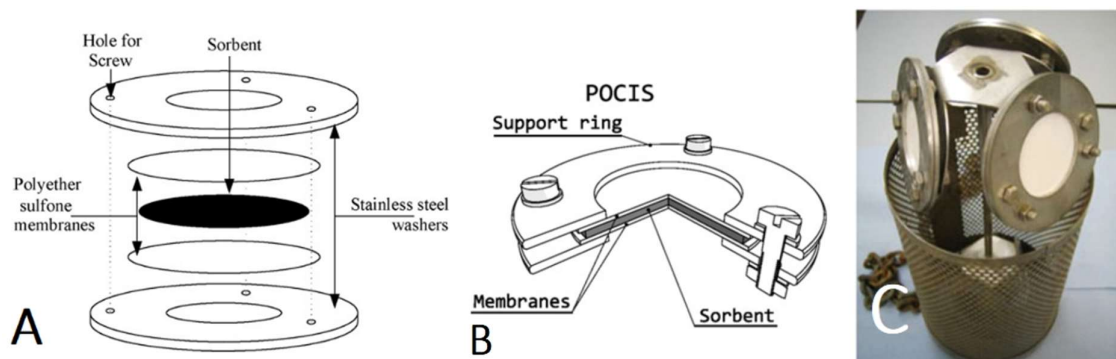


Figure 1-8. Schematic diagrams and typical deployment configuration of the POCIS for the passive sampling of hydrophilic organic compounds. A) and B) typical construction of POCIS; C) array of POCIS mounted on a support rod for field deployment. Figure 1-8A is reproduced from ref. [223] and 1-8B is reproduced from ref. [129], both with permission from Elsevier. Figure 1-8C is reproduced from ref. [236] with permission from the Springer eBook.

The POCIS is versatile as the receiving phase (sorbent) can be changed to target a specific chemical or class of compounds, and there are two commercially available configurations available, including the pesticide-POCIS and the pharmaceutical-POCIS. The pesticide-POCIS incorporates a receiving phase comprising a triphasic admixture of Isolute ENV+ (hyper cross-linked hydroxylated polystyrene-divinylbenzene polymeric resin) with Amborsorb 1500 (carbonaceous adsorbent) dispersed on S-X3 Bio Beads (styrene divinylbenzene copolymer), and the pharmaceutical-POCIS incorporates only one phase; an Oasis hydrophilic-lipophilic balanced (HLB) copolymer sorbent [109]. As the different sorbents are optimised for specific classes or types of hydrophilic organic compounds, it is common to co-deploy both pesticide- and pharmaceutical-POCIS simultaneously, to maximise the detection of these compounds at any given sampling site [228].

The triphasic admixture is considered the generic sorbent for hydrophilic organic compounds, however the Oasis configuration exhibits advantageous properties. Analyte molecules with multiple functional groups bind strongly to the carbonaceous component of the triphasic receiving phase resulting in difficult and complex extraction with poor recoveries [228], and more toxic elution solvents (dichloromethane as opposed to methanol) are required for analyte stripping with the pesticide-POCIS [237]. Vermeirssen et al. (2012) undertook a study using pesticide-POCIS to assess the partition of analytes between both sorbent and PES

membrane for a range of compounds (herbicides, pharmaceuticals and industrial chemicals) with log K_{ow} values between -2.6 to 3.8 [238], and Silvani et al. (2017) likewise undertook a similar study using pharmaceutical-POCIS to monitor a range of alkylphenols between log K_{ow} 2.5 to 5.8 [234]. Both studies showed that compounds with higher log K_{ow} values tended to be retained by the PES membrane with a lag-phase prior to their detection in the sorbent receiving phase where compounds with low log K_{ow} values were efficiently retained. This demonstrates the importance of analysing both the sorbent and membrane phases to correctly determine environmentally relevant concentrations of pollutants with a varying degree of hydrophilicity [234, 238].

More recently a number of specialised receiving phases have been reported in the literature specifically for strongly polar and ionisable compounds including a) the Strata™ weak anion exchange (X-AW) sorbent deployed in estuarine environments for the detection of perfluorinated chemicals [239], b) a commercially available molecularly imprinted polymer receiving phase for the determination of glyphosate and its degradation product aminomethylphosphonic acid [240, 241], c) imidazolium ionic liquids immobilised on silica gel used to monitor five perfluoroalkyl substances (PFAS) in waste water effluent [242], and d) the IL trihexyl(tetradecyl)phosphonium dicyanamide as the receiving phase for monitoring pharmaceuticals in a POCIS like passive sampling technique (termed PASSIL, short for passive sampling with ionic liquids) which has been applied to high salinity seawater matrices [243].

A number of calibration strategies for POCIS are outlined in the literature, namely static renewal, static depletion, flow-through systems and *in situ* calibration [133]. The choice of calibration method has been shown to have a significant impact on the sampling rate (R_s) [244], and one of the biggest challenges to the widespread use of POCIS for quantitative analysis is the lack of a robust method to correct for *in situ* environmental conditions such as hydrodynamics (flow rate and pattern), temperature, salinity, pH and dissolved organic matter [107, 109]. In order to obtain quantitative data from POCIS (i.e., C_{TWA} determination), a number of *in situ* calibration methods have been proposed with varying degrees of success, including the PRC approach, surrogate PRC systems based around the co-deployment with hydrophobic samplers, and calibration of the POCIS against the dissolution of calcium sulfate decahydrate casts [133]. Interactions between polar analyte molecules, polar sorbents and the PES diffusion limiting membrane in the POCIS are fundamentally different to isotropic uptake and exchange

dynamics in hydrophobic samplers between analytes and PRCs, and thus the classic PRC calibration approach may continue to provide limited success for POCIS-based passive sampling for polar and ionisable compounds [107].

1.4.3. Chemcatcher®

The Chemcatcher® was first described by Kingston et al. [245] and has been applied to measuring the C_{TWA} for both polar/non-polar organics [245, 246] and heavy metals [247], in aquatic environments. The Chemcatcher® comprises a reusable polytetrafluoroethylene (PTFE) assembly, a commercially available receiving phase (solid sorbent), and in some applications a diffusion-limiting membrane can be added to regulate and facilitate analyte uptake [245] (Figure 1-9).

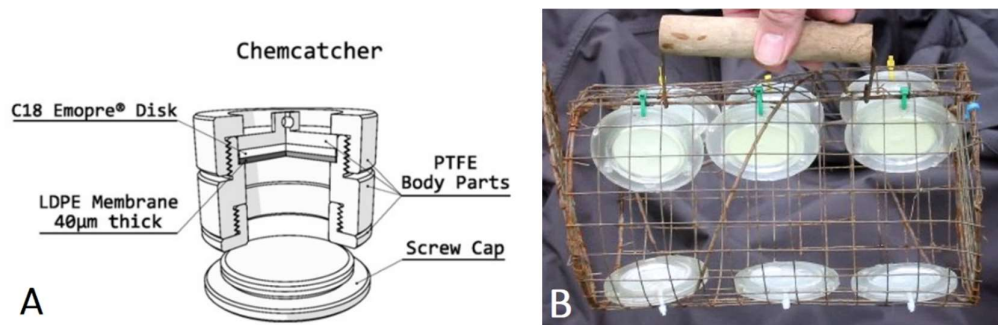


Figure 1-9. Schematic diagram and typical deployment configuration of the Chemcatcher®, (A) for non-polar analyte passive sampling, with B) showing multiple replicate devices mounted in a cage for field deployment. Figure 1-9A is reproduced from ref. [129] with permission from Elsevier, and 1-9B is from ref. [248] with permission from the Royal Society of Chemistry.

The most common Chemcatcher® prototype employs a 47-mm C₁₈ Empore™ disk as the receiving phase, and either a polysulfone (PES) or a low density polyethylene (LDPE) rate-limiting membrane for monitoring of polar or non-polar organic compounds, respectively [245]. Studies have shown that temperature impacts the rate of analyte accumulation in both polar and non-polar Chemcatcher®, with the authors concluding that it is necessary to determine the effects of temperature in the laboratory for each analyte of interest so that calibrations can be appropriately adjusted and field results corrected [245, 246]. The effect of water turbulence was likewise studied showing a quantifiable effect with increasing

turbulence, especially for smaller molecules, suggesting that uptake rates are analyte specific and controlled by both diffusion through the aqueous boundary layer and by affinity of the analyte for the diffusion-limiting membrane material [245, 246].

The applicability of using PRCs with Chemcatcher® samplers to compensate for the effects of environmental variables (i.e., temperature, turbulence/flow conditions and biofouling) and for *in situ* calibration has been investigated. Lissalde et al. [249] provided an extensive summary of their research into this topic, highlighting that PRCs have been successfully used, and are appropriate for establishing *in situ* sampling kinetics especially for the non-polar Chemcatcher®. However, for the polar configuration there has been limited success using this approach, with the authors suggesting further research was warranted.

The performance of the Chemcatcher® in high ionic strength matrices has rarely been evaluated, however, some Chemcatcher® studies have been undertaken in a range of marine environments where the PSD have been deployed as part of wider water quality monitoring programs and where optimisation studies were not central to the study.

Petersen et al. [108] undertook calibration experiments using a non-polar Chemcatcher® in fresh and seawater matrices for selected PBDEs, PCBs and organochlorine pesticides, showing a salinity effect, whereby a higher offload of PRCs and a slightly lower sampling rate (R_s) were observed as a function of increasing salinity. Allan et al. [250] recommended that the effect of water hardness (i.e., interference of Ca^{2+} and Mg^{2+}) on the Chemcatcher® measurements for metals should be investigated, however, this study is yet to be undertaken. It has been suggested that the pH could affect Chemcatcher® sampling rates through both pH effects influencing the properties of the sampler membrane and receiving phase, and modifications of analyte speciation or partition between protonated and deprotonated forms [249]. Other studies have also reported pH effects when monitoring inorganic mercury and organotin compounds [251], and for a range of herbicides and pesticides with differing polarities [252, 253].

A large variety of receiving phase and membrane combinations (spanning a wide range of $\log K_{ow}$ values) have been described in the literature for Chemcatcher® (Figure 1-10) covering a range of non-polar to polar organics, allowing for the Chemcatcher® sorbent and diffusion

membranes to be tailored to the polarity of the target analyte(s) and the desired deployment period/integration time [114].

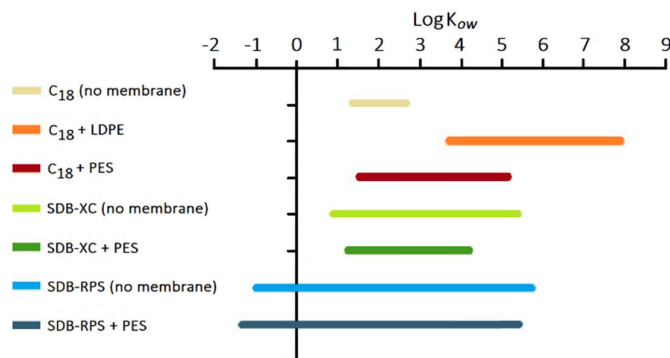


Figure 1-10. Summary of the $\log K_{ow}$ ranges successfully tested for various Chemcatcher® receiving phase and membrane combinations. This figure is reproduced from ref. [114] with permission from Elsevier.

1.4.3.1 Chemcatcher® for non-polar compounds

The Chemcatcher® used for monitoring non-polar compounds commonly employs a C₁₈ Empore™ disk as its receiving phase, overlain by a thin (40 μm thickness) commercially available LDPE membrane [245]. Vrana et al. [254] were able to significantly improve the performance of the hydrophobic Chemcatcher® by filling the interstitial space between the receiving sorbent phase and the diffusion-limiting membrane with a small volume of *n*-octanol, having a high permeability (solubility x diffusivity) for lipophilic HOCs, and reducing the internal resistance to mass transfer within the device [246].

In situ exchange kinetics of PRCs allowed for corrections to be made to laboratory derived sampling rates using an empirical model that corrected for environmental flow/turbulence and temperature conditions [255]. However, since their development, non-polar Chemcatcher® samplers have not been widely applied in marine or even more generally freshwater passive sampling field experiments. This is likely due to the costs involved with deployment given their small and restricted surface area, which may require the deployment of multiple devices to allow for the receiving phases to be combined in order to achieve the desired sensitivities, and this then becomes expensive compared to other commercially available passive samplers (SPMDs or LDPE/SR strips) for this class of compounds [245].

Only one publication has documented the deployment of the non-polar Chemcatcher® samplers in a high salinity marine environment. El-Shenawy et al. [256] describe the use of a Chemcatcher® sampler with C₁₈ Empore™ disk receiving phase and LDPE membrane, deployed alongside resident marine mussels used for biomonitoring in several harbour sites in Portsmouth, UK, to monitor a range of pesticides and PCB congeners. The authors suggest that the Chemcatcher®-based passive sampling and organism exposure approach were complimentary, as the Chemcatcher® samplers captured the dissolved fraction of contaminants, while the mussels were indicative of both dissolved and particulate-bound fractions [256].

1.4.3.2 Chemcatcher® for polar compounds

Kingston et al. [245] have reported the deployment of Chemcatcher® for the monitoring of polar compounds at two marine harbour sites for field trials. The PSD contained the C₁₈ Empore™ disk and PES membrane to monitor the slightly polar herbicides diuron and igarol. There was reasonable agreement between both spot and passive sampling methods, with replicate PSDs exhibiting good reproducibility [245].

The most extensive use of Chemcatcher® for the monitoring of polar compounds in marine environments has been located at the World Heritage listed Great Barrier Reef (GBR) Marine Park, in Australia. The first study used a C₁₈ receiving phase (with no diffusion limiting membrane), which was deployed for preliminary evaluation to monitor the presence of polar herbicides in the GBR coastal waters, showing that there were detectable levels of diuron, atrazine, simazine, hexazinone and flumetron being recorded throughout the catchment [159]. In a further study on the coral reef, Shaw et al. used a Chemcatcher® sampler with SDB-RPS Empore™ disks as the sorbent phase and with a 0.2 µm polyethersulfone Z-bind™ diffusion membrane to successfully detect a similar variety of agricultural pesticides [171]. The increase in photosynthesis inhibiting pesticides (PSII) was positively correlated to agricultural run-off resulting from seasonal flooding on the GBR. Kennedy et al. [257] deployed a Chemcatcher® PSD using a SDR-RPS receiving phase with a 0.45 µm PES diffusion membrane to determine if they could detect and quantify an increase in PSII contaminant loads exported to inshore waters as a result of extreme weather events (e.g., tropical cyclones during the wet season).

Two of the PSII herbicides, tebuthiuron and metolachlor, were shown to exceed their Water Quality Guideline values during the 2010 – 2011 wet season, and both passive and spot sampling methods were in good agreement highlighting the potential of this passive sampling tool to be used for long-term monitoring in remote areas of the GBR for this class of priority pesticides. Additional research was undertaken in which the passive sampling technology using Chemcatcher® was combined with remote sensing for coloured dissolved organic matter (a proxy for measuring incursions of freshwater and therefore run-off) to assess the possibility of integrating the two techniques to monitor improvements in water quality entering the GBR catchment [258].

1.4.3.3 Chemcatcher® for metals and organometallics

The majority of studies using Chemcatcher® for trace metals sampling has been undertaken in freshwater environments. Nevertheless, Chemcatcher® technology has been applied in high salinity matrices to monitor the concentrations of organometallic pollutants (monobutyltin, dibutyltin, tributyltin), and inorganic mercury [251, 259, 260]. The first sampler for the organotin pollutants comprised a C₁₈ Empore™ disk and cellulose acetate (CA) diffusion membrane. It was calibrated under laboratory conditions with the effect of water temperature and flow pattern/turbulence on the uptake rate evaluated. Limits of detection were reported for the different organotin compounds in the range of 0.2 – 7.5 ng L⁻¹. The PSDs were deployed in the Alicante Harbour, Spain, for a period of 14 days, with performance evaluated alongside spot sampling (every second day) [259]. However, there was a significant discrepancy between mean spot sample concentrations over the period of deployment and the C_{TWA} determined from passive sampling. The authors suggest that this is likely due to a) the spot samples containing both the dissolved fraction and the bound fractions (particulate and organic matter bound), where the PSD would only accumulate the dissolved fraction that can diffuse through the pores of the diffusion limiting membrane, and b) there was a significant variation in the concentrations returned in the spot samples over the monitoring period where the frequency of sample collection (every two days) may have been insufficient to provide a representative reflection of the true C_{TWA} concentration.

A Chemcatcher® sampler selective for inorganic mercury was developed and optimised under laboratory conditions, and subsequently applied in the Alicante Harbor in Spain. During this study, further optimisation experiments were also conducted for the monitoring of organotin using the Chemcatcher® sampler described above. Empore™ C₁₈ disks were used for monitoring the organotins, and two receiving phase sorbents were tested for the detection of inorganic mercury, namely the Empore™ SDB-RPS cation-exchange disks and the Empore™ chelating disks containing iminodiacetic (IDA) groups, with the latter being selected [260]. Optimisation studies for both the organotin and inorganic mercury sampler were undertaken to select an appropriate diffusion-limiting membrane for the target analytes, and to study the effect of pH, salinity and biofouling on sampler performance [260]. Cellulose acetate (CA), polyethersulfone (PES), polyethylene (PE) and dialysis membranes were tested, with CA and PES being chosen for the organotin and inorganic mercury Chemcatcher® samplers, respectively. Salinity appeared to have no significant effect on both samplers, however, a change in pH from 7 – 8 was found to affect the performance of the inorganic mercury PSD likely due to pH affecting the speciation of inorganic mercury to form more hydroxide complexes which are accumulated to a lesser extent in the PSD. However, the pH did not affect the performance of the organotin PSD. The use of PRCs could not be applied for this sampler, as the analytes exhibited anisotropic exchange kinetics, and thus a laboratory-based calibration was performed under controlled temperature and turbulence conditions that were chosen to mimic common environmental conditions. The authors suggest that for wider applicability of the device, further work is required under a range of hydrodynamic and temperature conditions to extend the calibration data available [260]. Extensive field trials in ten locations over Europe, featuring a diversity of aquatic matrices, were performed using the laboratory calibrated and optimised Chemcatcher® passive samplers for organotins and for inorganic mercury [251]. Spot sampling was conducted in tandem, however, once again the PSDs accumulated less of the target analytes when comparing with the average concentration recorded for the spot samples collected. This was likely due to the samplers only collecting the soluble fraction of the target pollutants. Nevertheless, the preconcentration capabilities of these PSDs have been identified as a significant advantage, especially in environments where concentrations in spot samples fall below the limits of detection of the analytical instrumentation.

A Chemcatcher® sampler was used by Petersen et al. [261] in the first passive sampling experiment to monitor rare earth elements in aquatic environments. The experiments were undertaken in estuarine waters, using the 3M Empore™ chelating disk as the receiving phase, and a CA diffusion limiting membrane (pore size of 0.45 µm). Temperature and water turbulence effects were studied, with turbulence shown to have a significant influence on uptake rates. The PSDs were shown to accumulate a number of rare earth metals commonly found in trace concentrations in matrices with high salt concentrations, highlighting this passive sampler as an effective monitoring tool [261]. A further improvement to this sampler was described where a continuous flow-through set-up was employed to minimise the artefacts from variable hydrodynamic conditions as the PRC calibration approach could not be used for this configuration of sampler [262].

1.4.4 Solid-phase adsorption toxin tracking (SPATT)

Algal blooms are a global phenomenon and a natural part of seasonal cycles in aquatic ecosystems [263]. However, increasing ecosystem disturbance and pollution has resulted in the proliferation of harmful algal blooms (HABs), having a deleterious impact on the health of fresh, brackish and marine waters. The solid-phase adsorption toxin tracking tool was first introduced by MacKenzie et al. [264], and was developed as an early HAB detection and surveillance tool to monitor the occurrence of potentially harmful microalgal and cyanobacterial blooms and their biotoxins [265, 266]. A SPATT passive sampler is conceptually similar to the Chemcatcher® and POCIS passive samplers. The receiving phase comprises beads of porous synthetic resin capable of adsorbing toxins from the water column, contained in an inert mesh, typically polyester [264] or nylon [266]. A suite of different resins have been investigated for a variety of lipophilic and hydrophilic toxins, with the most common resin Diaion® HP20 made from cross-linked styrene-divinylbenzene beads [267]. Similarly to other passive sampling devices, the challenges limiting the widespread adoption of SPATT samplers as a regulatory monitoring tool include calibration, and standardisation of methods and procedures [268]. However, SPATT samplers have been deployed in Monterey Bay, California, and were found to be successful in detecting the presence of phycotoxins in seawater three and seven weeks prior to a major HAB event, and seven to eight weeks prior to the detection

of toxins in sentinel shellfish [266], allowing for appropriate management strategies to be implemented predominantly to protect human health.

1.4.5. Diffusive gradients in thin-films (DGT)

Diffusive gradients in thin-films (DGT) technique was first proposed by Davison et al. (1994) for the determination of *in situ* trace-metal concentrations in natural waters, with zinc being the target analyte investigated in seawater [269]. A DGT passive sampler generally comprises a chelating resin or metal oxide adsorbent (analyte binding site) separated from the sample solution by a thin-film of an ion-permeable hydrogel where analyte mass transfer is controlled by diffusion through the gel. In addition, it contains a protective pre-filter membrane exposed to the sampled medium, which is employed to prevent suspended particles from adhering to the diffusive hydrogel, which may inhibit analyte uptake over time by minimising the surface area of the exposed PSD (Figure 1-11) [269].

Diffusion of analyte through the hydrogel is largely dependent on the physicochemical properties of the gel including pore size and density, and the swelling factor which reflects the uptake of water by the suspended/submerged gels [270]. Zhang and Davison (1999) reported that polyacrylamide gel cross-linked with agarose derivative produced an 'open-pore', high swelling gel with a water content of 95%, which allowed almost unrestricted diffusion of metal ions through the gel, and an indistinguishable analyte diffusion coefficient between water and the gel [270].

Early development of the DGT passive sampling method focused on the determination of cadmium (Cd), iron (Fe), manganese (Mg), and copper (Cu) in coastal environments using a Chelex-100 cation exchange resin, a polyacrylamide hydrogel and a cellulose nitrate pre-filter membrane [271]. Experiments undertaken showed that for the Chelex-100 resin, uptake of Cd was dependent on temperature, however, it was independent of a) ionic strength (10 nM – 1 M), b) pH in the range of 5 – 8.3, and c) hydrodynamic effects as long as solution flow rates were above a certain threshold [271].

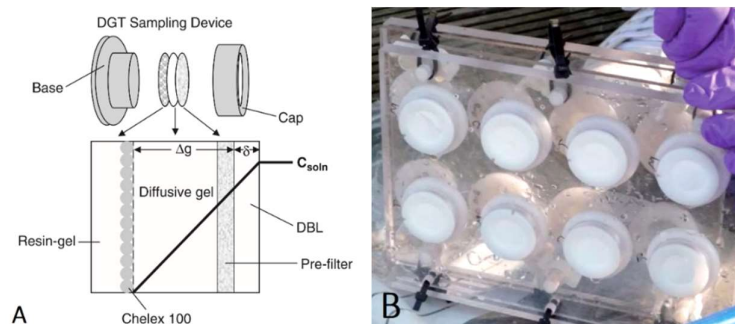


Figure 1-11. Schematic diagram and typical deployment configuration of the diffusive gradient in thin-films passive sampling device. A) Schematic representation of DGT showing analyte uptake mechanism through a pre-filter membrane, diffusive gel, and resin gel (binding site). B) replicates of DGT samplers mounted in a Perspex block which was deployed in the field. Figure 1-11A is reproduced from ref. [132] with permission from Elsevier, and Figure 1-11B is reproduced from ref. [272] with permission from The Royal Society of Chemistry.

Chelex-100 has been the most frequently applied resin binding gel for heavy metal determination, separated by an ion-permeable hydrogel layer of thickness Δg (Figure 1-11A). According to Fick's first law of diffusion, the concentration in bulk solution (C_b) can be determined from the mass (m) of accumulated analyte in the resin layer after a known deployment time (t) using Equation (1-2):

$$C_b = m\Delta g / (DA t) \quad (1-2)$$

Where D is the experimental diffusion coefficient of the metal in the gel, and A is the exposed surface area of the DGT sampler ($A = 3.14 \text{ cm}^2$).

Chelex-100 consists of a styrene divinylbenzene copolymer containing paired iminodiacetate ions, making it an effective polyvalent metal ion chelating resin. Garmo et al. [273] undertook a comprehensive study to determine diffusion coefficients and evaluate the performance of the Chelex-100 resin for 55 elements including alkali and alkaline earth metals and their respective halide ion pairs, transition metals and lanthanides. The authors found that 24 of the elements examined showed an affinity for the binding resin (mostly transition metals), and the alkali and alkaline earth metals and their halide ions did not appear to interfere, indicating that dissolved salts would be unlikely to compete with transition metals in high salinity matrices [273].

A comparison between uptake of dissolved aluminium (Al) species by Chelex-100 and Metsorb (titanium dioxide-based adsorbent) in fresh and marine waters found that both Chelex-100 and

Metsorb exhibited similar diffusion coefficients at pH 5.0. However, in the pH range of seawater, and with increasing ionic strength, a considerable underestimation of Al concentration was observed in the Chelex-100-DGT sampler (40 – 70% lower than predicted), while the Metsorb-DGT sampler measurements were described as independent of pH (5.0 – 8.5) and ionic strength (0.001 – 0.7 M NaNO₃) [274]. It was proposed that the Metsorb-DGT sampler generated more accurate results and that Chelex-100-DGT sampler, which was unsuitable for monitoring dissolved Al in seawater. Ferrihydrite-DGT containing a ferric oxyhydroxide mineral binding phase was compared to Metsorb for the determination of the oxyanions of dissolved reactive phosphorus (DRP), arsenic (As(V)), vanadium (V(V)), antimony (Sb(V)), molybdenum (Mo(VI)), and tungsten (W(VI)). The Metsorb-DGT exhibited superior performance in both fresh and seawaters for measuring As, Sb, W and DRP, nevertheless neither Metsorb-DGT nor Ferrihydrite-DGT samplers performed well at estimating Mo(VI) concentrations [275].

Mercury(II) ions bond covalently with the amide nitrogen groups of polyacrylamide gels, and thus both Chelex-100 binding resin and Spheron-thiol based resin were compared in terms of specificity for Hg, using an agarose gel as the diffusive layer [276]. Both resins exhibited different affinities for bound Hg and were therefore able to be used to differentiate measurable fractions of Hg complexes [276]. Ren et al. (2018) have proposed the use of a highly selective macroporous poly-isothiuronium chelating resin (Tulsion® CH-95) for the simultaneous measurement of methyl mercury and mercuric ion, with uptake rates being independent of both pH and ionic strength in the range of 4.1 – 8.1 pH units and 0.1 – 1000 mM respectively [277].

While DGT samplers have been successfully applied for widespread monitoring of heavy metals in marine environments, DGT technology does not easily discriminate between complexed metal ions (generally less bioavailable and therefore less toxic) and free metal ions (highly bioavailable exhibiting high toxicity), with the concentrations accumulated by DGT tending to reflect total dissolved concentrations [278, 279].

DGT samplers for inorganic nutrient monitoring have been developed for use in freshwater matrices, specifically for ammonium [140, 280], nitrate [139, 280] and phosphate [126, 141, 280, 281]. DGT samplers developed for inorganic nutrient monitoring utilise an ion-exchange resin as the binding phase, however, in high salinity matrices this phase is unable to

discriminate between the low concentration of analyte molecules compared to the high concentrations of dissolved salts.

While the DGT technology was initially developed for detecting *in situ* trace metals and labile inorganics in fresh and marine waters, the application and scope was extended by Chen et al. (2012) who developed the first DGT sampler for polar organic contaminants such as sulfamethoxazole antibiotics using a XAD18 binding resin and agarose hydrogel [282]. While most DGT samplers for organics have been applied to freshwater matrices, there are a few examples in the literature where they are applied to high salinity matrices. Xie et al. (2018) described a DGT sampler for monitoring a suite of 20 antibiotics in seawater using the XDA-1 binding resin as the receiving phase [283], and Ren et al. (2018) developed a porous carbon material derived from metal-organic frameworks as the binding phase for monitoring in synthetic and natural seawater, with both DGT samplers for the polar organics showing little sensitivity to pH and ionic strength [284]. Endocrine disrupting chemicals (three hormones, two pesticides and bisphenol A) were monitored in seawaters using XDA-1 resin as the binding agent, showing linear accumulation over the period of deployment and accumulation was independent of pH and salinity over the range pH 7 – 9 and ionic strength of 0.4 – 0.8 M [285]. Guibal et al. (2019) provide a comprehensive review on DGT passive samplers for polar organics, emphasising similarities with other polar organic passive samplers, and showing that environmental conditions including temperature, pH, analyte pKa, ionic strength and the concentration of dissolved organic matter can have a significant impact on the performance of these PSDs [134]. However, due to the ability of the diffusive gel to mitigate the effect of hydrodynamic conditions on the sampling rate, this makes the DGT samplers for organics inherently more reliable and easier to calibrate, making them a promising and competitive new tool for *in situ* monitoring of polar organic chemicals [286].

1.4.6 GELLYFISH for metals

The Gellyfish is an inexpensive, equilibrium-based passive sampler developed specifically for monitoring toxic free metal ions in the divalent form (M^{2+}) dissolved in seawater, using a thin disk of polyacrylamide gel with beads immobilised in the polymer matrix containing iminodiacetate groups (IDA) that are highly selective for divalent metal cations. The first

Gellyfish sampler developed was tested with the cupric ion (Cu^{2+}) [287]. Dong et al. (2015) described several improvements that were made to the Gellyfish-PSD, namely a significantly reduced equilibration time, and the capability to monitor multiple free metal ions simultaneously, including Cu, Zn, Ni, Pb and Cd ions [288]. The authors developed an R-based model (called GELLYMOD) to correct for ionic strength and account for competitive binding between the different metals and the IDA [288]. Large scale and repeated monitoring of the free ion concentrations of five metals was undertaken using Gellyfish at five inshore locations in the Boston Harbour, with concurrent measurements of ten biogeochemical variables being undertaken. Using the Gellyfish to obtain high resolution data over important spatiotemporal scales, the authors found that there were significant correlations among the metals which varied seasonally, with pH, salinity, temperature and rainfall as key determinants of free metal ion variability [289].

1.4.7 Liquid membrane-based passive samplers

Liquid membranes combine the concept of solvent extraction (i.e., liquid-liquid extraction) with that of membrane-based separation. A liquid membrane is composed of an organic liquid phase immiscible with water, containing an extractant (also known as carrier), and is used to separate two aqueous liquid phases, thus allowing simultaneous extraction and stripping (back-extraction) on each side of the membrane. In the context of passive sampling, the liquid membrane plays the role of the semi-permeable barrier between the aqueous sampled medium and an aqueous liquid receiving phase. The target analyte(s) are first extracted into the membrane, forming adducts with the extractant, which are transported across the membrane by diffusion, and then the analytes are back-extracted into the receiving solution containing a suitable stripping reagent [89, 290, 291]. The fact that the receiving phase is an aqueous liquid offers a great advantage because the receiving solution can be analysed directly without the necessity of analyte stripping from a solid receiving phase as is the case with most other PSDs, thus simplifying the overall analytical procedure [292].

Two types of liquid membranes have been applied in passive sampling, namely supported liquid membranes (SLMs) and polymer inclusion membranes (PIMs). Both consist of an organic liquid phase impregnated within a base polymer, although the binding interactions between

the two components are different in each case as described below. Recently, liquid membrane-based passive sampling techniques have been described in the literature and applied to freshwaters [143, 293, 294]. As their passive sampling mechanism is based on ion-exchange, the complex ionic composition of marine waters tends to suppress the extraction of the target ionic species of interest, thus limiting the use of SLM- and PIM-based passive samplers for such matrices. However, a few liquid membrane-based systems have been reported for application in seawaters, which have great potential to be used as passive samplers. These include a hollow fibre-SLM for the separation and preconcentration of cadmium (Cd) [295], and a PIM for the monitoring of Cd [296], and mercury (Hg) [297].

An SLM comprises an inert microporous thin-film polymeric support, whose pores are filled with a liquid phase (containing the extractant), which is held by capillary forces [298]. The SLM-based enrichment device developed for the monitoring of Cd consisted of a polyvinylidene difluoride (Durapore) support impregnated with the IL Aliquat 336 (a mixture of quaternary alkylammonium chlorides, $(R_3R'N)Cl$) as carrier dissolved in decaline [295]. Optimisation of the SLM was undertaken including the IL concentration and the receiving solution composition. The Cd present in the sampled source solution was extracted into the liquid membrane in the form of $CdCl_4^{2-}$ which was proposed to form an ion pair with the cationic component of the Aliquat 336 ($(R_3R'N)_2CdCl_4$) by exchange with Cl^- (Aliquat 336 anion). The performance of the device was not compromised by the highly saline matrix or due to the presence of other dissolved trace metals (Cu, Ni, Pb) [295].

A PIM-device was developed for Cd preconcentration from high salinity seawater matrices, showing little interference by the high ionic strength of seawater [296]. The PIM-device was composed of a PIM containing the IL trihexyl (tetradecyl)phosphonium chloride as the extractant, cellulose triacetate as the base polymer and nitrophenyl octyl ether as the plasticiser, and 0.5 M nitric acid as the receiving solution. The Cd transport from seawater samples containing $10 \mu\text{g L}^{-1}$ Cd was achieved in 24 h allowing for preconcentration and matrix separation in a single step [296].

A PIM-device was also developed for the monitoring of mercury (Hg) in natural waters including rivers, groundwater and seawater, again with no matrix effects observed [297]. The PIM composition was studied in terms of type of extractant to assess the performance between two ILs, both having the same cation (trioctylmethylammonium) and having different anions

(thiosalicylate or salicylate with acronyms TOMATS and TOMAS, respectively). The TOMATS-based PIM showed better performance than the PIM with TOMAS (using a solution of 10^{-3} M cysteine as the receiving phase) and was therefore chosen for field deployment experiments. Furthermore, the effect of biofilm growth on the performance of the device was assessed, showing that there was no measurable effect observed after a 7-day deployment. The method reported an LOD of $0.29 \mu\text{g L}^{-1}$ showing promise as a passive sampling tool for the monitoring of mercury pollution in waters with complex matrices.

1.4.8 Ammonium PSDs applied to freshwaters

As mentioned earlier, two passive sampling methods have been reported to monitor ammonium in low ionic strength matrices, including a PIM-based PSD [143], and a DGT sampler [138-142]. The PIM device consists of an acidic receiving solution (0.8 M HCl) separated from the sampled aquatic medium by a membrane composed of 55 wt% poly(vinyl chloride) as the base polymer, 35 wt% commercial dionyl naphthalene sulfonic acid as the extractant, and 10% 1-tetradecanol as a plasticiser [143]. This PSD exhibited a linear accumulation over a period of 7 days, and was deployed in the field as a water quality monitoring tool to track sources of fecal pollution in storm water drains [299]. Several DGT samplers are described in the literature and are constructed using a protective membrane filter overlaid on a diffusive hydrogel layer, with various sorbent receiving phases assessed including a) zeolite gel comprising microporous hydrated aluminosilicate [138], b) CMI-7000 or Microlite PrCH cation exchange resins [139, 140], c) a mixed inorganic nitrogen binding gel composed of ion exchange resins PrCH and A520E [141], and a mixed binding layer for simultaneous sampling of orthophosphate and ammonium using a micro-sized biochar-zeolite-zirconium oxide binding phase [142]. Both DGT and PIM-based passive samplers for ammonium monitoring are susceptible to interference from dissolved salts and are therefore not able to be used in high salinity matrices, such as estuarine and marine waters.

1.5 General comments and research objectives

Ammonia is an important nutrient in coastal and oceanic waters due to its role in the aquatic nitrogen cycle and its potential to cause eutrophication of marine environments when concentrations are sufficient to cause prolific algal growth [1, 9]. However, in the open ocean and oligotrophic environments the presence of this analyte at trace concentrations (nanomolar) and the high salinity and matrix complexity of the water make its analysis a real challenge [44].

Choosing an appropriate method for a particular environmental water quality monitoring application is important as no method can be universally applied, with every method exhibiting advantages and disadvantages. It is therefore essential to consider a number of important factors such as cost of analysis in terms of operational complexity, ease of instrumental set-up and operation, in addition to sensitivity and accuracy requirements, duration of analysis, reagent stability and potential interferences as well as logistics associated with sample availability and frequency of collection [91].

To ensure water quality standards are maintained now and into the future, it is important to understand the challenges of analysing ammonia in estuarine and marine waters. Historically, flow-based methodologies, such as segmented flow analysis [38, 54], and more recently flow injection analysis [45, 77], and sequential injection analysis [60, 71], have been used to assist with this difficult task. Several flow-based methodologies have been developed for monitoring ammonia in marine waters, and on-line sample pre-treatment strategies employed and different detection methods have been discussed, highlighting the need to improve limits of detection, need for miniaturisation and lower energy consumption, and to reduce and eliminate interferences.

While significant research efforts have been focused on the development of flow-based methodologies for measuring pollutants in aquatic environments, considerable advances have been made over the last three decades to develop passive sampling technologies for water quality monitoring particularly as a diagnostic tool to identify point-source and pollution events [89, 223]. Whilst passive sampling technologies are often semi-quantitative in that laboratory calibration does not always allow for sufficiently accurate C_{TWA} concentrations to be determined, they are an effective screening tool for many important aquatic pollutants, and

they can be used as an early detection method for areas of concern for regulators and water quality managers [91]. The advantages of passive sampling (i.e., affordability, ease of use, minimal sample handling required, and the capacity to provide time-weighted average concentrations of analytes for the period of deployment) make this a desirable technique for routine monitoring of pollutants, especially for identifying pollution hotspots and episodic pollution events.

Different types of passive sampling techniques have been developed to detect a wide range of important aquatic pollutants including both non-polar and polar organics, metallic/organometallic and some inorganic compounds, and a number of passive samplers have been described and evaluated, including for environmental monitoring of seawater [89, 102]. While many PSDs have been developed and applied to freshwater environments, seawater environments pose several additional challenges [102]. While two passive samplers have been developed for the monitoring of ammonium in low salinity freshwater matrices, including DGT- and PIM-based PSDs, these cannot be applied to estuarine or marine environments due to interference from the high concentration of dissolved salts [139, 140, 143].

The objective of this PhD research was therefore to develop novel analytical methods for the monitoring of ammonia in high salinity marine waters and dynamic estuarine environments, able to cover the revised water quality guideline values for high conservation value waters in Australia and New Zealand ($160 \mu\text{g NH}_3\text{-N L}^{-1}$ [3]), and with the additional capability of being able to be used over a wide range of environmental ammonia concentrations.

This thesis is presented in a 'thesis by publication' style and comprises 5 chapters. **Chapters 2, 3 and 4** are experimental chapters, and are written in a style accepted by journals for publication.

Chapter 1 includes a comprehensive literature review of flow methods developed for monitoring total ammonia in high salinity and complex matrices, including in estuarine, coastal, and open ocean environments, the subject of which was published in 2014 in the journal *Trends in Analytical Chemistry*. It also includes a comprehensive review of the passive sampling literature, focussing on PSDs applied to high salinity matrices.

Chapter 2 describes the development of a simple and environmentally-friendly flow-based analyser for the monitoring of total ammonia in marine waters over a wide range of concentrations, without the need to make any changes to the manifold or reagent solutions. This chapter has been published in the journal *Marine Chemistry*. This flow-based analytical system has also been used in the experimental work described in **Chapters 3** and **4** to analyse all samples collected from the sampled medium (generally containing very low ammonia concentrations) as well as the passive samplers' receiving solutions (containing ammonia concentrations several orders of magnitude higher than the sampled medium).

Chapter 3 reports the development of a passive sampler based on gas-diffusion separation, where dissolved molecular ammonia present in the sampled medium diffuses across a hydrophobic porous gas-diffusion membrane into an aqueous receiving solution, where it is accumulated. Since the membrane is only permeable to gaseous species, this approach effectively eliminates the interference of ionic species present in the high salinity sampled medium. This initial design was able to be applied to estuarine and coastal waters for a deployment period of 3-days, however significant biofouling impeded analyte accumulation after a period of 4 days thus limiting the usability of the device for periods longer than 3 days. This chapter has been published in the journal *Talanta*.

Chapter 4 describes a further improvement to the gas-diffusion passive sampling device by adopting an antifouling strategy. A number of biofouling resistance strategies were tested, allowing for a 7-day deployment period to be achieved. Moreover, a single calibration model was developed using a neural network based-calibration approach that was able to take into account the effects of several environmental factors that influence the sampling rate, including the environmental temperature and pH. The newly developed gas-diffusion passive sampling device was successfully applied to a range of field environments, and the neural network-based calibration approach allowed for one calibration only to be employed when the environmental conditions (temperature and pH) varied between different deployment sites. This chapter has been submitted for publication to the journal *Environmental Pollution* and is currently under review.

Chapter 5 summarises the main achievements of the research work described in this thesis, and several improvements are proposed which could be performed in future work.

References

1. Camargo, J.A. and A. Alonso, *Ecological and toxicological effects of inorganic nitrogen pollution in aquatic ecosystems: A global assessment*. Environ. Int., 2006. **32**: p. 831-849.
2. Borja, Á., *The European water framework directive: A challenge for nearshore, coastal and continental shelf research*. Continental Shelf Research, 2005. **25**(14): p. 1768-1783.
3. Batley, G.E. and S.L. Simpson, *Development of guidelines for ammonia in estuarine and marine water systems*. Mar. Pollut. Bull., 2009. **58** (10): p. 1472-1476.
4. ANZG, *Australian and New Zealand guidelines for fresh and marine water quality*. 2018, Australian and New Zealand Governments and Australian state and territory governments: Canberra ACT, Australia.
5. US Environmental Protection Agency, *Ambient Water Quality Criteria for Ammonia (Saltwater), EPA 440/5-88-004*. US EPA Office of Water, Washington, DC, USA. 1989.
6. I. Johnson, N. Sorokin, C. Atkinson, K. Rule, and S.J. Hope, *Proposed environmental quality standards for water framework directive annex viii substances: Ammonia (un-ionised)*, Environment Agency, UK. 2007.
7. Molins-Legua, C., S. Meseguer-Lloret, Y. Moliner-Martinez, and P. Campins-Falco, *A guide for selecting the most appropriate method for ammonium determination in water analysis*. Trends in Analytical Chemistry, 2006. **25**(3): p. 282-290.
8. US Environmental Protection Agency. *Update of Ambient Water Quality Criteria for Ammonia EPA 822-R-99-014*. 1999, US EPA Office of Water: Washington, DC, USA.
9. Vitousek, P.M.A., John D.; Howarth, Robert W.; Likens, Gene E.; Matson, Pamela A.; Schindler, David W.; Schlesinger, William H.; Tilman, David G., *Human Alteration of the Global Nitrogen Cycle: Sources and Consequences*. Ecological Applications, 1997. **7**(3): p. 737-750.
10. Diaz, R.J.R., Rutger, *Spreading Dead Zones and Consequences for marine Ecosystems*. Science, 2008. **321**: p. 926-929.
11. Wilkie, M.P., *Ammonia Excretion and Urea Handling by Fish Gills: Present Understanding and Future Research Challenges*. Journal of Experimental Zoology, 2002. **293**: p. 284-301.
12. Vosyliene, M.Z.S., G.; Kazlauskienė, N. *Fish Physiology, Toxicology, and Water Quality*. in *Proceedings of the Seventh International Symposium*. 2003. Tallinn, Estonia: Ecosystems Research Division.
13. Löscher, C.R., A. Kock, M. Könneke, J. LaRoche, H.W. Bange, and R.A. Schmitz, *Production of oceanic nitrous oxide by ammonia-oxidizing archaea*. Biogeosciences, 2012. **9**(7): p. 2419-2429.
14. United States Environmental Protection Agency. *Overview of Greenhouse Gases*. Accessed 16 August 2013; Available from: <http://epa.gov/climatechange/ghgemissions/gases/n2o.html>.
15. Boesch, D.F., *Challenges and opportunities for science in reducing nutrient over-enrichment in coastal ecosystems*. Estuaries, 2002. **25**: p. 886-900.
16. Pawar, P.R., *Anthropogenic threats to coastal and marine biodiversity : A review*. International Journal of Modern Biological Research, 2016. **4**: p. 35-45.
17. Aminot, A., R. Kérouel, and S. Coverly, *Chapter 8 Nutrients in Seawater Using Segmented Flow Analysis*, in *Practical Guidelines for the Analysis of Seawater*, O. Wurl, Editor. 2009, CRC Press, Taylor & Francis Group: Boca Raton. p. 143.

18. *Salinity in the Oceans in: Seawater: Its Composition, Properties and Behaviour*. 1995, The Open University. p. 29.
19. National Oceanic and Atmospheric Administration. *What is an estuary?* ; Available from: https://oceanservice.noaa.gov/education/tutorial_estuaries/est01_what.html, Accessed: 10 October 2020.
20. Levinton, J.S., *Marine Biology: Function, Biodiversity, Ecology*. Oxford University Press, New York, 3rd.ed. . 1995.
21. Talley, L.D.P., George L.; Emery, William J.; Swift, James H., *Descriptive Physical Oceanography: An Introduction*. 6th ed. 2011, United States: Academic Press.
22. MacKinnon, J., L. St Laurent, and A.C. Naveira Garabato, *Chapter 7 - Diapycnal Mixing Processes in the Ocean Interior*, in *International Geophysics*, G. Siedler, et al., Editors. 2013, Academic Press. p. 159-183.
23. Ma, J., L. Adornato, R.H. Byrne, and D. Yuan, *Determination of nanomolar levels of nutrients in seawater*. TrAC Trends in Analytical Chemistry, 2014. **60**: p. 1-15.
24. Grasshoff, K., M. Ehrhardt, and K. Kremling, *Methods of seawater analysis*. 1983, Weinheim: Verlag Chemie.
25. APHA, *Method 4500-NH₃ C. Titrimetric Method*, in *Standard Methods For the Examination of Water and Wastewater*. 2000, America Public Health Association: Washington, D.C.
26. Watson, R.J., E.C. Butler, L.A. Clementson, and K.M. Berry, *Flow-injection analysis with fluorescence detection for the determination of trace levels of ammonium in seawater*. Journal of Environmental Monitoring, 2005. **7**(1): p. 37-42.
27. Amornthammarong, N. and J.Z. Zhang, *Shipboard fluorometric flow analyzer for high-resolution underway measurement of ammonium in Seawater*. Analytical Chemistry, 2008. **80**(4): p. 1019-1026.
28. *Standard methods for the examination of water and wastewater*. 22nd ed, ed. E.W. Rice and L. Bridgewater. 2012, Washington, D.C.: American Public Health Association, American Water Works Association, Water Environment Federation.
29. Zhang, J., P.B. Ortner, C.J. Fischer, and L.D. Moore, *Method 349.0 Determination of ammonia in estuarine and coastal waters by gas segmented continuous flow colorimetric analysis*. U. S. Environmental Protection Agency, Washington, DC, EPA/600/R-15/013. 1997.
30. U.S. EPA. *Method 350.1: Nitrogen, Ammonia (Colorimetric, Automated Phenate), Revision 2.0*. Cincinnati, OH. 1993.
31. Víctor Cerdà, Jessica Avivar, and A. Cerdá, *Laboratory automation based on flow techniques*. Pure. Appl. Chem. , 2012. **84**: p. 1983-1998.
32. Coverly, S., R. K erouel, and A. Aminot, *A re-examination of matrix effects in the segmented-flow analysis of nutrients in sea and estuarine water*. Analytica Chimica Acta, 2012. **712**(0): p. 94-100.
33. Cerd , V. and C. Pons, *Multicommutated flow techniques for developing analytical methods*. TrAC Trends in Analytical Chemistry, 2006. **25**(3): p. 236-242.
34. Grasshoff, K. and H. Johannsen, *A New Sensitive and Direct Method for the Automatic Determination of Ammonia in Sea Water*. ICES Journal of Marine Science, 1972. **34**(3): p. 516-521.
35. Oliveira, S.M., T. Lopes, I.V. T th, and A.O.S.S. Rangel, *Determination of ammonium in marine waters using a gas diffusion multicommutated flow injection system with in-line*

- prevention of metal hydroxides precipitation*. Journal of Environmental Monitoring, 2009. **11**(1): p. 228-234.
36. Azzaro, F. and M. Galletta, *Automatic colorimetric analyzer prototype for high frequency measurement of nutrients in seawater*. Marine Chemistry, 2006. **99**(1-4): p. 191-198.
 37. T. R. Crompton, *Analysis of Seawater: A Guide for the Analytical and Environmental Chemist*, Springer, Berlin and Heidelberg, Germany. 2006.
 38. Jodo, M., K. Kawamoto, M. Tochimoto, and S.C. Coverly, *Determination of nutrients in seawater by segmented-flow analysis with higher analysis rate and reduced interference on ammonia*. Journal of Automatic Chemistry, 1992. **14**(5): p. 163-167.
 39. Ariza, A.C., P. Linares, M.D.L. Decastro, and M. Valcarcel, *Flow-injection analysis for online monitoring of nutrients (ammonia and nitrite) in aquaculture*. Journal of Automatic Chemistry, 1992. **14**(5): p. 181-183.
 40. Tovar, A., C. Moreno, M.P. Manuel-Vez, and M. Garcia-Vargas, *Simultaneous determination of nutrients (ammonium and phosphate) in marine aquaculture effluents by flow analysis*. Quimica Analitica, 2001. **20**(1): p. 37-45.
 41. Chen, G.H., M. Zhang, Z. Zhang, Y.M. Huang, and D.X. Yuan, *On-line solid phase extraction and spectrophotometric detection with flow technique for the determination of nanomolar level ammonium in seawater samples*. Analytical Letters, 2011. **44**(1-3): p. 310-326.
 42. Li, Q.P., J.Z. Zhang, F.J. Millero, and D.A. Hansell, *Continuous colorimetric determination of trace ammonium in seawater with a long-path liquid waveguide capillary cell*. Marine Chemistry, 2005. **96**(1-2): p. 73-85.
 43. Zhu, Y., D. Yuan, Y. Huang, J. Ma, S. Feng, and K. Lin, *A modified method for on-line determination of trace ammonium in seawater with a long-path liquid waveguide capillary cell and spectrophotometric detection*. Marine Chemistry, 2014. **162**: p. 114-121.
 44. Kodama, T., T. Ichikawa, K. Hidaka, and K. Furuya, *A highly sensitive and large concentration range colorimetric continuous flow analysis for ammonium concentration*. Journal of Oceanography, 2015. **71**(1): p. 65-75.
 45. Muraki, H., K. Higuchi, M. Sasaki, T. Korenaga, and K. Tōei, *Fully automated system for the continuous monitoring of ammonium ion in fish farming plant sea water by flow-injection analysis*. Analytica Chimica Acta, 1992. **261**(1): p. 345-349.
 46. Shoji, T. and E. Nakamura, *Flow injection analysis with spectrophotometry for ammonium ion with 1-naphthol and dichloroisocyanurate*. Journal of Flow Injection Analysis, 2009(26): p. 37-42.
 47. Lin, K., P. Li, Q. Wu, S. Feng, J. Ma, and D. Yuan, *Automated determination of ammonium in natural waters with reverse flow injection analysis based on the indophenol blue method with o-phenylphenol*. Microchemical Journal, 2018. **138**: p. 519-525.
 48. Li, P., Y. Deng, H. Shu, K. Lin, N. Chen, Y. Jiang, J. Chen, D. Yuan, and J. Ma, *High-frequency underway analysis of ammonium in coastal waters using an integrated syringe-pump-based environmental-water analyzer (iSEA)*. Talanta, 2019. **195**: p. 638-646.
 49. Hashihama, F., J. Kanda, A. Tauchi, T. Kodama, H. Saito, and K. Furuya, *Liquid waveguide spectrophotometric measurement of nanomolar ammonium in seawater based on the indophenol reaction with o-phenylphenol (OPP)*. Talanta, 2015. **143**: p. 374-380.

50. Y. Liang, Y. Pan, Q. Guo, H. Hu, C. Wu, and Q. Zhang, *A novel analytical method for trace ammonium in freshwater and seawater using 4-methoxyphthalaldehyde as fluorescent reagent*. *J. Anal. Methods. Chem*, 2015. **2015**(387207).
51. Zhang, M., T. Zhang, Y. Liang, and Y. Pan, *Toward sensitive determination of ammonium in field: A novel fluorescent probe, 4,5-dimethoxyphthalaldehyde along with a hand-held portable laser diode fluorometer*. *Sensors and Actuators B: Chemical*, 2018. **276**: p. 356-361.
52. Ma, J., P. Li, K. Lin, Z. Chen, N. Chen, K. Liao, and D. Yuan, *Optimization of a salinity-interference-free indophenol method for the determination of ammonium in natural waters using o-phenylphenol*. *Talanta*, 2018. **179**: p. 608-614.
53. Mansour, F.R. and N.D. Danielson, *Reverse flow-injection analysis*. *TrAC Trends in Analytical Chemistry*, 2012. **40**: p. 1-14.
54. K erouel, R. and A. Aminot, *Fluorometric determination of ammonia in sea and estuarine waters by direct segmented flow analysis*. *Marine Chemistry*, 1997. **57**(3): p. 265-275.
55. Jones, R.D., *An improved fluorescence method for the determination of nanomolar concentrations of ammonium in natural waters*. *Limnology and Oceanography*, 1991. **36**(4): p. 814-819.
56. P ascoa, R.N.M.J., I.V. T oth, and A.O.S.S. Rangel, *Review on recent applications of the liquid waveguide capillary cell in flow based analysis techniques to enhance the sensitivity of spectroscopic detection methods*. *Analytica Chimica Acta*, 2012. **739**: p. 1-13.
57. Cerd a, A., M.T. Oms, R. Forteza, and V. Cerd a, *Evaluation of flow injection methods for ammonium determination in wastewater samples*. *Anal. Chim. Acta*, 1995. **311**(2): p. 165-173.
58. Van Son, M., R.C. Schothorst, and G. Den Boef, *Determination of total ammoniacal nitrogen in water by flow-injection analysis and a gas-diffusion membrane*. *Analytica Chimica Acta*, 1983. **153**: p. 271-275.
59. Gray, S.M., P.S. Ellis, M.R. Grace, and I.D. McKelvie, *Spectrophotometric determination of ammonia in estuarine waters by hybrid reagent-injection gas-diffusion flow analysis*. *Spectroscopy Letters*, 2006. **39**(6): p. 737-753.
60. Segundo, R.A., R.B.R. Mesquita, M. Ferreira, C. Teixeira, A.A. Bordalo, and A.O.S.S. Rangel, *Development of a sequential injection gas diffusion system for the determination of ammonium in transitional and coastal waters*. *Analytical Methods*, 2011. **3**(9): p. 2049-2055.
61. Hunter, D.A. and R.F. Uglow, *A technique for the measurement of total ammonia in small volumes of seawater and hemolymph*. *Ophelia*, 1993. **37**(1): p. 31-40.
62. Plant, J.N., K.S. Johnson, J.A. Needoba, and L.J. Coletti, *NH₄-Digiscan: an in situ and laboratory ammonium analyzer for estuarine, coastal, and shelf waters*. *Limnology and Oceanography-Methods*, 2009. **7**: p. 144-156.
63. Henr quez, C., B. Horstkotte, and C. V ctor, *Conductometric determination of ammonium by a multisyringe flow injection system applying gas diffusion*. *International Journal of Environmental Analytical Chemistry*, 2013. **93**(12): p. 1236-1252.
64. Henr quez, C., B. Horstkotte, and V. Cerd a, *A highly reproducible solenoid micropump system for the analysis of total inorganic carbon and ammonium using gas-diffusion with conductimetric detection*. *Talanta*, 2014. **118**: p. 186-194.

65. Šrámková, I., B. Horstkotte, H. Sklenářová, P. Solich, and S.D. Kolev, *A novel approach to Lab-In-Syringe Head-Space Single-Drop Microextraction and on-drop sensing of ammonia*. *Analytica Chimica Acta*, 2016. **934**: p. 132-144.
66. Willason, S.W. and K.S. Johnson, *A rapid, highly sensitive technique for the determination of ammonia in seawater*. *Marine Biology*, 1986. **91**(2): p. 285-290.
67. Gibb, S.W., R.F.C. Mantoura, and P.S. Liss, *Analysis of ammonia and methylamines in natural waters by flow-injection gas-diffusion coupled to ion chromatography*. *Analytica Chimica Acta*, 1995. **316**(3): p. 291-304.
68. Gibb, S.W., J.W. Wood, R. Fauzi, and C. Mantoura, *Automation of flow injection gas diffusion ion chromatography for the nanomolar determination of methylamines and ammonia in seawater and atmospheric samples*. *Journal of Automatic Chemistry*, 1995. **17**(6): p. 205-212.
69. Zhu, Y., D. Yuan, H. Lin, and T. Zhou, *Determination of Ammonium in Seawater by Purge-and-Trap and Flow Injection with Fluorescence Detection*. *Analytical Letters*, 2016. **49**(5): p. 665-675.
70. Oliveira, S.M., T.I.M.S. Lopes, I.V. Tóth, and A.O.S.S. Rangel, *A multi-commuted flow injection system with a multi-channel propulsion unit placed before detection: Spectrophotometric determination of ammonium*. *Analytica Chimica Acta*, 2007. **600**(1–2): p. 29-34.
71. Kolev, S.D., P.R.L.V. Fernandes, D. Satinsky, and P. Solich, *Highly sensitive gas-diffusion sequential injection analysis based on flow manipulation*. *Talanta*, 2009. **79**(4): p. 1021-1025.
72. Wang, P.-Y., J.-Y. Wu, H.-J. Chen, T.-Y. Lin, and C.-H. Wu, *Purge-and-trap ion chromatography for the determination of trace ammonium ion in high-salinity water samples*. *Journal of Chromatography A*, 2008. **1188**(2): p. 69-74.
73. Ferreira, F.N., J.C. Afonso, F.V.M. Pontes, M.C. Carneiro, A.A. Neto, M.L.B. Tristão, and M.I.C. Monteiro, *Determination of low-molecular-weight amines and ammonium in saline waters by ion chromatography after their extraction by steam distillation*. *Journal of Separation Science*, 2016. **39**(8): p. 1454-1460.
74. Ferreira, F.N., J.C. Afonso, F.V.M. Pontes, M.C. Carneiro, A.A. Neto, R.E. Junior, and M.I.C. Monteiro, *Ultrasound-assisted purge-and-trap extraction for simultaneous determination of low-molecular weight amines and ammonium in high salinity waters by ion chromatography*. *Microchemical Journal*, 2017. **133**: p. 658-662.
75. Hongzhi Hu, Ying Liang, Shuo Li, Qing Guo, and C. Wu, *A modified o-phthalaldehyde fluorometric analytical method for ultratrace ammonium in natural waters using EDTA-NaOH as buffer*. *J. Anal. Methods. Chem*, 2014. **2014**(728068).
76. Masserini, R.T. and K.A. Fanning, *A sensor package for the simultaneous determination of nanomolar concentrations of nitrite, nitrate, and ammonia in seawater by fluorescence detection*. *Marine Chemistry*, 2000. **68**(4): p. 323-333.
77. Aminot, A., R. Kérouel, and D. Birot, *A flow injection-fluorometric method for the determination of ammonium in fresh and saline waters with a view to in situ analyses*. *Water Research*, 2001. **35**(7): p. 1777-1785.
78. Abi Kaed Bey, S.K., D.P. Connelly, F.-E. Legiret, A.J.K. Harris, and M.C. Mowlem, *A high-resolution analyser for the measurement of ammonium in oligotrophic seawater*. *Ocean Dynamics*, 2011. **61**(10): p. 1555-1565.

79. Frank, C., F. Schroeder, R. Ebinghaus, and W. Ruck, *A fast sequential injection analysis system for the simultaneous determination of ammonia and phosphate*. *Microchimica Acta*, 2006. **154**(1-2): p. 31-38.
80. Frank, C. and F. Schroeder, *Using sequential injection analysis to improve system and data reliability of online methods: Determination of ammonium and phosphate in coastal waters*. *Journal of Automated Methods & Management in Chemistry*, 2007. **2007**(49535): p. 1-6.
81. Horstkotte, B., C.M. Duarte, and V. Cerdà, *A miniature and field-applicable multipumping flow analyzer for ammonium monitoring in seawater with fluorescence detection*. *Talanta*, 2011. **85**(1): p. 380-385.
82. Amornthammarong, N., J.Z. Zhang, and P.B. Ortner, *An autonomous batch analyzer for the determination of trace ammonium in natural waters using fluorometric detection*. *Analytical Methods*, 2011. **3**(7): p. 1501-1506.
83. Amornthammarong, N., J.Z. Zhang, P.B. Ortner, J. Stamates, M. Shoemaker, and M.W. Kindel, *A portable analyser for the measurement of ammonium in marine waters*. *Environmental Science-Processes & Impacts*, 2013. **15**(3): p. 579-584.
84. Zhu, Y., D. Yuan, Y. Huang, J. Ma, and S. Feng, *A sensitive flow-batch system for on board determination of ultra-trace ammonium in seawater: method development and shipboard application*. *Analytica chimica acta*, 2013. **794**: p. 47-54.
85. Y. Zhu, J. Chen, X. Shi, D. Yuan, S. Feng, T. Zhou, and Y. Huang, *Development and application of a portable fluorescence detector for shipboard analysis of ammonium in estuarine and coastal waters*. *Analytical methods*, 2018. **v. 10**(no. 15): p. pp. 1781-1787-2018 v.10 no.15.
86. Genfa, Z. and P.K. Dasgupta, *Fluorometric measurement of aqueous ammonium ion in a flow injection system*. *Analytical Chemistry*, 1989. **61**(5): p. 408-412.
87. APHA, *Method 4500-NH₃ F. Phenate Method in Standard Methods For the Examination of Water and Wastewater*. 2000, America Public Health Association: Washington, D.C.
88. Taylor, A.C., G.R. Fones, B. Vrana, and G.A. Mills, *Applications for Passive Sampling of Hydrophobic Organic Contaminants in Water—A Review*. *Critical Reviews in Analytical Chemistry*, 2019: p. 1-35.
89. Vrana, B., I.J. Allan, R. Greenwood, G.A. Mills, E. Dominiak, K. Svensson, J. Knutsson, and G. Morrison, *Passive sampling techniques for monitoring pollutants in water*. *TrAC Trends Anal. Chem.*, 2005. **24** (10): p. 845-868.
90. Novic, A.J., D.S. O'Brien, S.L. Kaserzon, D.W. Hawker, S.E. Lewis, and J.F. Mueller, *Monitoring Herbicide Concentrations and Loads during a Flood Event: A Comparison of Grab Sampling with Passive Sampling*. *Environ. Sci. Tech.*, 2017. **51**(7): p. 3880-3891.
91. Dressing, S.A., D.W. Meals, J.B. Harcum, J. Spooner, J.B. Stribling, R.P. Richards, C.J. Millard, S.A. Lanberg, and J.G. O'Donnell. *Monitoring and Evaluating Nonpoint Source Watershed Projects*. 2016 10 October 2020]; Available from: <https://www.epa.gov/polluted-runoff-nonpoint-source-pollution/monitoring-and-evaluating-nonpoint-source-watershed>.
92. Lohmann, R. and D. Muir, *Global Aquatic Passive Sampling (AQUA-GAPS): Using Passive Samplers to Monitor POPs in the Waters of the World*. *Environmental Science & Technology*, 2010. **44**(3): p. 860-864.
93. ISO (International Organisation for Standardisation), *ISO 5667-23:2011 Water Quality - Sampling - Part 23: Guidance on Passive Sampling in Surface Waters; ISO (International Organisation for Standardisation)*. 2011: Switzerland.

94. Miège, C., N. Mazzella, I. Allan, V. Dulio, F. Smedes, C. Tixier, E. Vermeirssen, J. Brant, S. O'Toole, H. Budzinski, J.-P. Ghestem, P.-F. Staub, S. Lardy-Fontan, J.-L. Gonzalez, M. Coquery, and B. Vrana, *Position paper on passive sampling techniques for the monitoring of contaminants in the aquatic environment – Achievements to date and perspectives*. TrAC Trends Anal. Chem., 2015. **8**: p. 20-26.
95. Lohmann, R., D. Muir, E.Y. Zeng, L.-J. Bao, I.J. Allan, K. Arinaitwe, K. Booij, P. Helm, S. Kaserzon, J.F. Mueller, Y. Shibata, F. Smedes, M. Tsapakis, C.S. Wong, and J. You, *Aquatic Global Passive Sampling (AQUA-GAPS) Revisited: First Steps toward a Network of Networks for Monitoring Organic Contaminants in the Aquatic Environment*. Environmental Science & Technology, 2017. **51**(3): p. 1060-1067.
96. Booij, K., C.D. Robinson, R.M. Burgess, P. Mayer, C.A. Roberts, L. Ahrens, I.J. Allan, J. Brant, L. Jones, U.R. Kraus, M.M. Larsen, P. Lepom, J. Petersen, D. Pröfrock, P. Roose, S. Schäfer, F. Smedes, C. Tixier, K. Vorkamp, and P. Whitehouse, *Passive Sampling in Regulatory Chemical Monitoring of Nonpolar Organic Compounds in the Aquatic Environment*. Environ. Sci. Technol., 2016. **50** (1): p. 3-17.
97. Miège, C., S. Schiavone, A. Dabrin, M. Coquery, N. Mazzella, C. Berho, J.P. Ghestem, A. Togola, C. Gonzalez, J.L. Gonzalez, B. Lalere, S. Lardy-Fontan, B. Lepot, D. Munaron, and C. Tixier, *An in situ intercomparison exercise on passive samplers for monitoring metals, polycyclic aromatic hydrocarbons and pesticides in surface waters*. TrAC Trends in Analytical Chemistry, 2012. **36**: p. 128-143.
98. Górecki, T. and J. Namieśnik, *Passive sampling*. TrAC Trends in Analytical Chemistry, 2002. **21**(4): p. 276-291.
99. Booij, K., B. Vrana, J.N. Huckins, R. Greenwood, G. Mills, and B. Vrana, *Chapter 7 Theory, modelling and calibration of passive samplers used in water monitoring*, in *Comprehensive Analytical Chemistry*. 2007, Elsevier. p. 141-169.
100. Mayer, P., J. Tolls, J.L.M. Hermens, and D. Mackay, *Equilibrium Sampling Devices*. Environmental Science & Technology, 2003. **37**(9): p. 184A-191A.
101. Salim, F. and T. Górecki, *Theory and modelling approaches to passive sampling*. Environmental Science: Processes & Impacts, 2019. **21**(10): p. 1618-1641.
102. Schintu, M., A. Marrucci, and B. Marras, *Passive Sampling Technologies for the Monitoring of Organic and Inorganic Contaminants in Seawater*, in *Current Environmental Issues and Challenges*, G. Cao and R. Orrù, Editors. 2014, Springer Netherlands: Dordrecht. p. 217-237.
103. Booij, K., H.E. Hofmans, C.V. Fischer, and E.M. Van Weerlee, *Temperature-Dependent Uptake Rates of Nonpolar Organic Compounds by Semipermeable Membrane Devices and Low-Density Polyethylene Membranes*. Environmental Science & Technology, 2003. **37**(2): p. 361-366.
104. Gong, X., K. Li, C. Wu, L. Wang, and H. Sun, *Passive sampling for monitoring polar organic pollutants in water by three typical samplers*. Trends in Environmental Analytical Chemistry, 2018. **17**: p. 23-33.
105. Valenzuela, E.F., H.C. Menezes, and Z.L. Cardeal, *Passive and grab sampling methods to assess pesticide residues in water. A review*. Environmental Chemistry Letters, 2020.
106. Huckins, J.N., J.D. Petty, J.A. Lebo, F.V. Almeida, K. Booij, D.A. Alvarez, W.L. Cranor, R.C. Clark, and B.B. Mogensen, *Development of the Permeability/Performance Reference Compound Approach for In Situ Calibration of Semipermeable Membrane Devices*. Environmental Science & Technology, 2002. **36**(1): p. 85-91.

107. Harman, C., I.J. Allan, and P.S. B auerlein, *The Challenge of Exposure Correction for Polar Passive Samplers—The PRC and the POCIS*. Environmental Science & Technology, 2011. **45**(21): p. 9120-9121.
108. Petersen, J., A. Paschke, R. Gunold, and G. Sch u rmann, *Calibration of Chemcatcher® passive sampler for selected highly hydrophobic organic substances under fresh and sea water conditions*. Environmental Science: Water Research & Technology, 2015. **1**(2): p. 218-226.
109. Godlewska, K., P. Stepnowski, and M. Paszkiewicz, *Application of the Polar Organic Chemical Integrative Sampler for Isolation of Environmental Micropollutants – A Review*. Critical Reviews in Analytical Chemistry, 2020. **50**(1): p. 1-28.
110. Manov, D.V., G.C. Chang, and T.D. Dickey, *Methods for Reducing Biofouling of Moored Optical Sensors*. Journal of Atmospheric and Oceanic Technology, 2004. **21**(6): p. 958-968.
111. Smith, M.J., A. Kerr, and M.J. Cowling, *Effects of marine biofouling on gas sensor membrane materials*. J. Environ. Monitor., 2007. **9**(12): p. 1378-1386.
112. Nandakumar, K. and T. Yano, *Biofouling and Its Prevention: A Comprehensive Overview*. Biocontrol Science, 2003. **8**(4): p. 133-144.
113. Morin, N., C. Mi ege, M. Coquery, and J. Randon, *Chemical calibration, performance, validation and applications of the polar organic chemical integrative sampler (POCIS) in aquatic environments*. TrAC Trends in Analytical Chemistry, 2012. **36**: p. 144-175.
114. Charriau, A., S. Lissalde, G. Poulier, N. Mazzella, R. Buzier, and G. Guibaud, *Overview of the Chemcatcher® for the passive sampling of various pollutants in aquatic environments Part A: Principles, calibration, preparation and analysis of the sampler*. Talanta, 2016. **148**: p. 556-571.
115. Galceran, J. and J. Puy, *Interpretation of diffusion gradients in thin films (DGT) measurements: a systematic approach*. Environmental Chemistry, 2015. **12**(2): p. 112-122.
116. Booij, K., R. van Bommel, A. Mets, and R. Dekker, *Little effect of excessive biofouling on the uptake of organic contaminants by semipermeable membrane devices*. Chemosphere, 2006. **65**(11): p. 2485-2492.
117. Richardson, B.J., P.K.S. Lam, G.J. Zheng, K.E. McClellan, and S.B. De Luca-Abbott, *Biofouling confounds the uptake of trace organic contaminants by semi-permeable membrane devices (SPMDs)*. Marine Pollution Bulletin, 2002. **44**(12): p. 1372-1379.
118. Huckins, J.N., K. Booij, and J.D. Petty, *Monitors of Organic Chemicals in the Environment: Semipermeable Membrane Devices*, ed. J.N. Huckins, K. Booij, and J.D. Petty. 2006, Boston, MA: Springer US.
119. Ellis, G.S., C.E. Rostad, J.N. Huckins, C.J. Schmitt, J.D. Petty, and P. Maccarthy, *Evaluation of lipid-containing semipermeable membrane devices for monitoring organochlorine contaminants in the Upper Mississippi river*. Environmental Toxicology and Chemistry, 1995. **14**(11): p. 1875-1884.
120. Sch afer, R.B., A. Paschke, and M. Liess, *Aquatic passive sampling of a short-term thiacloprid pulse with the Chemcatcher: impact of biofouling and use of a diffusion-limiting membrane on the sampling rate*. J Chromatogr A, 2008. **1203**(1): p. 1-6.
121. Harman, C., O. B oyum, K.V. Thomas, and M. Grung, *Small but Different Effect of Fouling on the Uptake Rates of Semipermeable Membrane Devices and Polar Organic Chemical Integrative Samplers*. Environmental Toxicology and Chemistry, 2009. **28**(11): p. 2324-2332.

122. Devillers, D., R. Buzier, M. Grybos, A. Charriau, and G. Guibaud, *Key role of the sorption process in alteration of metal and metalloid quantification by fouling development on DGT passive samplers*. Environmental Pollution, 2017. **230**: p. 523-529.
123. Díez, S. and R. Giaggio, *Do biofilms affect the measurement of mercury by the DGT technique? Microcosm and field tests to prevent biofilm growth*. Chemosphere, 2018. **210**: p. 692-698.
124. Feng, Z., P. Zhu, H. Fan, S. Piao, L. Xu, and T. Sun, *Effect of Biofilm on Passive Sampling of Dissolved Orthophosphate Using the Diffusive Gradients in Thin Films Technique*. Analytical Chemistry, 2016. **88**(13): p. 6836-6843.
125. Uher, E., H. Zhang, S. Santos, M.-H. Tusseau-Vuillemin, and C. Gourlay-Francé, *Impact of Biofouling on Diffusive Gradient in Thin Film Measurements in Water*. Analytical Chemistry, 2012. **84**(7): p. 3111-3118.
126. Pichette, C., H. Zhang, W. Davison, and S. Sauvé, *Preventing biofilm development on DGT devices using metals and antibiotics*. Talanta, 2007. **72**(2): p. 716-722.
127. Namieśnik, J., B. Zabiegała, A. Kot-Wasik, M. Partyka, and A. Wasik, *Passive sampling and/or extraction techniques in environmental analysis: a review*. Analytical and Bioanalytical Chemistry, 2005. **381**(2): p. 279-301.
128. Stuer-Lauridsen, F., *Review of passive accumulation devices for monitoring organic micropollutants in the aquatic environment*. Environmental Pollution, 2005. **136**(3): p. 503-524.
129. Kot-Wasik, A., B. Zabiegała, M. Urbanowicz, E. Dominiak, A. Wasik, and J. Namieśnik, *Advances in passive sampling in environmental studies*. Analytica Chimica Acta, 2007. **602**(2): p. 141-163.
130. Mills, G.A., R. Greenwood, B. Vrana, I.J. Allan, and T. Ocelka, *Measurement of environmental pollutants using passive sampling devices – a commentary on the current state of the art*. Journal of Environmental Monitoring, 2011. **13**(11): p. 2979-2982.
131. Mills, G.A., A. Gravell, B. Vrana, C. Harman, H. Budzinski, N. Mazzella, and T. Ocelka, *Measurement of environmental pollutants using passive sampling devices – an updated commentary on the current state of the art*. Environmental Science: Processes & Impacts, 2014. **16**(3): p. 369-373.
132. Warnken, K.W., H. Zhang, and W. Davison, *Chapter 11 In situ monitoring and dynamic speciation measurements in solution using DGT*, in *Comprehensive Analytical Chemistry*, R. Greenwood, G. Mills, and B. Vrana, Editors. 2007, Elsevier. p. 251-278.
133. Harman, C., I.J. Allan, and E.L.M. Vermeirssen, *Calibration and use of the polar organic chemical integrative sampler--a critical review*. Environmental toxicology and chemistry, 2012. **31**(12): p. 2724-2738.
134. Guibal, R., R. Buzier, S. Lissalde, and G. Guibaud, *Adaptation of diffusive gradients in thin films technique to sample organic pollutants in the environment: An overview of o-DGT passive samplers*. Science of The Total Environment, 2019. **693**: p. 133537.
135. Taylor, A.C., G.R. Fones, and G.A. Mills, *Trends in the use of passive sampling for monitoring polar pesticides in water*. Trends in Environmental Analytical Chemistry, 2020. **27**: p. e00096.
136. Kot, A., B. Zabiegała, and J. Namieśnik, *Passive sampling for long-term monitoring of organic pollutants in water*. TrAC Trends in Analytical Chemistry, 2000. **19**(7): p. 446-459.
137. Mills, G.A., G.R. Fones, K. Booij, and R. Greenwood, *Passive Sampling Technologies*, in *Chemical Marine Monitoring: Policy Framework and Analytical Trends*, Philippe

- Quevauviller, Patrick Roose, and G. Verreet., Editors. 2011, John Wiley & Sons, Inc. p. 397-432.
138. Feng, Z., T. Guo, Z. Jiang, and T. Sun, *Sampling of ammonium ion in water samples by using the diffusive-gradients-in-thin-films technique (DGT) and a zeolite based binding phase*. *Microchimica Acta*, 2015. **182**(15): p. 2419-2425.
 139. Huang, J., W.W. Bennett, D.T. Welsh, and P.R. Teasdale, *Determining time-weighted average concentrations of nitrate and ammonium in freshwaters using DGT with ion exchange membrane-based binding layers*. *Environ. Sci. Proc. Imp.*, 2016. **18** (12): p. 1530-1539.
 140. Huang, J., W.W. Bennett, D.T. Welsh, T. Li, and P.R. Teasdale, *Development and evaluation of a diffusive gradients in a thin film technique for measuring ammonium in freshwaters*. *Anal. Chim. Acta*, 2016. **904** (Supplement C): p. 83-91.
 141. Huang, J., W.W. Bennett, P.R. Teasdale, N.R. Kankanamge, and D.T. Welsh, *A modified DGT technique for the simultaneous measurement of dissolved inorganic nitrogen and phosphorus in freshwaters*. *Anal. Chim. Acta*, 2017. **988**: p. 17-26.
 142. Feng, Z., N. Wang, M. He, L. Yang, Y. Wang, and T. Sun, *Simultaneous sampling of dissolved orthophosphate and ammonium in freshwaters using diffusive gradients in thin films with a mixed binding phase*. *Talanta*, 2018. **186**: p. 176-182.
 143. Almeida, M.I.G.S., A.M. Silva, R.A. Coleman, V.J. Pettigrove, R.W. Cattrall, and S.D. Kolev, *Development of a passive sampler based on a polymer inclusion membrane for total ammonia monitoring in freshwaters*. *Anal. Bioanal. Chem.*, 2016. **408** (12): p. 3213-22.
 144. Huckins, J.N., M.W. Tubergen, and G.K. Manuweera, *Semipermeable membrane devices containing model lipid: A new approach to monitoring the bioavailability of lipophilic contaminants and estimating their bioconcentration potential*. *Chemosphere*, 1990. **20**(5): p. 533-552.
 145. Esteve-Turrillas, F.A., A. Pastor, V. Yusà, and M. de la Guardia, *Using semi-permeable membrane devices as passive samplers*. *TrAC Trends in Analytical Chemistry*, 2007. **26**(7): p. 703-712.
 146. Esteve-Turrillas, F.A., V. Yusà, A. Pastor, and M. de la Guardia, *New perspectives in the use of semipermeable membrane devices as passive samplers*. *Talanta*, 2008. **74**(4): p. 443-457.
 147. Huckins, J.N., K. Booij, and J.D. Petty, *Chapter 2 Fundamentals of SPMDs*, in *Monitors of Organic Chemicals in the Environment, Semipermeable Membrane Devices*. 2006, Springer: Boston, MA.
 148. Moldoveanu, S. and V. David, *Chapter 5 - Phase Transfer in Sample Preparation*, in *Modern Sample Preparation for Chromatography*, S. Moldoveanu and V. David, Editors. 2015, Elsevier: Amsterdam. p. 105-130.
 149. Huckins, J.N., H.F. Prest, J.D. Petty, J.A. Lebo, M.M. Hodgins, R.C. Clark, D.A. Alvarez, W.R. Gala, A. Steen, R. Gale, and C.G. Ingersoll, *Overview and comparison of lipid-containing semipermeable membrane devices and oysters (*Crassostrea gigas*) for assessing organic chemical exposure*. *Environmental Toxicology and Chemistry*, 2004. **23**(7): p. 1617-1628.
 150. Huckins, J.N., K. Booij, and J.D. Petty, *Chapter 4 Study Considerations*, in *Monitors of Organic Chemicals in the Environment, Semipermeable Membrane Devices*. 2006, Springer: Boston, MA.

151. NOAA. *Semipermeable Membrane Devices*. 2013 Revised April 16 2013 [cited 2020 16 April 2020]; Available from: <http://oceanexplorer.noaa.gov/technology/tools/spmds/spmds.html>.
152. Booij, K., R. van Bommel, H.M. van Aken, H. van Haren, G.-J.A. Brummer, and H. Ridderinkhof, *Passive sampling of nonpolar contaminants at three deep-ocean sites*. Environmental Pollution, 2014. **195**: p. 101-108.
153. Huckins, J.N., G.K. Manuweera, J.D. Petty, D. Mackay, and J.A. Lebo, *Lipid-containing semipermeable membrane devices for monitoring organic contaminants in water*. Environmental Science & Technology, 1993. **27**(12): p. 2489-2496.
154. Booij, K., H.M. Sleiderink, and F. Smedes, *Calibrating the uptake kinetics of semipermeable membrane devices using exposure standards*. Environmental Toxicology and Chemistry, 1998. **17**(7): p. 1236-1245.
155. Huckins, J.N., K. Booij, and J.D. Petty, *Chapter 3 Theory and Modelling*, in *Monitors of Organic Chemicals in the Environment, Semipermeable Membrane Devices*. 2006, Springer: Boston, MA. p. 45-85.
156. Chang, W.-T., M.-D. Fang, C.-L. Lee, and P. Brimblecombe, *Measuring bioavailable PAHs in estuarine water using semipermeable membrane devices with performance reference compounds*. Mar. Pollut. Bull., 2014. **89**(1): p. 376-383.
157. Bustamante, J., G. Arana, A. de Diego, and J.M. Madariaga, *The use of SPMDs and implanted oysters for monitoring PAHs and PCBs in an aquatic environment in the estuary of Urdaibai (Western Pyrenees)*. Environmental Engineering & Management Journal (EEMJ), 2012. **11**(9): p. 1707-1714.
158. Vetter, W., P. Haase-Aschoff, N. Rosenfelder, T. Komarova, and J.F. Mueller, *Determination of Halogenated Natural Products in Passive Samplers Deployed along the Great Barrier Reef, Queensland/Australia*. Environmental Science & Technology, 2009. **43**(16): p. 6131-6137.
159. Shaw, M. and J.F. Müller, *Preliminary evaluation of the occurrence of herbicides and PAHs in the Wet Tropics region of the Great Barrier Reef, Australia, using passive samplers*. Marine Pollution Bulletin, 2005. **51**(8): p. 876-881.
160. Schintu, M., A. Marrucci, B. Marras, M. Atzori, and D. Pellegrini, *Passive sampling monitoring of PAHs and trace metals in seawater during the salvaging of the Costa Concordia wreck (Parbuckling Project)*. Marine Pollution Bulletin, 2018. **135**: p. 819-827.
161. Cleveland, L., E.E. Little, J.D. Petty, B.T. Johnson, J.A. Lebo, C.E. Orazio, J. Dionne, and A. Crockett, *Toxicological and chemical screening of Antarctica sediments: Use of whole sediment toxicity tests, microtox, mutatox and semipermeable membrane devices (SPMDs)*. Marine Pollution Bulletin, 1997. **34**(3): p. 194-202.
162. Booij, K. and B.L. van Drooge, *Polychlorinated biphenyls and hexachlorobenzene in atmosphere, sea-surface microlayer, and water measured with semi-permeable membrane devices (SPMDs)*. Chemosphere, 2001. **44**(2): p. 91-98.
163. Zhao, Z., L. Zhang, J. Wu, and C. Fan, *Application of Semipermeable Membrane Devices (SPMDs) and Benthic Mussels to Evaluate the Bioavailability of Sediment-associated DDTs*. Soil and Sediment Contamination: An International Journal, 2013. **22**(3): p. 351-364.
164. Hong, Y., D. Wetzel, E.L. Pulster, P. Hull, D. Reible, H.-M. Hwang, P. Ji, E. Rifkin, and E. Bouwer, *Significant spatial variability of bioavailable PAHs in water column and sediment porewater in the Gulf of Mexico 1 year after the Deepwater Horizon oil spill*. Environmental Monitoring and Assessment, 2015. **187**(10): p. 646.

165. Eek, E., G. Cornelissen, and G.D. Breedveld, *Field Measurement of Diffusional Mass Transfer of HOCs at the Sediment-Water Interface*. Environmental Science & Technology, 2010. **44**(17): p. 6752-6759.
166. Baussant, T., S. Sanni, G. Jonsson, A. Skadsheim, and J.F. Børseth, *Bioaccumulation of polycyclic aromatic compounds: 1. Bioconcentration in two marine species and in semipermeable membrane devices during chronic exposure to dispersed crude oil*. Environmental Toxicology and Chemistry, 2001. **20**(6): p. 1175-1184.
167. Granmo, Å., R. Ekelund, M. Berggren, E. Brorström-Lundén, and P.-A. Bergqvist, *Temporal Trend of Organochlorine Marine Pollution Indicated by Concentrations in Mussels, Semipermeable Membrane Devices, and Sediment*. Environmental Science & Technology, 2000. **34**(16): p. 3323-3329.
168. Booij, K., F. Smedes, E.M. Van Weerlee, and P.J.C. Honkoop, *Environmental Monitoring of Hydrophobic Organic Contaminants: The Case of Mussels versus Semipermeable Membrane Devices*. Environmental Science & Technology, 2006. **40**(12): p. 3893-3900.
169. Bergqvist, P.-A., B. Strandberg, R. Ekelund, C. Rappe, and Å. Granmo, *Temporal Monitoring of Organochlorine Compounds in Seawater by Semipermeable Membranes following a Flooding Episode in Western Europe*. Environmental Science & Technology, 1998. **32**(24): p. 3887-3892.
170. Zhao, D., P. Zhang, L. Ge, G.J. Zheng, X. Wang, W. Liu, and Z. Yao, *The legacy of organochlorinated pesticides (OCPs), polycyclic aromatic hydrocarbons (PAHs) and polychlorinated biphenyls (PCBs) in Chinese coastal seawater monitored by semi-permeable membrane devices (SPMDs)*. Marine Pollution Bulletin, 2018. **137**: p. 222-230.
171. Shaw, M., M.J. Furnas, K. Fabricius, D. Haynes, S. Carter, G. Eaglesham, and J.F. Müller, *Monitoring pesticides in the Great Barrier Reef*. Marine Pollution Bulletin, 2010. **60**(1): p. 113-122.
172. Shaw, M., I.R. Tibbetts, and J.F. Müller, *Monitoring PAHs in the Brisbane River and Moreton Bay, Australia, using semipermeable membrane devices and EROD activity in yellowfin bream, *Acanthopagrus australis**. Chemosphere, 2004. **56**(3): p. 237-246.
173. Røe Utvik, T.I. and S.a. Johnsen, *Bioavailability of Polycyclic Aromatic Hydrocarbons in the North Sea*. Environmental Science & Technology, 1999. **33**(12): p. 1963-1969.
174. Marrucci, A., B. Marras, S.S. Campisi, and M. Schintu, *Using SPMDs to monitor the seawater concentrations of PAHs and PCBs in marine protected areas (Western Mediterranean)*. Marine Pollution Bulletin, 2013. **75**(1): p. 69-75.
175. Berge, J.A., K. Hylland, M. Schlabach, and A. Ruus, *Accumulation of Polychlorinated Dibenzo-p-Dioxins and Furans in Atlantic Cod (*Gadus morhua*)—Cage Experiments in a Norwegian Fjord*. Journal of Toxicology and Environmental Health, Part A, 2011. **74**(7-9): p. 455-465.
176. Cornelissen, G., K. Wiberg, D. Broman, H.P.H. Arp, Y. Persson, K. Sundqvist, and P. Jonsson, *Freely Dissolved Concentrations and Sediment-Water Activity Ratios of PCDD/Fs and PCBs in the Open Baltic Sea*. Environmental Science & Technology, 2008. **42**(23): p. 8733-8739.
177. Roach, A.C., R. Muller, T. Komarova, R. Symons, G.J. Stevenson, and J.F. Mueller, *Using SPMDs to monitor water column concentrations of PCDDs, PCDFs and dioxin-like PCBs in Port Jackson (Sydney Harbour), Australia*. Chemosphere, 2009. **75**(9): p. 1243-1251.

178. Booij, K., B.N. Zegers, and J.P. Boon, *Levels of some polybrominated diphenyl ether (PBDE) flame retardants along the Dutch coast as derived from their accumulation in SPMDs and blue mussels (Mytilus edulis)*. Chemosphere, 2002. **46**(5): p. 683-688.
179. Følsvik, N., E.M. Brevik, and J.A. Berge, *Organotin compounds in a Norwegian fjord. A comparison of concentration levels in semipermeable membrane devices (SPMDs), blue mussels (Mytilus edulis) and water samples*. Journal of Environmental Monitoring, 2002. **4**(2): p. 280-283.
180. Følsvik, N., E.M. Brevik, and J.A. Berge, *Monitoring of organotin compounds in seawater using semipermeable membrane devices (SPMDs)—tentative results*. Journal of Environmental Monitoring, 2000. **2**(4): p. 281-284.
181. Allan, I.J., G. Christensen, K. Bæk, and A. Evenset, *Photodegradation of PAHs in passive water samplers*. Marine Pollution Bulletin, 2016. **105**(1): p. 249-254.
182. Wenzel, K.D., B. Vrana, A. Hubert, and G. Schüürmann, *Dialysis of Persistent Organic Pollutants and Polycyclic Aromatic Hydrocarbons from Semipermeable Membranes. A Procedure Using an Accelerated Solvent Extraction Device*. Analytical Chemistry, 2004. **76**(18): p. 5503-5509.
183. Leonard, A.W., R.V. Hyne, and F. Pablo, *Trimethylpentane-containing passive samplers for predicting time-integrated concentrations of pesticides in water: Laboratory and field studies*. Environmental Toxicology and Chemistry, 2002. **21**(12): p. 2591-2599.
184. Zhao, W., M. Han, S. Dai, J. Xu, and P. Wang, *Ionic liquid-containing semipermeable membrane devices for monitoring the polycyclic aromatic hydrocarbons in water*. Chemosphere, 2006. **62**(10): p. 1623-1629.
185. Brumbaugh, W.G., J.D. Petty, T.W. May, and J.N. Huckins, *A passive integrative sampler for mercury vapor in air and neutral mercury species in water*. Chemosphere - Global Change Science, 2000. **2**(1): p. 1-9.
186. Müller, J.F., K. Manomanii, M.R. Mortimer, and M.S. McLachlan, *Partitioning of polycyclic aromatic hydrocarbons in the polyethylene/water system*. Fresenius' Journal of Analytical Chemistry, 2001. **371**(6): p. 816-822.
187. Booij, K., F. Smedes, and E.M. van Weerlee, *Spiking of performance reference compounds in low density polyethylene and silicone passive water samplers*. Chemosphere, 2002. **46**(8): p. 1157-1161.
188. Carls, M.G., L.G. Holland, J.W. Short, R.A. Heintz, and S.D. Rice, *Monitoring polynuclear aromatic hydrocarbons in aqueous environments with passive low-density polyethylene membrane devices*. Environ Toxicol Chem, 2004. **23**(6): p. 1416-24.
189. Belles, A., C. Alary, and Y. Mamindy-Pajany, *Thickness and material selection of polymeric passive samplers for polycyclic aromatic hydrocarbons in water: Which more strongly affects sampler properties?* Environmental Toxicology and Chemistry, 2016. **35**(7): p. 1708-1717.
190. Bayen, S., E. Segovia Estrada, H. Zhang, W.K. Lee, G. Juhel, F. Smedes, and B.C. Kelly, *Partitioning and Bioaccumulation of Legacy and Emerging Hydrophobic Organic Chemicals in Mangrove Ecosystems*. Environmental Science & Technology, 2019. **53**(5): p. 2549-2558.
191. Lohmann, R., J. Klanova, P. Kukucka, S. Yonis, and K. Bollinger, *Concentrations, Fluxes, and Residence Time of PBDEs Across the Tropical Atlantic Ocean*. Environmental Science & Technology, 2013. **47**(24): p. 13967-13975.

192. Lang, S.-C., P. Mayer, A. Hursthouse, D. Kötke, I. Hand, D. Schulz-Bull, and G. Witt, *Assessing PCB pollution in the Baltic Sea - An equilibrium partitioning based study*. Chemosphere, 2018. **191**: p. 886-894.
193. Tucca, F., H. Moya, and R. Barra, *Ethylene vinyl acetate polymer as a tool for passive sampling monitoring of hydrophobic chemicals in the salmon farm industry*. Marine Pollution Bulletin, 2014. **88**(1): p. 174-179.
194. St. George, T., P. Vlahos, T. Harner, P. Helm, and B. Wilford, *A rapidly equilibrating, thin film, passive water sampler for organic contaminants; characterization and field testing*. Environmental Pollution, 2011. **159**(2): p. 481-486.
195. Adams, R.G., R. Lohmann, L.A. Fernandez, and J.K. MacFarlane, *Polyethylene Devices: Passive Samplers for Measuring Dissolved Hydrophobic Organic Compounds in Aquatic Environments*. Environmental Science & Technology, 2007. **41**(4): p. 1317-1323.
196. Rusina, T.P., F. Smedes, J. Klanova, K. Booij, and I. Holoubek, *Polymer selection for passive sampling: A comparison of critical properties*. Chemosphere, 2007. **68**(7): p. 1344-1351.
197. Rusina, T.P., F. Smedes, and J. Klanova, *Diffusion coefficients of polychlorinated biphenyls and polycyclic aromatic hydrocarbons in polydimethylsiloxane and low-density polyethylene polymers*. Journal of Applied Polymer Science, 2010. **116**(3): p. 1803-1810.
198. Lohmann, R., *Critical Review of Low-Density Polyethylene's Partitioning and Diffusion Coefficients for Trace Organic Contaminants and Implications for Its Use As a Passive Sampler*. Environmental Science & Technology, 2012. **46**(2): p. 606-618.
199. Allan, I.J., K. Booij, A. Paschke, B. Vrana, G.A. Mills, and R. Greenwood, *Field Performance of Seven Passive Sampling Devices for Monitoring of Hydrophobic Substances*. Environmental Science & Technology, 2009. **43**(14): p. 5383-5390.
200. Aminot, Y., A. Belles, C. Alary, and J.W. Readman, *Near-surface distribution of pollutants in coastal waters as assessed by novel polyethylene passive samplers*. Marine Pollution Bulletin, 2017. **119**(1): p. 92-101.
201. Friedman, C.L., M.G. Cantwell, and R. Lohmann, *Passive sampling provides evidence for Newark Bay as a source of polychlorinated dibenzo-p-dioxins and furans to the New York/New Jersey, USA, atmosphere*. Environmental Toxicology and Chemistry, 2012. **31**(2): p. 253-261.
202. Fernandez, L.A., W. Lao, K.A. Maruya, C. White, and R.M. Burgess, *Passive Sampling to Measure Baseline Dissolved Persistent Organic Pollutant Concentrations in the Water Column of the Palos Verdes Shelf Superfund Site*. Environmental Science & Technology, 2012. **46**(21): p. 11937-11947.
203. Fernandez, L.A., W. Lao, K.A. Maruya, and R.M. Burgess, *Calculating the Diffusive Flux of Persistent Organic Pollutants between Sediments and the Water Column on the Palos Verdes Shelf Superfund Site Using Polymeric Passive Samplers*. Environmental Science & Technology, 2014. **48**(7): p. 3925-3934.
204. Yates, K., I. Davies, L. Webster, P. Pollard, L. Lawton, and C. Moffat, *Passive sampling: partition coefficients for a silicone rubber reference phase*. Journal of Environmental Monitoring, 2007. **9**(10): p. 1116-1121.
205. Jonker, M.T.O., S.A. van der Heijden, M. Kotte, and F. Smedes, *Quantifying the Effects of Temperature and Salinity on Partitioning of Hydrophobic Organic Chemicals to Silicone Rubber Passive Samplers*. Environmental Science & Technology, 2015. **49**(11): p. 6791-6799.

206. Baltussen, E., C. Cramers, and P. Sandra, *Sorptive sample preparation – a review*. Analytical and Bioanalytical Chemistry, 2002. **373**(1): p. 3-22.
207. Seethapathy, S. and T. Górecki, *Applications of polydimethylsiloxane in analytical chemistry: A review*. Analytica Chimica Acta, 2012. **750**: p. 48-62.
208. Vrana, B., L. Komancová, and J. Sobotka, *Calibration of a passive sampler based on stir bar sorptive extraction for the monitoring of hydrophobic organic pollutants in water*. Talanta, 2016. **152**: p. 90-97.
209. David, F. and P. Sandra, *Stir bar sorptive extraction for trace analysis*. Journal of Chromatography A, 2007. **1152**(1): p. 54-69.
210. DiFilippo, E.L. and R.P. Eganhouse, *Assessment of PDMS-Water Partition Coefficients: Implications for Passive Environmental Sampling of Hydrophobic Organic Compounds*. Environmental Science & Technology, 2010. **44**(18): p. 6917-6925.
211. Ouyang, G. and J. Pawliszyn, *SPME in environmental analysis*. Analytical and Bioanalytical Chemistry, 2006. **386**(4): p. 1059-1073.
212. Lin, K., W. Lao, Z. Lu, F. Jia, K. Maruya, and J. Gan, *Measuring freely dissolved DDT and metabolites in seawater using solid-phase microextraction with performance reference compounds*. Science of The Total Environment, 2017. **599-600**: p. 364-371.
213. O'Connell, S.G., L.D. Kincl, and K.A. Anderson, *Silicone Wristbands as Personal Passive Samplers*. Environmental Science & Technology, 2014. **48**(6): p. 3327-3335.
214. Donald, C.E., R.P. Scott, K.L. Blaustein, M.L. Halbleib, M. Sarr, P.C. Jepson, and K.A. Anderson, *Silicone wristbands detect individuals' pesticide exposures in West Africa*. Royal Society Open Science, 2016. **3**(8): p. 160433.
215. Anderson, K.A., G.L. Points, 3rd, C.E. Donald, H.M. Dixon, R.P. Scott, G. Wilson, L.G. Tidwell, P.D. Hoffman, J.B. Herbstman, and S.G. O'Connell, *Preparation and performance features of wristband samplers and considerations for chemical exposure assessment*. J Expo Sci Environ Epidemiol, 2017. **27**(6): p. 551-559.
216. Donald, C.E., R.P. Scott, G. Wilson, P.D. Hoffman, and K.A. Anderson, *Artificial turf: chemical flux and development of silicone wristband partitioning coefficients*. Air Quality, Atmosphere & Health, 2019. **12**(5): p. 597-611.
217. Burgess, R.M., R. Lohmann, J.P. Schubauer-Berigan, P. Reitsma, M.M. Perron, L. Lefkovitz, and M.G. Cantwell, *Application of passive sampling for measuring dissolved concentrations of organic contaminants in the water column at three marine superfund sites*. Environmental Toxicology and Chemistry, 2015. **34**(8): p. 1720-1733.
218. Monteyne, E., P. Roose, and C.R. Janssen, *Application of a silicone rubber passive sampling technique for monitoring PAHs and PCBs at three Belgian coastal harbours*. Chemosphere, 2013. **91**(3): p. 390-398.
219. Smedes, F. and K. Booij, *Guidelines for passive sampling of hydrophobic contaminants in water using silicone rubber samplers*. ICES Techniques in Marine Environmental Sciences, 2012. **52**: p. 20.
220. Claessens, M., E. Monteyne, K. Wille, L. Vanhaecke, P. Roose, and C.R. Janssen, *Passive sampling reversed: Coupling passive field sampling with passive lab dosing to assess the ecotoxicity of mixtures present in the marine environment*. Marine Pollution Bulletin, 2015. **93**(1): p. 9-19.
221. Sheikh, M.A., M.M. Fasih, J. Strand, H.R. Ali, A.H. Bakar, and H.M. Sharif, *Potential of silicone passive sampler for Tributyltin (TBT) detection in tropical aquatic systems*. Regional Studies in Marine Science, 2020. **35**: p. 101171.

222. Ouyang, G., W. Zhao, M. Alaei, and J. Pawliszyn, *Time-weighted average water sampling with a diffusion-based solid-phase microextraction device*. *J. Chromatog. A.*, 2007. **1138**(1): p. 42-46.
223. Seethapathy, S., T. Górecki, and X. Li, *Passive sampling in environmental analysis*. *J. Chromatogr. A.*, 2008. **1184**(1): p. 234-253.
224. Jonker, M.T.O., R.M. Burgess, U. Ghosh, P.M. Gschwend, S.E. Hale, R. Lohmann, M.J. Lydy, K.A. Maruya, D. Reible, and F. Smedes, *Ex situ determination of freely dissolved concentrations of hydrophobic organic chemicals in sediments and soils: basis for interpreting toxicity and assessing bioavailability, risks and remediation necessity*. *Nature Protocols*, 2020. **15**(5): p. 1800-1828.
225. Endo, S., S.E. Hale, K.-U. Goss, and H.P.H. Arp, *Equilibrium Partition Coefficients of Diverse Polar and Nonpolar Organic Compounds to Polyoxymethylene (POM) Passive Sampling Devices*. *Environmental Science & Technology*, 2011. **45**(23): p. 10124-10132.
226. Sobek, A., H.P.H. Arp, K. Wiberg, J. Hedman, and G. Cornelissen, *Aerosol–Water Distribution of PCDD/Fs and PCBs in the Baltic Sea Region*. *Environmental Science & Technology*, 2013. **47**(2): p. 781-789.
227. Warren, J.K., P. Vlahos, R. Smith, and C. Tobias, *Investigation of a new passive sampler for the detection of munitions compounds in marine and freshwater systems*. *Environmental Toxicology and Chemistry*, 2018. **37**(7): p. 1990-1997.
228. Alvarez, D.A., J.N. Huckins, J.D. Petty, T. Jones-Lepp, F. Stuer-Lauridsen, D.T. Getting, J.P. Goddard, A. Gravell, R. Greenwood, G. Mills, and B. Vrana, *Chapter 8 Tool for monitoring hydrophilic contaminants in water: polar organic chemical integrative sampler (POCIS)*, in *Comprehensive Analytical Chemistry*. 2007, Elsevier. p. 171-197.
229. Bergqvist, P.-A. and A. Zaliauskiene, *Chapter 14 Field study considerations in the use of passive sampling devices in water monitoring*, in *Comprehensive Analytical Chemistry*, R. Greenwood, G. Mills, and B. Vrana, Editors. 2007, Elsevier. p. 311-328.
230. Groshart, C.P., P.C. Okkerman, W.B.A. Wassenberg, and A.M. Pijnenburg, *Chemical Study on Alkylphenols*. 2001, Report: RIKZ/2001.029. Directoraat-General Rijkswaterstaat.
231. Hansch, C., A. Leo, and D. Hoekman, *Exploring QSAR - Hydrophobic, Electronic, and Steric Constants*. 1995, Washington DC: American Chemical Society. 16.
232. Alvarez, D.A., J.D. Petty, J.N. Huckins, T.L. Jones-Lepp, D.T. Getting, J.P. Goddard, and S.E. Manahan, *Development of a passive, in situ, integrative sampler for hydrophilic organic contaminants in aquatic environments*. *Environmental Toxicology and Chemistry*, 2004. **23**(7): p. 1640-1648.
233. Alvarez, D.A., *Guidelines for the Use of the Semipermeable Membrane Device (SPMD) and the Polar Organic Chemical Integrative Sampler (POCIS) in Environmental Monitoring Studies*. U. S. Geological Survey, Techniques and Methods, 2010. **1-D4**(28): p. 1-28.
234. Silvani, L., C. Riccardi, E. Eek, M.P. Papini, N.A.O. Morin, G. Cornelissen, A.M.P. Oen, and S.E. Hale, *Monitoring alkylphenols in water using the polar organic chemical integrative sampler (POCIS): Determining sampling rates via the extraction of PES membranes and Oasis beads*. *Chemosphere*, 2017. **184**: p. 1362-1371.
235. Miège, C., H. Budzinski, R. Jacquet, C. Soulier, T. Pelte, and M. Coquery, *Polar organic chemical integrative sampler (POCIS): application for monitoring organic micropollutants in wastewater effluent and surface water*. *Journal of Environmental Monitoring*, 2012. **14**(2): p. 626-635.

236. Budzinski, H. and M.-H. Dévier, *POCIS Passive Samplers in Combination with Bioassay-Directed Chemical Analyses*, in *Encyclopedia of Aquatic Ecotoxicology*, J.-F. Féraud and C. Blaise, Editors. 2013, Springer Netherlands: Dordrecht. p. 873-882.
237. Li, H., E.L.M. Vermeirssen, P.A. Helm, and C.D. Metcalfe, *Controlled field evaluation of water flow rate effects on sampling polar organic compounds using polar organic chemical integrative samplers*. *Environmental Toxicology and Chemistry*, 2010. **29**(11): p. 2461-2469.
238. Vermeirssen, E.L.M., C. Dietschweiler, B.I. Escher, J. van der Voet, and J. Hollender, *Transfer Kinetics of Polar Organic Compounds over Polyethersulfone Membranes in the Passive Samplers Pocis and Chemcatcher*. *Environmental Science & Technology*, 2012. **46**(12): p. 6759-6766.
239. Kaserzon, S.L., K. Kennedy, D.W. Hawker, J. Thompson, S. Carter, A.C. Roach, K. Booij, and J.F. Mueller, *Development and Calibration of a Passive Sampler for Perfluorinated Alkyl Carboxylates and Sulfonates in Water*. *Environmental Science & Technology*, 2012. **46**(9): p. 4985-4993.
240. Berho, C., B. Claude, E. Coisy, A. Togola, S. Bayoudh, P. Morin, and L. Amalric, *Laboratory calibration of a POCIS-like sampler based on molecularly imprinted polymers for glyphosate and AMPA sampling in water*. *Analytical and Bioanalytical Chemistry*, 2017. **409**(8): p. 2029-2035.
241. Claude, B., C. Berho, S. Bayoudh, L. Amalric, E. Coisy, R. Nehmé, and P. Morin, *Preliminary recovery study of a commercial molecularly imprinted polymer for the extraction of glyphosate and AMPA in different environmental waters using MS*. *Environmental Science and Pollution Research*, 2017. **24**(13): p. 12293-12300.
242. Wang, L., X. Gong, R. Wang, Z. Gan, Y. Lu, and H. Sun, *Application of an immobilized ionic liquid for the passive sampling of perfluorinated substances in water*. *Journal of Chromatography A*, 2017. **1515**: p. 45-53.
243. Męczykowska, H., P. Stepnowski, and M. Caban, *Effect of salinity and pH on the calibration of the extraction of pharmaceuticals from water by PASSIL*. *Talanta*, 2018. **179**: p. 271-278.
244. Zhang, Z., A. Hibberd, and J.L. Zhou, *Analysis of emerging contaminants in sewage effluent and river water: Comparison between spot and passive sampling*. *Analytica Chimica Acta*, 2008. **607**(1): p. 37-44.
245. Kingston, J.K., R. Greenwood, G.A. Mills, G.M. Morrison, and L. Björklund Persson, *Development of a novel passive sampling system for the time-averaged measurement of a range of organic pollutants in aquatic environments*. *Journal of Environmental Monitoring*, 2000. **2**(5): p. 487-495.
246. Vrana, B., G.A. Mills, E. Dominiak, and R. Greenwood, *Calibration of the Chemcatcher passive sampler for the monitoring of priority organic pollutants in water*. *Environmental Pollution*, 2006. **142**(2): p. 333-343.
247. Persson, L.B., G.M. Morrison, J.-U. Friemann, J. Kingston, G. Mills, and R. Greenwood, *Diffusional behaviour of metals in a passive sampling system for monitoring aquatic pollution*. *Journal of Environmental Monitoring*, 2001. **3**(6): p. 639-645.
248. Ahkola, H., S. Herve, and J. Knuutinen, *Study of different Chemcatcher configurations in the monitoring of nonylphenol ethoxylates and nonylphenol in aquatic environment*. *Environmental Science and Pollution Research*, 2014. **21**(15): p. 9182-9192.
249. Lissalde, S., A. Charriau, G. Poulhier, N. Mazzella, R. Buzier, and G. Guibaud, *Overview of the Chemcatcher® for the passive sampling of various pollutants in aquatic*

- environments Part B: Field handling and environmental applications for the monitoring of pollutants and their biological effects.* Talanta, 2016. **148**(Supplement C): p. 572-582.
250. Allan, I.J., J. Knutsson, N. Guigues, G.A. Mills, A.M. Fouillac, and R. Greenwood, *Chemcatcher and DGT passive sampling devices for regulatory monitoring of trace metals in surface water.* J. Environ. Monit., 2008. **10** (7): p. 821-9.
 251. Aguilar-Martínez, R., M.M. Gómez-Gómez, and M.A. Palacios-Corvillo, *Mercury and organotin compounds monitoring in fresh and marine waters across Europe by Chemcatcher passive sampler.* International Journal of Environmental Analytical Chemistry, 2011. **91**(11): p. 1100-1116.
 252. Tran, A.T.K., R.V. Hyne, and P. Doble, *Calibration of a passive sampling device for time-integrated sampling of hydrophilic herbicides in aquatic environments.* Environmental Toxicology and Chemistry, 2007. **26**(3): p. 435-443.
 253. Bernal-González, M. and C. Durán-Domínguez-de-Bazúa, *Development of a Passive Sampler for Monitoring of Carbamate and s-Triazine Pesticides in Surface Waters.* Water, Air, & Soil Pollution, 2012. **223**(8): p. 5071-5085.
 254. Vrana, B., G. Mills, R. Greenwood, J. Knutsson, K. Svensson, and G. Morrison, *Performance optimisation of a passive sampler for monitoring hydrophobic organic pollutants in water.* Journal of Environmental Monitoring, 2005. **7**(6): p. 612-620.
 255. Vrana, B., G.A. Mills, M. Kotterman, P. Leonards, K. Booiij, and R. Greenwood, *Modelling and field application of the Chemcatcher passive sampler calibration data for the monitoring of hydrophobic organic pollutants in water.* Environmental Pollution, 2007. **145**(3): p. 895-904.
 256. El-Shenawy, N., Z. Nabil, I. Abdel-Nabi, and R. Greenwood, *Comparing the passive and active sampling devices with biomonitoring of pollutants in Langstone and Portsmouth Harbour, UK.* Journal of Environmental Science and Technology, 2010. **3**(1): p. 1-17.
 257. Kennedy, K., T. Schroeder, M. Shaw, D. Haynes, S. Lewis, C. Bentley, C. Paxman, S. Carter, V.E. Brando, M. Bartkow, L. Hearn, and J.F. Müller, *Long term monitoring of photosystem II herbicides – Correlation with remotely sensed freshwater extent to monitor changes in the quality of water entering the Great Barrier Reef, Australia.* Marine Pollution Bulletin, 2012. **65**(4): p. 292-305.
 258. Kennedy, K., M. Devlin, C. Bentley, K. Lee-Chue, C. Paxman, S. Carter, S.E. Lewis, J. Brodie, E. Guy, S. Vardy, K.C. Martin, A. Jones, R. Packett, and J.F. Mueller, *The influence of a season of extreme wet weather events on exposure of the World Heritage Area Great Barrier Reef to pesticides.* Marine Pollution Bulletin, 2012. **64**(7): p. 1495-1507.
 259. Aguilar-Martínez, R., M.A. Palacios-Corvillo, R. Greenwood, G.A. Mills, B. Vrana, and M.M. Gómez-Gómez, *Calibration and use of the Chemcatcher® passive sampler for monitoring organotin compounds in water.* Analytica Chimica Acta, 2008. **618**(2): p. 157-167.
 260. Aguilar-Martínez, R., R. Greenwood, G.A. Mills, B. Vrana, M.A. Palacios-Corvillo, and M.M. Gómez-Gómez, *Assessment of Chemcatcher passive sampler for the monitoring of inorganic mercury and organotin compounds in water.* International Journal of Environmental Analytical Chemistry, 2008. **88**(2): p. 75-90.
 261. Petersen, J., D. Pröfrock, A. Paschke, J.A.C. Broekaert, and A. Prange, *Laboratory calibration and field testing of the Chemcatcher-Metal for trace levels of rare earth elements in estuarine waters.* Environmental Science and Pollution Research, 2015. **22**(20): p. 16051-16059.

262. Petersen, J., D. Pröfrock, A. Paschke, J.A.C. Broekaert, and A. Prange, *Development and field test of a mobile continuous flow system utilizing Chemcatcher for monitoring of rare earth elements in marine environments*. Environmental Science: Water Research & Technology, 2016. **2**(1): p. 146-153.
263. Sarkar, S.K., *Marine Algal Bloom: Characteristics, Causes and Climate Change Impacts*. 2018, Singapore: Springer.
264. MacKenzie, L., V. Beuzenberg, P. Holland, P. McNabb, and A. Selwood, *Solid phase adsorption toxin tracking (SPATT): a new monitoring tool that simulates the biotoxin contamination of filter feeding bivalves*. Toxicon, 2004. **44**(8): p. 901-918.
265. Roué, M., H.T. Darius, and M. Chinain, *Solid Phase Adsorption Toxin Tracking (SPATT) Technology for the Monitoring of Aquatic Toxins: A Review*. Toxins, 2018. **10**(4): p. 167.
266. Lane, J.Q., C.M. Roddam, G.W. Langlois, and R.M. Kudela, *Application of Solid Phase Adsorption Toxin Tracking (SPATT) for field detection of the hydrophilic phycotoxins domoic acid and saxitoxin in coastal California*. Limnology and Oceanography: Methods, 2010. **8**(11): p. 645-660.
267. Kudela, R.M., *Chapter Eleven - Passive Sampling for Freshwater and Marine Algal Toxins*, in *Comprehensive Analytical Chemistry*, J. Diogène and M. Campàs, Editors. 2017, Elsevier. p. 379-409.
268. MacKenzie, L.A., *In situ passive solid-phase adsorption of micro-algal biotoxins as a monitoring tool*. Current Opinion in Biotechnology, 2010. **21**(3): p. 326-331.
269. Davison, W. and H. Zhang, *In situ speciation measurements of trace components in natural waters using thin-film gels*. Nature, 1994. **367**(6463): p. 546-548.
270. Zhang, H. and W. Davison, *Diffusional characteristics of hydrogels used in DGT and DET techniques*. Analytica Chimica Acta, 1999. **398**(2): p. 329-340.
271. Zhang, H. and W. Davison, *Performance Characteristics of Diffusion Gradients in Thin Films for the in Situ Measurement of Trace Metals in Aqueous Solution*. Anal. Chem., 1995. **67**(19): p. 3391-3400.
272. Turner, G.S.C., G.A. Mills, M.J. Bowes, J.L. Burnett, S. Amos, and G.R. Fones, *Evaluation of DGT as a long-term water quality monitoring tool in natural waters; uranium as a case study*. Environmental Science: Processes & Impacts, 2014. **16**(3): p. 393-403.
273. Garmo, Ø.A., O. Røyset, E. Steinnes, and T.P. Flaten, *Performance Study of Diffusive Gradients in Thin Films for 55 Elements*. Analytical Chemistry, 2003. **75**(14): p. 3573-3580.
274. Panther, J.G., W.W. Bennett, P.R. Teasdale, D.T. Welsh, and H. Zhao, *DGT Measurement of Dissolved Aluminum Species in Waters: Comparing Chelex-100 and Titanium Dioxide-Based Adsorbents*. Environmental Science & Technology, 2012. **46**(4): p. 2267-2275.
275. Panther, J.G., R.R. Stewart, P.R. Teasdale, W.W. Bennett, D.T. Welsh, and H. Zhao, *Titanium dioxide-based DGT for measuring dissolved As(V), V(V), Sb(V), Mo(VI) and W(VI) in water*. Talanta, 2013. **105**: p. 80-86.
276. Dočekalová, H. and P. Diviš, *Application of diffusive gradient in thin films technique (DGT) to measurement of mercury in aquatic systems*. Talanta, 2005. **65**(5): p. 1174-1178.
277. Ren, M., Y. Wang, S. Ding, L. Yang, Q. Sun, and L. Zhang, *Development of a new diffusive gradient in the thin film (DGT) method for the simultaneous measurement of CH₃Hg⁺ and Hg²⁺*. New Journal of Chemistry, 2018. **42**(10): p. 7976-7983.

278. Twiss, M.R. and J.W. Moffett, *Comparison of Copper Speciation in Coastal Marine Waters Measured Using Analytical Voltammetry and Diffusion Gradient in Thin-Film Techniques*. Environmental Science & Technology, 2002. **36**(5): p. 1061-1068.
279. Dunn, R.J.K., P.R. Teasdale, J. Warnken, and R.R. Schleich, *Evaluation of the Diffusive Gradient in a Thin Film Technique for Monitoring Trace Metal Concentrations in Estuarine Waters*. Environ. Sci. Tech., 2003. **37**(12): p. 2794-2800.
280. Ren, M., S. Ding, D. Shi, Z. Zhong, J. Cao, L. Yang, D.C.W. Tsang, D. Wang, D. Zhao, and Y. Wang, *A new DGT technique comprised in a hybrid sensor for the simultaneous measurement of ammonium, nitrate, phosphorus and dissolved oxygen*. Sci. Total. Environ., 2020. **725**: p. 138447.
281. Huang, J., W.W. Bennett, D.T. Welsh, T. Li, and P.R. Teasdale, *"Diffusive Gradients in Thin Films" Techniques Provide Representative Time-Weighted Average Measurements of Inorganic Nutrients in Dynamic Freshwater Systems*. Environ. Sci. Technol., 2016. **50** (24): p. 13446-13454.
282. Chen, C.-E., H. Zhang, and K.C. Jones, *A novel passive water sampler for in situ sampling of antibiotics*. Journal of Environmental Monitoring, 2012. **14**(6): p. 1523-1530.
283. Xie, H., J. Chen, Q. Chen, C.-E.L. Chen, J. Du, F. Tan, and C. Zhou, *Development and evaluation of diffusive gradients in thin films technique for measuring antibiotics in seawater*. Science of The Total Environment, 2018. **618**: p. 1605-1612.
284. Ren, S., J. Tao, F. Tan, Y. Cui, X. Li, J. Chen, X. He, and Y. Wang, *Diffusive gradients in thin films based on MOF-derived porous carbon binding gel for in-situ measurement of antibiotics in waters*. Science of The Total Environment, 2018. **645**: p. 482-490.
285. Xie, H., Q. Chen, J. Chen, C.-E.L. Chen, and J. Du, *Investigation and application of diffusive gradients in thin-films technique for measuring endocrine disrupting chemicals in seawaters*. Chemosphere, 2018. **200**: p. 351-357.
286. Challis, J.K., M.L. Hanson, and C.S. Wong, *Development and Calibration of an Organic-Diffusive Gradients in Thin Films Aquatic Passive Sampler for a Diverse Suite of Polar Organic Contaminants*. Analytical Chemistry, 2016. **88**(21): p. 10583-10591.
287. Senn, D.B., S.B. Griscom, C.G. Lewis, J.P. Galvin, M.W. Chang, and J.P. Shine, *Equilibrium-Based Sampler for Determining Cu²⁺ Concentrations in Aquatic Ecosystems*. Environmental Science & Technology, 2004. **38**(12): p. 3381-3386.
288. Dong, Z., C.G. Lewis, R.M. Burgess, and J.P. Shine, *The Gellyfish: An in situ equilibrium-based sampler for determining multiple free metal ion concentrations in marine ecosystems*. Environmental Toxicology and Chemistry, 2015. **34**(5): p. 983-992.
289. Dong, Z., C.G. Lewis, R.M. Burgess, B. Coull, and J.P. Shine, *Statistical evaluation of biogeochemical variables affecting spatiotemporal distributions of multiple free metal ion concentrations in an urban estuary*. Chemosphere, 2016. **150**: p. 202-210.
290. Almeida, M.I.G.S., R.W. Cattrall, and S.D. Kolev, *Polymer inclusion membranes (PIMs) in chemical analysis - A review*. Analytica Chimica Acta, 2017. **987**: p. 1-14.
291. Kuswandi, B., F. Nitti, M.I.G.S. Almeida, and S.D. Kolev, *Water monitoring using polymer inclusion membranes: a review*. Environmental Chemistry Letters, 2020. **18**(1): p. 129-150.
292. Kolev, S.D., M.I.G.S. Almeida, and R.W. Cattrall, *Chapter 27, Polymer Inclusion Membranes*, in *Handbook of Membrane Separations: Chemical, Pharmaceutical, Food and Biotechnological Applications*, S.S.H.R. Editors: A. K. Pabby, A. M. S. Requena, Editor. 2015: CRC Press, Boca Raton. p. 723-739.

293. Almeida, M.I.G.S., C. Chan, V.J. Pettigrove, R.W. Cattrall, and S.D. Kolev, *Development of a passive sampler for Zinc(II) in urban pond waters using a polymer inclusion membrane*. Environmental Pollution, 2014. **193**(Supplement C): p. 233-239.
294. Garcia-Rodríguez, A., C. Fontàs, V. Matamoros, M.I.G.S. Almeida, R.W. Cattrall, and S.D. Kolev, *Development of a polymer inclusion membrane-based passive sampler for monitoring of sulfamethoxazole in natural waters. Minimizing the effect of the flow pattern of the aquatic system*. Microchemical Journal, 2016. **124**(Supplement C): p. 175-180.
295. Pont, N., V. Salvadó, and C. Fontàs, *Applicability of a Supported Liquid Membrane in the Enrichment and Determination of Cadmium from Complex Aqueous Samples*. Membranes, 2018. **8**(2): p. 21.
296. Ait Khaldoun, I., L. Mitiche, A. Sahmoune, and C. Fontàs, *An Efficient Polymer Inclusion Membrane-Based Device for Cd Monitoring in Seawater*. Membranes, 2018. **8**(3): p. 61.
297. Elias, G., S. Díez, and C. Fontàs, *System for mercury preconcentration in natural waters based on a polymer inclusion membrane incorporating an ionic liquid*. Journal of Hazardous Materials, 2019. **371**: p. 316-322.
298. Dzygiel, P. and P.P. Wiczorek, *Chapter 3 - Supported Liquid Membranes and Their Modifications: Definition, Classification, Theory, Stability, Application and Perspectives*, in *Liquid Membranes*, V.S. Kislik, Editor. 2010, Elsevier: Amsterdam. p. 73-140.
299. Tillett, B.J., D. Sharley, M.I.G.S. Almeida, I. Valenzuela, A.A. Hoffmann, and V. Pettigrove, *A short work-flow to effectively source faecal pollution in recreational waters – A case study*. Sci. Total. Environ., 2018. **644**: p. 1503-1510.

CHAPTER 2: Determination of trace levels of ammonia in marine waters using a simple environmentally-friendly ammonia (SEA) analyser

Foreword

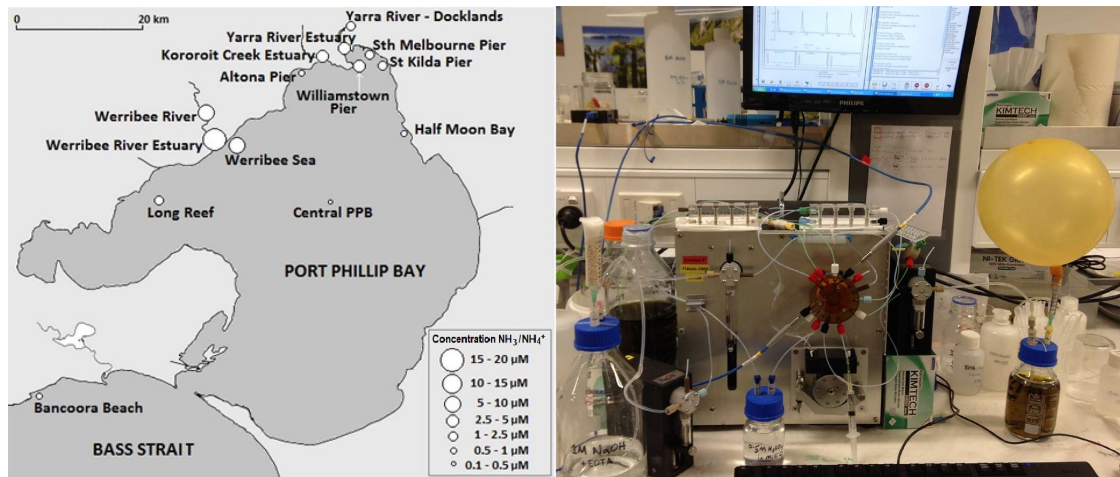
In **Chapter 1**, a comprehensive review of the literature regarding flow-based methodologies for ammonia monitoring and analysis in marine environments (including estuarine, coastal and oligotrophic ocean waters) was undertaken to develop an understanding of the advantages and limitations of existing analytical techniques already described in the literature. While many of the described methods were sensitive (e.g., fluorometric method), they often exhibited a narrow working range with a complicated manifold (e.g., requiring heating of manifold components) and or custom-made parts. This chapter describes the development and validation of a sensitive and robust analyser, capable of ammonia determination in complex matrices over a wide range of concentrations (relevant to both monitoring and analysis of environmental samples and passive sampling receiving solutions), with a reasonable sample throughput, and without requiring expensive or toxic reagents with stability issues.

The following section contains an original research paper describing the development of a simple and environmentally-friendly ammonia (SEA) analyser to measure ammonia concentrations in coastal and estuarine waters, the content of which was published in 2017 in the journal *Marine Chemistry*.

The SEA analyser was used for the analysis of ammonia in aqueous samples collected in the context of the development of the gas-diffusion passive sampler (**Chapters 3 and 4**).

O'Connor Šraj, L., Almeida, M. I. G. S., McKelvie, I. D., Kolev, S. D., (2017) *Determination of trace levels of ammonia in marine waters using a simple environmentally-friendly ammonia (SEA) analyser*, *Marine Chemistry*, 194, 133-145, doi.org/10.1016/j.marchem.2017.06.008

Graphical abstract



Contents

Abstract	87
2.1 Introduction	88
2.2 Materials and methods	91
2.2.1 Reagents	91
2.2.2 Acceptor solution	91
2.2.3 Donor solution	92
2.2.4 Ammonia standards	93
2.2.5 Sample flushing solution	93
2.2.6 Seawater samples	93
2.2.7 Apparatus and manifold	94
2.2.8 Gas-diffusion cell and membranes	97
2.2.9 Program	98
2.2.10 Data processing	98
2.3 Results and discussion	99
2.3.1 Flow system optimisation	99
2.3.2 Flow rate and sample volume	99
2.3.3 Gas-diffusion apparatus	101
2.3.4 Acid-base indicator dyes	103
2.4 SEA analyser system and performance	105
2.4.1 Analytical figures of merit	105
2.5 Validation of SEA analyser	107
2.5.1 Measurement of certified reference materials	107
2.5.2 Spike-and-recovery studies	108
2.6 Conclusions	109
2.7 Appendix	111
Acknowledgements	112
References	113

Abstract

A simple and environmentally-friendly ammonia (SEA) analyser based on programmable flow was developed for the determination of trace levels of ammonia nitrogen in marine waters. The proposed SEA analyser was based on a gas-diffusion spectrophotometric method. High sensitivity was achieved through the use of large sample volumes and a programmable-flow approach. The degree of pre-concentration of ammonia in the acceptor stream was determined by the controlled and programmable delivery of the sample to the gas-diffusion unit, and the sensitivity of the method was tailored to the concentration range of interest by simple modification of the sample volume used for analysis. Three different working concentration ranges were defined by varying the volume of the sample, thus making the SEA analyser versatile and applicable for use in estuarine or coastal seawaters: 0.028 – 5.6 μM (2.0 mL), 0.28 – 13.9 μM (1.0 mL), and 1.4 – 55.6 μM (0.25 mL). Typical limits of detection of 15, 88 and 440 nM, and repeatability of 0.71, 1.2 and 0.97% RSD ($n = 10$), were attained for each range, respectively. Good sample throughput was achieved with approximately 20 samples per hour for the lower concentration range, 30 samples per hour for the middle concentration range, and 40 samples per hour for the upper concentration range. Method validation involved the analysis of a certified reference material in artificial seawater, and spike-and-recovery analysis for seawater and estuarine samples collected from various locations around *Nerm* (Port Phillip Bay, Victoria, Australia). Small volumes of waste (i.e. alkaline seawater feedstock and 1.5 mL indicator solution) were generated per sample. The reagents used were non-toxic, suitable for long-term storage, and cheap, costing as little as \$2.40 AUD per 1,000 determinations.

Keywords: Ammonia; Flow analysis; Environmental monitoring; Seawater, Estuarine water

2.1 Introduction

Ammonia nitrogen is naturally found at low concentrations in the marine environment and is cycled in the water column by a number of different biological processes with perhaps the most important of these processes being the assimilation of ammonium (NH_4^+) by phytoplankton, nitrification and de-nitrification by bacteria and the excretion of both ammonia (NH_3) and ammonium (NH_4^+) by fish, invertebrates and other marine biota. It is estimated that between 70 - 90% of gross primary production in the open oceans is based on the uptake and assimilation of nitrogen in the ammonium form, via a process referred to as regenerated production [1].

Higher levels of ammonia nitrogen in the marine environment can be directly and indirectly toxic to many marine organisms. Nitrogenous pollution is increasing in aquatic ecosystems as a result of large-scale anthropogenic run-off from agricultural land and industrial processes, resulting in nitrogenous compounds accumulating in estuarine waters and coastal environments [2]. Estuaries form part of a network of important nursery habitat for many marine fish species, and high nitrogen loads in these environments can have a deleterious impact on organism and ecosystem health [3]. Additionally, episodic pollution events may result in large phytoplankton blooms, rapid algal growth and eutrophication, which can result in the development of hypoxic waters [4], and/or the release of algal toxins into the water body [5].

Monitoring of ammonia nitrogen is important in providing information about water quality to policy makers, regulatory bodies and the community, and supports the development of strategies to manage and conserve important fisheries, catchments and marine reserves. In order to develop an understanding of how this chemical enters, cycles and persists in the environment, sensitive, reliable, and preferably fast analytical methods with a wide working concentration range are required.

Flow analysis techniques have played an important role in water analysis and monitoring [6, 7]. Several flow-based methods have been described in the literature for the photometric determination of ammonia nitrogen in marine waters based on different chemistries, namely the phenate method, gas-diffusion methods and the orthophthaldialdehyde (OPA) based fluorimetric method [8]. The phenate method, known also as the Berthelot method, involves

the reaction between ammonia and hypochlorite to form monochloroamine, which then reacts with phenol in the presence of catalytic quantities of nitroprusside to form the coloured product indophenol blue [9-11]. This method is commonly employed as the standard reference photometric method [12], however it requires the use of toxic reagents such as phenol and nitroprusside [13], which are harmful to human health and aquatic life. Salicylate [11] and 1-naphthol [14] have been proposed as less toxic phenolic alternatives, however, when using these reagents method sensitivity is compromised. In order to increase sensitivity, large amounts of these reagents are required to achieve a sensitivity comparable to that in the case of the use of phenol [15]. Furthermore, since the reaction is slow, reaction temperature of around 80 °C is required, adding extra complexity to the flow system. The use of long-path liquid waveguide capillary cells (LWCC) (2 – 2.5 m) has been shown to provide a substantial increase in sensitivity for the phenol-hypochlorite reaction for ammonia determination (i.e. limit of detection in the range of 3.6 – 5 nM) [16, 17], however LWCCs are susceptible to in-cell bubble formation as a function of increased cell length and sample filtration despite being time consuming and laborious, is advisable to prevent difficulties with cleaning particulate blockages [18]. In-line solid-phase extraction (SPE) has also been employed to improve method sensitivity (i.e. limit of detection 3.5 nM), however, this is at the expense of sample throughput with a sampling rate of 3 samples per hour achievable [19]. Hence, the use of toxic reagents, matrix effects (such as Schlieren effects), interference from precipitation of divalent metal cations and lack of sensitivity are the main drawbacks of the phenate method and its less toxic versions.

Flow-based methodologies using gas-diffusion separation coupled with colorimetric pH sensitive indicator dyes have also been employed for monitoring ammonia nitrogen in marine water environments. By introducing a gas-diffusion unit (GDU) into the flow analysis system, total ammonia nitrogen can be determined by alkalinising the sample, converting the soluble ammonium to gaseous ammonia, which can then diffuse across a hydrophobic porous membrane into an acceptor solution containing an acid-base indicator, whose absorbance can be measured using photometry [20-22]. The GDU effectively separates the analyte from the sample matrix, allowing for improved selectivity. Refractive index (Schlieren) effects are eliminated with the use of a GDU, and an acidic flushing solution can be used periodically to remove any build-up of divalent metal hydroxide precipitate [22]. Unless samples are very

turbid, and likely to block the flow manifold, filtration is not normally needed when using a GDU, as its hydrophobic membrane physically separates the donor stream, where the sample is injected, from the acceptor stream, where detection takes place, thus minimizing sample pretreatment and associated contamination risks. This method involves non-toxic reagents that are easy to prepare and are stable. Specific flow pattern manipulations (e.g. oscillating flow, stop-flow) [23] as well as increasing diffusion area [24] have been described to improve method sensitivity, however, until now, reported detection limits for spectrophotometric gas-diffusion methods have been characteristically high when compared to other methods described in the literature (i.e. best limits of detection in the range of 50 – 210 nM) [20, 22, 25].

The fluorometric method is the most sensitive method described in the literature for the determination of ammonia nitrogen in marine waters, with detection limits reported to be as low as 1 - 13 nM [26-34]. The method involves the reaction of OPA with ammonia in the presence of a reducing agent, commonly 2-mercaptoethanol or sodium sulphite, resulting in the formation of an intensely fluorescing product. The fluorescence method has also been coupled with gas-diffusion separation [26, 28, 32] in order to reduce interference from primary amines and dissolved amino acids when 2-mercaptoethanol has been used as the reducing agent [26, 28]. Sodium sulphite, which has exhibited higher selectivity towards ammonia over primary amines, is non-toxic and easier to handle compared to 2-mercaptoethanol because of its superior stability, making it suitable for long-term storage and ship-board analysis [27, 32]. Under ambient temperature conditions, the OPA chemistry has a slow reaction rate (typically 3 – 4 h), requiring the incorporation of a heating unit into the manifold [35] and similarly to the indophenol blue method, adding complexity to the analytical system. However, the major drawbacks of the fluorescence method are the toxicity and cost of the OPA reagent.

In addition to the frequently used spectrophotometric detection, conductometric detection has also been utilised in several flow analysis systems with gas-diffusion separation for the determination of ammonia nitrogen in seawater [36, 37]. Conductometric detection does not require in most cases the use of additional reagents which could be toxic, unstable or expensive and generally provides a linear response. However, the temperature of the flow must be strictly controlled [36] or temperature compensation mechanisms must be used [37]. Henríquez et al. reported a limit of detection in the range of 2.5 – 5 μ M with a sample

throughput of 32 samples per hour [36] while Plant et al. achieved limits of detection for coastal and shelf waters of 200 and 14 nM, respectively, with a sample throughput of 9 and 3 samples per hour [37].

The method described in this work aims to utilise enhanced flow manipulation in a gas-diffusion flow system with spectrophotometric detection. Rather than injecting a discrete sample into a flowing stream of reagents (i.e. Flow Injection Analysis) or sequential aspiration of sample and reagents into a holding coil (i.e. Sequential Injection Analysis), both methods being restricted by sample volume, the SEA analyser involves the continuous merging and mixing of large sample volumes and small reagent volumes for a given period of time depending only on the volumes necessary to achieve the desired sensitivity.

The method sensitivity was tailored to cover the range of ammonia concentrations usually found in marine waters by simple flow manipulation, in order to achieve a limit of detection comparable to flow-based fluorimetric methods. Hence, a simple and environmentally-friendly ammonia (SEA) analyser is proposed.

2.2 Materials and methods

2.2.1 Reagents

Analytical grade chemicals were used for the preparation of all reagent solutions and were used without further purification. Deionized water from a Millipore Milli-Q system (Synergy 185, France, resistivity >18 M Ω cm) was used throughout this study if not stated otherwise.

2.2.2 Acceptor solution

A 5 mM stock solution of indicator dye was prepared by dissolving 313 mg of bromothymol blue (BDH Chemicals – pKa 7.3) and 1 mL of 1 M NaOH in 99 mL Milli-Q water and stored at room temperature away from ambient light. The acceptor solution was prepared by 50 fold dilution of the bromothymol blue stock into a 0.68 M NaCl solution, resulting in a final concentration of 100 μ M. Spectral scanning over the range 350 – 750 nm was used to determine the wavelength at the absorbance maximum of the basic form of the deprotonated

dye (I^{2-}), which was selected for absorbance monitoring. The pH of the acceptor solution was adjusted by drop wise addition of 0.01 M NaOH and/or 0.01 M HCl to achieve an absorbance of between 0.180 - 0.200 absorbance units at 615 nm, corresponding to the baseline absorbance.

Prior to analysis, the acceptor solution was sonicated for 20 min in a glass bottle and a syringe barrel filled with self-indicating soda lime was fitted to one of two airtight ports on the cap of the bottle. After degassing, the headspace of the bottle was flushed with N_2 , and before use, the soda lime syringe was replaced with a N_2 -filled balloon. As the indicator solution was consumed during the course of analysis, the same volume of N_2 was replaced in the air-tight bottle thus preventing contact between the acceptor solution and the ambient air.

5 mM stock solutions of the indicator dyes (all Indicator Grade chemicals) bromocresol green (BDH Chemicals – pKa 4.9), bromocresol purple (BDH Chemicals – pKa 6.4), cresol red (May & Baker Laboratory Chemicals – pKa 8.3), meta-cresol purple (ACROS Organics – pKa 8.3), and thymol blue (May & Baker Laboratory Chemicals– pKa 9.2) were likewise prepared according to the procedure outlined above, resulting in final acceptor solution concentrations of 100 μ M dye. For each indicator, the wavelength at the absorbance maximum of the fully deprotonated basic form of the dye (I^{2-}) was determined, i.e. bromocresol green (610 nm), bromocresol purple (590 nm), cresol red (572 nm), meta-cresol purple (578 nm), and thymol blue (596 nm). In order to determine which dye, or dye combination exhibited the highest sensitivity, all indicator acceptor solutions were set to a baseline absorbance of 0.200 ± 0.005 units for comparison. For mixed indicator solutions, the desired ratios of stock solutions were mixed and diluted with 0.68 M NaCl solution as described above, and for the dye mixtures wavelengths were selected to fall in between the two basic absorbance maxima for the respective indicator species.

2.2.3 Donor solution

40 g of NaOH (Chem Supply, Analytical Reagents, 98% purity) and 150 g ethylenediaminetetraacetic acid disodium salt dihydrate (EDTA) (Chem Supply, Analytical Reagents, $\geq 99\%$) were dissolved in 1 L of water and used to convert the ammonium ions

present in the sample solution into molecular ammonia. This solution was prepared weekly, stored at 4 °C and sonicated for 20 min prior to use.

2.2.4 Ammonia standards

A primary stock solution of ammonium was prepared by dissolving 741.4 mg of ammonium chloride salt (BDH Chemicals, 99.8%), oven dried at 105 °C overnight, in 250.0 mL water, having a final concentration of 55.56 mM NH_4^+ . A secondary stock solution was prepared by 100 times dilution of the primary stock solution into water (i.e. 0.5556 mM NH_4^+). Both solutions were stored in Teflon sealed glass bottles in the dark at 4 °C. Working solutions were prepared by dilution of the secondary stock solution into solutions comprising 0.6 M NaCl, or with real seawater samples for recovery and standard addition experiments.

A certified reference material (CRM) for ammonia as NH_3 $1,000 \pm 6 \text{ mg L}^{-1}$ (ERA, A Waters Company, Lot no. 080715, Traceability against NIST SRM (194) 99.1%) was diluted and used to determine the method accuracy by preparing solutions with known concentrations of NH_4^+ in 0.6 M NaCl in Milli-Q water.

2.2.5 Sample flushing solution

A solution of approximately 5 mM HCl was used to flush the donor channel of the **GDU** prior to the introduction of each new sample, in order to avoid cross-contamination. A mildly acidic solution was used instead of water, in the event that a small amount of divalent metal cation precipitation would accumulate over long periods of analysis time, contributing to membrane clogging, as was observed by Willason and Johnson [22].

2.2.6 Seawater samples

Sea and estuarine water samples were collected from locations in the area of *Nerm* (Port Phillip Bay), Victoria, Australia. Samples were collected in 500 mL amber glass bottles and immediately acidified with 50 μL of 10.2 M HCl to achieve an approximate pH of 3 (monitored with universal indicator paper) and kept on ice during transport. All samples were transferred

to high density polyethylene plastic bottles and stored for no longer than 3 days in the dark at 4 °C. The clean-up protocol for all collection and storage containers, and other equipment that came into contact with the samples involved a 3 x wash with water, followed by 3 x wash with 5 mM HCl, and finally a 3 x wash with water. Clean equipment was dried and stored in zip-lock bags, and clean glassware was dried, and lids were used to seal containers from dust.

The seawater samples collected at the Werribee study sites were visibly turbid and required filtration using 0.45 µm syringe filters. Spike-and-recovery tests were performed for seven marine water samples, including estuarine water samples collected from the Yarra River at Docklands.

2.2.7 Apparatus and manifold

The flow manifold of the SEA analyser developed for the spectrophotometric detection of ammonia nitrogen in seawater using gas-diffusion separation is shown in Figure 2-1.

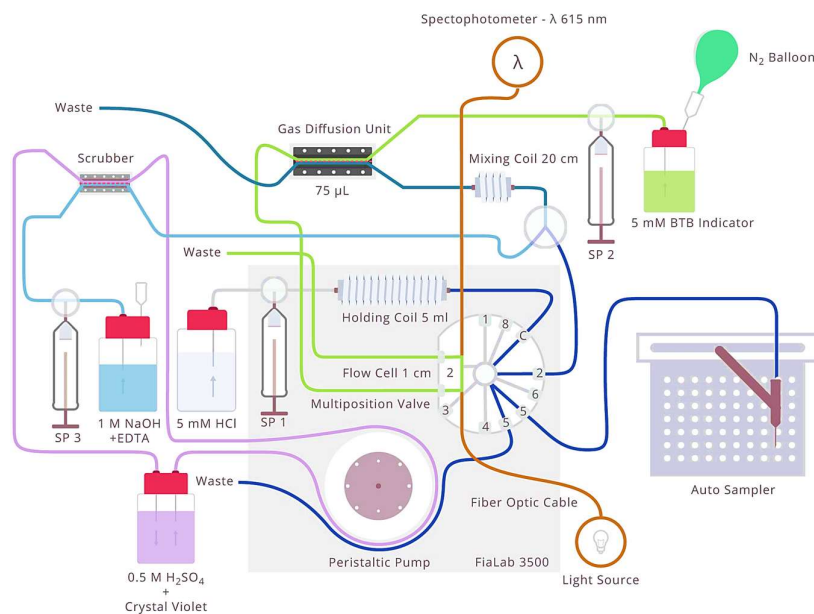


Figure 2-1. Schematic diagram of the fully automatic SEA analyser using a FiaLab 3500 flow system and Cetac autosampler. SP, syringe pump; BTB, bromothymol blue; N₂, nitrogen.

A FIALab 3500 flow injection analyser fitted with a 10 mL syringe pump (Tecan, Cavro XLP), an 8 port multiposition valve (MPV) and a peristaltic pump (FIALab instruments, Bellevue, WA,

USA) controlled by FIAlab software (version 5.9.314 for Windows) was used for all experiments. The syringe pump (SP 1) was connected to a 5 mL holding coil, constructed from Teflon® tubing (1/8" OD and 0.062" ID) and two Peek flangeless nuts. Teflon tubing (1/16" OD and 0.03" ID) and a mixture of Peek and Acetal flangeless nuts were used for connecting all other parts of the flow system.

Two GDUs were used in the SEA analyser: one for the alkaline solution clean-up (the 'scrubber') and another for the separation and pre-concentration of ammonia from the marine samples into a solution containing a pH sensitive colorimetric indicator dye. The 'scrubber' comprised a straight-channelled sandwich style GDU with 31.5 cm channel length, 2 mm width and 1.5 mm depth (i.e. 945 µL volume). The acceptor stream of this GDU contained a stripping solution (i.e. 0.5 M H₂SO₄ and crystal violet indicator), which was recirculated via the peristaltic pump and removed trace ammonia contamination from the NaOH/EDTA reagent solution. Crystal violet was added to this solution to indicate if the membrane in the scrubber had become compromised.

The main GDU used for the majority of the experiments comprised a sandwich-type configuration, with serpentine-shaped channels made from 9.5 cm Perspex blocks that were sandwiched together with 8 stainless steel screws. The height and width of the unit were 1.5 cm and 2.3 cm, respectively. Two identical 100 mm long serpentine channels were bored into each piece of Perspex at a depth of 0.5 mm and width of 2 mm [23]. Each end of the Perspex blocks had an inlet and an outlet port that were connected to the tubing with flangeless nuts (for 1/16" tubing). The donor channel was always facing downwards and the acceptor channel was always facing upwards in order to facilitate the migration of ammonia gas from the donor to the acceptor channel [23]. Both channels of the GDU were separated by a mechanically stable, super hydrophobic gas-diffusion membrane with 0.1 µm pore size (SureVent®, Merck Millipore), which was suitable for use under high flow rate conditions. Flow rates of 4.5 mL min⁻¹ and 1.2 mL min⁻¹ were used for delivery of the indicator solution to the acceptor channel, and the sample and alkaline solutions to the donor channel of the GDU, respectively (refer to the Programmable Flow Procedure, Table A2-1 in the Appendix).

Where possible, short lines were used to reduce sample dispersion and enhance sensitivity. Therefore, the tubing connecting the acceptor channel to the flow cell was 11.5 cm in length,

allowing for the reference absorbance measurement to be taken before the indicator sample plug entered the flow cell. The two external Cavo Tecan syringe pumps (SP 2 and SP 3), fitted with 2.5 mL syringe barrels (Tecan, Cavo, XC/XP), and the autosampler (Teledyne, CETAC Technologies, ASX-260) were programmed for use with the FIALab 3500 analyser.

The detection system comprised a USB4000 CCD spectrophotometer (Ocean Optics) and a LS-1 tungsten-halogen light source (Ocean Optics) connected by two 200 μm quartz optical fibres (Ocean Optics) to the 1 cm flow cell of the in-built MPV (Figure 2-1). SP 1 was used for the aspiration of large sample volumes into the holding coil, subsequent propulsion of the sample to the 20 cm mixing coil and donor channel of the GDU, and for cleaning the lines with a mildly acidic sample flushing solution (5 mM HCl). A 20 μL air bubble was aspirated into the holding coil to separate the sample plug from the 5 mM HCl in order to prevent dispersion when aspirating or dispensing the sample.

SP 2 was used to deliver the indicator solution to the acceptor channel of the main GDU, which was connected to the 1 cm flow cell of the MPV. Bromothymol blue in 0.68 M NaCl solution was the indicator used for most experiments and monitoring of the basic indicator species was undertaken at 615 nm. A reference wavelength of 750 nm was selected to correct for any optical interferences in the acceptor solution.

SP 3 was used to deliver a solution of NaOH and EDTA to the two GDUs, the former being the 'scrubber' and the latter being the main GDU (Figure 2-1). The NaOH and EDTA stream passed through the 'scrubber' GDU, prior to being merged with the sample stream.

The peristaltic pump was operated with Tygon pump tubing (TACS, Australia), orange-yellow (0.51 mm ID) for the recirculation of 0.5 M H_2SO_4 stripping solution and grey-grey (1.30 mm ID) for sample delivery to Port 5 (sample port) of the MPV. Approximately 1.5 mL of sample is required to prime the autosampler tubing and the sample port of the MPV, prior to introduction of a sample into the holding coil.

The autosampler tubing was modified to allow for rapid aspiration of samples into the holding coil, by connecting the autosampler needle to Port 5 of the MPV with white-white (1.02 mm ID) Tygon tubing.

2.2.8 Gas-diffusion cells and membranes

A number of different GDU configurations (Figure 2-2) were performance tested alongside a number of different porous hydrophobic membranes, with the specifications listed in Tables 2-1 and 2-2, respectively.

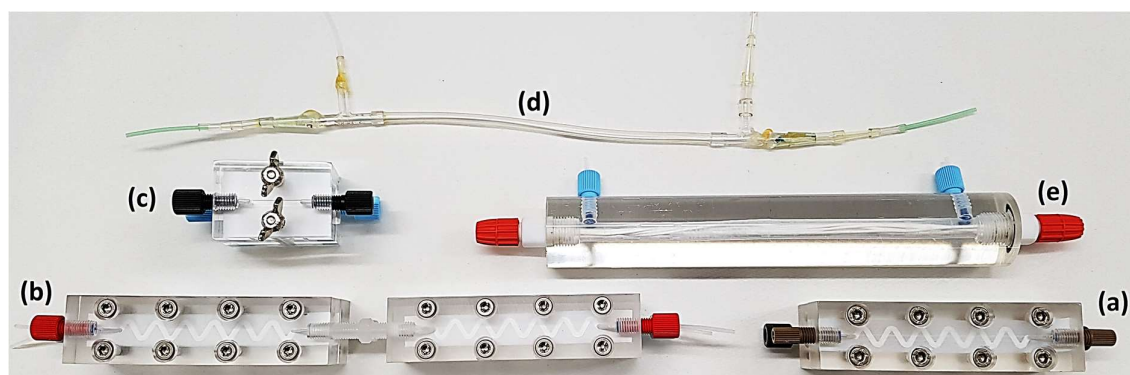


Figure 2-2. Different **GDU** configurations tested in order to select the configuration that achieved the highest sensitivity. The SureVent® membrane was used for the sandwich type **GDU**s, including the single (Serpentine x1) (a), double (Serpentine x2) (b), micro (μ **GDU**) (c). Accurel® capillaries were used for the construction of the single (d), and multi hollow fibre (e) tubular **GDU**s.

Table 2-1. Gas-diffusion configurations comparing various aspect ratios (exposed membrane area to channel volume ratio).

Configuration	Aspect ratio ($\text{cm}^2 \text{mL}^{-1}$)	Channel length (mm)	Width (mm)	Depth (mm)	Diameter (mm)	Pore size (μm)	Hydrophobic membrane (supplier)
Sandwich – serpentine channel (Figure 2-2a)	20	100	2	0.5	-	0.1	SureVent super hydrophobic PVDF (Millipore)
Sandwich – double serpentine channel (Figure 2-2b)	20	220	2	0.5	-	0.1	SureVent super hydrophobic PVDF (Millipore)
Sandwich – straight channel μ GDU (Figure 2-2c)	10	20	1	1	-	0.1	SureVent super hydrophobic PVDF (Millipore)
Single tubular membrane (Figure 2-2d)	52	110	-	-	0.75	0.2	Accurel PP capillary (Membrana)
Multi tubular membrane (n=6) (Figure 2-2e)	241	150	-	-	0.75	0.2	Accurel PP capillary (Membrana)

PP – polypropylene

Table 2-2. Hydrophobic membranes tested.

Configuration	Hydrophobic membrane	Pore size (µm)	Channel length (mm)	Width (mm)	Diffusion area (mm ²)
Flat membrane, serpentine flow path	SureVent Superhydrophobic PVDF (Millipore)	0.1	100	2	200
Flat membrane serpentine flow path	Durapore PVDF (Millipore)	0.2	100	2	200
Flat membrane serpentine flow path	Plumbers tape PTFE (Reece)	Un-specified	100	2	200
Flat membrane serpentine flow path	High density PTFE (Shamban)	Un-specified	100	2	200
Flat membrane serpentine flow path	Heavy duty pink PTFE (Boston)	Un-specified	100	2	200
Single tubular membrane	Accurel PP hollow fibre (Membrana)	0.2	110	-	260

PVDF – polyvinylidene difluoride, PTFE – polytetrafluoroethylene, PP – polypropylene

The sandwich type single block serpentine GDU described above using SureVent[®] superhydrophobic 0.1 µm pore size membrane was robust under high flow rates and provided good sensitivity. Therefore, it was used for all experiments except for the GDU and membrane optimisation experiments.

2.2.9 Program

Determination of ammonia nitrogen in seawater using the SEA analyser was achieved using the programmable flow procedure outlined in Table A2-1 (Appendix).

2.2.10 Data processing

FIAlab software version 5.9.314 for Windows was used with Microsoft Excel for data processing of all experimental data. Peak maximum ('local maximum') was used as the analytical signal, and each sample was measured in triplicate with the average signal used for all calculations. The Excel Solver function was used to compute the sample concentrations utilizing non-linear calibration equations, and the limits of detection and quantification were determined using

the error of the lower linear portion of the calibration equations, as described by Miller and Miller [38].

2.3 Results and discussion

2.3.1 Flow system optimization

Flow system optimisation experiments were undertaken to improve method sensitivity and are described in detail below. The effects of varying matrix salinity and interference from primary, secondary and tertiary amines were not assessed in this work, as such studies were undertaken and described in detail by Segundo et al. [21] and Oliviera et al. [24], respectively, showing there was no interference from solutions prepared with differing salinities, and no statistically significant difference in peak response between spiked and un-spiked samples for a number of ammine species, even when present in concentrations higher than those expected in marine waters.

2.3.2 Flow rate and sample volume

A stop-flow approach [24] was chosen as a strategy to maximize the SEA analyser efficiency. In all optimization experiments the acceptor stream was stopped in the GDU until the sample zone had passed through the donor channel of the GDU.

The flow rate of the donor stream is expected to affect how much ammonia can pass through the hydrophobic membrane into the acceptor solution. A low flow rate will result in the sample zone spending a longer duration of time in the GDU, thus facilitating the diffusion of molecular ammonia into the acceptor stream. However, this is at the expense of sample throughput. In turn a higher flow rate will result in the sample passing through the GDU more quickly and thus the efficiency of mass transfer of molecular ammonia across the membrane is reduced. There is a trade-off between achieving high sensitivity whilst simultaneously achieving an acceptable sample throughput. Low flow rates provided relatively higher absorbance signals when compared to higher flow rates (Figure 2-3a), however, sample throughput was reduced by decreasing the flow rates. For a 1 mL sample volume (where 0.2 mL alkaline solution was used to increase the sample pH), the flow rate of 1.2 mL min⁻¹ was chosen as the optimum flow rate, as it allowed for sufficient amount of molecular ammonia to diffuse into the acceptor solution,

whilst ensuring a reasonable sample throughput of 2 min per sample volume of 1 mL. However, whilst lower flow rates prolonged the lifetime of the GDU membrane (i.e. Millipore SureVent® ‘super-hydrophobic’ membrane), flow rates higher than 4 mL min⁻¹ required the membrane to be changed more frequently, and given that priming the membrane was a time-consuming process, it was decided that such high flow rates for sample delivery should be avoided.

Similarly, to flow rate, the sample volume is likewise expected to affect how much analyte can be pre-concentrated into the acceptor solution. By simply increasing the sample volume dispensed through the donor channel of the GDU, the number of ammonia molecules diffusing across the porous hydrophobic membrane into the stagnant acceptor solution also increased, thus improving analyte pre-concentration (Figure 2-3b). However, larger sample volumes allowed for an increase in sensitivity at the expense of sample throughput. Therefore, it was important to determine the appropriate sample volume to use for each ammonia concentration range of interest. A 2 mL sample with 0.4 mL of alkaline reagent, 1 mL sample with 0.2 mL of alkaline reagent and 0.25 mL sample with 0.05 mL of alkaline reagent were the optimal sample and reagent volumes found to provide good sensitivity and sample throughput for the concentration ranges 0.028 – 5.6, 0.28 – 13.9, 1.4 – 55.6 μM NH₄⁺, respectively.

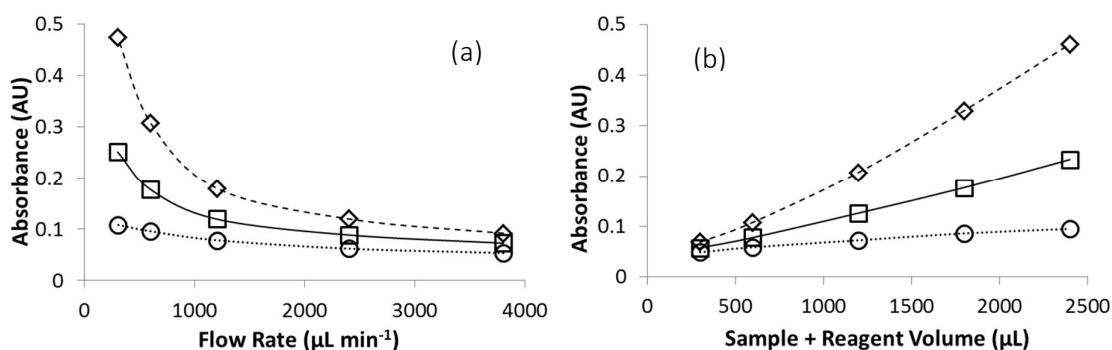


Figure 2-3. (a) Effect of the donor stream flow rate on the analytical signal for three different ammonium standards: blank (○), 1.4 μM (□) and 2.8 μM (◇). The conditions of the experiment are as follows: Sample volume, 1 mL; alkaline solution volume (NaOH and EDTA), 0.2 mL; acceptor stream flow rate, stop-flow, each data point is the average of 3 replicate injections. (b) Effect of the sample and reagent volume on the maximum absorbance for three different ammonium standards: blank (○), 1.4 μM (□) and 2.8 μM (◇). The conditions of the experiment are as follows: Alkaline solution volume (NaOH and EDTA), 0.2 mL; donor stream flow rate, 1.2 mL min⁻¹; acceptor stream flow rate, stop-flow, each data point is the average of 3 replicate injections.

2.3.3 Gas-diffusion apparatus

Parameters such as surface area, GDU configuration and membrane porosity, are known to affect gas-diffusion and were investigated. For large sample volumes, GDUs with a large aspect ratio are desirable to facilitate high contact between the sample and the membrane, which will in turn allow for greater diffusion and mass transfer of molecular ammonia to the indicator solution resulting in enhanced sensitivity. Pore size is likewise an important factor to consider in terms of mass transfer efficiency.

Several GDU configurations (Figure 2-2, Table 2-1) were tested, namely sandwich-style GDUs and hollow fibre type [39]. A small increase in sensitivity was achieved using the double serpentine GDU (i.e. two serpentine GDUs) when compared to the single serpentine GD cell (Figure 2-4a). However, as the double serpentine GDU consisted of two single GDUs joined together by two Teflon two-way flangeless connectors for 1/16" tubing (one connecting the donor channels and the other connecting the acceptor channels), a double-humped peak appeared, where the dip between the two humps resulted from the acceptor solution held static in the connecting tubing, where no diffusion had occurred. For this reason, it was not used further.

A tubular GDU was constructed using a single hydrophobic microporous hollow fibre (0.03" ID, Accurel®, Membrana) inserted into a piece of silicone tubing (red – red, Tygon) where each end was fitted with a glass T-piece, with the hollow fibre being fixed into place using epoxy glue and pipette tips. The space between the silicone tube and the hollow fibre corresponded to the donor channel, and the hollow fibre was the acceptor channel. The pipette tips and the glass T-piece ends were connected to the two ends of the hollow fibre using small pieces of silicone tubing. Whilst this GDU provided an approximate three-fold increase in sensitivity compared to the sandwich style GDUs (Figure 2-4a), there was a significant contamination problem when using epoxy glue to fix the hollow fibre in place. Many commercial epoxy resin glues consist of one part epoxide and one part tertiary ammine. The unreacted amines on the surface of the hardened resin, when in contact with the alkaline solution, diffused across the hollow fibre walls resulting in a very large blank response. After several hours of flushing with water to remove unreacted tertiary ammine on the surface of the epoxy glue, the blank signal appeared to decrease. However, it was still present and the standard deviation for replicate samples was high. Due to these interference effects the tubular GDU was discarded.

The small surface area of the μ GDU resulted in insufficient sensitivity (Figure 2-4a), and the multi hollow fibre in chamber GDU had substantial problems with bubbles getting trapped in-between each of the fibres, where it was impossible to dislodge them, reducing the sensitivity of this type of GDU despite the high aspect ratio (Figure 2-4a, Table 2-1). Moreover, it was similarly constructed with epoxy glue, which also meant it had a large blank response.

The sandwich-style single serpentine GDU was therefore chosen for further experiments. It was easy to use, as bubbles did not present as a problem, and it could be easily flushed out with each new sample. High flow rates were able to be used with this GDU configuration with little problem.

A number of different porous hydrophobic membranes were tested (Figure 2-4b), with pore sizes specified for some, and pore sizes un-specified for commercial plumbing membranes (Table 2-2). All membranes required some degree of priming (a process where water is continuously flushed through the GDU to remove all bubbles appearing on the surface of the porous hydrophobic membrane), with the PTFE membrane requiring on average a couple of hours compared to the SureVent[®] and Durapore[®] membranes requiring between one to two days. However, despite longer priming times when compared to their PTFE counterparts, both Durapore[®] and SureVent[®] membranes exhibited superior mechanical stability. Durapore[®] was able to be used for approximately 1 week under high flow rate conditions, and SureVent[®] for several months. All other membranes exhibited some degree of membrane deformation under high flow rate conditions. Despite the long priming time, and slightly lower sensitivity (Figure 2-4b) SureVent[®] was the membrane of choice. SureVent[®] is a mechanically stable membrane, which has been treated to give extra hydrophobicity compared to its Durapore[®] counterpart. As a result of this treatment, these membranes lasted longer under high flow rate conditions. The smaller pore size of the SureVent[®] membrane is likewise desirable, as although it may compromise sensitivity a little, it provides better membrane stability at higher flow rates and can be expected to be more effective at reducing interference from large molecular mass amines. All commercial plumbing tapes were very soft and prone to distortion.

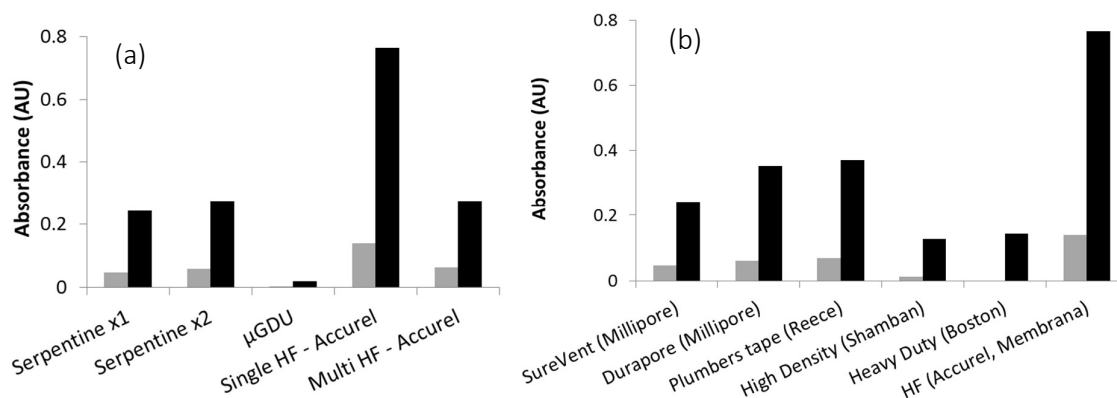


Figure 2-4. (a) Performance of different GDU configurations where the blank response which was different for each type of GDU configuration, was subtracted from the two ammonium standards (grey bar, 1.4 μM and the black bar, 5.6 μM) in order to simplify the comparison of GDU configuration sensitivity. The SureVent® membrane was used for the single (Serpentine x1), double (Serpentine x2), and micro (μGDU) sandwich type GDUs and Accurel® filaments were used in the construction of the single and multi hollow fibre tubular GDUs. Each data point is the average of 3 replicate injections. (b) Performance of different porous hydrophobic membranes was examined using the sandwich type GDU for all membranes except for the Accurel® tubular filaments from Membrana. The blank signal for each different membrane was subtracted from the signals for the two ammonium standards (grey bar, 1.4 μM; black bar, 5.6 μM) to allow for a comparison of membrane sensitivity. HF is defined as hollow fibre for both figures (a) and (b). Each data point is the average of 3 replicate injections.

2.3.4 Acid-base indicator dyes

In order to determine the optimum acceptor solution composition for trace determination of ammonia nitrogen in seawater, a number of spectrophotometric acid-base indicator dyes were examined. Factors known to affect the sensitivity of the acceptor solution are the pKa and molar absorptivity of the indicator [40], acceptor solution pH, buffering capacity and indicator concentration [41-43], and ionic strength [22]. Additionally, Schulze et al. [40] describe that the pH of the acceptor solution should be adjusted close to the equivalence point of the indicator in order to achieve maximum sensitivity. However, it should be taken into consideration that the higher the baseline absorbance, the narrower the working range. The baseline absorbance for this method was therefore set to between 0.180 - 0.200 (Figure 2-5a) when running real samples.

Several indicator dyes and dye mixtures were selected for analysis according to their respective pKa values. Acceptor solutions were prepared by making small adjustments to the pH in order

to achieve a baseline absorbance of 0.200 ± 0.005 for each solution. The analytical signals for the ammonium standards (1.4 and 2.8 μM) after blank correction, were used to compare the sensitivity of each acceptor solution (Figure 2-5b). Bromothymol blue (BTB) was the indicator chosen for method development, because it exhibited the highest sensitivity compared to all indicator solutions tested.

A mixture of several indicators can increase the working range of the method, whilst maintaining sensitivity, provided there is a maximum of 1 pH unit difference between the pKa values of the individual indicators, the basic forms have similar molar absorptivity values and that the respective indicator dyes absorb at approximately the same wavelength [44].

The dynamic range of the method using a quadratic calibration equation can be extended by simply combining two or more different indicators as shown in Figure 2-5c, where the range was extended by 2.8 μM NH_4^+ when thymol blue was used in combination with BTB. However, whilst the working range of the method can be extended by using a combination of indicators, sensitivity is slightly compromised. Therefore, one must decide which of these factors is more important when choosing an appropriate acceptor solution composition.

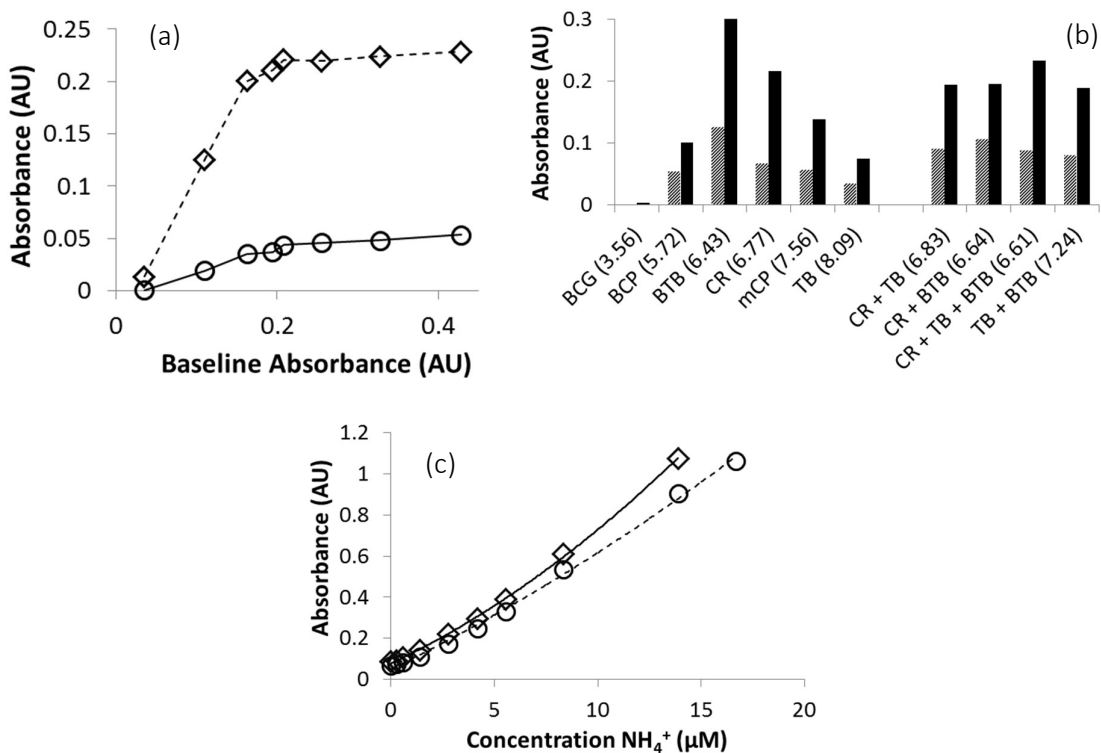


Figure 2-5. (a) Blank corrected absorbance response for for 1.4 μM (○) and 2.8 μM (◇) ammonium standards as a function of baseline absorbance (100 μM bromothymol blue acceptor solution containing 0.68 M NaCl). Each data point is the average of 3 replicate injections. (b) Absorbance response for different colour indicator dye solutions, as single dyes or as mixtures. The graph shows the blank corrected response for 1.4 μM (grey bar) and 2.8 μM (black bar) ammonium standards to highlight the sensitivity in the case of each indicator solution. Mixed indicator solutions were prepared in equal proportions of each indicator, and the numbers in brackets indicate the pH of the indicator solution at which the experiment was undertaken. Each data point is the average of 3 replicate injections. (c) The working range of the method can be extended when mixed indicator solutions are used, provided the pKa's of the respective indicators selected do not vary by more than 1 pH unit. The range of the 1:1 ratio **BTB** + thymol blue solution (○) ($y = (8.1186 \times 10^{-4})x^2 + (4.8406 \times 10^{-2})x + 5.0921 \times 10^{-2}$, $R^2 = 99.737$) could be extended by up to 2.4 μM NH₄⁺ compared to the solution of **BTB** only (◇) ($y = (1.7778 \times 10^{-3})x^2 + (4.7322 \times 10^{-2})x + 7.7463 \times 10^{-2}$, $R^2 = 99.938$). Each data point is the average of 3 replicate injections.

2.4 SEA analyser system performance

2.4.1 Analytical figures of merit

Three different working ranges were obtained by simple manipulation of the analyser control program, specifically by setting different sample volumes, namely 2.0, 1.0 and 0.25 mL, with typical calibration curves provided in Figure 2-6. For low concentration ammonia nitrogen

samples, larger volumes were required to achieve sufficient pre-concentration in the GDU, and conversely for high concentration samples, smaller volumes sufficed. Hence, an overall range of 0.028 – 55.6 μM NH_4^+ could be covered.

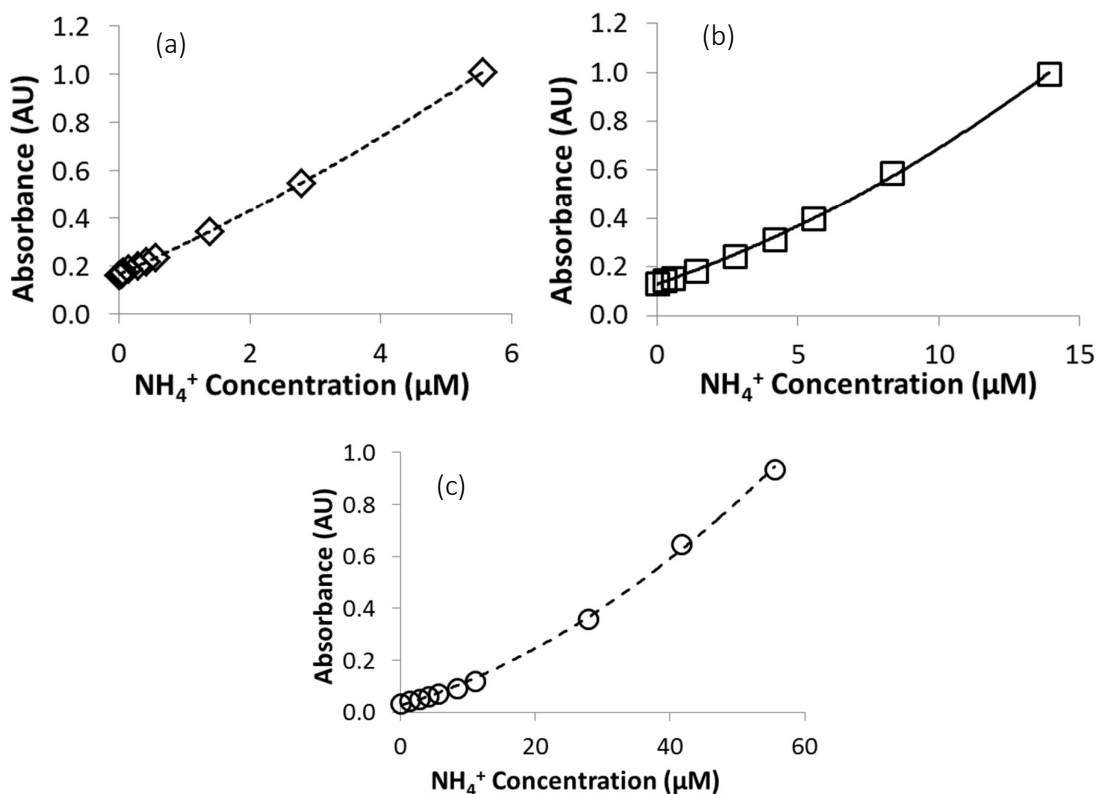


Figure 2-6. Three typical concentration working ranges based on sample volume: (a) (\diamond) 0.028 – 5.6 μM NH_4^+ , sample volume 2.0 mL; (b) (\square) 0.28 – 13.9 μM NH_4^+ , sample volume 1.0 mL; and (c) (\circ) 1.4 – 55.6 μM NH_4^+ , sample volume 0.25 mL. The corresponding calibration equations and coefficients of determination are shown in Table 2-3. Each data point is the average of 3 replicate injections.

The respective analytical figures of merit for each typical working range are outlined in Table 2-3. The limits of detection and limits of quantification were determined using the error of the regression described by Miller and Miller [38], and second order polynomial regressions were used to describe the dynamic range. The LINEST function in Microsoft Excel was used to calculate the standard deviation of the estimate of the regression coefficients.

Table 2-3. Analytical figures of merit of the SEA analyser for three typical working ranges (Figure 2-6).

Ammonium concentration range	0.028 – 5.6 μM Figure 2-6(a)	0.28 – 13.9 μM Figure 2-6(b)	1.4 – 55.6 μM Figure 2-6(c)
Repeatability (% RSD) n=10	± 0.71 (0.556 μM)*	± 1.2 (4.16 μM)*	± 0.97 (13.89 μM)*
LOD (nM)	15	88	440
LOQ (nM)	50	290	1,500
Sampling rate (h^{-1})	20	30	40
Sample volume (mL)	2.0	1.0	0.25
Calibration equation	$y = (1.6157 \pm 0.0852) \times 10^{-5} x^2 + (6.8460 \pm 0.0827) \times 10^{-3} x + (1.6499 \pm 0.0089)$	$y = (5.0627 \pm 0.5173) \times 10^{-6} x^2 + (2.2094 \pm 0.1280) \times 10^{-3} x + (0.12862 \pm 0.0052)$	$y = (4.8545 \pm 0.4860) \times 10^{-7} x^2 + (4.3545 \pm 0.4725) \times 10^{-4} x + (2.6182 \pm 0.6314) \times 10^{-2}$
Coefficient of determination, R^2	99.994	99.921	99.886

* Concentration used to determine the repeatability

2.5 Validation of the SEA analyser

2.5.1 Measurement of certified reference materials

The accuracy of the newly developed SEA system was determined using a Certified Reference Material (CRM). Four different dilutions of the CRM spanning the concentration range 0.28 – 11.1 μM NH_4^+ were analysed. The results for the lower concentrations (0.28 and 0.56 μM) had predictably higher errors than those for the higher concentrations (5.0 and 11.1 μM NH_4^+), as shown in Table 2-4. These observations are consistent with results achieved for similar analytical methods developed for the monitoring of nutrients [45], and dissolved Fe(II) [46] in complex matrices, and in line with guidelines established for the validation of analytical methods that specify that the concentration of CRMs should be between 75 % - 80 % at the lower end, and 120% - 125% at the upper end of the stated or known value [47, 48].

Table 2-4. Method validation using a diluted CRM in 0.6 M NaCl, for the calibration range 0.28 – 13.9 μM NH_4^+ (Table 2-3).

Nominal Concentration of Standards (μM NH_4^+)	Concentration of Standards Measured (μM NH_4^+)	Relative Standard Deviation (%)	Relative Error (%)
0.28	0.20 ± 0.03	12.6	± 29.3
0.56	0.60 ± 0.04	6.5	± 8.5
5.0	4.9 ± 0.05	1.0	± 1.9
11.1	11.2 ± 0.04	0.4	± 0.5

2.5.2 Spike-and-recovery studies

Seawater and estuarine samples collected from around *Nerm* (Port Phillip Bay) and Bancoora Surf Beach, (Victoria, Australia) were analysed directly by the proposed SEA analyser and the results are shown in Figure 2-7.

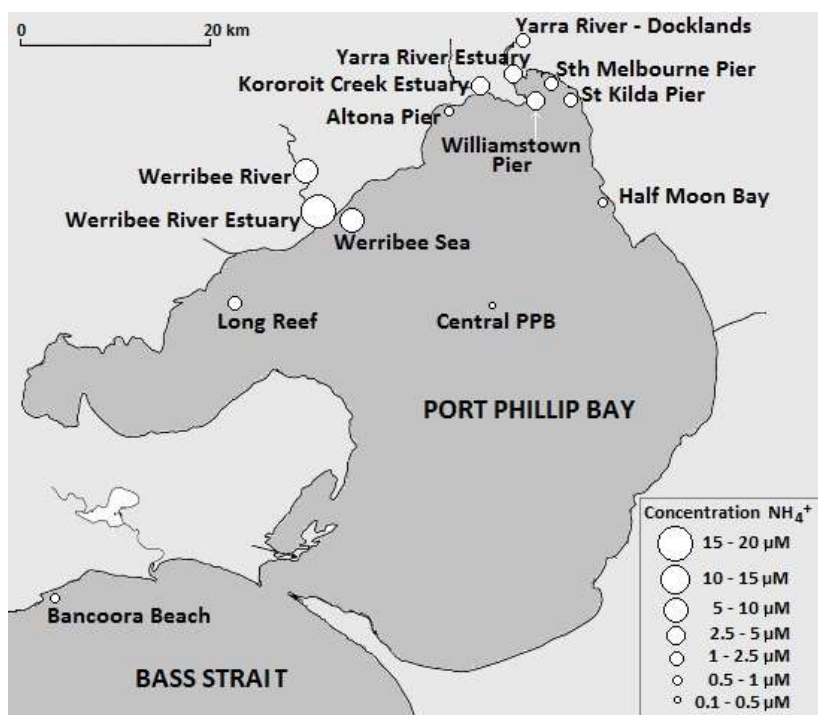


Figure 2-7. Sampling sites around the Port Phillip Bay Study Area with the average range of concentrations of ammonia nitrogen measured with the SEA analyser (○).

Seawater and estuarine water of seven locations was used for spike-and-recovery analysis. In one of the locations (South Melbourne) seawater was collected on two different days. The concentrations obtained fell between 0.56 – 2.2 μM NH₄⁺ at the different locations, allowing for the 0.28 – 13.9 μM calibration equation (Table 2-3) to be used with 1.0 mL sample volumes. These samples were spiked with three different concentrations of ammonium stock solution, namely 0.56, 5.0 and 10.6 μM, which were selected in order to test the performance of the method at the low, mid and upper sections of the calibration range. The recoveries obtained for the spiked samples are presented in Figure 2-8. At the lower end of the range (i.e. samples spiked with 0.56 μM ammonia) some variability was observed with recoveries between 83.5 –

116.5 %, which is reasonable considering this falls at the lower end of the calibration curve where there is a greater inherent error due to the lower signal to noise ratio. Recoveries within 90.0 – 99.4 % and 97.0 – 103.3 % were obtained for the samples spiked with 5.0 and 10.6 μM , respectively.

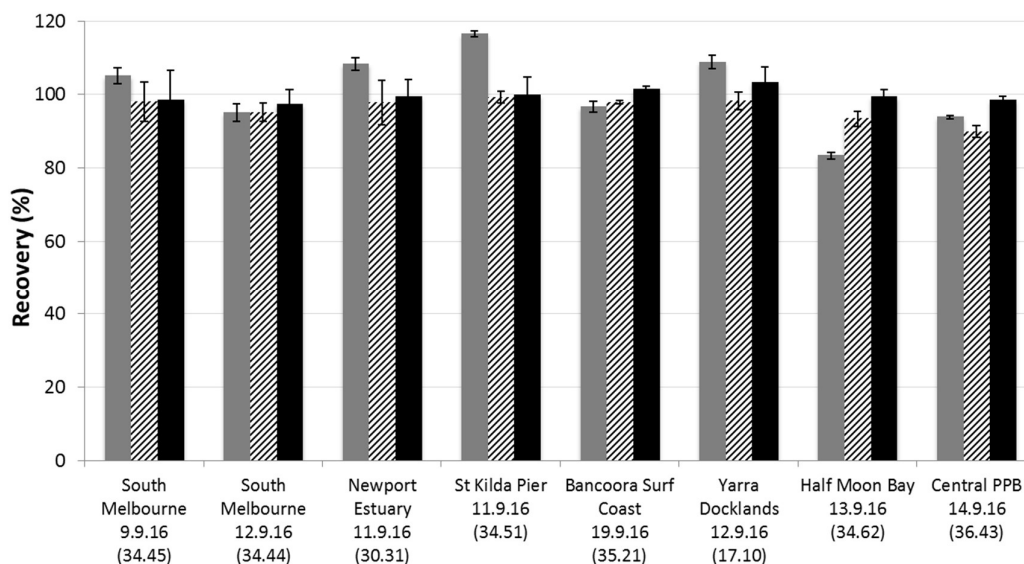


Figure 2-8. Spiked recoveries of seawater samples of varying salinity from around Port Phillip Bay (PPB), and Bancoora Surf Beach. Three different ammonium concentrations were used to spike the samples: 0.56 (grey bar), 5.0 (crosshatched bar) and 10.6 μM (black bar), respectively. The numeric values after the location description indicate the date of sample collection (dd.mm.yy) and the value in brackets corresponds to the salinity of the samples using the Practical Salinity Scale 1978 [49].

2.6 Conclusions

A highly sensitive programmable flow analysis method for the trace determination of ammonia nitrogen in seawater has been described using the newly developed SEA analyser. This flow system enables the sensitivity of the method to be tailored to the concentration range of interest, by simple modification of the program involving appropriate adjustment of the sample volume. Manifold changes are not necessary to achieve a wide working range, making this method practical, versatile and applicable for use in coastal and oceanic environments.

The method developed employs a novel flow approach whereby large sample volumes and small reagent volumes are continuously merged and delivered to the donor channel of the

GDU under stop-flow conditions, rather than using discrete sample plugs as described in the literature for flow injection and sequential injection analysis methods for ammonia nitrogen determination in natural waters [20-22, 26, 28, 50]. Whilst Segundo et al. described a spectrophotometric sequential injection method capable of achieving two dynamic ranges by making small changes in the protocol sequence (i.e. 5.5 – 55 and 55 - 222 $\mu\text{M NH}_4^+$) for example by doubling the number of sample and sodium hydroxide plugs aspirated into the holding coil [21], the range achieved was narrower than that of the newly developed method, with a detection limit of two orders of magnitude higher (i.e. 1.5 $\mu\text{M NH}_4^+$). The conductometric method developed by Plant et al. provided comparable detection limits to those described in this work (i.e. 14 nM for shelf waters), by increasing the number of sample pulses delivered to the GDU and decreasing the flow rate, however the sample throughput was compromised allowing for a little over 3 samples per hour to be measured [37]. Whilst this sampling frequency may be appropriate for *in situ* analysis, it would be unsuitable for use during shipboard analysis or for use in a laboratory setting. In addition, while the components used in the method of Plant et al. are commercially available, the in-house modification of the conductivity cell, manufacturer modification of the micro solenoid pumps and detector board, and the use of custom software to control the data logger/controller may impede the accessibility of this method to potential users.

In the proposed method, high flow rates of the donor stream under stop-flow conditions for the acceptor stream were achievable using the mechanically stable superhydrophobic SureVent® microfiltration membrane (Millipore) in the GDU, allowing for good sample throughput to be achieved for all ranges with approximately 20 samples per hour achieved for the low concentration range, 30 samples per hour for the mid-range and 40 samples per hour for the upper range. The following working ranges were obtained by sample volume adjustment, 0.028 – 5.6 (2.0 mL sample volume), 0.28 – 13.9 (1.0 mL sample volume), 1.4 – 55.6 $\mu\text{M NH}_4^+$ (0.25 mL sample volume). These ranges are characterised by typical limits of detection of 0.015, 0.088 and 0.44 $\mu\text{M NH}_4^+$, respectively, with the sensitivity for the lowest range comparable to some fluorometric detection methods described in the literature [30, 33, 51].

Spike-and-recovery analysis produced good results, and method validation using a CRM showed that in the mid-to upper calibration range the error was minimal. These results

illustrate the potential of the newly developed method for reliably determining ammonia nitrogen in seawater samples over a wide and realistic concentration range.

2.7 Appendix

Table A2-1. Programmable flow procedure for the determination of ammonia nitrogen in seawater.

Step	Commands	Corresponding Actions
0	Hardware Settings Wavelength 1 (nm) 615 Hardware Settings Wavelength 4 (nm) 750 Hardware Use Wavelength 4 as Reference Hardware Settings Optimize Integration Peristaltic Pump Clockwise(%) 65	Instrument settings and measurement parameters defined at the outset of experiment. Ensure all lines have been primed, bubbles expelled and syringe barrels emptied prior to analysis.
1	Loop Start (#) 3 Next Sample Analyte New Sample Peristaltic Pump On SP Sample Valve Out SP Sample Flowrate (microliter/sec) 200 SP Sample Aspirate (microliter) 1500* SP Indicator Valve Out SP Indicator Flowrate (microliter/sec) 200 SP Indicator Aspirate (microliter) 1500 SP NaOH Valve Out SP NaOH Flowrate (microliter/sec) 100 SP NaOH Aspirate (microliter) 200* SP Indicator Delay Until Done Autosampler Pump Off	Define next sample, and send autosampler to sample reservoir. 3 replicates to be analysed defined by Loop Start (#) 3. SP-Sample, SP-Indicator and SP-NaOH syringes fill, whilst the peristaltic pump delivers sample to port 5 of MPV ensuring that ample sample passes through the tubing to prime lines. SP-Sample fills with an acidic flushing solution, which is delivered to the GDU after each aliquot of sample, to prevent clogging of the gas-diffusion membrane by divalent cations precipitating from the highly alkaline seawater. Autosampler pump switched off after washing from previous sample.
2	SP Indicator Valve In SP Indicator Flowrate (microliter/sec) 75 SP Indicator Dispense (microliter) 750 Peristaltic Pump Off SP Sample Valve In Multiposition Valve AIR SP Sample Aspirate (microliter) 20 SP Sample Delay Until Done Multiposition Valve Sample SP Sample Flowrate (microliter/sec) 200 SP Sample Aspirate (microliter) 1000* SP Sample Delay Until Done	Indicator solution is dispensed to the acceptor chamber of the GDU where it is held static. A 20 µL air bubble is aspirated into the holding coil to prevent contact and subsequent dispersion of the sample with the acidic flushing solution. Sample is aspirated into the holding coil at a high flow rate of 200 µL min ⁻¹ .
3	SP NaOH Valve In Multiposition Valve GD Cell SP Sample Flowrate (microliter/sec) 20 SP Sample Dispense (microliter) 2500* SP NaOH Flowrate (microliter/sec) 4 SP NaOH Dispense (microliter) 200** SP NaOH Delay Until Done	Sample and alkaline solution are merged in the mixing coil and continuously delivered to the donor chamber of the GDU. During this time, the acceptor channel is held static allowing pre-concentration of ammonia into the acceptor solution in the GDU. Once the sample has passed through the GDU, the bubble will pass and the acidic flushing solution will clean the donor chamber of the GDU and all tubing.
4	SP Indicator Flowrate (microliter/sec) 10 SP Indicator Dispense (microliter) 750 Spectrometer Reference Scan Spectrometer Absorbance Scanning Autosampler Pump On Delay (sec) 10 SP Indicator Flowrate (microliter/sec) 30	SP-Indicator is engaged and the spectrometer takes the reference scan, immediately followed by continuous absorbance scanning. It takes approximately 5 seconds before the plug of indicator where the ammonia has been concentrating passes through the spectrophotometric flow-through cell.

Continued on next page

5	SP Sample Flowrate (microliter/sec) 75 Delay (sec) 2 Spectrometer Stop Scanning Peristaltic Pump On Autosampler Wash Autosampler Wash Peristaltic Pump Off SP Sample Stop*** Multiposition Valve Waste*** SP Sample Flowrate (microliter/sec) 200*** SP Sample Empty*** SP Sample Delay Until Done*** Loop End	The autosampler pump is turned on to flush the needle washing chamber with fresh water. Peristaltic pump is switched on whilst the autosampler needle is washed. This allows for small volumes of water to be drawn into the tubing flushing any residual sample to waste prior to aspiration of next sample. ***Any remaining flushing solution is expelled from the SP-Sample and holding coil via the waste port of the MPV.
----------	---	---

* Commands highlighted in **BOLD** can be modified to achieve desired sensitivity and concentration range. ** For every 1 mL sample, 200 µL NaOH/citrate are needed, therefore this volume is adjusted according to the sample volume used. *** These commands are only used for samples larger than 1 mL. This is because it takes longer for the SP-Sample to deliver 1.5 mL of flushing solution, than it does for the program to run to the end of the loop. Therefore, for samples larger than 1 mL SP-Sample is flushed with acidic flushing solution whilst the absorbance measurements are being collected, however, after the run is finished and prior to the loop end, the MPV is directed to waste, and the remaining solution is dispensed to at a rate much more rapid than what could be passed through the GDU. No carryover was observed.

Acknowledgements

We are grateful to the Australian Research Council (Linkage Grant LP110200595)) for financial support and to Mr Andrew Longmore and the Centre for Aquatic Pollution Identification and Management in assisting with the collection of samples in the *Nerm* (Port Phillip Bay study area). Lenka O'Connor Šraj is grateful to the University of Melbourne for the award of a postgraduate scholarship.

References

1. Karl, D.M., R.R. Bidigare, M.J. Church, J.E. Dore, R.M. Letelier, C. Mahaffey, and J.P. Zehr, *Chapter 16 - The Nitrogen Cycle in the North Pacific Trades Biome: An Evolving Paradigm*, in *Nitrogen in the Marine Environment (2nd Edition)*. 2008, Academic Press: San Diego. p. 705-769.
2. Camargo, J.A. and A. Alonso, *Ecological and toxicological effects of inorganic nitrogen pollution in aquatic ecosystems: A global assessment*. *Environ. Int.*, 2006. **32**: p. 831-849.
3. Schlacher, T.A., J.A. Mondon, and R.M. Connolly, *Estuarine fish health assessment: Evidence of wastewater impacts based on nitrogen isotopes and histopathology*. *Marine Pollution Bulletin*, 2007. **54**(11): p. 1762-1776.
4. CENR, *An Assessment of Coastal Hypoxia and Eutrophication in U.S. Waters*, N.S.a.T.C.C.o.E.a.n. Resources, Editor. 2003: Washington D.C.
5. Anderson, D.M., P.M. Glibert, and J.M. Burkholder, *Harmful algal blooms and eutrophication: Nutrient sources, composition, and consequences*. *Estuaries*, 2002. **25** (4): p. 704-726.
6. Gray, S., G. Hanrahan, I. McKelvie, A. Tappin, F. Tse, and P. Worsfold, *Flow analysis techniques for spatial and temporal measurement of nutrients in aquatic systems*. *Environmental Chemistry*, 2006. **3**(1): p. 3-18.
7. Worsfold, P.J., R. Clough, M.C. Lohan, P. Monbet, P.S. Ellis, C.R. Quetel, G.H. Floor, and I.D. McKelvie, *Flow injection analysis as a tool for enhancing oceanographic nutrient measurements-A review*. *Analytica Chimica Acta*, 2013. **803**: p. 15-40.
8. O'Connor Šraj, L., M.I.G.S. Almeida, S.E. Swearer, S.D. Kolev, and I.D. McKelvie, *Analytical challenges and advantages of using flow-based methodologies for ammonia determination in estuarine and marine waters*. *TrAC Trend. Anal. Chem.*, 2014. **59**: p. 83-92.
9. Jodo, M., K. Kawamoto, M. Tochimoto, and S.C. Coverly, *Determination of nutrients in seawater by segmented-flow analysis with higher analysis rate and reduced interference on ammonia*. *Journal of Automatic Chemistry*, 1992. **14**(5): p. 163-167.
10. Ariza, A.C., P. Linares, M.D.L. Decastro, and M. Valcarcel, *Flow-injection analysis for online monitoring of nutrients (ammonia and nitrite) in aquaculture*. *Journal of Automatic Chemistry*, 1992. **14**(5): p. 181-183.
11. Muraki, H., K. Higuchi, M. Sasaki, T. Korenaga, and K. Toei, *Fully automated system for the continuous monitoring of ammonium ion in fish farming plant seawater by flow-injection analysis*. *Analytica Chimica Acta*, 1992. **261**(1-2): p. 345-349.
12. Eaton, A., L.S. Clesceri, and A.E. Greenberg, *Standard Methods for the Examination of Water and Wastewater*. 19th ed ed. 1995, Alexandria, VA: American Public Health Association, American Water Works Association, Water Environment Federation.
13. Molins-Legua, C., S. Meseguer-Lloret, Y. Moliner-Martinez, and P. Campins-Falco, *A guide for selecting the most appropriate method for ammonium determination in water analysis*. *Trends in Analytical Chemistry*, 2006. **25**(3): p. 282-290.
14. Shoji, T. and E. Nakamura, *Flow injection analysis with spectrophotometry for ammonium ion with 1-naphthol and dichloroisocyanurate*. *Journal of Flow Injection Analysis*, 2009(26): p. 37-42.
15. Kempers, A.J. and C.J. Kok, *Re-examination of the determination of ammonium as the indophenol blue complex using salicylate*. *Analytica Chimica Acta*, 1989. **221**: p. 147-155.
16. Li, Q.P., J.Z. Zhang, F.J. Millero, and D.A. Hansell, *Continuous colorimetric determination of trace ammonium in seawater with a long-path liquid waveguide capillary cell*. *Marine Chemistry*, 2005. **96**(1-2): p. 73-85.
17. Zhu, Y., D. Yuan, Y. Huang, J. Ma, S. Feng, and K. Lin, *A modified method for on-line determination of trace ammonium in seawater with a long-path liquid waveguide capillary cell and spectrophotometric detection*. *Marine Chemistry*, 2014. **162**: p. 114-121.

18. Páscoa, R.N.M.J., I.V. Tóth, and A.O.S.S. Rangel, *Review on recent applications of the liquid waveguide capillary cell in flow based analysis techniques to enhance the sensitivity of spectroscopic detection methods*. *Analytica Chimica Acta*, 2012. **739**: p. 1-13.
19. Chen, G.H., M. Zhang, Z. Zhang, Y.M. Huang, and D.X. Yuan, *On-line solid phase extraction and spectrophotometric detection with flow technique for the determination of nanomolar level ammonium in seawater samples*. *Analytical Letters*, 2011. **44**(1-3): p. 310-326.
20. Hunter, D.A. and R.F. Uglow, *A technique for the measurement of total ammonia in small volumes of seawater and hemolymph*. *Ophelia*, 1993. **37**(1): p. 31-40.
21. Segundo, R.A., R.B.R. Mesquita, M. Ferreira, C. Teixeira, A.A. Bordalo, and A. Rangel, *Development of a sequential injection gas diffusion system for the determination of ammonium in transitional and coastal waters*. *Analytical Methods*, 2011. **3**(9): p. 2049-2055.
22. Willason, S.W. and K.S. Johnson, *A rapid, highly sensitive technique for the determination of ammonia in seawater*. *Marine Biology*, 1986. **91**(2): p. 285-290.
23. Kolev, S.D., P.R.L.V. Fernandes, D. Satinsky, and P. Solich, *Highly sensitive gas-diffusion sequential injection analysis based on flow manipulation*. *Talanta*, 2009. **79**(4): p. 1021-1025.
24. Oliveira, S.M., T. Lopes, I.V. Toth, and A. Rangel, *Determination of ammonium in marine waters using a gas diffusion multicommutated flow injection system with in-line prevention of metal hydroxides precipitation*. *Journal of Environmental Monitoring*, 2009. **11**(1): p. 228-234.
25. Gray, S.M., P.S. Ellis, M.R. Grace, and I.D. McKelvie, *Spectrophotometric determination of ammonia in estuarine waters by hybrid reagent-injection gas-diffusion flow analysis*. *Spectroscopy Letters*, 2006. **39**(6): p. 737-753.
26. Jones, R.D., *An improved fluorescence method for the determination of nanomolar concentrations of ammonium in natural waters*. *Limnology and Oceanography*, 1991. **36**(4): p. 814-819.
27. Kérrouel, R. and A. Aminot, *Fluorometric determination of ammonia in sea and estuarine waters by direct segmented flow analysis*. *Marine Chemistry*, 1997. **57**(3): p. 265-275.
28. Masserini, R.T. and K.A. Fanning, *A sensor package for the simultaneous determination of nanomolar concentrations of nitrite, nitrate, and ammonia in seawater by fluorescence detection*. *Marine Chemistry*, 2000. **68**(4): p. 323-333.
29. Amornthammarong, N. and J.-Z. Zhang, *Shipboard Fluorometric Flow Analyzer for High-Resolution Underway Measurement of Ammonium in Seawater*. *Analytical Chemistry*, 2008. **80**(4): p. 1019-1026.
30. Amornthammarong, N., J.Z. Zhang, and P.B. Ortner, *An autonomous batch analyzer for the determination of trace ammonium in natural waters using fluorometric detection*. *Analytical Methods*, 2011. **3**(7): p. 1501-1506.
31. Zhu, Y., D. Yuan, Y. Huang, J. Ma, and S. Feng, *A sensitive flow-batch system for on board determination of ultra-trace ammonium in seawater: method development and shipboard application*. *Analytica chimica acta*, 2013. **794**: p. 47-54.
32. Watson, R.J., E.C. Butler, L.A. Clementson, and K.M. Berry, *Flow-injection analysis with fluorescence detection for the determination of trace levels of ammonium in seawater*. *Journal of Environmental Monitoring*, 2005. **7**(1): p. 37-42.
33. Horstkotte, B., C.M. Duarte, and V. Cerdà, *A miniature and field-applicable multipumping flow analyzer for ammonium monitoring in seawater with fluorescence detection*. *Talanta*, 2011. **85**(1): p. 380-385.
34. Abi Kaed Bey, S.K., D.P. Connelly, F.-E. Legiret, A.J.K. Harris, and M.C. Mowlem, *A high-resolution analyser for the measurement of ammonium in oligotrophic seawater*. *Ocean Dynamics*, 2011. **61**(10): p. 1555-1565.
35. Kerouel, R. and A. Aminot, *Fluorometric determination of ammonia in sea and estuarine waters by direct segmented flow analysis*. *Marine Chemistry*, 1997. **57**(3-4): p. 265-275.

36. Henríquez, C., B. Horstkotte, and C. Víctor, *Conductometric determination of ammonium by a multisyringe flow injection system applying gas diffusion*. International Journal of Environmental Analytical Chemistry, 2013. **93**(12): p. 1236-1252.
37. Plant, J.N., K.S. Johnson, J.A. Needoba, and L.J. Coletti, *NH₄-Digiscan: an in situ and laboratory ammonium analyzer for estuarine, coastal, and shelf waters*. Limnology and Oceanography-Methods, 2009. **7**: p. 144-156.
38. Miller, J.N. and J.C. Miller, *Statistics and chemometrics for analytical chemistry*. 2005: Pearson Education.
39. Luque de Castro, M.D., *Chapter 8. Membrane Based-Separation Techniques: Dialysis, Gas Diffusion and Pervaporation*, in *Advances in Flow Injection Analysis and Related Techniques*, S.D. Kolev and I.D. McKelvie, Editors. 2008, Elsevier: Hungary.
40. Schulze, G., C.Y. Liu, M. Brodowski, O. Elsholz, W. Frenzel, and J. Möller, *Different approaches to the determination of ammonium ions at low levels by flow injection analysis*. Analytica Chimica Acta, 1988. **214**: p. 121-136.
41. Van Der Linden, W.E., *Membrane separation in flow injection analysis*. Analytica Chimica Acta, 1983. **151**: p. 359-369.
42. Nakata, R., T. Kawamura, H. Sakashita, and A. Nitta, *Determination of ammonium ion in a flow-injection system with a gas-diffusion membrane*. Analytica Chimica Acta, 1988. **208**: p. 81-90.
43. Van Son, M., R.C. Schothorst, and G. Den Boef, *Determination of total ammoniacal nitrogen in water by flow-injection analysis and a gas-diffusion membrane*. Analytica Chimica Acta, 1983. **153**: p. 271-275.
44. Ramsing, A., J. Růžička, and E.H. Hansen, *A new approach to enzymatic assay based on flow-injection spectrophotometry with acid-base indicators*. Analytica Chimica Acta, 1980. **114**: p. 165-181.
45. Dafner, E.V., *Segmented continuous-flow analyses of nutrient in seawater: intralaboratory comparison of Technicon AutoAnalyzer II and Bran+Luebbe Continuous Flow AutoAnalyzer III*. Limnology and Oceanography: Methods, 2015. **13**(10): p. 511-520.
46. Paluch, J., P. Kościelniak, I. Molęda, K. Machowski, S. Kalinowski, S. Koronkiewicz, and J. Kozak, *Novel approach to determination of Fe(II) using a flow system with direct-injection detector*. Monatshefte für Chemie - Chemical Monthly, 2020. **151**(8): p. 1305-1310.
47. Food and Drug Administration Office of Regulatory Affairs. *Methods, Methods Verification and Validation*. ORA-LAB 5.4.5 Laboratory Manual Volume II 2020; Available from: <https://www.fda.gov/media/73920/download>, Accessed: 10 October 2020.
48. Australian Pesticides & Veterinary Medicines Authority. *Guidelines for the Validation of Analytical Methods for Active Constituent, Agricultural and Veterinary Chemical Products*. 2004; Available from: <https://apvma.gov.au/sites/default/files/docs/guideline-69-analytical-methods.pdf>, Accessed: 10 October 2020.
49. Lewis, E., *The practical salinity scale 1978 and its antecedents*. IEEE Journal of Oceanic Engineering, 1980. **5**(1): p. 3-8.
50. Frank, C. and F. Schroeder, *Using sequential injection analysis to improve system and data reliability of online methods: Determination of ammonium and phosphate in coastal waters*. Journal of Automated Methods & Management in Chemistry, 2007. **2007**(49535): p. 1-6.
51. Aminot, A., R. Kérouel, and D. Birot, *A flow injection-fluorometric method for the determination of ammonium in fresh and saline waters with a view to in situ analyses*. Water Research, 2001. **35**(7): p. 1777-1785.

CHAPTER 3: Gas-diffusion based passive sampler for ammonia monitoring in marine waters

Foreword

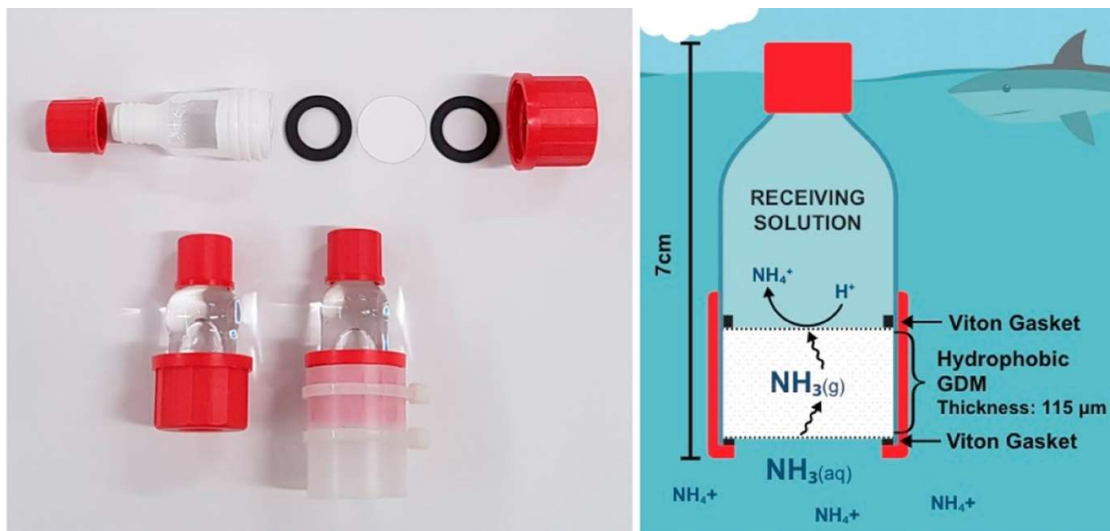
Chapter 2 outlines the development and validation of a simple yet sensitive, environmentally friendly ammonia analyser, whereby large volumes of sample can be used to achieve the required high sensitivity for environmental waters, and programmable flow allows the analysis to be tailored to the concentration range of interest (with three ranges described and validated). The development of this analyser was an enabling step toward developing the gas-diffusion-based ammonia passive sampler, as it enabled easy determination of ammonia concentrations in both typically low concentration marine field samples and in high concentration acidic passive sampling receiving solutions. The first prototype of a gas-diffusion based passive sampling device (GD-PS) for ammonia monitoring in marine waters is described in this chapter, showing that the developed GD-PS is efficient at determining a time-weighted average ammonia concentration over the period of deployment, and is able to overcome several disadvantages associated with the use of spot sampling for water quality monitoring.

The content of this chapter was published in 2017 in the journal *Talanta*, and later the research was featured on Elsevier's, *New Chemistry Research* news page in 2018:

<https://www.elsevier.com/physical-sciences-and-engineering/chemistry/journals/new-chemistry-research/stopping-aquatic-ammonia-pollution>

O'Connor Šraj, L., Almeida, M. I. G. S., Bassett, C., McKelvie, I. D., Kolev, S. D., (2017) *Gas-diffusion based passive sampler for ammonia monitoring in marine waters*, *Talanta*, 181, 52-56, doi.org/10.1016/j.talanta.2017.12.076

Graphical abstract



Contents

Abstract	119
3.1 Introduction	120
3.2 Materials and methods	121
3.2.1 Reagents and solutions	121
3.2.2 pH and total ammonia determination	121
3.2.3 Gas-diffusion membranes	122
3.2.4 Passive sampling experiments and assemblage	123
3.3 Results and discussion	124
3.3.1 Gas-diffusion based passive sampler	124
3.3.2 Membrane permeability study and receiving solution optimisation	125
3.3.3 Flow pattern effects on the ammonia uptake	127
3.3.4 Calibration of the GD-PS	128
3.3.5 Validation	129
3.3.5.1 Laboratory application	129
3.3.5.2 Field application	130
3.4 Conclusions	130
Acknowledgements	131
References	132

Abstract

A novel passive sampler based on gas-diffusion across a hydrophobic membrane is described for the determination of the time-weighted average concentration of dissolved molecular ammonia in high ionic strength aquatic environments, such as sea, coastal and estuarine waters, for a period of 3 days. The passive sampler developed is cheap, easy-to-use, reusable, and has a dynamic concentration range of 1.0 to 12 μM , which covers the water quality guideline trigger value of 11.4 μM ($160 \mu\text{g L}^{-1} \text{NH}_3\text{-N}$) for high conservation value waters, making this a powerful new tool for water quality managers involved in long-term ammonia monitoring. The gas-diffusion-based passive sampler was calibrated under laboratory conditions and deployed in a tank of seawater in the laboratory and at an estuarine site for proof of concept, and a good agreement between passive and spot sampling was achieved in both cases.

Keywords: Passive sampling; Ammonia; Seawater sampling; Gas-diffusion membrane.

3.1 Introduction

Ammonia nitrogen is a biologically important nutrient found naturally at low concentrations in aquatic environments. However, inorganic nitrogen runoff as a result of anthropogenic activity is increasing the nutrient loading of estuarine and coastal waters [1]. Ammonia is therefore monitored in these ecosystems as an indicator of water quality [2]. Effective monitoring of this analyte is not without its challenges. Most water quality monitoring programs involve periodic 'spot' sampling (i.e. the collection of discrete water samples). The overall analytical process involves sample collection, preservation, storage, and analysis, which can be laborious, time consuming, and expensive, without the guarantee that episodic pollution events will be detected, resulting in a poor understanding of nutrient sources and fluxes.

Integrative and passive sampling techniques are an efficient alternative to 'spot' sampling as they allow for the collection and accumulation of the analyte from the aquatic environment to be performed *in situ* and over extended periods of time [3]. Linear uptake passive samplers, such as Chemcatcher®, polar organic chemical integrative samplers (POCIS), semipermeable membrane devices (SPMDs), and diffusion gradients in thin-film (DGT) samplers have been described in the literature for the monitoring of a wide range of analytes of environmental interest [4, 5], and allow for the time-weighted average concentration (C_{TWA}) of an analyte to be determined for the period of deployment. To the best of our knowledge, only two passive sampling devices have been reported for the determination of C_{TWA} of ammonium (NH_4^+) in environmental waters, namely DGT with a Microlite cation-exchange resin [6] and polymer inclusion membrane based passive sampler (PIM-PS) [7]. However, both devices were applied to low salinity freshwater matrices only. Neither of these samplers is suitable for monitoring ammonia in marine waters (viz. estuarine and coastal waters), because of interference from alkali and alkaline earth metals in the ion-exchange process, which are found in concentrations several orders of magnitude higher than the ammonia concentration. The aim of the present work is thus to develop a passive sampler which can be applied to the monitoring of total ammonia nitrogen in marine waters, and for this purpose a gas-diffusion membrane (GDM) was used as the selective barrier between the sampled medium and the receiving solution.

3.2 Materials and methods

3.2.1 Reagents and solutions

Analytical grade chemicals were used without further purification for the preparation of synthetic seawater and for the GD-PS receiving solutions. Deionized water (Synergy 185, Millipore, France, resistivity $\geq 18 \text{ M}\Omega \text{ cm}$) was used throughout this study.

A stock solution of 55.56 mM NH_4^+ was prepared by dissolving NH_4Cl (BDH Chemicals, 99.8%), previously oven dried at $105 \text{ }^\circ\text{C}$ overnight, in 250.0 mL of deionised water.

The un-buffered source solution (2 L) used in the GDM study contained $2 \text{ g L}^{-1} \text{ NaCl}$ (Merck Millipore). Its pH was adjusted to 7.2 using a few drops of a 0.1 M NaOH (Chem-supply) solution.

Synthetic seawater was composed of $34 \text{ g L}^{-1} \text{ NaCl}$ and $1 \text{ g L}^{-1} \text{ Trizma}^\circledast$ base (Aldrich), and the desired pH was achieved by the addition of concentrated HCl (32 % RCI Labscan) solution. This synthetic seawater solution was then spiked with the appropriate volumes of ammonium stock solution to prepare source solutions with different ammonium concentrations.

The GD-PS receiving solution comprised 0.1 M HCl and 0.2 M NaCl when the salinity of the source solution was between 33 – 35, and 0.1 M HCl and 0.02 M NaCl when the source solution salinity was below 25. For the receiving solution optimisation study, varying concentrations of HCl and NaCl were tested.

A solution of 7.2 mM methylene blue (UniLab) in deionised water with a few drops of a 1 M NaOH solution was used to determine the degree of biofouling of the GDMs [8].

3.2.2 pH and total ammonia determination

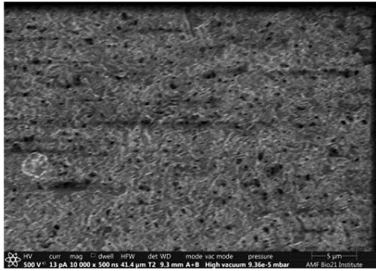
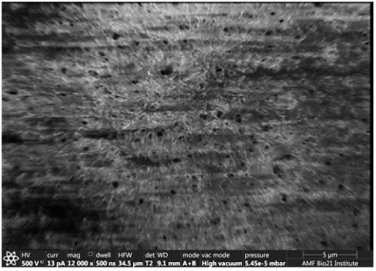
The pH of marine and estuarine water samples and synthetic seawater was measured using the standard reference spectrophotometric method in a flow system, following the procedure outlined in SOP 6b by Dickson et al [9]. The pH of the un-buffered source solution used in the GDM study was measured using a multi-parameter laboratory analyser (smartChem-Lab, TPS, Australia) fitted with an intermediate junction pH electrode (TPS, Australia).

The concentration of accumulated ammonium in the receiving solution and total ammonia in the source solution was determined using the flow analysis method developed for trace determination of ammonia nitrogen in marine waters described by O'Connor Šraj et al [10]. A portable conductivity meter (TPS WP-84, TPS, Australia) and a thermometer coupled with a high accuracy immersion probe (Precision Plus, ThermoWorks, USA) were used to measure solution conductivity and temperature, respectively.

3.2.3 Gas diffusion membranes

Three commercially available porous and hydrophobic GDMs supplied by Merck Millipore were tested. These included SureVent®, Fluoropore™ and Durapore®, and the membrane characteristics are described in Table 3-1.

Table 3-1. Membrane characteristics.

	SureVent	Durapore	Fluoropore
Product code*	VVSP	GVHP	GPTFEPE
Membrane Material*	Modified PVDF	PVDF	PTFE - polyester support
Average pore size (µm)*	0.1	0.22	0.22
Thickness (µm)*	115	125	150
Water breakthrough pressure (psi)	≥ 73	≥ 30	≥ 60
SEM Image**			N/A

VVSP, GVHP, GPTFEPE – Manufacturer product codes

PVDF – poly(vinylidene fluoride), PTFE – polytetrafluoroethylene

* Information obtained from Millipore, Product Selection Guide for Microfiltration Membranes [11].

** Scanning Electron Microscope images were obtained on a FEI Teneo Volumescopie system under high vacuum with an accelerating voltage of 500 V, beam deceleration of -4 kV and a beam current of 13 pA at a magnification 10,000x. The PTFE membrane was incompatible with the scanning process of the SEM, and thus membrane images for this material were not able to be captured.

3.2.4 Passive sampling experiments and assemblage

The passive sampling device was assembled as described by Almeida et al. [7], however a GDM was used rather than a PIM, and two Viton gaskets (Gasketech, Australia) replaced the Teflon washer and the rubber O-ring (Figure 3-1a). Laboratory-based passive sampling experiments were conducted as described by Almeida et al. [7], using aquarium pumps to promote flow, and adhesive door/window strips (Raven, Australia) to seal the 10 L plastic containers and lids. Flow pattern effects on ammonia accumulation were studied under laboratory conditions using cylindrical flow shields made from pieces of polypropylene (11 cm diameter x 4 cm height), which were tightly fixed to the passive sampling devices' caps with aperture, leaving approximately 2 cm of the shield exposed to the source solution (Figures 3-1a(1) and 1b) [12]. The same study was also conducted in the Yarra River estuary at Newport (37° 50'31.5"S, 144°53'51.1"E), and at the Environment Protection Authority - Victoria water sampling site at Long Reef (38° 01'50.9"S, 144°35'29.8"E), 1.8 km off the Werribee Coast. The receiving solution compositions used were 0.1 M HCl and 0.1 M NaCl, and 0.1 M HCl and 0.2 M NaCl, respectively.

Laboratory-based calibration of the passive sampling devices was performed using synthetic seawater (34 g L⁻¹ NaCl, 1 g L⁻¹ Trizma® base and 4.85 mM HCl, salinity of 35, and pH 8.0) as the source solution. The corresponding experiments were undertaken at 22.2 °C in a temperature-controlled cabinet (Clegg, Australia; with E5CN OMRON temperature controller). The calibration was performed over a range of ammonia concentrations spanning between 0.97 – 11.5 µM NH₄⁺ using a second order polynomial. A linear calibration curve, based on the lower concentration range between 0.97 and 6.62 µM NH₄⁺, was utilised for determining the limit of detection using the error of the regression described by Miller and Miller [13].

For validation purposes, a laboratory-based experiment using seawater collected from the Lagoon Pier in Port Melbourne (37° 50'45.0"S, 144°56'20.7"E) was undertaken by spiking it with 8.02 µM ammonium, and testing the performance of the passive samplers under the same experimental conditions as those used for the construction of the laboratory-based calibration curve. Real seawater was collected and stored in the dark at 4 °C, and was used unfiltered, without the addition of biocides. A field-based passive sampling experiment was also conducted in the Werribee River estuary (37° 56'34.0"S, 144°40'12.3"E) over a period of 3 days. Daily spot samples were collected during the 3-day deployment period to allow total

ammonia monitoring alongside temperature, pH, and salinity. The receiving solution composition used in both studies was 0.1 M HCl and 0.02 M NaCl.

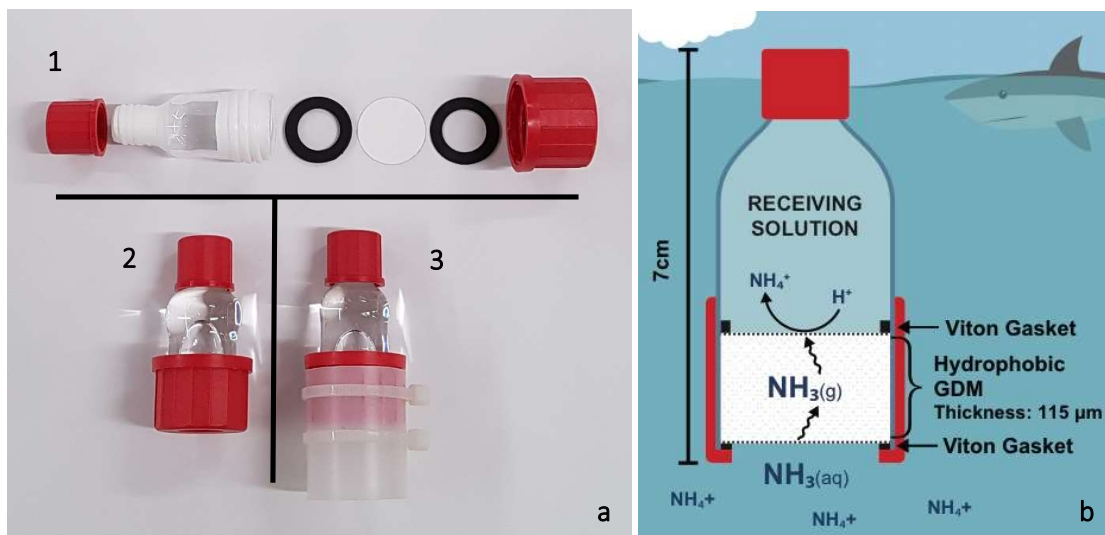


Figure 3-1. (a) GD-PS assembly (1) and PSs without (2) and with (3) a flow shield. (b) Cross section of the GD-PS (membrane thickness not drawn to scale), and schematic illustration of the diffusion process of dissolved ammonia ($\text{NH}_3(\text{aq})$) from the source solution through the pores of the hydrophobic GDM ($\text{NH}_3(\text{g})$) and its reaction with hydrogen ions in the receiving solution resulting in its conversion to the ammonium cation ($\text{NH}_4^+(\text{aq})$).

3.3 Results and discussion

3.3.1 Gas-diffusion based passive sampler

A schematic of the GD-PS, developed in this study, is shown in Figure 3-1b. The sampler contains an acidic receiving solution (10 mL), which is separated from the source solution by a porous and hydrophobic GDM. The ammonia accumulation mechanism involves ammonia evaporating from the source solution into the pores of hydrophobic GDM and then diffusing to the membrane/acidic receiving solution interface to readily react with hydrogen ions and forming ammonium. Molecular ammonia is effectively accumulated in the receiving solution as the ammonium ion, as GDMs are highly impermeable to ions and polar molecules. Due to the hydrophobic character of the membrane and the high acidity of the receiving solution, interference from solutes and dissolved gases with acidic character such as CO_2 and SO_2 can be eliminated.

The sum of both the molecular (NH_3) and ionised (NH_4^+) forms of ammonia is referred to as total ammonia. In the marine environment the speciation of ammonia is largely dependent on pH, temperature and to a lesser extent to salinity [14]. At pH 8.0 and a temperature of 20 °C, molecular ammonia is 2.98% of total ammonia, however, even a small increase of 0.2 pH units and 2 °C will result in a relatively large increase in the percentage of molecular ammonia, i.e. 3.38% [14].

3.3.2 Membrane permeability study and receiving solution optimisation

When the salt concentrations of the solutions on both sides of the membrane are different, mild osmotic pressure effects involving movement of water from a region of low to high salt concentration can be observed which is accompanied by diffusive transport of solutes along their concentration gradients. These effects are undesirable in the operation of the GD-PS and therefore possibilities for their minimization were explored (Table 3-2). The GD-PSs were submerged in 2 L of un-buffered source solution to determine the degree of the osmotic effects mentioned above. After 19 h, the pH of the source solution was measured. The SureVent® membrane exhibited the best performance since insignificant pH change in the source solution was observed (Table 3-2). This is due most likely to the membrane smaller pore size in comparison with the other two GDMs (0.1 μm versus 0.22 μm) and the manufacturer's treatment of the membrane to enhance its hydrophobicity (proprietary information not provided by manufacturer). The SureVent® membrane was thus selected for all further experiments.

Table 3-2. Study of the gas-diffusion membranes and the receiving solution composition.

Membrane type	Receiving solution composition	pH drop after 19 h (pH units)	[NH ₄ ⁺] in the receiving solution (μM)
SureVent ^{®a}	1 M HCl	0.06	-
Fluoropore ^{™a}	1 M HCl	3.17	-
Durapore ^{®a}	1 M HCl	4.46	-
SureVent ^{®b}	0.01 M HCl, 0.56 M NaCl	-	43.3 ± 0.8
SureVent ^{®b}	0.1 M HCl, 0.2 M NaCl	-	45.7 ± 5.0
SureVent ^{®b}	0.15 M HCl	-	69.3 ± 11.4
SureVent ^{®b}	0.3 M HCl	-	21.4 ± 5.4

^a Study of membrane stability under osmotic pressure. Source solution (2 L) composition: 2 g L⁻¹ NaCl, pH 7.2 was achieved by the addition of a few drops of a 0.1 M NaOH solution (no ammonium was added). Duration of experiment: 19 h. As these solutions were un-buffered, a control experiment was conducted to evaluate the pH changes related to the uptake of atmospheric CO₂. The solution pH of each membrane experiment was corrected accordingly.

^b Receiving solution composition optimisation study. Source solution composition: synthetic seawater (34 g L⁻¹ NaCl, 1 g L⁻¹ Trizma[®] base, 4.85 mM HCl) containing 15.7 μM NH₄⁺. Experimental conditions: temperature 21 – 22 °C, pH 7.97, duration 7 days, 9 replicates for each receiving solution composition.

Different receiving solution compositions were then studied (Table 3-2), and by matching the receiving solution composition as closely as possible to the source solution matrix in terms of salinity (except for 0.3 M HCl which had a conductivity double that of the source solution), it was possible to minimise the effects of osmotic pressure. It was noticed that both 0.15 M HCl and 0.3 M HCl receiving solutions exhibited on average between 5 – 25% volume loss over the course of the experiment, respectively. The receiving solutions containing both NaCl and HCl exhibited a negligible volume loss, good ammonia accumulation, and were therefore considered suitable for further studies. A receiving solution composition of 0.1 M HCl with the appropriate NaCl concentration (dependant on the salinity of the source solution) was chosen for the subsequent experiments.

3.3.3 Flow pattern effects on the ammonia uptake

The effect of the aquatic flow patterns on the analyte uptake has been studied by comparing the accumulation of GD-PSs with and without flow shields (Figures 3-1a and 3-1b) as described by Garcia-Rodríguez et al [12]. Laboratory-based experiments were conducted by dipping devices with and without flow shields ($n = 8$ each) in 9 L of synthetic seawater spiked with $6.62 \mu\text{M}$ of ammonium for a period of 7 days and using aquarium pumps to promote synthetic seawater mixing. The uptake of the un-shielded and shielded samplers was $10.7 \pm 0.98 \mu\text{M}$ and $9.46 \pm 0.80 \mu\text{M}$, respectively. A 2-tail Student's t-test was performed, where the null hypothesis was accepted (i.e. no statistically significant difference between the two experimental results) if the calculated t-value was lower than the critical t-value at the selected confidence level. The t-value calculated for the laboratory-based flow pattern study was 2.72 and the critical t-value was 2.15 at the 95% confidence level. Therefore, there was a statistically significant difference between the results for the un-shielded and shielded sampling devices. These results are in accordance with the observations published by Garcia-Rodríguez et al [12].

The same experiment was repeated in estuarine water (Yarra River at Newport) and in seawater (Long Reef, Port Phillip Bay). The total ammonia concentrations of spot samples were measured as $2.77 - 2.95 \mu\text{M}$ between the two sites, with temperature and salinity ranging between $14.0 - 14.4 \text{ }^\circ\text{C}$ and $31.3 - 34.5$, respectively. The ammonia uptake of the un-shielded and shielded samplers at the Yarra River estuary site was $3.67 \pm 0.61 \mu\text{M}$ and $3.18 \pm 0.70 \mu\text{M}$, respectively, and at Long Reef - $2.52 \pm 1.06 \mu\text{M}$ and $2.92 \pm 1.35 \mu\text{M}$, respectively. A 2-tail Student's t-test was performed for both locations showing no statistically significant difference between the results for un-shielded and shielded samplers at the 95% confidence level (Yarra estuary: $0.697 < 2.12$ and Long Reef: $1.59 < 2.12$).

In the marine environment, water movement tends to be multi-directional as a result of wave and tidal action, however, in rivers and streams it tends to be unidirectional. Whilst flow shields have been shown to assist in minimising the effects of the aquatic flow pattern under laboratory conditions [12], in marine and estuarine environments, the use of flow shields did not provide any benefits and thus they were not used in the subsequent experiments.

3.3.4 Calibration of the GD-PS

The GD-PS accumulates dissolved ammonia from the source solution, and by performing its laboratory-based calibration under controlled environmental conditions (temperature, pH and salinity) it is possible to determine the C_{TWA} of total ammonia at the sampling site in the aquatic system over the period of sampling time. However, the ability of these devices to accumulate molecular ammonia from the source solution was drastically inhibited after a period of 4-5 days (Figure 3-2a). In order to assess whether biofouling was inhibiting uptake, the membranes were immersed in a solution of 7.2 mM methylene blue, which is commonly used as a biological stain, before and after use. Prior to immersion in the source solution, the GDMs did not take up the stain, but post 7 day immersion, all GDMs exhibited some degree of staining, indicative of the presence of bacterial biofilms on their surfaces, which has likely resulted in some degree of blockage of their pores thus suppressing ammonia uptake. Despite this issue, the ammonia uptake was linear up to 3 days, and hence a calibration curve was plotted for this sampling period (Figure 3-2b). Under the experimental conditions described for the laboratory-based calibration (Section 3.2.4) the detection limit of the passive samplers was determined as $1.64 \mu\text{M NH}_4^+$ and the repeatability (%RSD) at a source solution concentration of $3.54 \mu\text{M}$ was 11.9% ($n = 7$).

The rate of molecular ammonia uptake from the source solution to the receiving solution appears to have a non-linear response at higher concentrations (Figure 3-2b.), which may be due to the equilibrium partition of $\text{NH}_3/\text{NH}_4^+$ favouring greater production of molecular ammonia as it is removed from the solution by the GD-PS. Additionally, while the first data point on the calibration curve (i.e. 0.97 mM) was supposed to represent the blank, daily measurements of ammonia nitrogen present in the source solution blank indicated the presence of trace contamination of ammonia, most likely originating from atmospheric inputs, and/or from reagents used to prepare the artificial seawater.

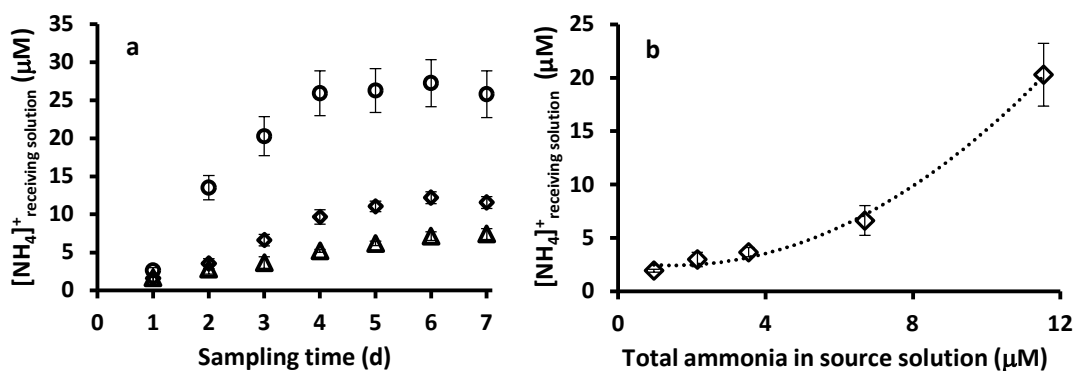


Figure 3-2. (a) Transient concentration of ammonium in the receiving solution versus sampling time for the following total ammonia concentrations in the source solutions: (Δ) 3.54 μM, (◊) 6.70 μM, (○) 11.5 μM. (b) Laboratory-based calibration of the GD-PS: concentration of ammonium in the receiving solution versus the total ammonia concentration in the source solution after 3 days of sampling time. (◊) ($y = 1.753 \times 10^{-2}x^2 - (5.213 \times 10^{-1})x + 2.812$), $R^2 = 9.9524 \times 10^{-1}$. Receiving solution composition: 0.1 M HCl and 0.2 M NaCl. Source solution composition: 34 g L⁻¹ NaCl, 1 g L⁻¹ Trizma® base, 4.85 mM HCl (pH 8.0 ± 0.2), temperature 22.2 ± 0.3 °C, and total ammonia concentrations between 0.97 – 11.5 μM NH₄⁺. Error bars = ± standard deviation of 7 replicate samplers.

3.3.5 Validation

While ammonia speciation is dependent on pH, temperature and salinity, the proposed GD-PS is expected to perform well in ocean and sea environments, where fluctuations in pH, temperature and salinity are characteristically small over long time scales. However, in estuarine environments a larger error would be expected, where high daily changes in pH, temperature and salinity may be experienced with the tidal cycle and with freshwater influx as a result of rainfall in the upstream catchments. For this reason, validation experiments were performed under laboratory conditions using seawater, and in the field at an estuarine site, in order to assess the performance of the GD-PS in different water matrices.

3.3.5.1 Laboratory application

The experiment involved 4 samplers and was conducted for a period of 3 days under controlled experimental conditions (described in Section 3.2.4) using aquarium pumps to promote flow. The temperature, salinity, pH, and total ammonia concentration of the seawater source solution were measured daily and the following average values were obtained: temperature - 22.2 ± 0.84 °C, salinity - 33.6 ± 0.03, pH - 7.98 ± 0.09, and total ammonia concentration - 4.60

$\pm 3.32 \mu\text{M}$. The initial ammonia concentration of the seawater source solution of $8.02 \mu\text{M}$ decreased to $0.31 \mu\text{M}$ at the end of the sampling period due to the rapid growth of bacteria. The laboratory-based calibration (Figure 3-2b) was used to determine the C_{TWA} for total ammonia and was found to be $4.42 \pm 0.20 \mu\text{M}$ ($n=5$). No statistically significant difference was found at the 95% confidence level (2-tail Student's t-test: $0.111 < 2.37$) between the average total ammonia concentration measured in the seawater source solution mentioned above and the total ammonia C_{TWA} . The excellent agreement between the two sampling methods characterised by a relative error of 4.03% demonstrated the suitability of the newly developed GD-PS for environmental monitoring of ammonia in sea and ocean environments.

3.3.5.2 Field application

A field study was undertaken in the Werribee River estuary for a 3-day deployment period, with 5 gas-diffusion passive sampling devices, containing receiving solution (0.1 M HCl and 0.02 M NaCl) with a salinity similar to that of the matrix. Spot samples were collected daily at different tidal heights, and the average temperature ($22.5 \pm 2.8 \text{ }^\circ\text{C}$), salinity (23.2 ± 5.2) and pH (8.04 ± 0.16) were determined over the period of deployment. The C_{TWA} for total ammonia was determined on the basis of the concentrations of ammonia in the receiving solutions of the five samplers after a 3-day deployment. The laboratory-based calibration curve (Figure 3-2b) was used. No statistically significant difference was found at the 95% confidence level (2-tail Student's t-test: $0.735 < 2.37$) between the average total ammonia concentration measured in the estuarine spot samples ($5.41 \pm 0.30 \mu\text{M}$) and the total ammonia C_{TWA} ($6.21 \pm 2.18 \mu\text{M}$). There was thus good agreement between the two sampling methods, with a relative error of 13.0%, which is considered to be reasonable for passive sampling in waters with a highly complex and variable matrix [15].

3.4 Conclusions

A novel passive sampler based on gas-diffusion has been developed and applied as a proof of concept for the monitoring of ammonia in marine waters. The performance of the GD-PS device was tested under laboratory conditions using seawater under stable and controlled pH, temperature and salinity conditions, and in the field at an estuarine site. The relative error

between the concentration of ammonia nitrogen measured, and the experimentally determined time weighted average concentration for the seawater matrix was 4.03% and for the estuarine environment it was 13.0%. In an environment where the variables affecting ammonia speciation (pH, temperature and salinity) are stable over long periods of time, these devices can be used for studies aimed at understanding complex biogeochemical cycling of ammonia nitrogen in the water column, however, in more complex and variable environments the same GD-PS devices would be more suitable for monitoring point-source nutrient inputs and episodic pollution events. While the GD-PS described in this study was successfully applied in the field for a 3-day deployment period, this time-frame may be short for large-scale environmental monitoring. Therefore, a number of different strategies to minimise the effects of biofouling are currently being investigated, in addition to a detailed evaluation of the effect of temperature, matrix pH and salinity. On the basis of the results obtained it can be concluded that the newly developed gas-diffusion-based passive sampling approach offers a cheap, easy-to-use and reliable alternative to conventional spot sampling, and it does not require sample pre-treatment steps prior to analysis unlike existing passive sampling techniques. All these features make the GD-PS an attractive new tool for marine and estuarine water quality monitoring.

Acknowledgements

This article is dedicated to Professor Purnendu (Sandy) Dasgupta, the recipient of the 2017 Talanta Medal.

The authors would like to thank the Australian Research Council (ARC) and Melbourne Water Corporation for funding this research in the framework of the ARC Linkage Scheme (Grant LP160100687). We also acknowledge Mr. Edward Nagul for assisting with the collection of SEM images, and Mr. Marcus Hammarstedt for creating Figure 3-1b. L. O'Connor Šraj is grateful to the University of Melbourne for the award of a postgraduate scholarship

References

1. Camargo, J.A. and A. Alonso, *Ecological and toxicological effects of inorganic nitrogen pollution in aquatic ecosystems: A global assessment*. Environ. Int., 2006. **32**: p. 831-849.
2. Batley, G.E. and S.L. Simpson, *Development of guidelines for ammonia in estuarine and marine water systems*. Mar. Pollut. Bull., 2009. **58** (10): p. 1472-1476.
3. Roll, I.B. and R.U. Halden, *Critical review of factors governing data quality of integrative samplers employed in environmental water monitoring*. Water Res, 2016. **94**: p. 200-7.
4. Vrana, B., I.J. Allan, R. Greenwood, G.A. Mills, E. Dominiak, K. Svensson, J. Knutsson, and G. Morrison, *Passive sampling techniques for monitoring pollutants in water*. TrAC Trends Anal. Chem., 2005. **24** (10): p. 845-868.
5. Zabiegała, B., A. Kot-Wasik, M. Urbanowicz, and J. Namieśnik, *Passive sampling as a tool for obtaining reliable analytical information in environmental quality monitoring*. Analytical and Bioanalytical Chemistry, 2010. **396**(1): p. 273-296.
6. Huang, J., W.W. Bennett, D.T. Welsh, T. Li, and P.R. Teasdale, *Development and evaluation of a diffusive gradients in a thin film technique for measuring ammonium in freshwaters*. Anal. Chim. Acta, 2016. **904** (Supplement C): p. 83-91.
7. Almeida, M.I.G.S., A.M. Silva, R.A. Coleman, V.J. Pettigrove, R.W. Cattrall, and S.D. Kolev, *Development of a passive sampler based on a polymer inclusion membrane for total ammonia monitoring in freshwaters*. Anal. Bioanal. Chem., 2016. **408** (12): p. 3213-22.
8. Aneja, K.R., *Experiments in Microbiology, Plant Pathology and Biotechnology*. Fourth Edition ed. 2003, New Delhi: New Age International. 97-100.
9. Dickson, A.G., C.L. Sabine, J.R. Christian, and Eds, *SOP 6B Determination of the pH of sea water using the indicator dye m-cresol purple*. In *Guide to Best Practices for Ocean CO₂ Measurements*. PICES Special Publication 3. 2007: p. 1-7.
10. O'Connor Šraj, L., M.I.G.S. Almeida, I.D. McKelvie, and S.D. Kolev, *Determination of trace levels of ammonia in marine waters using a simple environmentally-friendly ammonia (SEA) analyser*. Mar. Chem., 2017. **194** (Supplement C): p. 133-145.
11. Corporation, M., *Microfiltration Membranes, Microfiltration Membranes for Filtration and Venting Applications*. 2009: USA.
12. Garcia-Rodríguez, A., C. Fontàs, V. Matamoros, M.I.G.S. Almeida, R.W. Cattrall, and S.D. Kolev, *Development of a polymer inclusion membrane-based passive sampler for monitoring of sulfamethoxazole in natural waters. Minimizing the effect of the flow pattern of the aquatic system*. Microchemical Journal, 2016. **124**(Supplement C): p. 175-180.
13. Li, Q.P., J.Z. Zhang, F.J. Millero, and D.A. Hansell, *Continuous colorimetric determination of trace ammonium in seawater with a long-path liquid waveguide capillary cell*. Marine Chemistry, 2005. **96**(1-2): p. 73-85.
14. Bower, C.E. and J.P. Bidwell, *Ionization of Ammonia in Seawater: Effects of Temperature, pH, and Salinity*. J. Fish. Res. Board Can., 1978. **35** (7): p. 1012-1016.
15. EU, *Commission Directive 2009/90/EC of 31 July 2009 laying down, pursuant to Directive 2000/60/EC of the European Parliament and of the Council, technical specifications for chemical analysis and monitoring of water status*. Official Journal of the European Union, L210: 36–38. 2009.

CHAPTER 4: Monitoring of ammonia in marine waters using a passive sampler with biofouling resistance and neural network-based calibration

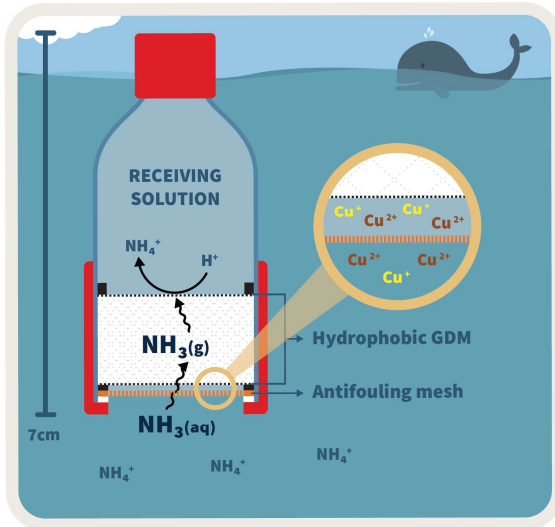
Foreword

In **Chapter 3**, the development of the first prototype of a gas-diffusion based passive sampling device (GD-PS) for ammonia monitoring in marine waters and its application as a proof of concept for a 3-day deployment in an estuary and in a tank with recirculated natural seawater is described. Whilst the device showed promise, it was unable to be deployed for periods of more than three days due to biofilm formation on the surface of the gas-diffusion membrane thus limiting the uptake of ammonia from the sampled medium. Additionally, in order to determine the time-weighted average concentration during the period of deployment, calibration of the device was required in the laboratory under the same environmental temperature and pH conditions at which the GD-PS was deployed, which limited the usability of the device for widespread water quality monitoring programs.

The research described in this chapter looks at a) a number of different antifouling strategies to reduce the impact of biofouling on the device and improve its deployment longevity, b) assessing the impact of the environmental variables temperature, pH and salinity on the performance of the device, and c) developing a universal calibration model over a range of commonly occurring environmental conditions, by applying the Group Method Data Handling algorithm as a neural network-based calibration approach. The content of this chapter was published in 2020 in the journal *Environmental Pollution*.

O'Connor Šraj, L., Almeida, M. I. G. S., Sharp, S., McKelvie, I. D., Morrison, R., Kolev, S. D., (2020) *Monitoring of ammonia in marine waters using a passive sampler with biofouling resistance and neural network-based calibration*, *Environmental Pollution*, 267, 115457, <https://doi.org/10.1016/j.envpol.2020.115457>

Graphical abstract



Contents

Abstract	136
4.1 Introduction	137
4.2 Materials and methods	139
4.2.1 Reagents and solution	139
4.2.2 Analytical tools and methods	140
4.2.3 Gas-diffusion membranes	141
4.2.4 Antifouling strategies	141
4.2.5 Passive sampler assembly and calibration	141
4.2.6 Field deployment	143
4.3 Results and discussion	144
4.3.1 Membrane selection and receiving solution optimisation	144
4.3.2 Membrane antifouling strategies	145
4.3.3 Influence of temperature, salinity and pH on the GD-PS performance	148
4.3.4 GD-PS calibration using GMDH model	152
4.3.5 Field validation	153
4.3.6 Method performance	155
4.3.7 GD-PS: A tool for ammonia screening	156
4.4 Conclusions	157
4.5 Appendix	158
Acknowledgements	171
References	172

Abstract

A biofouling resistant passive sampler for ammonia, where the semi-permeable barrier is a microporous hydrophobic gas-diffusion membrane, has been developed for the first time and successfully applied to determine the time-weighted average concentration of ammonia in estuarine and coastal waters for 7 days. Strategies to control biofouling of the membrane were investigated by covering it with either a copper mesh or a silver nanoparticle functionalised cotton mesh, with the former approach showing better performance. The effects of temperature, pH and salinity on the accumulation of ammonia in the newly developed passive sampler were studied and the first two parameters were found to influence it significantly. A universal calibration model for the passive sampler was developed using the Group Method Data Handling algorithm based on seawater samples spiked with known concentrations of total ammonia under conditions ranging from 10 to 30 °C, pH 7.8 to 8.2 and salinity 20 to 35. The newly developed passive sampler is affordable, user-friendly, reusable, sensitive, and can be used to detect concentrations lower than the revised default guideline value of 160 µg total NH₃-N L⁻¹, for a 99% species protection level, with the lowest concentration measured at 17 nM molecular NH₃ (i.e., 8 µg total NH₃-N L⁻¹ at pH 8.0 and 20 °C). It was deployed at four field sites in the coastal waters of *Nerm* (Port Phillip Bay), Victoria, Australia. Good agreement was found between molecular ammonia concentrations obtained with passive and discrete grab sampling methods (relative difference, - 12% to - 19%).

Keywords: Passive sampling; ammonia; marine water sampling; gas-diffusion membrane.

4.1 Introduction

Globally nutrient pollution is a major threat to the health of aquatic ecosystems [1, 2]. Increasingly large-scale anthropogenic run-off from agricultural land, industrial processes and atmospheric deposition, results in the nutrient enrichment of natural waters causing increased primary production and eutrophication [1-4]. Estuarine and coastal waters are susceptible to eutrophication from total nitrogen and total phosphorus, which can lead to oxygen depletion in the water column and benthic environments [5].

Ammonia is commonly monitored as an indicator of water quality by regulatory bodies responsible for monitoring and providing information about the health of aquatic ecosystems. The sources, dispersal and fate of ammonia are of concern to water quality managers, and efficient and reliable monitoring approaches are needed, especially during pollution events.

The speciation of ammonia in aquatic environments ($\text{NH}_3/\text{NH}_4^+$) is dependent on pH and temperature, and to a lesser extent salinity [6]; the sum of both molecular ammonia (NH_3) and ammonium (NH_4^+) are referred to as total ammonia.

Current Australian and New Zealand Guidelines (ANZG) for fresh and marine water quality specify the default guideline value for total ammonia in marine waters as $500 \mu\text{g NH}_3\text{-N L}^{-1}$ (equivalent to $1.06 \mu\text{M}$ molecular NH_3 at pH 8 and 20°C) for a 99% species protection level [7]. However, additional data will likely result in further revisions to these guidelines, with a guideline value of $160 \mu\text{g NH}_3\text{-N L}^{-1}$ (i.e., 340 nM molecular NH_3 at pH 8 and 20°C) determined to be more appropriate for maintaining ecosystem function and health [8], highlighting the need for more sensitive, but still reliable, ammonia monitoring methods.

Most water quality monitoring programs involve intermittent (i.e., in response to pollution events) or routine (baseline) spot sampling during daylight hours, preservation and sample pre-treatment (i.e., filtration) prior to sample analysis. Such methods can be time-consuming, expensive, weather dependent (or unsafe), and prone to sample contamination [9]. Passive sampling techniques overcome many of the disadvantages of grab sampling by collecting and accumulating the analyte of interest *in-situ*, providing a time-weighted average concentration for the period of deployment [9, 10]. The advantages of passive sampling make this a desirable tool for routine monitoring and for identifying pollution hotspots. Over the last three decades, various passive sampling techniques were developed to monitor a wide range of important aquatic pollutants [9-11]. Passive sampling allows for the time-weighted average concentration

of the analyte(s) of interest to be determined over the period of deployment. This technique has been successfully used to overcome a number of limitations of traditional water quality monitoring programs using intermittent spot sampling. The fundamental advantages of passive sampling include allowing for lower levels of target species to be detected (due to the preconcentration ability of passive samplers) [12], and more representative data to be collected, especially in highly dynamic environments such as estuaries, and over large spatiotemporal scales to account for tidal cycles, flood events and even seasonal variability over longer deployment times [13-15].

Diffusive gradients in thin films (DGT) samplers have been described in the literature for monitoring nutrient concentrations including ammonia [16, 17], nitrate [17, 18] and phosphate [17, 19-23]. Using ion-exchange resins as binding agents, DGTs have been applied to different freshwater systems, including streams and wetlands, as well as in the assessment of lake sediment remediation techniques [16, 18-20, 24]. A passive sampling device using a polymer inclusion membrane (PIM) for ammonia monitoring in freshwaters has been successfully developed [25]. This device consists of a receiving solution separated from the sampled aquatic medium by a PIM. Subsequent ammonia monitoring using PIM-based passive samplers in combination with standard microbial faecal indicators was applied to identify dry-weather leaks (i.e., cracked sewer pipe) and episodic pollution events (e.g., sewer spills) [26]. However, both DGT- and PIM-based passive samplers are susceptible to interference from dissolved salts and therefore not appropriate for use in high salinity matrices, such as estuarine and marine waters.

Ammonia determination using gas-diffusion separation has been widely used in automated flow analysis methods [27], in potentiometric ion selective electrodes (ISEs) [28-34], and more recently in a gas-permeable membrane-based conductivity (GPMCP) probe deployed in an estuary for 24 hours [35]. Automated methods commonly require the use of expensive and sometimes custom-made equipment, a high degree of operator skill and are predominantly used in a laboratory setting, although *in situ* and shipboard underway applications have been described [27]. ISEs require the use of a gas-diffusion membrane to eliminate interference from K^+ , Na^+ and Ca^{2+} ions whose concentrations are commonly several orders of magnitude higher in seawater than that of the NH_4^+ ion. This results in characteristically poor sensitivities and slow response times, which can be improved by the addition of an alkalisng reagent to the sample. Ammonia ISEs are typically used in laboratories for measuring ammonia [31, 32], and

have not been tested and validated for long-term, *in situ* field deployment in saline waters. While the GPMCP probe shows promise in terms of *in situ* monitoring capability, the sensitivity of the sensor decreases as a function of deployment time [36], and the complexity and cost of fabrication of custom-made electronic components and the need for power to operate the instrument may limit its usability in widespread environmental monitoring campaigns.

An ammonia gas-diffusion passive sampler (GD-PS) for use in marine waters using a gas-diffusion membrane instead of a PIM has previously been described [37], however, membrane biofouling inhibited the performance of the GD-PS after three days. In addition, this passive sampler required calibration at the specific temperature and pH of the water of each deployment site. Hence, in the present work, strategies to overcome the effects of biofilm formation on the ammonia accumulation by the GD-PS were investigated and they involved covering the GD membrane with either a copper mesh or a silver nanoparticle functionalised mesh. This article also reports the development of a single calibration model, involving the use of the Group Method Data Handling (GMDH) algorithm [38], to calibrate the GD-PS over a range of environmental pH (7.8 to 8.2), temperature (10 to 30 °C) and salinity (20 – 35) conditions, allowing for a universal calibration to be used in determining the ammonia time-weighted average concentration ($[\text{NH}_3]_{\text{TWA}}$) in a wide range of marine waters.

4.2 Materials and methods

4.2.1. Reagents and solutions

The preparation of reagents, GD-PS receiving solutions, and synthetic source solutions are described in Section A (Appendix).

4.2.2 Analytical tools and methods

The pH of synthetic seawater and discrete grab samples (also known as spot samples) was measured using a flow system utilising a spectrophotometric method [39, 40]. The system was assembled using an Ocean Optics spectrophotometer (USB4000), a tungsten halogen light source (LS-1) with a blue filter (BG-34), and a 10 cm optical path length flow cell. A certified reference material (Batch 141 Certified Seawater) from the Scripps Institute of Oceanography was used to assess the performance of the pH flow system, which was accurate to within ± 0.005 pH units of the reported value (pH 7.887 at 25 °C) and with an interquartile range of 0.001.

The concentration of accumulated ammonia in the receiving solution (measured as ammonium) and total ammonia in the sample source solution were determined using a Sensitive Environmentally-friendly Ammonia (SEA) analyser [41]. Two working ranges were used, namely 0.28 – 13.9 μM for the source solution samples and 1.4 – 55.6 μM for the GD-PS receiving solutions. Typical limits of detection were 88 nM and 440 nM for the lower and upper concentration ranges, respectively. A certified reference material (ERA A Waters Company, Lot no. 080715 Traceability against NIST SRM (194) 99.1% concentration $1,000 \pm 6 \text{ mg L}^{-1}$) diluted to 5.0 μM for the lower range and 30.0 μM for the upper range was used to assess the performance of the SEA analyser with errors in the order of $\pm 1.9\%$ for the lower range and $\pm 1.3\%$ for the upper range. Molecular ammonia in the sample source solution was calculated by multiplying the total ammonia concentration by the fraction of un-ionised ammonia in solution, which was determined using an empirical model described by Bower and Bidwell [6], when the temperature (°C), pH values, and salinity were known.

To measure solution conductivity and temperature, a portable conductivity meter (TPS WP-84, TPS, Australia) calibrated using a 36 ppK salinity standard (TPS, Australia) alongside a high accuracy thermometer coupled with a platinum resistance temperature detector (RTD) immersion probe (Precision Plus Thermometer with RTD High Accuracy Freezer Probe, 1/10 DIN, ThermoWorks, USA) were used.

4.2.3 Gas-diffusion membranes

Three commercially available hydrophobic gas-diffusion membranes (GDM's) were tested, viz. SureVent® (0.1 µm pore size), Fluoropore™ (0.22 µm pore size) and Durapore™ (0.22 µm pore size) (Merck Millipore). Membrane characteristics have been described previously [37].

4.2.4 Antifouling strategies

Two types of copper mesh and a cotton mesh functionalised with silver nanoparticles (AgNP) were investigated for control of membrane biofouling. The copper mesh (TWP Inc., California) was supplied in an overall thickness of 112 µm and two different weave densities (100 wires per inch with 60% opening, and 200 wires per inch with 35% opening). The AgNP cotton mesh was prepared according to the method described by Rehan et al. [42] using 45 g of muslin (Grade 80, thread count 40 x 32 per square inch), 1 L solution of 1200 mg L⁻¹ AgNO₃ (Chem-Supply) and 5% (w/w) solution of trisodium citrate (Chem-Supply) added drop wise. In order to test the efficacy of the silver nanoparticle treatment, three layers of the AgNP cotton mesh were sandwiched together as the muslin cloth had a low specific surface area, due to a low thread count. A single layer of copper mesh was employed in the copper-based experiments. Biofouling on the surface of each GDM was quantified by immersion of the membrane in a methylene blue stain for 60 seconds [43], followed by photo scanning of the stained membrane using a CanoScan Lide220. The image was processed using ImageJ software, using the red colour channel to determine the extent of biofouling by monitoring the intensity of colour change between the unstained and stained GDM immersed in the field, or in real seawater solutions in the laboratory.

4.2.5 Passive sampler assembly and calibration

The GD-PSs were assembled as described previously [37], with the addition of an antifouling mesh between the outer surface of the GDM and the sampled medium (i.e., source solution) (Figure).

Laboratory experiments were performed using unfiltered low-nutrient seawater collected from Half Moon Bay, Victoria, Australia as the source solution (Figure S4-1, Table S4-1, Appendix), spiked with the appropriate volume of ammonia stock solution prepared by using NH_4Cl . Experiments were conducted as previously described [37], using 10 L tanks in a temperature controlled cabinet with 500 L h^{-1} aquarium pumps to promote flow. For laboratory calibration experiments, the pH was adjusted by the addition of small volumes of 5 M HCl or NaOH solutions, and the salinity was adjusted with the addition of deionized water. All experiments were conducted for a period of 7 days, except for the field biofouling experiment that was conducted over 8 days, with 10 GD-PSs used for each condition/concentration tested.

The Group Method Data Handling (GMDH) algorithm [38] was used to model the behaviour of the GD-PS under a wide range of environmental variables (salinity 20 – 36, temperature 10 – 30 °C and pH 7.8 – 8.2), using the commercially available GMDH predictive analytics software package (GMDH Shell version 3.8.9) [44]. Seawater pH was adjusted and thermostated at the desired temperatures. Daily pH, temperature and total ammonia measurements of the source solution were performed over a 7-day period. Receiving solutions were analysed at the completion of the experiments (i.e., after 7 days) and used to determine the $[\text{NH}_3]_{\text{TWA}}$. The concentrations greater than the 90th or less than the 10th percentile were removed (10 percent trimmed mean) in order to minimise the influence of outliers, and to provide a better estimation of central tendency of data both for model calibration and validation [45]. The temperature, pH, average molecular ammonia concentration of the source solution, and the 10 percent trimmed mean receiving solution ammonia concentration were used to develop the GMDH calibration model.

The linear concentration range of the proposed GD-PS was determined using a range of standard source solutions prepared under the following conditions: salinity 35, 20 °C and pH 8.0.

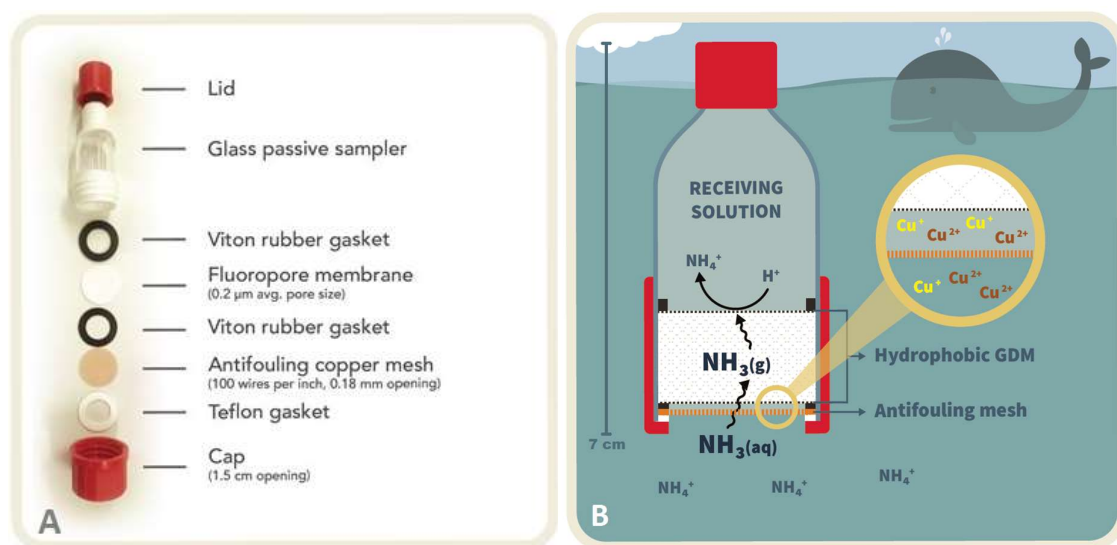


Figure 4-1. A) GD-PS assemblage with antifouling mesh. B) Cross-section of the GD-PS showing the process of selective accumulation of dissolved $\text{NH}_3(\text{aq})$ from the source solution, where the gas diffuses into the pores of the hydrophobic gas-diffusion membrane (not to scale) and the subsequent reaction of $\text{NH}_3(\text{g})$ at the membrane/receiving solution interface where the molecular ammonia is converted to ammonium ion ($\text{NH}_4^+(\text{aq})$) by reaction with a hydrogen ion ($\text{H}^+(\text{aq})$) in the receiving solution. Inset: Proposed antifouling mechanism when using the copper mesh, involving the oxidation of elemental copper and subsequent generation of the toxic cuprous and cupric ions.

4.2.6 Field deployment

Four field-based passive sampling experiments were conducted in Victoria, Australia, i.e., the *Birrarung* (Yarra River) estuary (Site 1), Hobsons Bay (Site 2), the Werribee River estuary mouth (Site 3) and approximately 5 kilometres upstream (Site 4) (Figure S4-1, Table S4-1, Appendix). These sites are part of the larger coastal area of *Nerm* (Port Phillip Bay).

During the GD-PS deployment, 250 mL discrete grab samples were collected every 2 hours at each site during the 7 day deployment period, using a Hach Sigma autosampler (model 900) fitted with 24 x 1 L polyethylene bottles, each of which contained 50 μL H_2SO_4 (98% RCI Labscan) to preserve samples. Samples remained in the dark and on ice until collection, and new bottles and ice were replaced every 48 hours. A Durapore™ 0.45 μm syringe filter (Millipore) was used for sample filtration, and samples were kept at $\leq 4^\circ\text{C}$ and analysed within 3 days of collection using the SEA analyser described above.

Multiparameter water quality sondes with sensors for pH, electrical conductivity (EC) and temperature were deployed at each site during field work. Hanna Instruments (H17629829)

was deployed at Sites 1, 2 and 3, the Hydrolab (DS5X) was used at Site 4, and YSI (EXO2) was used at Site 4 for the biofouling experiment. The GD-PSs were fitted to a floating cage [26], to which an autonomous sonde was attached prior to submerging both just beneath the surface of the water. At Sites 1 and 3, the GD-PS and sondes were deployed from a floating jetty, at Site 2 from a fixed pier, and at Site 4 the GD-PS were deployed from a partially submerged tree where the sonde had been secured to a steel post driven into the river bed.

A three-point calibration of the pH glass electrodes was carried out using standard pH buffers, pH 4, 7 and 10 (TPS, Australia). Such electrodes are susceptible to liquid junction potential errors in saline matrices [46]. Hence, five grab samples were manually collected from each site during the 7-day deployment period (on days 0, 2, 4, 6 and 7, with day 0 being the deployment day, and day 7 the collection day), and pH and temperature were measured using the instrumentation described in the '*Analytical tools and methods*' Section 4.2.2. This allowed for liquid junction potential errors to be corrected on the multiparameter autonomous sondes used in the field. A 36 ppK calibration solution (TPS, Australia) was used to calibrate the EC probes of the sondes at the beginning of each experiment and was used again at the completion of the experiment to check for sensor drift.

GD-PS receiving solutions contained 0.01 M HCl and an appropriate concentration of NaCl to approximately match the conductivity of the source solution. For Site 2 and 3, a receiving solution composition of 0.01 M HCl and 0.56 M NaCl was used, for Site 1 a 0.01 M HCl and 0.48 M NaCl receiving solution was used, and for Site 4 a 0.01 M HCl and 0.40 M NaCl receiving solution was used.

4.3 Results and discussion

4.3.1 Membrane selection and receiving solution optimisation

Three different hydrophobic porous GDMs were tested in a tris-buffered synthetic seawater source solution (salinity 35, 20 °C) with different receiving solution compositions to determine which combination provided the highest ammonia accumulation and best precision (Figure S4-2, Appendix). It was previously shown that maintaining a similar conductivity between source

and receiving solutions was important to minimise the movement of water by osmosis across the porous hydrophobic GDM [37]. Thus all three membranes, SureVent[®], Fluoropore[™] and Durapore[™] were tested with solutions containing mixtures of HCl and NaCl (viz., 0.01 M HCl + 0.56 M NaCl and 0.1 M HCl + 0.2 M NaCl) alongside 0.15 M and 0.3 M HCl (all with conductivities of approximately 5.0 S m⁻¹, except for the 0.3 M HCl solution, which was approximately twice as high).

Whilst the GD-PS with the SureVent[®] membrane exhibited an overall higher precision when compared to those with Fluoropore[™] and Durapore[™] membranes, it exhibited lower accumulation of ammonia, likely due to the smaller pore size of the SureVent[®] membrane in comparison with that of the other two (0.1 µm vs. 0.2 µm).

In the previous study, a 0.1 M HCl + 0.02 M NaCl receiving solution was used [37], which allowed the GD-PS to be applied to water salinity of around 25. However, in this study both low- and high-conductivity marine waters were monitored. Hence, a 0.01 M HCl solution was selected as it allowed for greater flexibility in terms of matching the conductivity of the receiving solution to that of the sampled medium by adding NaCl to achieve the final desired conductivity. There was no flexibility with the 0.15 M HCl receiving solution as its conductivity was effectively the same as seawater with a salinity of 35. Hence, a receiving solution composed of 0.01 M HCl and 0.56 M NaCl was selected as it provided the highest overall precision while allowing for the GD-PS to be deployed in a range of ionic strength environments, from low ionic strength estuarine to high ionic strength marine environments with good ammonia accumulation. The Fluoropore[™] membrane was selected for further experiments because it provided the best compromise between ammonia accumulation and precision in comparison with the other two membranes with 0.01 M HCl and 0.56 M NaCl as the receiving solution.

4.3.2 Membrane antifouling strategies

Bacterial and microalgal biofilm formation on the surface of the porous hydrophobic GDM impacted the previously described GD-PS, where the accumulation of ammonia in the device was observed to 'plateau' after a period of 3-4 days limiting its usability [37]. Membrane biofouling is known to limit the operating lifetime of gas sensing instruments deployed in

marine environments [47], and both copper and silver have successfully been used as biocides to limit biofilm formation in membrane facilitated separation technologies [21, 48, 49]. Hence, several antifouling strategies were tested with the aim of extending the sampling period of the GD-PS, namely, two different wire count densities of copper mesh, including Cu-100 (60% opening) and Cu-200 (35% opening), and three layers of a silver nanoparticle (AgNP) functionalised cotton mesh.

When performing laboratory-based experiments it is difficult to simulate the specific environmental conditions experienced in the field, especially in relation to the volume of water into which the GD-PSs are submerged in the laboratory (i.e., 10 L), and the composition of microorganisms in the matrix. Therefore, the likelihood of bacterial and microalgal growth in this low volume, nutrient enhanced, closed body of water is very high, and may not mimic real conditions. These experiments were therefore performed under both laboratory and field conditions.

The performance of the different antifouling strategies tested using the Fluoropore™ membrane-based GD-PS is illustrated in Figure.

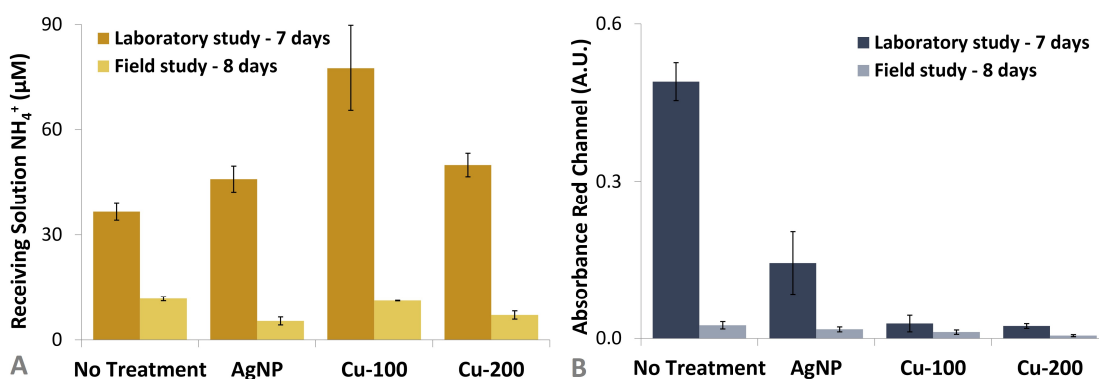


Figure 4-2. Membrane antifouling strategies under laboratory conditions. A) Effect of the different antifouling strategies on the ammonium concentration accumulated in the receiving solution after 7 or 8 days of sampling in the laboratory or field study – Site 2, respectively. B) Effect of the different antifouling strategies on the extent of biofilm formation on the surface of the GDMs, where the intensity of blue colour after staining with methylene blue is proportional to the extent of biofouling. Laboratory experimental conditions: receiving solution, 10 mL of 0.01 M HCl + 0.56 M NaCl; source solution mean ammonia concentration 223 ± 10.7 nM at salinity 34.5, temperature 21 °C, pH 7.9, $n_{(GD-PS)} = 5$. Field study conditions: receiving solution, 10 mL of 0.01 M HCl + 0.56 M NaCl; source solution mean ammonia concentration 29.4 ± 14.9 nM at salinity 34.6, temperature 17 °C, pH 8.0, $n_{(GD-PS)} = 3$. Error bars = \pm standard deviation (SD) for $n_{(GD-PS)} = 5$ (laboratory experiments) and $n_{(GD-PS)} = 3$ (field study).

In the laboratory-based antifouling experiments, receiving solution samples were collected daily and measured to monitor the uptake of ammonia into the GD-PS. In the presence of antifouling treatments Cu-100, Cu-200 and AgNP, the ammonia accumulation was linear over the course of seven days (Figure S4-3, Appendix), while for the control experiment (No Treatment) the accumulation was non-linear. This is consistent with our previous work and emphasises the importance of inhibiting biofilm formation which otherwise adversely affects the performance of the GDM.

The results observed in Figure 4-2A can be understood in the context of Fick's first law of diffusion (Eqn. 1) [50], whereby the flux of total ammonia (J_{TA}) will be reduced with any increase in the diffusive pathlength from the bulk solution to the GDM, thus affecting the overall accumulation rate in the receiving solution, where D_{TA} is the effective diffusion coefficient of total ammonia, C is the total ammonia concentration and x is distance.

$$J_{TA} = -D_{TA} \frac{\partial C}{\partial x} \quad (\text{Eqn. 1})$$

A diffusive boundary layer (DBL) will exist at the interface of any solid object in a flowing solution such as the GDM of the GD-PS studied, where the mass transfer rate (M_{TA}) (Eqn. 2) and thus the amount of ammonia accumulated in the receiving solution of the newly developed GD-PS, is controlled solely by molecular diffusion through the DBL [51], and S is defined as the surface area through which diffusion takes place.

$$M_{TA} = S \times J_{TA} \quad (\text{Eqn. 2})$$

The presence of an antifouling mesh placed in front of the GDM will create static solution pockets between the mesh threads and the GDM, and depending on the diameter of the threads (defining the mesh thickness), will increase the diffusional pathway. At the same time, the presence of the mesh will decrease S (Eqn. 2). These two effects explain the observed lower accumulation of ammonia in both the GD-PS fitted with the high density copper mesh (Cu-200) and the sandwiched-three layers of AgNP functionalised cotton mesh (FigureA). The low accumulation for the control GD-PS with no antifouling mesh (No Treatment) can be solely attributed to the presence of a biofilm on the surface of the GDM. The tortuous diffusion pathway of the ammonia molecules through the biofilm increases significantly the overall diffusional pathway between the bulk source solution and the GDM of the GD-PS, which will reduce the amount of ammonia accumulated in the sampler's receiving solution [52, 53]

(Figure 4-2A). The GD-PS fitted with copper mesh (both densities Cu-100 and Cu-200) exhibited minimal biofouling when compared to the AgNP and No Treatment conditions in the laboratory (FigureB). This is likely due to the generation of the unstable cuprous ($\text{Cu}^+_{(\text{aq})}$) ion, which rapidly oxidises to the toxic cupric ($\text{Cu}^{2+}_{(\text{aq})}$) ion, adjacent to the surface of the GDM creating a micro-environment unfavourable for bacterial and microalgal colonisation [54, 55].

The antifouling strategy with the lower density copper mesh (Cu-100) characterised by 60% opening, exhibited higher ammonia accumulation than the Cu-200 mesh with 35% opening because of the difference in their respective diffusional areas (i.e., S , Eqn. 2). Additionally, the copper itself was effective at inhibiting biofilm formation on the surface of the GDM, as well as growth and multiplication of suspended bacteria and algae in the source solution.

In the biofouling field experiment, performed in the Hobsons Bay study, Williamstown (Site 2), the highest ammonia accumulation was observed for the Cu-100 mesh-based GD-PS and the control GD-PS (No Treatment), whose values were not statistically significantly different from each other (2-Tail Student t -test 95% confidence interval: absolute value $1.63 <$ critical value 2.78 ; p -value: 0.179) (FigureA). Interestingly, since the amount of biofouling on the surface of the GDMs in all cases was quite low for field deployed GD-PSs (FigureB), the above findings suggested that the Cu-100 mesh did not present a significant analyte mass-transfer barrier. In this field study, biofouling may not have presented as a significant issue in the accumulation performance of the GD-PS likely due to low primary productivity in this environment, characterised by the low ammonia concentration registered for the period of deployment (29.4 ± 14.9 nM). However, when calibrating the GD-PS, and deploying in highly productive environments (e.g., nutrient enhanced calibration solutions, eutrophic water bodies, such as Sites 1, 3 and 4), biofouling control is imperative. As a compromise between the amount of ammonia accumulated and the minimisation of the GDM biofouling, the Cu-100 mesh was adopted for all further work.

4.3.3 Influence of temperature, salinity and pH on the GD-PS performance

In seawater, ammonia exists predominantly in the ammonium form ($\text{NH}_4^+_{(\text{aq})}$), with a small fraction being in the more toxic form of molecular ammonia ($\text{NH}_3_{(\text{aq})}$). The ammonia speciation

in marine waters has been well described, and is dependent on the environmental variables temperature, pH and to a lesser extent salinity [6].

The mechanism of ammonia accumulation by the GD-PS involves the diffusion of dissolved molecular ammonia present in the source solution through the pores of the hydrophobic GDM into the GDM/receiving solution interface where it is ionised forming the ammonium ion as it reacts with the hydrogen ions present in the receiving solution ($\text{NH}_{3(g)} + \text{H}^+_{(aq)} \rightarrow \text{NH}_4^+_{(aq)}$). Ammonia is therefore selectively accumulated into the GD-PS receiving solution as ammonium (Figure). However, in order to determine the time-weighted average molecular ammonia concentration ($[\text{NH}_3]_{\text{TWA}}$), it is necessary to calibrate the GD-PS to establish the relationship between the ammonium concentration in the receiving solution and ammonia concentration in the sampled source solution.

To assess if the ammonia accumulation was independent of the environmental variables, temperature, pH and salinity, an experiment was performed based on the empirical model of Bower and Bidwell (1978). While varying the matrix conditions (i.e., salinity, pH and temperature) appropriate amounts of ammonia were spiked into the source solutions to maintain a constant molecular ammonia concentration between experiments, as determined by the Bower and Bidwell model (Table S4-2, Appendix).

Two different total ammonia concentrations were assessed, namely, $4.4 \pm 0.2 \mu\text{M}$ and $8.5 \pm 0.1 \mu\text{M}$ (Figure S4-4, Appendix) in three different matrix compositions, each having effectively the same concentration of molecular ammonia available to the GD-PS (2.93% to 2.99% NH_3). If no appreciable difference was observed in the amount of ammonia accumulated in the receiving solutions, then the calibration of the GD-PS could be performed as a function of available molecular ammonia independent of the variables, temperature, pH and salinity. However, there was a statistically significant difference between each of the experiments in the multivariate study, which is unsurprising, since it is well established that environmental factors such as temperature will affect the analyte accumulation rate of diffusion-based PSDs [56] (Figure S4-4, Appendix).

Since it is well known that diffusion rates are temperature dependent, and can be corrected for by adjusting the diffusion coefficient for a given temperature [51, 53], it was necessary to determine if the other variables, pH and salinity also exhibited an effect on the sampling rate. The effect of the temperature, salinity and pH was therefore examined through the univariate

approach, where each variable was studied independently, again using the Bower and Bidwell, (1978) ammonia speciation model (Table S4-3, Appendix).

The salinity study examined two concentrations of molecular ammonia in the source solution at two different salinities (Figure A). There was no statistically significant difference between the results for the different salinity matrices for the two concentrations analysed, and it was thus concluded that this variable did not affect the performance of the GD-PS.

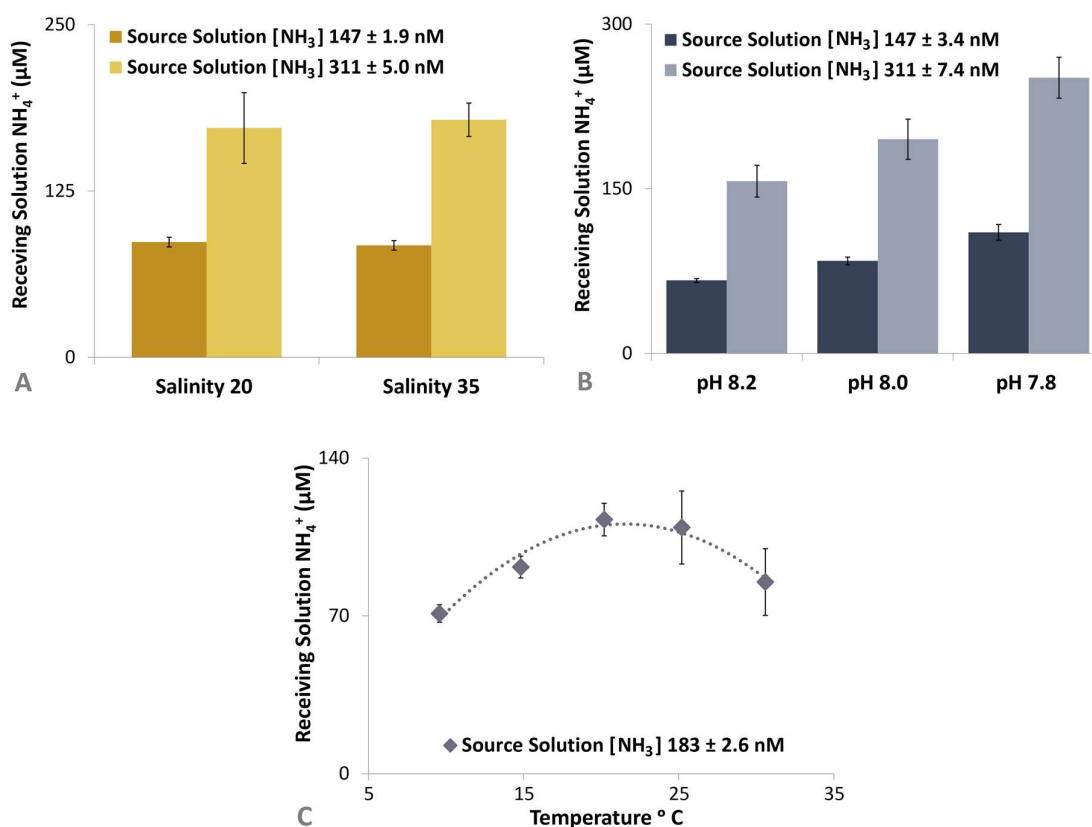


Figure 4-3. Effect of salinity (A), pH (B) and temperature (C) on the GD-PS accumulation. A) Salinity study experimental conditions: source solution, seawater (temperature 20 °C, pH 8.0); $n_{(GD-PS)} = 8$; receiving solution composition (salinity 20) = 0.01 M HCl and 0.34 M NaCl, and (salinity 35) = 0.01 M HCl and 0.56 M NaCl; statistical analysis using a 2-tail student t-test at the 95% confidence interval ($t\text{-value} < 2.145$), and $t\text{-value}_{[147\text{ nM}]} 1.376$, $t\text{-value}_{[311\text{ nM}]} 0.414$. B) pH study experimental conditions: source solution, seawater (salinity 34.5, temperature 20 °C); $n_{(GD-PS)} = 8$. C) Temperature study experimental conditions: source solution, seawater (salinity 34.5, pH 8.0). Error bars = ± SD ($n_{(GD-PS)} = 8$).

The pH study involved two ammonia concentrations and three different pH conditions, separated by 0.2 pH units (7.8 – 8.2), spanning the pH range commonly found in estuarine and

marine waters (FigureB). A statistically significant difference was observed for each data set, and the GD-PS ammonia accumulation increased as pH was decreased. This result may seem contrary to expectations, given the lower fraction of NH_3 at lower pH values. However, it was necessary to vary the source solution total ammonia concentration ($[\text{NH}_3] + [\text{NH}_4^+]$) in order to achieve the same molecular ammonia concentration ($[\text{NH}_3]$) between the experiments with matrices of different pH (Table S4-3, Appendix). This is because as the pH decreases, the percentage of molecular ammonia also decreases, and as a result the total ammonia concentration had to be increased in order to maintain the same concentration of molecular ammonia for all source solutions with different pH. As molecular ammonia diffuses into the pores of the GDM at the interface between the static solution layer and the membrane, additional NH_3 is rapidly formed from ammonium ions ($\text{NH}_4^+ \leftrightarrow \text{NH}_3 + \text{H}^+$) to compensate for the depletion of NH_3 so that the equilibrium described by $K = \frac{[\text{NH}_3][\text{H}^+]}{[\text{NH}_4^]}$ at the source solution pH is satisfied. Therefore, it is suggested that the higher concentration of total ammonia in the bulk solution will thus sustain a higher concentration of total ammonia at the GDM/source solution interface due to Fickian diffusion (Eqn. 1), thus resulting in increased NH_3 uptake and accumulation by the GD-PS. It is therefore reasonable to suggest that the total ammonia concentration may be an important factor in the observed results, as the rate of diffusion and thus the concentration at the membrane surface, depends on the total ammonia concentration in the bulk solution. It is therefore not possible to undertake an examination of the effect of pH on the accumulation efficiency of the GD-PS independent of the total ammonia concentration.

The temperature study involved the use of source solutions at five different temperatures from 10 to 30 °C in 5 °C increments. The concentration of total ammonia was again varied between solutions set at different temperatures, in order to maintain the same molecular ammonia concentration available to the GD-PS (FigureC, Table S4-3, Appendix).

There was a statistically significant difference between the data sets, except for the data sets at 20 °C and 25 °C. The response observed from the temperature study shows that the accumulation efficiency of the GD-PS increased as a function of increasing temperature up to approximately 20 °C, after which it decreased. In this instance, there are two competing effects influencing the ability of the GD-PS to accumulate ammonia from the source solution. Increased temperature will increase the rate of diffusion of total ammonia in the source solution/DBL, and of gaseous ammonia through the pores of the GDM thus promoting

increased ammonia accumulation in the GD-PS. However, in order to maintain a constant ammonia concentration in the source solution at different temperatures the total ammonia concentration in this solution was decreased for experiments conducted at higher temperatures (Table S4-3, Appendix). As a result of this, the concentration of total ammonia at the GDM/source solution interface was likewise reduced at higher temperatures, and the availability of NH_3 for gas diffusion into the pores of the GDM was therefore lower at higher temperatures. The dominance of the latter effect at higher temperatures may explain the lower accumulation efficiencies for the GD-PS above 25 °C.

Given that pH, temperature and total ammonia concentration appear to affect the GD-PS accumulation efficiency in a complex way, a simple regression equation would not be appropriate for calibration of the GD-PS, as it would be necessary to perform a calibration at every possible pH and temperature combination. In order to overcome this issue, the Group Method Data Handling algorithm (GMDH Shell software version 3.8.9 [44]) was used, which allowed for a high order polynomial regression model to be developed, applicable between the pH range 7.8 – 8.2 and temperature range of 10 °C – 30 °C (refer to the Appendix Section E GD-PS calibration).

4.3.4. GD-PS calibration using GMDH model

The GMDH algorithm introduced by Ivakheneko [38], was used to develop a calibration model allowing the $[\text{NH}_3]_{\text{TWA}}$ to be calculated in the sampled medium on the basis of the amount of ammonia accumulated as ammonium in the receiving solution of the GD-PS after 7 days of sampling, for pH and temperature of the sampled medium ranging from 7.8 to 8.2 and from 10 to 30 °C, respectively. Forty-nine laboratory experiments under different pH, temperature, and total ammonia concentrations were performed, and these data were used to develop the calibration model. The model (Figure S4-5) and its analytical figures of merit (Figure S4-6) are discussed in Section E of the Appendix. While hydrodynamic conditions are known to affect the thickness of the DBL of diffusion-based passive samplers and thus their accumulation rates [53, 57, 58], calibration experiments for the GD-PS studied were undertaken under one single flow condition designed to be representative of moderately fast moving waters such as tidal

estuaries, estuary openings and coastal seas. The impact of using only one flow condition is discussed in Section 3.5. *Field validation*, and in Section H, Appendix.

4.3.5. Field validation

Four study sites were selected to assess the performance of the GD-PS in the field (Figure S4-1, Table S4-1, Appendix). These sites were chosen as they were identified as significant nutrient sources to the waters of *Nerm* (Port Phillip Bay, PPB). The *Birrarung* (Yarra River) and its tributaries, the Western Treatment Plant, and the Werribee river contribute up to 32%, 54% and 6% of the yearly nitrogen load to PPB respectively [59], and the Werribee river estuary has been identified as a major source of ammonia nitrogen especially during periods of heavy rainfall [60]. The physical characteristics and ecological importance of the coastal area of PPB and surrounds are described in Section F (Appendix).

The GD-PSs, with the copper mesh (Cu-100) antifouling strategy, were deployed for 7 days at each location. Discrete grab samples were collected every two hours and total ammonia concentrations were measured for comparative purposes. Salinity, pH and temperature measurements were taken at half-hour intervals, and these data were used to determine the concentration of molecular ammonia in the source solution available to the GD-PS using the empirical model [6]. The concentration of accumulated ammonium in the GD-PS receiving solutions was measured and the mean pH and temperature values over the period of deployment was used to calculate the $[\text{NH}_3]_{\text{TWA}}$ using the GMDH model (Table 4-1 and Figure 4-4 for Sites 1 and 3, and Table 4-1 and Figure S4-7 for Sites 2 and 4).

There was good agreement between measured ammonia concentrations obtained by discrete grab sampling and $[\text{NH}_3]_{\text{TWA}}$ determined by the GD-PS over a range of environmental (pH, temperature and salinity) conditions, with a percentage difference in the order of -12% to -19% for the four field study sites (Table 4-1).

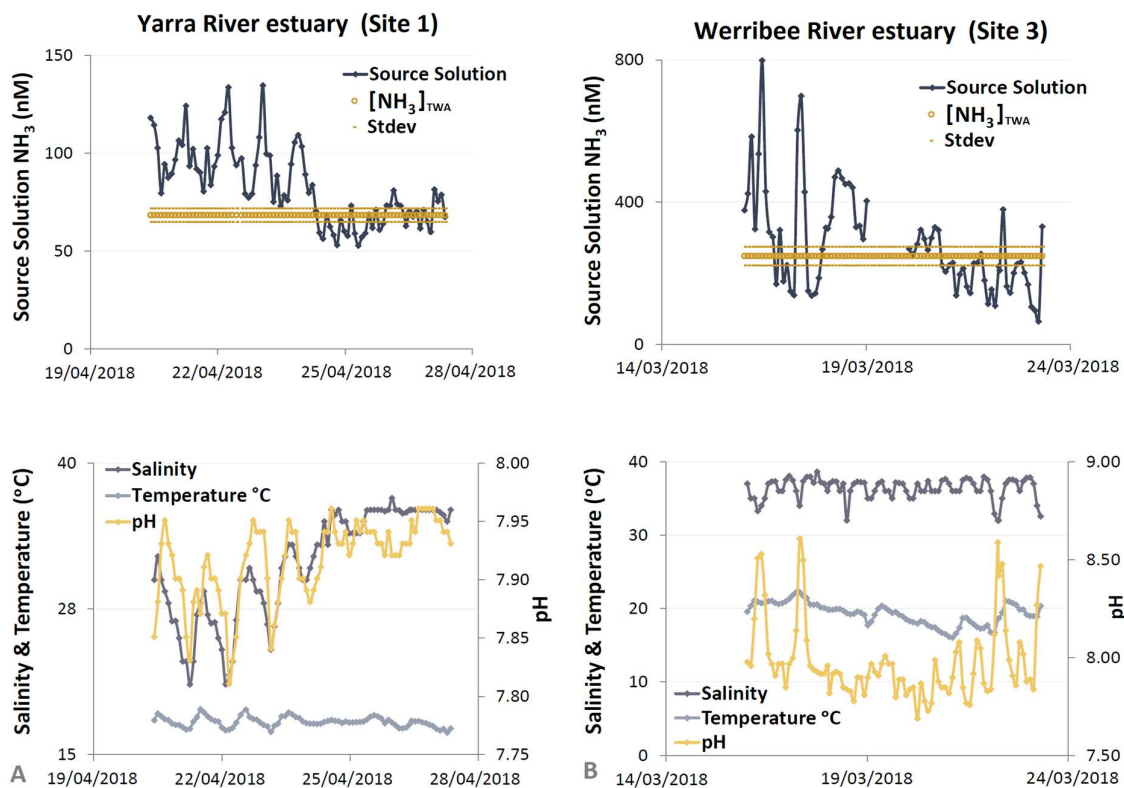


Figure 4-4. Field validation of the GD-PS with copper mesh (Cu-100) using the GMDH calibration model. The top graphs for both figures A) *Birrarung* (Yarra River) estuary (Site 1) and B) Werribee River estuary mouth (Site 3) compare the ammonia concentrations obtained from discrete grab samples (2 h sampling frequency) with the $[\text{NH}_3]_{\text{TWA}}$ determined using the GD-PS in conjunction with the GMDH calibration model. The salinity, temperature ($^{\circ}\text{C}$) and pH were monitored during the period of deployment and are represented in the bottom graphs.

Table 4-1. Comparison between discrete grab sampling and GD-based passive sampling (time-weighted average ammonia concentration ($[\text{NH}_3]_{\text{TWA}}$)) using the GMDH model.

Site	Temperature ($^{\circ}\text{C}$)	pH	Discrete grab sampling $[\text{NH}_3]/\text{nM}$	GD-PS $[\text{NH}_3]_{\text{TWA}}/\text{nM}$	% Difference	$n_{(\text{GD-PS})}$
Site 1	17.8 ± 0.5	7.91 ± 0.04	82.7 ± 19.6	68.2 ± 3.5	-19.3	8
Site 2*	17.6 ± 0.3	7.92 ± 0.02	49.1 ± 11.6	43.3 ± 5.0	-12.4	8
Site 3	19.4 ± 1.5	8.00 ± 0.19	285 ± 143	248 ± 26.7	-13.8	8
Site 4	19.9 ± 1.2	8.30 ± 0.27	575 ± 414	507 ± 22.8	-12.7	8

Site 2* due to accidental removal of the GD-PSs, the receiving solution data from this site was linearly extrapolated from a 5-day study that was performed simultaneously with the 7-day study.

During field studies a systematic error was observed, with the $[\text{NH}_3]_{\text{TWA}}$ being consistently lower than the mean ammonia concentration in the source solution measured. It was hypothesised, that the overall flow rate (promoted by the aquarium pump) in the calibration experiments was higher than that in the field, resulting in a thinner DBL [61]. Therefore, this resulted in a more rapid diffusional mass transfer of ammonia to the source solution/GDM interface and thus resulted in an enhanced ammonia accumulation by the GD-PS. As a result of this effect, the GMDH model would consistently underestimate the $[\text{NH}_3]_{\text{TWA}}$. Laboratory-based experiments were therefore performed to assess the impact of flow pattern on the accumulation of ammonia in the GD-PS (Table S4-4, Appendix), and the respective implications for using the GMDH model to determine the $[\text{NH}_3]_{\text{TWA}}$ (Section H, Appendix). By reducing the flow on every second day to the minimum setting of the aquarium pump, as well as using static flow conditions, it was observed that the flow rate and pattern were the likely cause of the systematic error.

Water velocity and flow pattern are constantly changing variables in the field, which are difficult to mimic under laboratory conditions. This limitation may be overcome by performing in-field calibration [62, 63], the use of passive flow devices [64], or by employing the flow-through passive sampling system described by Nitti et al., where a micropump was used to deliver a constant flow of sample source solution to the passive sampling device [65]. However, these options are either laborious, increase the overall cost and/or add additional layers of complexity to the operation of the passive sampler.

4.3.6 Method performance

To determine the working range of the GD-PS, the sampler protected by the Cu-100 mesh was immersed for 7 days in source solutions with different total ammonia concentrations, salinity 35, temperature of 20 °C and pH 8.0, after which time the total ammonia concentration was monitored. A linear relationship between the source solution molecular ammonia concentration and the accumulated ammonium in the receiving solution was obtained within the range 17 to 413 nM NH_3 (8 to 194 μg total $\text{NH}_3\text{-N L}^{-1}$) (Figure S4-8, Appendix). The repeatability (expressed as % RSD) at source solution concentrations of 19 nM, 113 nM and 256 nM was 7.7 %, 6.4 % and 4.9 %, respectively ($n_{\text{GD-PS}} = 8$).

4.3.7 GD-PS: A tool for ammonia screening

The Werribee river flows through Melbourne's main market garden area, where 10 % of the State of Victoria's vegetables are grown [66]. A total of 62 km of agricultural drainage channels discharge into the Werribee River estuary, which then flows into the coastal waters of PPB. Study Sites 4 and 3 were located adjacent to an agricultural drainage discharge point, and downstream of six drainage discharge points, respectively [67]. Over the last decade, the water quality for the lower Werribee River, including at the estuary mouth, has been classified as having poor to very poor river health [68], with blue green algal blooms common in the summer months [67].

The observed spikes in pH at both Werribee estuary Sites 3 and 4, are likely due to the incursion of fresh waters from up-stream during periods of low tide, where photosynthetic activity from algal blooms are causing an increase in both pH and the concentration of dissolved oxygen (Figure S4-9, Appendix). The decomposition of organic matter from senescent algae may be contributing to the high concentrations of ammonia nitrogen in the water column, as may surface run-off and the leaching of fertilisers and soil additives into the water body from surrounding farmland, especially in areas where there are agricultural drainage discharge points into the river (Figure S4-10, Appendix), and or areas with little to no riparian buffer along the river's edge to protect the estuary from wind and rain facilitated deposition. Nutrient loading of the estuary is likely facilitating increased primary production and algal blooms, resulting in periodic spikes in pH, and resulting in a higher percentage of the total ammonia in the water column existing in the toxic molecular ammonia form.

The GD-PSs deployed in the upper and lower Werribee River estuary effectively identified elevated concentrations of ammonia (Table 4-1), highlighting their applicability for monitoring and detecting diffuse and point source pollution, especially in proximity to high intensity agricultural areas. By using the GD-PS as a diagnostic tool to identify impacted environments, water quality managers could develop strategies to identify areas requiring restoration or comprehensive land use planning to mitigate adverse effects from intensive agricultural, industrial or urban expansion.

4.4 Conclusions

A biofouling resistant ammonia passive sampler based on gas-diffusion with a single calibration for application to a wide range of marine waters was developed. The described GD-PS is cheap to produce as it requires no mechanical or electronic components for operation. It is reusable as only the GDM and copper mesh need to be replaced between deployments, and both are commercially available. It is simple to fabricate and deploy requiring no specialised skills or technical expertise, and it is sensitive, with the lowest concentration measured at 17 nM molecular NH_3 corresponding to 8 μg total $\text{NH}_3\text{-N L}^{-1}$ (pH 8.0 and 20 °C). The GD-PS can be used to detect concentrations lower than the revised default guideline value of 160 μg total $\text{NH}_3\text{-N L}^{-1}$ (i.e., 340 nM molecular NH_3 at pH 8 and 20 °C) for a 99% species protection level, and its performance is well within the minimum criteria set out in the European Union's directive on technical specifications for chemical analysis and monitoring of surface waters [69]. Fluoropore™ was chosen as the optimum GDM because it showed the best compromise between ammonia accumulation and precision. The optimum receiving solution composition was found to be 0.01 M HCl with an appropriate NaCl concentration according to the salinity of the sampled source solution (e.g., estuarine or marine waters).

Covering the GDM with a copper mesh (Cu-100 mesh with 60% opening) was the preferred antifouling strategy as it was shown to effectively inhibit biofilm formation while ensuring the highest ammonia accumulation. This protective mesh allowed the deployment period to be extended from 3 to 7 days. The accumulation of ammonia in the receiving solution was affected by sample pH and temperature, but not salinity. Hence, to avoid the need to prepare a calibration for every possible sample composition, a single calibration model based on the GMDH algorithm was developed. Together with the GD-PS, this model was applied successfully to the determination of the $[\text{NH}_3]_{\text{TWA}}$ in estuarine and coastal waters in and around *Nerm* (Port Phillip Bay), Australia. These results demonstrate that the GD-PS with GMDH calibration can be universally applied to marine waters with typical ranges of temperature between 10 and 30 °C, pH between 7.8 and 8.2, and salinity from 20 to 35.

4.5 Appendix

Section A Reagents and solutions

Analytical grade chemicals were used for the preparation of all synthetic seawater and passive sampling receiving solutions. Deionized water (Synergy 185, Millipore, France, resistivity ≥ 18 M Ω cm) was used for all solution preparation throughout this study.

NH₄Cl (BDH Chemicals, 99.8%) was oven dried at 105 °C overnight and used to prepare a stock solution of 55.6 mM NH₄⁺ in deionised water.

Synthetic seawater was prepared using 34 g L⁻¹ NaCl (Merck) and 1 g L⁻¹ Trizma® base (Aldrich). The desired pH was achieved by the addition of aliquots of concentrated HCl solution (RCI Labscan 32%). Synthetic and natural seawaters were spiked with the appropriate volumes of 55.6 mM NH₄⁺ stock solution to prepare source solutions with different total ammonia concentrations for optimisation and calibration experiments.

For the receiving solution optimisation study, varying concentrations of HCl and NaCl were tested including 0.01 M HCl and 0.56 M NaCl, 0.1 M HCl and 0.2 M NaCl, as well as 0.15 M HCl and 0.3 M HCl (all 10 mL). For experiments where the source solution salinity deviated from 35, receiving solutions were prepared by modifying the added concentration of NaCl, to match the conductivity of the source solution.

A solution of 7.2 mM methylene blue (UniLab) was prepared in deionised water with a few drops of 1 M NaOH (Chem-Supply) solution to deprotonate the dye. This solution was used to quantify the extent of biofouling on the surface of the porous gas-diffusion membranes of the GD-PS after being deployed for 7 or 8 days under laboratory conditions or in the field, respectively.

Section B Field deployment

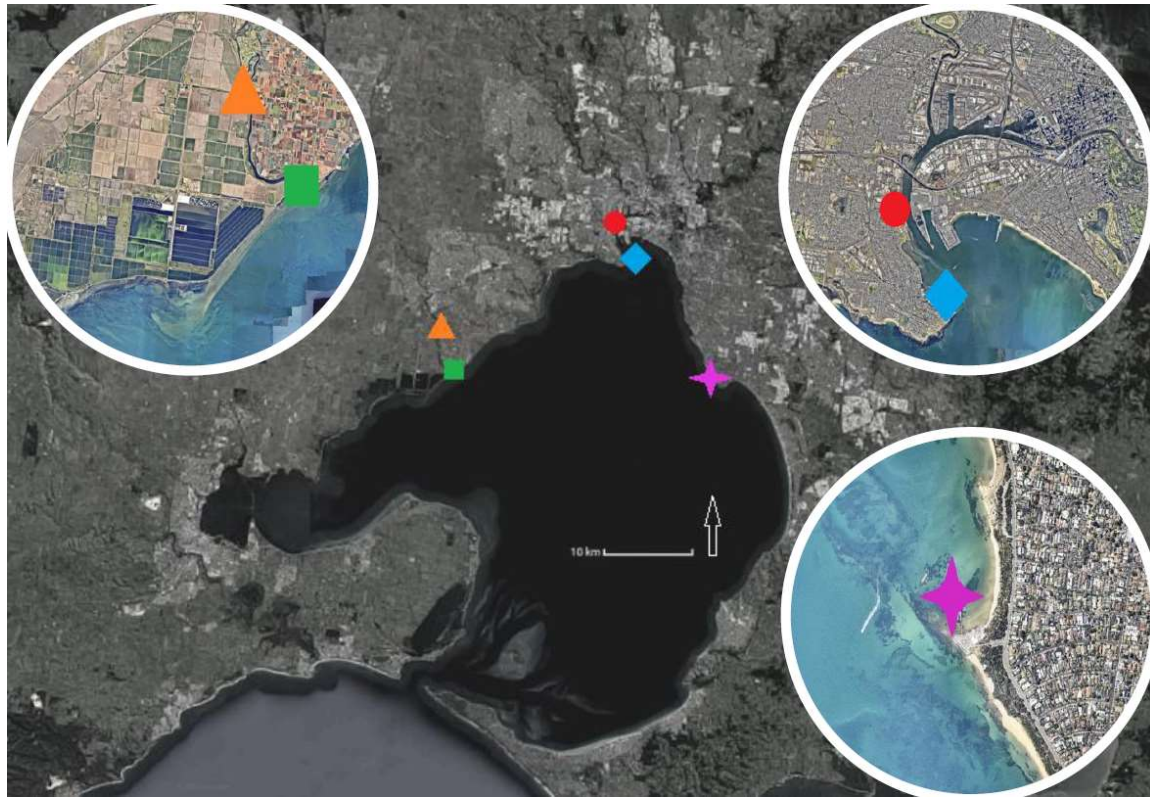


Figure S4-1. Port Phillip Bay field study sites and water collection point (datum: GDA94). Red circle = Site1 (37°50'34.9"S 144°53'51.7"E); Blue diamond = Site 2 (37°51'37.2"S 144°54'28.4"E); Green square = Site 3 (37°58'22.0"S 144°41'11.7"E); Orange triangle = Site 4 (37°56'32.0"S 144°40'13.2"E); Pink star = Site 5 (37°58'05.8"S 145°00'35.1"E) (Source: NearMap accessed on 04/08/2019 <http://maps.au.nearmap.com/>)

Table S4-1. Field site codes, location and GPS coordinates (datum: GDA94)

Site Code	Location	Position	Latitude	Longitude
Site 1	Birrarung (Yarra River) estuary, Newport	Estuary	37°50'34.9"S	144°53'51.7"E
Site 2	Hobsons Bay, Royal Yacht Club of Victoria, Williamstown	Embayment	37°51'37.2"S	144°54'28.4"E
Site 3	Werribee River estuary mouth	Embayment	37°58'22.0"S	144°41'11.7"E
Site 4	Werribee River estuary at K-Road car park, approximately 5 kilometres upstream	Estuary	37°56'32.0"S	144°40'13.2"E
Site 5	Half Moon Bay, Black Rock	Embayment	37°58'05.8"S	145°00'35.1"E

Section C Membrane selection & receiving solution optimisation

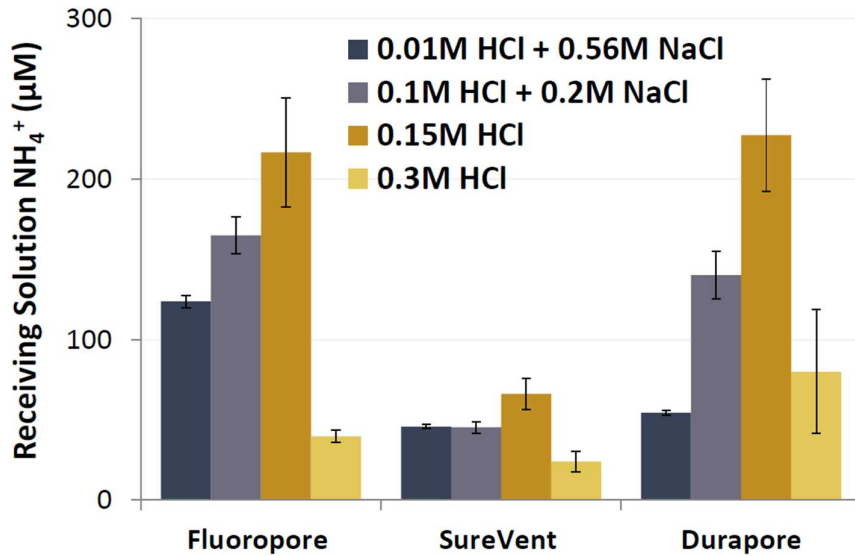


Figure S4-2. Receiving solution composition and membrane optimisation. Experimental conditions: receiving solution volume, 10 mL; source solution, 10 L of tris-buffered synthetic seawater, mean ammonia concentration 350 ± 6 nM NH_3 at salinity 35, temperature 20 °C, pH 8, $n_{(\text{GD-PS})} = 5$.

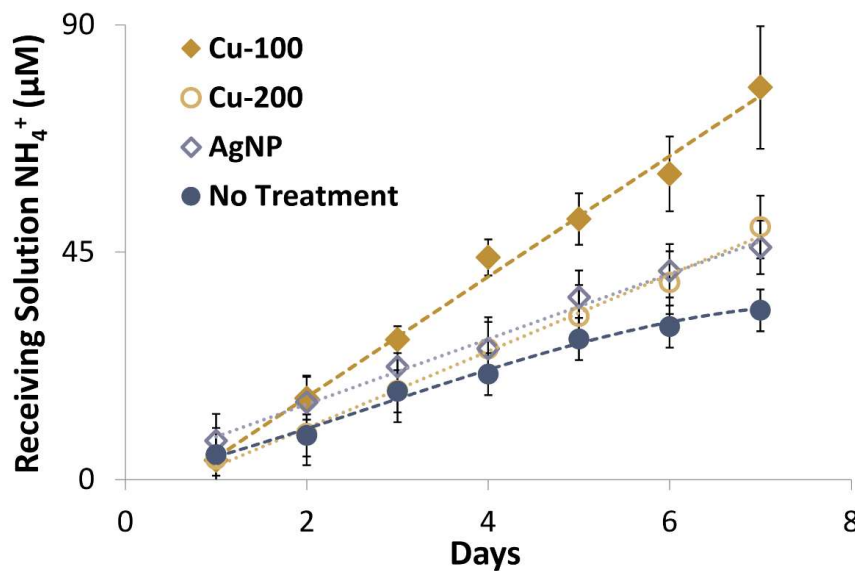


Figure S4-3. GD-PS accumulation over 7 days using Cu-100 (◆), Cu-200 (○) and AgNP (◇) antifouling mesh and no treatment (●). Laboratory experimental conditions: receiving solution, 10 mL of 0.01 M HCl + 0.56 M NaCl; source solution natural seawater, mean ammonia concentration 223 ± 10.7 nM NH_3 at salinity 34.5, temperature 21 °C, pH 7.9, $n_{(\text{GD-PS})} = 5$. Error bars = \pm standard deviation (SD) for $n_{(\text{GD-PS})} = 5$.

Section D Influence of temperature, salinity and pH on GD-PS performance

Table S4-2. Experimental conditions for the multivariate study. The values of the environmental variables salinity, temperature, and pH were chosen to ensure approximately 3% NH₃ concentration in the source solution (SS) of each experiment. RS, receiving solution.

Salinity	pH	Temperature (°C)	% NH ₃ *	SS [NH ₃]+[NH ₄ ⁺] μM	SS [NH ₃] μM	SS [NH ₄ ⁺] μM	SS [NH ₄ ⁺] μM
20	8.2	12	2.99	4.40	0.13	4.27	42.2 ± 5.3
36	8.0	20	2.98	4.40	0.13	4.27	73.6 ± 3.0
25	7.8	25	2.93	4.40	0.13	4.27	125 ± 11
20	8.2	12	2.99	8.50	0.25	8.25	94.6 ± 9.0
36	8.0	20	2.98	8.50	0.25	8.25	135 ± 11
25	7.8	25	2.93	8.50	0.25	8.25	205 ± 21

* The Bower and Bidwell (1978) ammonia ionisation model was used to determine the % NH₃ under the experimental salinity, pH and temperature conditions.

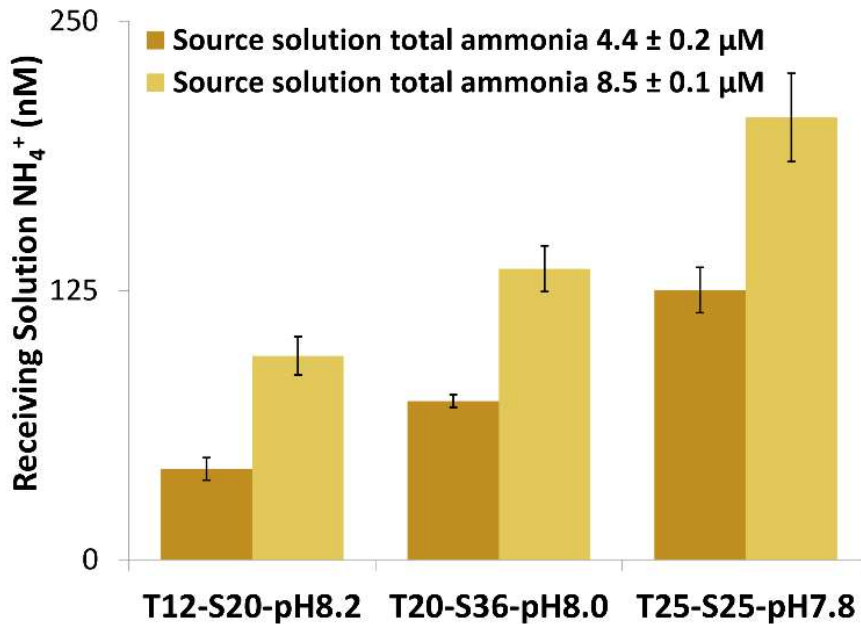


Figure S2-4. Multivariate study of temperature, salinity and pH parameters. T12-S20-pH8.2 = temperature 12 °C, salinity 20, pH 8.2, % NH₃ = 2.99; T20-S36-pH8.0 = temperature 20 °C, salinity 36, pH 8.0, % NH₃ = 2.98; T25-S25-pH7.8 = temperature 25 °C, salinity 25, pH 7.8, % NH₃ = 2.93.

Table S4-3. Experimental conditions for the univariate study. The appropriate concentration of total ammonia ($[\text{NH}_3]+[\text{NH}_4^+]$) was chosen to ensure the same molecular ammonia (NH_3) concentration in the source solution (SS) at different pH, salinity and temperature conditions used. RS, receiving solution.

Salinity	pH	Temperature (°C)	% NH_3 *	SS $[\text{NH}_3]+[\text{NH}_4^+]$ μM	SS $[\text{NH}_3]$ μM	SS $[\text{NH}_4^+]$ μM	SS $[\text{NH}_4^+]$ μM
20	8.0	20	3.41	4.31	0.147	4.16	86.7 ± 3.7
35	8.0	20	2.98	4.93	0.147	4.78	84.2 ± 3.6
20	8.0	20	3.41	9.12	0.311	8.81	172 ± 26
35	8.0	20	2.98	10.4	0.311	10.1	179 ± 12
35	7.8	20	1.90	7.73	0.147	7.58	110 ± 7.1
35	8.0	20	2.98	4.93	0.147	4.78	84.2 ± 3.6
35	8.2	20	4.65	3.16	0.147	3.01	66.4 ± 1.8
35	7.8	20	1.90	16.4	0.311	16.1	251 ± 19
35	8.0	20	2.98	10.4	0.311	10.13	195 ± 18
35	8.2	20	4.65	6.69	0.311	6.38	157 ± 14
35	8.0	10	1.44	12.7	0.183	12.5	71.0 ± 3.9
35	8.0	15	2.07	8.84	0.183	8.66	91.7 ± 4.9
35	8.0	20	2.98	6.14	0.183	5.96	113 ± 7.2
35	8.0	25	4.28	4.28	0.183	4.10	109 ± 16
35	8.0	30	6.09	3.01	0.183	2.83	85.0 ± 15

* The Bower and Bidwell (1978) ammonia ionisation model was used to determine the % NH_3 under the experimental salinity, pH and temperature conditions.

Section E GD-PS calibration

The GMDH algorithm is ideal for complex, multivariate systems, as the algorithm is able to discriminate between relevant and irrelevant input variables, removing bias that could be introduced by a researcher with prior knowledge [38]. The variables presented to the model were temperature, and pH, with the output defined as the estimated concentration of molecular ammonia in the source solution $[\text{NH}_3]_{\text{TWA}}$. The algorithm selected both temperature and pH as relevant variables. As salinity between the ranges of 20 to 35 does not affect the performance of the GD-PS (Figure 4-3A), salinity as a variable was not used for model development.

The GMDH model has a self-organising approach, built with 'layers' of polynomial regressions, whose coefficients are determined sequentially [38, 70]. The coefficients of the algorithm are defined using inductive learning procedures that sort and select the most appropriate regression, using the least squares fitting method [38, 70]. Once a 'layer' or polynomial regression is defined, the algorithm proceeds to define and test the next, until the relationship between input and output variables has been appropriately defined, and a model generated (Figure S4-5). The input data for the development of the model are segregated into 80% training and 20% randomly selected data used for model validation, and the model developed had an inherent error of up to 10% according to the plot of residuals (Figure S4-6). GMDH Shell (version 3.8.9) software was used for model generation [44], and the data was randomly sorted prior to model generation.

$Y1 = 0.00228306 - T*N10*0.00110564 + N10*1.02203$ $N10 = 1.15587 - pH*0.145014 + N26*1.00139$ $N26 = 0.176148 - N201*0.759038 + N68*1.7025$ $N68 = 0.492823 - N168*2.66956 + N168*N78*0.0452712 + N78*3.34612$ $N78 = -0.108832 + N165*0.705486 + N200*0.329447$ $N200 = -3.13477 + T*0.146979 - T*N226*0.0441373 + N226*1.92981$ $N226 = -1.05388 - RS*N248*0.000134602 + N248*1.61923$ $N165 = -0.00444923 - T*N181*0.00790556 + N181*1.16561$ $N181 = -2.22276e-11 + N196*0.49414 + N196*N255*0.162371$ $N196 = -12.2894 + pH*1.61754 + pH*RS*0.00137084 - RS*0.00950839$ $N168 = -0.670104 + T*0.0291933 + N195*1.02126$ $N195 = -0.320381 + pH*N248*0.943363 - N248*6.43417$ $N201 = -1.26068 + N243*4.0543 - N243*N249*0.124507 - N249*2.20323$ $N249 = -0.127495 - T*N250*0.0196021 + N250*1.4531$ $N250 = 1.01359 + RS*0.000624039 + RS*N255*0.000190735$ $N243 = -5.68889e-16 + N255*N234*0.167738 + N234*0.477419$ $N243 = -5.68889e-16 + N255*N234*0.167738 + N234*0.477419$ $N234 = -2.17316e-13 + N248*0.475292 + N248*N255*0.168421$ $N248 = 0.942538 - T*RS*3.62524e-05 + RS*0.00202773$ $N255 = 3.11546$	<table border="1"> <thead> <tr> <th>Error measure</th> <th>Absolute</th> <th>Target: SS</th> </tr> </thead> <tbody> <tr> <td colspan="3">Postprocessed results</td> </tr> <tr> <td></td> <td>Model Fit</td> <td>Predictions</td> </tr> <tr> <td>Number of observations</td> <td>39</td> <td>10</td> </tr> <tr> <td>Max. negative error</td> <td>-0.48004</td> <td>-1.02976</td> </tr> <tr> <td>Max. positive error</td> <td>0.647298</td> <td>0.95362</td> </tr> <tr> <td>Mean absolute error (MAE)</td> <td>0.206643</td> <td>0.324992</td> </tr> <tr> <td>Root mean square error (RMSE)</td> <td>0.250089</td> <td>0.46961</td> </tr> <tr> <td>Residual sum</td> <td>-3.09475E-14</td> <td>0.866145</td> </tr> <tr> <td>Standard deviation of residuals</td> <td>0.250089</td> <td>0.461554</td> </tr> <tr> <td>Coefficient of determination (R²)</td> <td>0.965462</td> <td>0.925164</td> </tr> <tr> <td>Correlation</td> <td>0.982579</td> <td>0.96782</td> </tr> </tbody> </table> <p>Model generated by GMDH Shell 3.8.9</p>	Error measure	Absolute	Target: SS	Postprocessed results				Model Fit	Predictions	Number of observations	39	10	Max. negative error	-0.48004	-1.02976	Max. positive error	0.647298	0.95362	Mean absolute error (MAE)	0.206643	0.324992	Root mean square error (RMSE)	0.250089	0.46961	Residual sum	-3.09475E-14	0.866145	Standard deviation of residuals	0.250089	0.461554	Coefficient of determination (R ²)	0.965462	0.925164	Correlation	0.982579	0.96782
Error measure	Absolute	Target: SS																																			
Postprocessed results																																					
	Model Fit	Predictions																																			
Number of observations	39	10																																			
Max. negative error	-0.48004	-1.02976																																			
Max. positive error	0.647298	0.95362																																			
Mean absolute error (MAE)	0.206643	0.324992																																			
Root mean square error (RMSE)	0.250089	0.46961																																			
Residual sum	-3.09475E-14	0.866145																																			
Standard deviation of residuals	0.250089	0.461554																																			
Coefficient of determination (R ²)	0.965462	0.925164																																			
Correlation	0.982579	0.96782																																			

Figure S4-5. GMDH model for GD-PS between pH 7.8 to 8.2 and temperature 10 to 30 °C. Experimental conditions: seawater, salinity 20 to 35, temperature 10 to 30 ° C, pH 7.8 to 8.2, total ammonia concentration 0.5 – 19 μM.

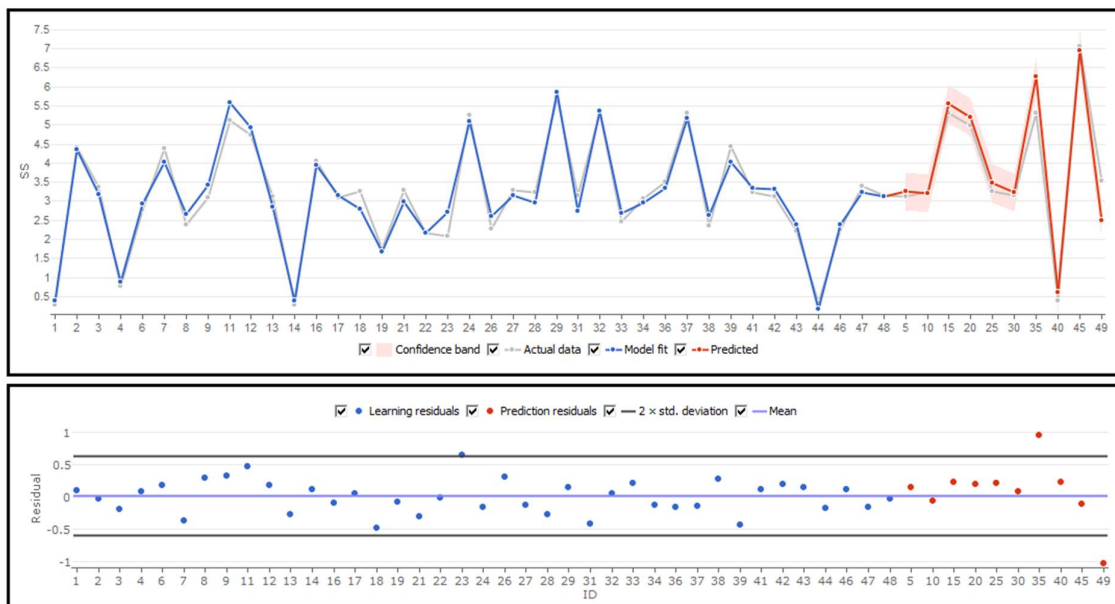


Figure S4-6. GMDH figures of merit. Blue data = 80% training; red data = 20% validation; pink shaded area around the red data points = error of prediction.

Section F *Nerm* (Port Phillip Bay)

The coastal areas and waterways feeding into *Nerm* (Port Phillip Bay), have for thousands of years been inhabited and managed by the Kulin nations, the waters which are today an area of cultural, social, environmental and economic importance to all Victorians [71-75]. Port Phillip Bay (PPB) is a semi-enclosed bay in south-eastern Australia, surrounded by the city of Melbourne, Geelong and surrounding suburbs with an area just under 2,000 km² (Figure S4-1) [76]. The land catchment area of PPB comprises 21 natural drainage basins, the largest of these being the Yarra River (known as *Birrarung/Birrarang* in the Woiwurrung and Boon Wurrung languages) with 13 tributaries [76]. PPB is shallow for its size (24 meters maximum depth) with flushing times of approximately ½ - 1 year in the farthest reaches, making it susceptible to nutrient pollution leading to poor water quality due to eutrophication [76]. PPB is a dynamic and self-sustaining ecosystem regulated by various important aquatic ecosystem processes including the biogeochemical cycling of nutrients in the water column and sediments. However, nutrient loading, particularly that of nitrogen, has been recognised as one of the major threats to the health of the bay [76, 77], with treated wastewater from the Western Treatment Plant (WTP), urban stormwater, agricultural runoff, and atmospheric deposition identified as the main contributors to nutrient inputs. Ammonia is the major form of nitrogen discharged from the WTP outfall into the coastal waters of Long Reef in western PPB [76]. It is estimated that the Werribee Treatment Plant and the Yarra River contribute around 54% and 32% of the total annual nitrogen load to PPB, respectively, and the Werribee river contributes around 6% [59].

The waters of PPB have been classified as nitrogen-limited, largely due to complex biogeochemical cycling facilitated by phytoplankton and microphytobenthos in the water column, the benthic bacterial and microalgal communities, and the burrowing invertebrates and the subsequent redox environment created by these organisms in the sediments [76]. Microbial denitrification in the sediments has been identified as fundamental to the 'assimilative capacity' of nitrogen in the ecosystem, defined as the largest amount of nitrogen loading that can be accommodated in the semi-enclosed bay, without there being a negative impact on water quality, a deleterious impact on ecosystem function, or a rapid and irreversible onset of eutrophication [76, 78]. Water quality managers are concerned with the fate and dispersal of nutrients near input points, modelling biogeochemical nutrient cycling, in addition

to implementing programs and strategies to mitigate and reduce nutrient pollution from entering the PPB catchment [78, 79]. Interestingly, the removal of bioavailable nitrogens, known as the ‘denitrification efficiency’, has been identified as an important ecosystem service to the cities of Melbourne, Geelong and surrounding suburbs, valued at an estimated \$11 billion per year [80].

Section G Field validation

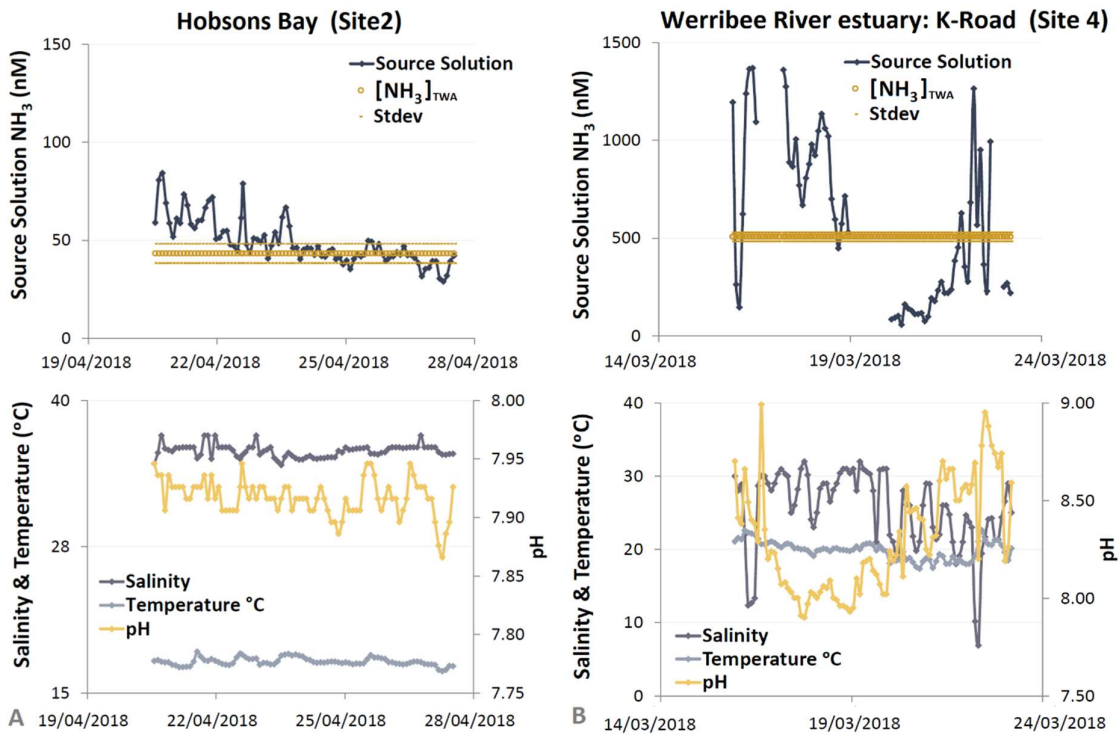


Figure S4-7. Field validation of the GD-PS with copper mesh (Cu-100) using the GMDH calibration model. The top graphs for both figures A) Hobsons Bay (Site 2) and B) Werribee River estuary 5 km upstream from river mouth (Site 4), highlight molecular ammonia concentrations measured by discrete grab sampling compared to the $[NH_3]_{TWA}$ determined using the GD-PS in conjunction with the GMDH calibration model. The salinity, temperature (°C) and pH were monitored during the period of GD-PS deployment and are represented in the bottom graphs.

Section H Systematic error

Calibration experiments were conducted with a near constant flow of 500 L h^{-1} , however environmental flow conditions in the field were very irregular. Some days water movement especially in the upper estuaries appeared to flow very slowly and on other days wave action and wind caused significant turbulence at the sea sites, followed by consecutive days where there was very little water movement observed.

To assess if the flow rate was the cause of the systematic error, a number of laboratory-based experiments (Table S4-4) were performed under three different flow conditions over the course of 7 days, and the GMDH model was then used to predict the $[\text{NH}_3]_{\text{TWA}}$. In the first series of experiments with maximum mixing, the 500 L h^{-1} aquarium pump in 10 L of solution was set to the maximum setting for the duration of the experiment. This setting was used to generate all calibration data used to develop the GMDH model, and a percentage difference of -9% was recorded between the calculated source solution ammonia concentration and the $[\text{NH}_3]_{\text{TWA}}$. In the second series of experiments, the intensity of mixing was reduced by adjusting the aquarium pump speed to its minimal flow setting and switching this every second day to the higher setting of 500 L h^{-1} . Under these conditions the percentage difference recorded was in the range of -21% to -22% between the calculated source solution ammonia concentration and the $[\text{NH}_3]_{\text{TWA}}$. The percentage difference for the two mixing intensities mentioned above are of a similar magnitude of that obtained during field work. A third series of experiments was conducted by removing the aquarium pump from the tank altogether, and conducting the passive sampling experiment under completely static conditions resulting in a difference of -74% recorded between the calculated source solution ammonia concentration and the $[\text{NH}_3]_{\text{TWA}}$ (Table S4-4). These results confirm that the flow pattern is likely responsible for the systematic error observed when comparing spot sampling with GD-based passive sampling.

Table S4-4. Effect of the flow pattern on the percentage difference (%) obtained when comparing discrete grab sampling (SS) and GD-based passive sampling ($[\text{NH}_3]_{\text{TWA}}$ determined using the GMDH model).

Lab flow studies	Temperature (°C)	pH	SS $[\text{NH}_3]/\text{nM}$	GD-PS $[\text{NH}_3]_{\text{TWA}}$ nM	% Difference	$n_{(\text{GD-PS})}$
Intensive mixing	25.5 ± 0.3	7.99 ± 0.10	180 ± 59	164 ± 11.4	-9.4	5
Moderate mixing	28.0 ± 2.3	7.86 ± 0.06	154 ± 42	125 ± 15.6	-21.4	5
Moderate mixing	14.0 ± 7.1	8.13 ± 0.07	281 ± 184	225 ± 17.2	-22.2	5
No mixing	19.2 ± 3.7	7.88 ± 0.16	198 ± 151	91 ± 4.7	-74.2	5

Section I Method performance

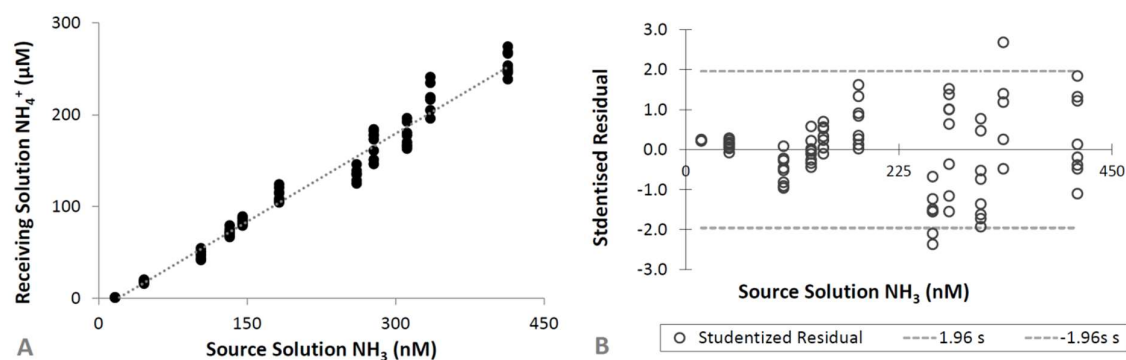


Figure S4-8. Linear calibration with studentised residuals. Calibration of the GD-PS under the following experimental conditions: salinity 35, temperature 20 °C, pH 8.0, and source solution ammonia concentrations 17 nM to 413 nM. The accumulated ammonia in the receiving solutions was measured as ammonium, and the source solution molecular ammonia was calculated by multiplying the total ammonia concentration by the fraction of un-ionised ammonia in solution, which was determined using the model described by Bower and Bidwell [6], when the temperature (°C), pH values, and salinity were known. A) Linear regression: $y = (6.396 \pm 0.1111) \times 10^{-1} x - (12.359 \pm 2.587)$, $R^2 = 9.753 \times 10^{-1}$; B) Studentized residuals showing a degree of increasing variance in the experiment, and an estimate of experimental error.

Section J GD-based passive sampling: A tool for ammonia screening and monitoring

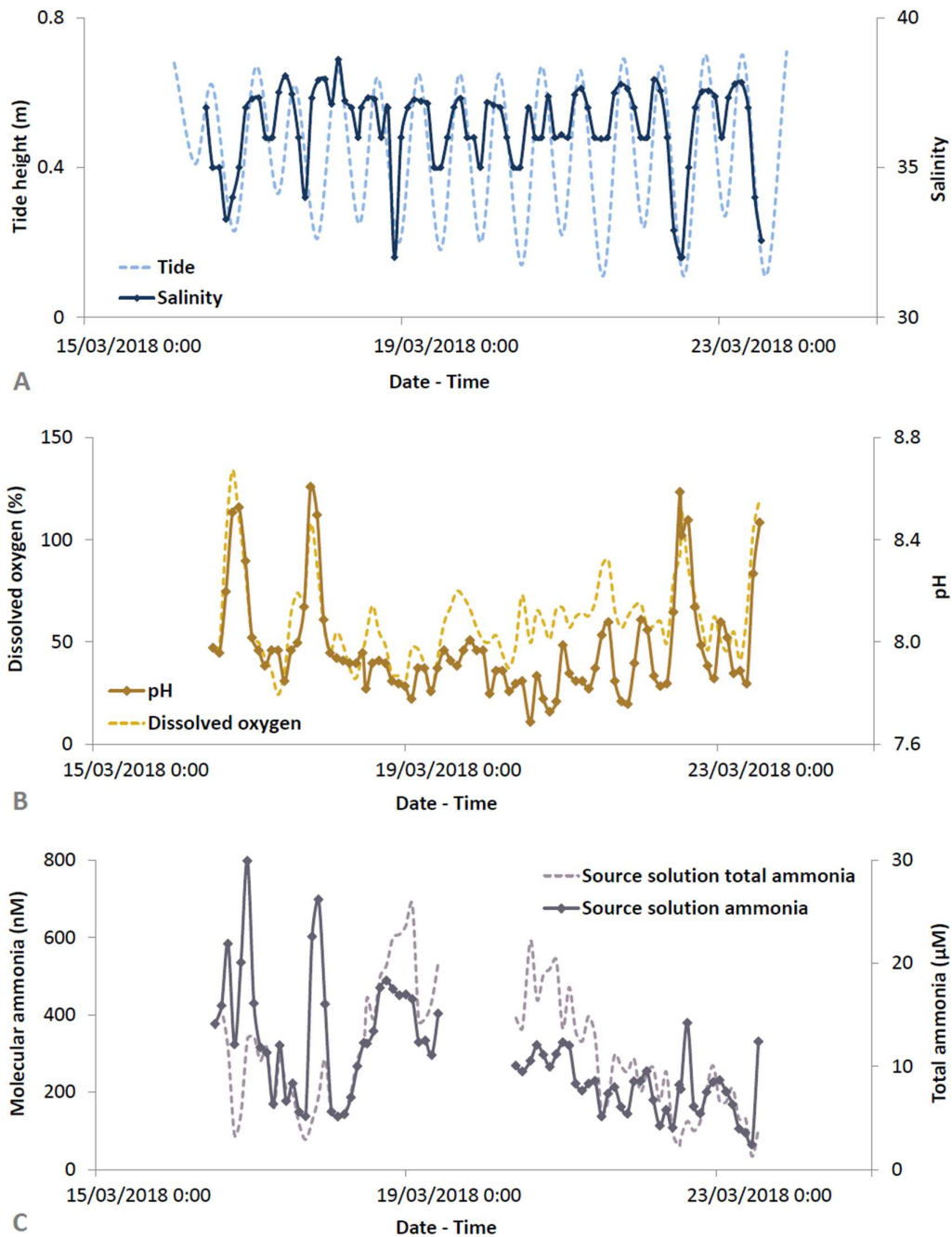


Figure S4-9. Werribee river estuary mouth (Site 3) dissolved oxygen and tidal data. A) Tide and salinity data; B) pH and dissolved oxygen data; C) calculated source solution molecular ammonia and measured total ammonia data.



Figure S4-10. Satellite images showing proximity of stockpiled agricultural chemicals to Werribee River estuary (Sites 3 and 4). Red stars mark the location of GD-PS deployment along the Werribee River estuary, blue circles mark the approximate location of the agricultural drainage discharge points [67], and insets are magnified images of stockpiled fertiliser and agricultural chemicals on the banks of the estuary approximately 20 – 40 m from the river edge. (Source of satellite images: NearMap, accessed on 04/08/2019 <http://maps.au.nearmap.com/>)

Acknowledgements

The authors of this work acknowledge the Boon Wurrung, Wurrundjerri and Wathaurong Sovereign Clans of the Kulin Nation as the Traditional Custodians of the waterways and lands upon which this research was undertaken. The authors acknowledge that the original placename for Port Phillip Bay (PPB) is *Nerm* or *Nairm* in the Boon Wurrung language [46], and the Yarra River is named *Birrarung* by the Wurundjeri and Boon Wurrung peoples meaning ‘river of mists’ [47, 48]. The Indigenous place names have been used, italicised, together with the colonial place names, in brackets.

The authors would like to thank the EPA Victoria and CAPIM, for the loan of field equipment and assistance from staff, namely, Chris Garland, Adele McKenzie and Mick Ernest, also Professor Vincent Pettigrove (RMIT University, former CEO of CAPIM), and Mr. Andrew Longmore for assistance with field work and sampling guidance. The authors would also like to thank Mr. Roger Eastham and the Royal Yacht Club of Victoria for allowing field work in the marina, Parks Victoria for permitting field work in the coastal waters of *Nerm* (PPB) and Werribee River estuary, and Melbourne Ports for allowing field work in the *Birrarung* (Yarra River) estuary. Mr. Marcus Hammarstedt assisted with the graphic design of Figure 4-1, and Lenka O’Connor Šraj is grateful to the University of Melbourne for the award of a postgraduate scholarship.

References

1. Anderson, D.M., P.M. Glibert, and J.M. Burkholder, *Harmful algal blooms and eutrophication: Nutrient sources, composition, and consequences*. Estuaries, 2002. **25** (4): p. 704-726.
2. Smith, V.H., *Eutrophication of freshwater and coastal marine ecosystems a global problem*. Environ. Sci. Pollut. Res., 2003. **10** (2): p. 126-139.
3. Smith, V.H., G.D. Tilman, and J.C. Nekola, *Eutrophication: impacts of excess nutrient inputs on freshwater, marine, and terrestrial ecosystems*. Environ. Pollut., 1999. **100** (1): p. 179-196.
4. Battye, W., V.P. Aneja, and W.H. Schlesinger, *Is nitrogen the next carbon?* Earth's Future, 2017. **5** (9): p. 894-904.
5. Camargo, J.A. and A. Alonso, *Ecological and toxicological effects of inorganic nitrogen pollution in aquatic ecosystems: A global assessment*. Environ. Int., 2006. **32**: p. 831-849.
6. Bower, C.E. and J.P. Bidwell, *Ionization of Ammonia in Seawater: Effects of Temperature, pH, and Salinity*. J. Fish. Res. Board Can., 1978. **35** (7): p. 1012-1016.
7. ANZG, *Australian and New Zealand guidelines for fresh and marine water quality*. 2018, Australian and New Zealand Governments and Australian state and territory governments: Canberra ACT, Australia.
8. Batley, G.E. and S.L. Simpson, *Development of guidelines for ammonia in estuarine and marine water systems*. Mar. Pollut. Bull., 2009. **58** (10): p. 1472-1476.
9. Vrana, B., I.J. Allan, R. Greenwood, G.A. Mills, E. Dominiak, K. Svensson, J. Knutsson, and G. Morrison, *Passive sampling techniques for monitoring pollutants in water*. TrAC Trends Anal. Chem., 2005. **24** (10): p. 845-868.
10. Allan, I.J., J. Knutsson, N. Guigues, G.A. Mills, A.M. Fouillac, and R. Greenwood, *Chemcatcher and DGT passive sampling devices for regulatory monitoring of trace metals in surface water*. J. Environ. Monit., 2008. **10** (7): p. 821-9.
11. Booij, K., C.D. Robinson, R.M. Burgess, P. Mayer, C.A. Roberts, L. Ahrens, I.J. Allan, J. Brant, L. Jones, U.R. Kraus, M.M. Larsen, P. Lepom, J. Petersen, D. Pröfrock, P. Roose, S. Schäfer, F. Smedes, C. Tixier, K. Vorkamp, and P. Whitehouse, *Passive Sampling in Regulatory Chemical Monitoring of Nonpolar Organic Compounds in the Aquatic Environment*. Environ. Sci. Technol., 2016. **50** (1): p. 3-17.
12. ICES. 2013, *Report of the Workshop on the Application of Passive Sampling and Pas-sive Dosing to Contaminants in Marine Media (WKPSPD)*. 29–31 January 2013, ICES CM 2013/SSGHIE:02. Copenhagen, Denmark.
13. Dunn, R.J.K., P.R. Teasdale, J. Warnken, M.A. Jordan, and J.M. Arthur, *Evaluation of the in situ, time-integrated DGT technique by monitoring changes in heavy metal concentrations in estuarine waters*. Environ. Pollut., 2007. **148**(1): p. 213-220.
14. Vrana, B., V. Klučárová, E. Benická, N. Abou-Mrad, R. Amdany, S. Horáková, A. Draxler, F. Humer, and O. Gans, *Passive sampling: An effective method for monitoring seasonal and spatial variability of dissolved hydrophobic organic contaminants and metals in the Danube river*. Environ. Pollut., 2014. **184**: p. 101-112.
15. Novic, A.J., D.S. O'Brien, S.L. Kaserzon, D.W. Hawker, S.E. Lewis, and J.F. Mueller, *Monitoring Herbicide Concentrations and Loads during a Flood Event: A Comparison of Grab Sampling with Passive Sampling*. Environ. Sci. Tech., 2017. **51**(7): p. 3880-3891.
16. Huang, J., W.W. Bennett, D.T. Welsh, T. Li, and P.R. Teasdale, *Development and evaluation of a diffusive gradients in a thin film technique for measuring ammonium in freshwaters*. Anal. Chim. Acta, 2016. **904** (Supplement C): p. 83-91.
17. Ren, M., S. Ding, D. Shi, Z. Zhong, J. Cao, L. Yang, D.C.W. Tsang, D. Wang, D. Zhao, and Y. Wang, *A new DGT technique comprised in a hybrid sensor for the simultaneous measurement of ammonium, nitrate, phosphorus and dissolved oxygen*. Sci. Total. Environ., 2020. **725**: p. 138447.

18. Huang, J., W.W. Bennett, D.T. Welsh, and P.R. Teasdale, *Determining time-weighted average concentrations of nitrate and ammonium in freshwaters using DGT with ion exchange membrane-based binding layers*. Environ. Sci. Proc. Imp., 2016. **18** (12): p. 1530-1539.
19. Huang, J., W.W. Bennett, P.R. Teasdale, N.R. Kankanamge, and D.T. Welsh, *A modified DGT technique for the simultaneous measurement of dissolved inorganic nitrogen and phosphorus in freshwaters*. Anal. Chim. Acta, 2017. **988**: p. 17-26.
20. Huang, J., W.W. Bennett, D.T. Welsh, T. Li, and P.R. Teasdale, *"Diffusive Gradients in Thin Films" Techniques Provide Representative Time-Weighted Average Measurements of Inorganic Nutrients in Dynamic Freshwater Systems*. Environ. Sci. Technol., 2016. **50** (24): p. 13446-13454.
21. Pichette, C., H. Zhang, W. Davison, and S. Sauvé, *Preventing biofilm development on DGT devices using metals and antibiotics*. Talanta, 2007. **72**(2): p. 716-722.
22. Panther, J.G., P.R. Teasdale, W.W. Bennett, D.T. Welsh, and H. Zhao, *Titanium Dioxide-Based DGT Technique for In Situ Measurement of Dissolved Reactive Phosphorus in Fresh and Marine Waters*. Environ. Sci. Tech., 2010. **44**(24): p. 9419-9424.
23. Panther, J.G., P.R. Teasdale, W.W. Bennett, D.T. Welsh, and H. Zhao, *Comparing dissolved reactive phosphorus measured by DGT with ferrihydrite and titanium dioxide adsorbents: Anionic interferences, adsorbent capacity and deployment time*. Anal. Chim. Acta, 2011. **698**(1): p. 20-26.
24. Zhu, Y., B. Shan, J. Huang, P.R. Teasdale, and W. Tang, *In situ biochar capping is feasible to control ammonia nitrogen release from sediments evaluated by DGT*. Chem. Eng. J., 2019. **374**: p. 811-821.
25. Almeida, M.I.G.S., A.M. Silva, R.A. Coleman, V.J. Pettigrove, R.W. Catrall, and S.D. Kolev, *Development of a passive sampler based on a polymer inclusion membrane for total ammonia monitoring in freshwaters*. Anal. Bioanal. Chem., 2016. **408** (12): p. 3213-22.
26. Tillett, B.J., D. Sharley, M.I.G.S. Almeida, I. Valenzuela, A.A. Hoffmann, and V. Pettigrove, *A short work-flow to effectively source faecal pollution in recreational waters – A case study*. Sci. Total Environ., 2018. **644**: p. 1503-1510.
27. O'Connor Šraj, L., M.I.G.S. Almeida, S.E. Swearer, S.D. Kolev, and I.D. McKelvie, *Analytical challenges and advantages of using flow-based methodologies for ammonia determination in estuarine and marine waters*. TrAC Trend. Anal. Chem., 2014. **59**: p. 83-92.
28. Gilbert, T.R. and A.M. Clay, *Determination of ammonia in aquaria and in sea water using the ammonia electrode*. Anal. Chem., 1973. **45**(9): p. 1757-1759.
29. Merks, A.G.A., *Determination of ammonia in sea water with an ion-selective electrode*. Neth. J. Sea. Res., 1975. **9**(3): p. 371-375.
30. Walters, F.H., K.B. Griffin, and D.F. Keeley, *Use of ammonia-sensing electrodes in salt media*. Analyst, 1984. **109**(5): p. 663-665.
31. APHA, *Method 4500-NH₃ D. Ammonia-Selective Electrode Method*, in *Standard Methods For the Examination of Water and Wastewater*. 2000, America Public Health Association: Washington, D.C.
32. APHA, *Method 4500-NH₃ E. Ammonia-Selective Electrode Method Using Known Addition*, in *Standard Methods For the Examination of Water and Wastewater*. 2000, America Public Health Association: Washington, D.C.
33. Ding, L., J. Ding, B. Ding, and W. Qin, *Solid-contact Potentiometric Sensor for the Determination of Total Ammonia Nitrogen in Seawater*. Int. J. Electrochem. Sci., 2017. **12**(4): p. 3296-3308.
34. Cuartero, M., N. Colozza, B.M. Fernández-Pérez, and G.A. Crespo, *Why ammonium detection is particularly challenging but insightful with ionophore-based potentiometric sensors – an overview of the progress in the last 20 years*. Analyst, 2020. **145**(9): p. 3188-3210.
35. Li, T., J. Panther, Y. Qiu, C. Liu, J. Huang, Y. Wu, P.K. Wong, T. An, S. Zhang, and H. Zhao, *Gas-Permeable Membrane-Based Conductivity Probe Capable of In Situ Real-Time Monitoring of Ammonia in Aquatic Environments*. Environ. Sci. Tech., 2017. **51**(22): p. 13265-13273.

36. Li, T., M. Zhou, Y. Qiu, J. Huang, Y. Wu, S. Zhang, and H. Zhao, *Membrane-based conductivity probe for real-time in-situ monitoring rice field ammonia volatilization*. *Sensor. Actuat. B-Chem.*, 2019. **286**: p. 62-68.
37. O'Connor Šraj, L., M.I.G.S. Almeida, C. Bassett, I.D. McKelvie, and S.D. Kolev, *Gas-diffusion-based passive sampler for ammonia monitoring in marine waters*. *Talanta*, 2018. **181**: p. 52-56.
38. Farlow, S.J., *The GMDH Algorithm of Ivakhnenko*. *Am. Stat.*, 1981. **35** (4): p. 210-215.
39. Dickson, A.G., C.L. Sabine, and J.R. Christian, *SOP 6B Determination of the pH of sea water using the indicator dye m-cresol purple*. In *Guide to Best Practices for Ocean CO₂ Measurements. PICES Special Publication 3*. 2007: p. 1-7.
40. Douglas, N.K. and R.H. Byrne, *Achieving accurate spectrophotometric pH measurements using unpurified meta-cresol purple*. *Mar. Chem.*, 2017. **190**: p. 66-72.
41. O'Connor Šraj, L., M.I.G.S. Almeida, I.D. McKelvie, and S.D. Kolev, *Determination of trace levels of ammonia in marine waters using a simple environmentally-friendly ammonia (SEA) analyser*. *Mar. Chem.*, 2017. **194** (Supplement C): p. 133-145.
42. Rehan, M., H.M. Mashaly, S. Mowafi, A. Abou El-Kheir, and H.E. Emam, *Multi-functional textile design using in-situ Ag NPs incorporation into natural fabric matrix*. *Dyes Pigm.*, 2015. **118**: p. 9-17.
43. Aneja, K.R., *Experiments in Microbiology, Plant Pathology and Biotechnology*. Fourth Edition ed. 2003, New Delhi: New Age International. 97-100.
44. GMDH, *GMDH Shell Predictive Analytics Software, Version 3.8.9*. 2019.
45. Helsel, D.R. and R.M. Hirsch, *3A. Statistical Methods in Water Resources*, in *Techniques of Water Resources Investigations*. 2002, U.S. Geological Survey.
46. Illingworth, J.A., *A common source of error in pH measurement*. *Biochem. J.*, 1981. **195**: p. 259-262.
47. Smith, M.J., A. Kerr, and M.J. Cowling, *Effects of marine biofouling on gas sensor membrane materials*. *J. Environ. Monitor.*, 2007. **9**(12): p. 1378-1386.
48. Ouyang, G., W. Zhao, M. Alaei, and J. Pawliszyn, *Time-weighted average water sampling with a diffusion-based solid-phase microextraction device*. *J. Chromatog. A.*, 2007. **1138**(1): p. 42-46.
49. Li, J., X. Liu, J. Lu, Y. Wang, G. Li, and F. Zhao, *Anti-bacterial properties of ultrafiltration membrane modified by graphene oxide with nano-silver particles*. *J. Colloid. Interf. Sci.*, 2016. **484**: p. 107-115.
50. Crank, J., *The Mathematics of Diffusion*. 2nd ed. 1975, Oxford, UK: Oxford Clarendon Press.
51. Zhang, H. and W. Davison, *Performance Characteristics of Diffusion Gradients in Thin Films for the in Situ Measurement of Trace Metals in Aqueous Solution*. *Anal. Chem.*, 1995. **67**(19): p. 3391-3400.
52. Booij, K., B. Vrana, J.N. Huckins, R. Greenwood, G. Mills, and B. Vrana, *Chapter 7 Theory, modelling and calibration of passive samplers used in water monitoring*, in *Comprehensive Analytical Chemistry*. 2007, Elsevier. p. 141-169.
53. Warnken, K.W., H. Zhang, and W. Davison, *Chapter 11 In situ monitoring and dynamic speciation measurements in solution using DGT*, in *Comprehensive Analytical Chemistry*, R. Greenwood, G. Mills, and B. Vrana, Editors. 2007, Elsevier. p. 251-278.
54. Radford, G.J.W., F.C. Walsh, J.R. Smith, C.D.S. Tuck, and S.A. Campbell, *3 - Electrochemical and atomic force microscopy studies of a copper-nickel alloy in sulfide-contaminated sodium chloride solutions*, in *Developments in Marine Corrosion*, S.A. Campbell, N. Campbell, and F.C. Walsh, Editors. 1998, Woodhead Publishing. p. 41-63.
55. Brooks, S. and M. Waldock, *Chapter 19, The use of copper as a biocide in marine antifouling paints*. In *Hellio, C and Yebara, D. (Eds.), In Advances in Marine Antifouling Coatings and Technologies, Woodhead Publishing Series in Metals and Surface Engineering*, 492-521 2009.
56. Seethapathy, S., T. Górecki, and X. Li, *Passive sampling in environmental analysis*. *J. Chromatogr. A.*, 2008. **1184**(1): p. 234-253.

57. Warnken, K.W., H. Zhang, and W. Davison, *Accuracy of the diffusive gradients in thin-films technique: diffusive boundary layer and effective sampling area considerations*. *Anal Chem*, 2006. **78**(11): p. 3780-7.
58. Guibal, R., S. Lissalde, and G. Guibaud, *Experimental Estimation of 44 Pharmaceutical Polar Organic Chemical Integrative Sampler Sampling Rates in an Artificial River under Various Flow Conditions*. *Environ. Toxicol. Chem.*, 2020. **39**(6): p. 1186-1195.
59. DEWLP, *Yarra River Protection Ministerial Advisory Committee, Protecting the Yarra River (Birrarrung) Discussion Paper, Department of Environment, Land, Water & Planning, The State Government of Victoria*, https://www.planning.vic.gov.au/data/assets/pdf_file/0037/99766/Protecting-the-Yarra-River-Birrarrung-discussion-paper-summary.pdf (accessed on: 10 October 2019). 2016.
60. Longmore, A.R., R.A. Cowdell, and R. Flint, *Nutrient status of the water in Port Phillip Bay 1990-1994. Technical Report 24, CSIRO Port Phillip Bay Environmental Study*. 1996.
61. Schlichting, H., *Boundary Layer Theory*. 7th ed. 1979, New York, USA: McGraw-Hill.
62. Ibrahim, I., A. Togola, and C. Gonzalez, *In-situ calibration of POCIS for the sampling of polar pesticides and metabolites in surface water*. *Talanta*, 2013. **116**: p. 495-500.
63. Moschet, C., E.L.M. Vermeirssen, H. Singer, C. Stamm, and J. Hollender, *Evaluation of in-situ calibration of Chemcatcher passive samplers for 322 micropollutants in agricultural and urban affected rivers*. *Water Res.*, 2015. **71**: p. 306-317.
64. Sara O'Brien, D., B. Chiswell, and J.F. Mueller, *A novel method for the in situ calibration of flow effects on a phosphate passive sampler*. *J. Environ. Monit.*, 2009. **11** (1): p. 212-219.
65. Nitti, F., M.I.G.S. Almeida, R. Morrison, R.W. Cattrall, V.J. Pettigrove, R.A. Coleman, and S.D. Kolev, *Development of a portable 3D-printed flow-through passive sampling device free of flow pattern effects*. *Microchem. J.*, 2018. **143**: p. 359-366.
66. Sheridan, J., K. Larsen, and R. Carey, *Melbourne's foodbowl: Now and at seven million, Victorian Eco-Innovation Lab, The University of Melbourne* https://research.unimelb.edu.au/_data/assets/pdf_file/0008/2355155/Melbournes-Foodbowl-Now-and-at-seven-million.pdf (accessed on 12 November 2019). 2015.
67. SRW, *Western Irrigation Futures Atlas, Southern Rural Water*, [http://www.srw.com.au/files/Technical_reports/Western Irrigation Futures WIF atlas.pdf](http://www.srw.com.au/files/Technical_reports/Western_Irrigation_Futures_WIF_atlas.pdf) (accessed on 20 November 2019). 2009.
68. SGV. *Werribee Catchment Report Card for July 2017 - June 2018, Yarra and Bay, State Government of Victoria* <https://yarraandbay.vic.gov.au/report-card/report-card-2018/port-phillip/werribee> (accessed on 20 November 2019). 2019 4 June 2019; Available from: https://yarraandbay.vic.gov.au/report-card/report-card-2018/port-phillip/werribee#top_of_report.
69. EU, *Commission Directive 2009/90/EC of 31 July 2009 laying down, pursuant to Directive 2000/60/EC of the European Parliament and of the Council, technical specifications for chemical analysis and monitoring of water status. Official Journal of the European Union, L210: 36-38*. 2009.
70. Anastaski, I. and N. Mort, *The Developemnt of Self-Organization Techniques in Modelling: A Review of the Group Method of Data Handling (GMDH), Department of Automatic Control & Systems Engineering, The University of Sheffield, Research Report No. 813*, [https://gmdhsoftware.com/GMDH %20Anastasakis and Mort 2001.pdf](https://gmdhsoftware.com/GMDH%20Anastasakis%20and%20Mort%202001.pdf) (accessed on 10 October 2019). 2001.
71. BWF, *Ngargee to Nerm: from ancient tree to ancient sea, Boon Wurrung Foundation; Port Phillip EcoCentre, City of Port Phillip*, [http://www.portphillip.vic.gov.au/default/Ngargee to Nerm DL V12-min.pdf](http://www.portphillip.vic.gov.au/default/Ngargee%20to%20Nerm%20DL%20V12-min.pdf) (accessed on 20 November 2019). 2016.

72. Briggs, C., *Boon Wurrung: The Filling of the Bay – The Time of Chaos*, Culture Victoria, State Government of Victoria, <https://cv.vic.gov.au/stories/aboriginal-culture/nyernila/boon-wurrung-the-filling-of-the-bay-the-time-of-chaos/> (accessed on 20 November 2019). 2016.
73. Garvey-Wandin, D. *Woiwurrung: The Durrung of the Yan-yan*, Culture Victoria, Victorian Government, <https://cv.vic.gov.au/stories/aboriginal-culture/nyernila/woiwurrung-the-durrung-of-the-yan-yan/> (accessed on 20 November 2019). 2016; Available from: <https://cv.vic.gov.au/stories/aboriginal-culture/nyernila/woiwurrung-the-durrung-of-the-yan-yan/>.
74. CV, *Boon Wurrung: The Journey of the Ilk – Ilkyawa*, Culture Victoria, State Government of Victoria, <https://cv.vic.gov.au/stories/aboriginal-culture/nyernila/boon-wurrung-the-filling-of-the-bay-the-time-of-chaos/> (accessed on 20 November 2019). 2016.
75. Eidelson, M., *Yalukit Willam: The River People of Port Phillip*, City of Port Phillip, Art & Heritage Unit, https://heritage.portphillip.vic.gov.au/Aboriginal_heritage/Yalukit_Willam_The_River_People_of_Port_Phillip (accessed on 20 November 2019). 2014.
76. Harris, G., G. Batley, D. Fox, D. Hall, P. Jernakoff, R. Molloy, A. Murray, B. Newell, J. Parslow, G. Skyring, and S. Walker, *Port Phillip Bay Environmental Study Final Report*, CSIRO, Canberra, Australia. 1996.
77. EPA, *Port Phillip Bay Water Quality Long-term Trends in Nutrients Status and Clarity, 1984 - 1999*, Publication 806, Environment Protection Authority Victoria, Southbank, Victoria. 2002.
78. Murray, A.G. and J.S. Parslow, *Modelling of nutrient impacts in Port Phillip Bay - a semi-enclosed marine Australian ecosystem*. *Mar. Fresh. Res.*, 1999. **50** (6): p. 597-612.
79. DELWP, *Port Phillip Bay Environmental Management Plan 2017 - 2027*, Department of Land Water and Planning, State Government of Victoria, <https://www.marineandcoasts.vic.gov.au/coastal-programs/port-phillip-bay> (accessed 5 October 2019). 2017.
80. DELWP, *Marine and Coastal Ecosystem Accounting: Port Phillip Bay*, Report to the Commissioner for Environmental Sustainability, Department of Environment, Land, Water & Planning, https://www.environment.vic.gov.au/data/assets/pdf_file/0025/49813/Marine-and-Coastal-Ecosystem-Accounting-Port-Phillip-Bay.pdf (accessed on 5 October 2019). 2016.
81. Shaun, C. and F. Thiele, *Indigenous Cultural Heritage and History within the Metropolitan Melbourne Investigation Area*, A Report to the Victorian Environmental Assessment Council <http://www.veac.vic.gov.au/documents/Indigenous%20Cultural%20Heritage%20and%20History%20within%20the%20VEAC%20Melbourne%20Metropolitan%20Investigation%20Area.pdf> (accessed on 20 November 2019).

CHAPTER 5: Conclusions and future work

This thesis reports on the development of novel analytical tools for the monitoring of ammonia in marine waters, including a flow-based analyser and a gas-diffusion-based passive sampler.

In **Chapter 2**, a simple and environmentally-friendly ammonia (SEA) analyser, was developed for the determination of ammonia in a wide range of concentrations. The SEA analyser was designed so that the desired concentration range could be tailored by simple modification of the program used to control the system hardware, including suitable adjustments to the sample and reagent volumes, making this an easy-to-use and versatile method. A gas-diffusion unit (GDU) was used for analyte separation and pre-concentration, and instead of using discrete, fixed volume samples, a flow approach was established where large sample volumes were continuously delivered to the donor channel of the GDU, while the acceptor solution, containing an acid-base indicator, was held static during this time. The acceptor stream was then re-started and monitored spectrophotometrically, and the absorbance, corresponding to the pH change caused by ammonia accumulated in the acceptor solution, was directly proportional to its concentration in the sample stream.

Several GDUs were tested, to determine which would give the highest sensitivity and repeatability, with two main configurations considered, including a sandwich style that comprised a sheet of hydrophobic porous gas-diffusion membrane (GDM) in between two Perspex blocks with drilled channels (identical in size), and a tubular design where either single or multiple hollow fibre GDMs were fitted into a larger diameter tubing. While the tubular configurations had a high membrane surface to solution volume ratio, these GDUs were difficult to use and suffered from a large blank response due to interference from the adhesives required for their fabrication which reacted with the acid-base indicator. The sandwich-style serpentine unit was chosen as it exhibited good sensitivity and repeatability. The performance of several different GDMs made from different porous hydrophobic materials and with different pore sizes were tested, with the super hydrophobic SureVent® membrane chosen as

it exhibited good mechanical stability and durability, especially under high flow rate conditions which allowed for increased sample throughput over prolonged periods of time.

Several acid-base indicators were tested to improve sensitivity and the working concentration range, including mixtures of indicators with similar pKa values and colour changes. Bromothymol blue exhibited the highest sensitivity and was therefore chosen as the preferred indicator; however, the dynamic range could be extended by using the combination bromothymol blue and thymol blue indicators in a 50:50 concentration ratio. The buffering capacity of the acceptor stream was also examined, showing that large increases in sensitivity could be achieved by a small adjustment in solution pH to achieve an initial absorbance in the range of 0.180 – 0.200.

Three working ranges and their analytical figures of merit were described, including a low concentration range (0.028 – 5.6 $\mu\text{M NH}_4^+$, 2.0 mL sample volume, LOD of 0.015 $\mu\text{M NH}_4^+$, and a sample throughput of 20 h^{-1}), a mid-concentration range (0.28 – 13.9 $\mu\text{M NH}_4^+$, 1.0 mL sample volume, LOD of 0.088 $\mu\text{M NH}_4^+$, and a sample throughput of 30 h^{-1}), and an upper concentration range (1.4 – 55.6 $\mu\text{M NH}_4^+$, 0.25 mL sample volume, LOD of 0.44 $\mu\text{M NH}_4^+$, and a sample throughput of 40 h^{-1}). The method is versatile and can be modified by simple adjustment of the sample and reagent volumes. Hence, an infinite number of working ranges could theoretically be defined. The system was validated against a certified reference material and spike-and-recovery of estuarine and coastal seawater samples, showing good agreement, especially in the middle to upper concentration ranges where the error was minimal. The reagents used were affordable, non-toxic, suitable for long-term storage, and costing as little as \$2.40 per 1,000 determinations.

The SEA analyser was used as an analytical tool in the development of the gas-diffusion-based passive sampling (GD-PS) device for ammonia monitoring in marine waters described in **Chapters 3** and **4**, enabling the easy determination of ammonia in both typically low concentrations found in marine water samples, and in high concentrations found in the passive sampler's acidic receiving solutions, without requiring any changes to the manifold.

The first prototype of an ammonia GD-PS for marine waters is described in **Chapter 3**. This device utilises a porous hydrophobic GDM to separate the sampled medium from a 10 mL acidic receiving solution. The dissolved ammonia present in the sampled medium diffuses through the pores of the GDM towards the membrane/receiving solution interface, where it is protonated to form the ammonium ion, and is thus accumulated in the receiving solution. The described GD-PS selectively transfers ammonia molecules from the sample matrix into its receiving solution, essentially acting as a zero sink by trapping the ammonia molecules as ammonium in the receiving solution, which can be directly analysed using a variety of methods, including the newly developed SEA analyser described in **Chapter 2**.

Membrane permeability and receiving solution optimisation studies showed that it was necessary to match the ionic strength of the receiving solution as closely as possible to that of the sampled medium, to minimise undesirable osmotic transport of solutes across the GDM. This was achieved by adding sodium chloride to the acidic receiving solution (0.1 M HCl) in order to achieve ion concentrations which would match that of the sampled medium where the sampler would be deployed. The effect of flow pattern on the ammonia uptake was also investigated, showing that in environments where multi-directional flow dominated (e.g., coastal areas subject to wave action and tidal estuaries) the use of flow restriction shields did not provide any benefits.

Calibration of the GD-PS was performed under laboratory conditions using recirculated synthetic seawater spiked with known concentrations of an ammonium stock solution. However, after a period of approximately 4-5 days, biofouling inhibited further uptake of ammonia into the receiving solution, limiting the use of the GD-PS to a deployment period of 3 days.

Validation experiments to assess the GD-PS performance for a sampling period of 3 days were undertaken in the field at an estuarine site. Daily spot samples of the sampled medium were collected in the field, and a comparison between the mean ammonia concentration found in the spot samples and the time-weighted average concentration (C_{TWA}) of ammonia determined using the calibrated GD-PS was performed. Good agreement between the two sampling methods was observed (relative error of 13.0%).

Chapter 4 describes how the limitations of the GD-PS outlined in **Chapter 3** were overcome. These limitations include the GDM biofouling after 3 days of deployment, and the need to perform a calibration under matrix conditions (e.g., temperature and pH) that closely resemble those of the aquatic system being sampled. Biofouling of the GDMs severely inhibited the performance of the GD-PS after 4-5 days, and thus membrane antifouling strategies were assessed. Each antifouling strategy was placed between the GDM and the sampled medium, and included a silver nanoparticle (AgNP) functionalised mesh and two different weave densities of a copper mesh. All antifouling strategies tested minimised the amount of biofilm formation on the surface of the GDM after exposure to samples containing microalga, however the copper meshes were more effective than the AgNP mesh. As expected, the control (with no treatment) had the highest fouling. The GD-PS with the open weave copper mesh (Cu-100 with a weave of 100 wires per inch) exhibited the highest ammonia uptake in the high fouling environment (nutrient enriched seawater) and this mesh was therefore chosen as the most efficient antifouling strategy for all future experiments allowing for linear ammonia uptake in the GD-PS for up to 7 days.

It is well documented that environmental variables, such as temperature, pH and salinity, may affect the performance of passive sampling technologies in aquatic environments, as summarised in **Chapter 1**. These environmental variables were also expected to affect the performance of the described GD-PS, as the ammonia speciation in solution is affected by temperature, pH, and to a lesser extent salinity. It was therefore important to assess the impact of these variable on the performance of the GD-PS.

While salinity (in the range 20 – 35) did not impact the performance of the GD-PS in terms of accumulation of ammonia in the receiving solution, both temperature and pH exhibited a significant effect. Therefore, to enable use of the GD-PS in a wide range of matrix conditions, numerous calibration experiments under different pH and temperature conditions were undertaken. The Group Method Data Handling (GMDH) algorithm allows for the modelling of complex systems affected by multiple variables. It was therefore chosen to model the GD-PS behaviour allowing for the development of one single calibration model applicable over the range of environmental conditions that were presented, that being temperature conditions

between 10–30° C and pH conditions within the range 7.8–8.2. These conditions were chosen as they are commonly found in coastal and marine ecosystems around the world. The input data for the model development were separated so that 80% were used for model development and 20% were withheld and used for model validation. The model had an approximate error of $\pm 10\%$ according to the plot of residuals.

The model was used to determine the C_{TWA} of ammonia at four field sites where the GD-PSs were deployed, including three estuarine sites and one coastal site. At each location, an autosampler was concurrently deployed to collect water spot samples every 2 hours over the course of GD-PS deployment. The ammonia in these samples was measured and the mean concentration was compared to the C_{TWA} determined using the GD-PS and the GMDH calibration model, and a good agreement between the two sampling methods was achieved. However, a systematic error was observed, which was attributed to the effect of flow pattern. In order to confirm this hypothesis, laboratory experiments were performed by immersing the GD-PS under different flow conditions, and it was concluded that the systematic error was likely due to differences in hydrodynamic conditions experienced by the GD-PS in the laboratory-based calibration compared to the field environments. Whilst this was shown to be most pronounced in near static solutions, estuaries and coastal aquatic environments should have sufficient water movement to allow for the developed calibration model to be used with minimal error.

While the use of performance reference compounds to overcome the effects of environmental variables has been successful for some passive samplers, this approach is suitable when partitioning is the dominant sorption mechanism. Hence, it would not be suitable for passive samplers that act as a chemical trap, such as the GD-PS studied. The concurrent deployment of passive flow monitors (containing gypsum or calcium sulfate dihydrate) have been successfully applied by O'Brien et al. [1] to correct for changes in hydrodynamic conditions experienced by passive phosphate samplers in estuarine and marine waters, and it is possible that such an approach could be applied to correct for the hydrodynamic exposure conditions experienced by the newly developed GD-PSs, although this remains to be tested.

In order to determine the ammonia C_{TWA} using the newly developed GD-PS, it is necessary to measure the environmental variables temperature and pH over the course of the sampler's deployment, as these variables have been identified as inputs for the GMDH calibration model. While accurate and affordable submersible temperature loggers are readily available (e.g., Tinytag and Hobo pendant), the accurate measurement of pH in high salinity matrices is far more challenging, as commercial probes are expensive and generally require a certain level of operator skill to perform the necessary calibrations. In highly dynamic estuarine environments, a pH logging device would be necessary, as diurnal changes in pH can be significant. However, in coastal seawaters that are buffered against pH changes, it would be possible to measure *in situ* pH only on the GD-PS deployment and collection days, and input the average of these two measurements into the GMDH calibration model.

A microfluidic paper-based analytical device (μ PAD) calibrated for measuring seawater pH is currently being developed by the author and will be used in the future in combination with the newly developed GD-PS for ammonia monitoring in high salinity aquatic systems. Additionally, the analysis of ammonia in the GD-PSs receiving solution could be further simplified and even performed in the field, by using the μ PADs for the determination of ammonia in wastewater samples using gas-diffusion separation [2] and in freshwaters using micro distillation analyte separation [3].

The newly developed GD-PS is affordable, user-friendly, reusable and can detect ammonia concentrations lower than the revised water quality guideline value of $160 \mu\text{g N L}^{-1}$ (total ammonia) for high conservation marine ecosystems, making this an exciting new tool for regulators and managers responsible for monitoring the health of our estuaries and coastal environments.

References

1. O'Brien, D.S., K. Booij, D.W. Hawker, and J.F. Mueller, *Method for the in Situ Calibration of a Passive Phosphate Sampler in Estuarine and Marine Waters*. Environmental Science & Technology, 2011. 45(7): p. 2871-2877.
2. Jayawardane, B.M., I.D. McKelvie, and S.D. Kolev, *Development of a Gas-Diffusion Microfluidic Paper-Based Analytical Device (μ PAD) for the Determination of Ammonia in Wastewater Samples*. Analytical Chemistry, 2015. 87(9): p. 4621-4626.
3. Peters, J.J., M.I.G.S. Almeida, L. O'Connor Šraj, I.D. McKelvie, and S.D. Kolev, *Development of a micro-distillation microfluidic paper-based analytical device as a screening tool for total ammonia monitoring in freshwaters*. Analytica Chimica Acta, 2019. 1079: p. 120-128.